Bio-engineering

A01 MICRO PARTICLE IMAGE VELOCIMETRY FOR IN VITRO ASSESSMENT OF PATIENT SPECIFIC WHOLE BLOOD RHEOLOGY

[1]Erdem Kucukal, [2]Yuncheng Man, [3]Ran An, [4]Jane A Little, [2]Umut A Gurkan. *[1]Case Western Reserve University, Cleveland Heights, OH; [2]Case Western Reserve University, OH; [3]Case Western Reserve University, Cleveland, OH; [4]University of North Carolina, NC*

10.1136/jim-2020-MW.1

Introduction/Background Whole blood visocity (WBV) is a pivotal biophysical parameter in many cardiovascular diseases and hematological disorders such as sickle cell disease (SCD). It can be influenced by a variety of factors including plasma viscosity, RBC deformability, hematocrit, and plasma protein levels. Although the separate effects of these factors on WBV determination have been well documented, a more comprehensive approach that takes into account all these factors in a patient-specific fashion is needed to better understand the role of WBV in SCD pathophysiology. Here, we describe a microfluidic platform integrated with the micro particle image velocimetry (PIV) technique to quantify WBV using unprocessed whole blood samples from individuals with SCD. Further, for the first time, we report both WBV and RBC adhesion levels simultaneously using this microfluidic system.

Objective(s) To assess whole blood viscosity (WBV) of subjects with sickle cell disease (SCD) using a high-throughput microfluidic system integrated with a micro particle image velocimetry (PIV) technique under normoxic or hypoxic conditions, and to examine its clinical associations and impact.

Methods Blood collection – Whole blood samples from de-identified healthy donors and SCD subjects (≥18) were collected in EDTA (Ethylenediaminetetraacetic acid) containing vacutainers based on an Institution Review Board (IRB) approved protocol. Subject clinical information, including medical treatments and previous comorbidities, were acquired after patients had provided a written consent from the Adult Sickle Cell Clinic at University Hospitals Cleveland Medical Center (UHCMC) in Cleveland, Ohio. A total number of 10 samples from healthy subjects (HbAA), 14 samples from subjects with HbSC, and 29 samples from subjects with HbSS were tested.

Micro PIV for velocity measurements – Whole blood samples were injected into rectangular microfluidic devices (4 mm x 0.05 mm) under constant physiological pressure (20 mm. Hg), and high resolution images of the blood flow were acquired via an inverted microscope (Olympus IX83). The images were then cross-correlated to compute the mean flow velocities in a given region of interest, which was a function of fluid viscosity. The conversion from mean blood velocity to microfluidic WBV was carried out using a standard curve generated by using clinically measured viscosity values (piston style viscometer).

RBC adhesion assay – The adhesion tests were performed in laminin-functionalized microfluidic channels. The blood samples with a volume of 15 µl were first injected into the microchannels at a shear stress of 1 dyne/cm^2, and then non-adherent cells were removed by flowing a buffer solution (1% BSA in PBS) at the same shear stress.

Results Our results showed that individuals with homozygous SCD (HbSS) had significantly higher WBV compared to healthy controls when the hematocrit of the samples were adjusted to 50% (4.8±0.41 cP vs 4.15±0.07 cP, $p<0.05$, Mann-Whiney U-test). However, HbSS SCD usually leads to significant anemia and lower hematocrit, which may lead to a lower WBV compared to the non-SCD population. Interestingly, HbSS SCD samples displayed significantly lower WBV compared to the healthy controls when unprocessed whole blood samples were tested (3.8±0.67 cP vs 4.49±0.32 cP, $p<0.05$, Mann-Whitney U-test). We observed a significant heterogeneity in terms of WBV among the HbSS subjects, where the WBV values ranged between 3.12 cP and 5.82 cP. Notably, subjects with a recent blood transfusion (<3 months, n=9) had a significantly higher WBV compared to those who were on hydroxyurea (HU) (n=15; 4.01±0.71 cP vs 3.74 ±0.71 cP, $p<0.05$, Mann-Whitney U-test). Subjects who were both on HU and with recent transfusion history were excluded from this analysis.

RBC adhesion to laminin (LN) has been repeatedly shown to correlate with disease severity in SCD. Since our results here also suggest a significantly heterogeneous WBV profile among the study group, we next sought to determine whether an association between RBC adhesion and WBV existed. Because the lowest WBV of HbAA samples that we tested was approximately 4 cP, we segregated the SCD study population into two groups: lower WBV group (<4 cP, N=8) and higher WBV (>4 cP, N=21). Interestingly, subjects with a lower WBV exhibited significantly greater RBC adhesion to LN compared to those with a higher WBV (mean adhesion ± SD: 957±767 per fov vs 452±331 per fov, $p<0.05$, Student's t-test, fov: field of view). These findings suggest that WBV and RBC adhesion may play distinct roles in the pathophysiology of homozygous SCD.

Hypoxia plays a crucial role in SCD pathophysiology as it leads to the formation of abnormally adhesive and stiff red blood cells due to hemoglobin polymerization. Consequently, we integrated a micro gas exchanger to our microfluidic system, as we have previously described, in order to probe the change in WBV as well as RBC adhesion to LN from normoxic to hypoxic conditions. The hypoxic viscosity results showed that WBV of control blood samples (HbAA, N=3) remained relatively unchanged, while the HbSS samples (N=10) became more viscous under hypoxia ($p=0.007$, student's t-test). More interestingly, we observed an inverse relationship between hypoxic WBV and RBC adhesion to LN in hypoxia, a similar behavior as in normoxic conditions (Pearson's correlation coefficient = -0.6, $p=0.03$, one-way ANOVA). In other words, RBCs from samples with a lower hypoxic WBV had an increased propensity to adhere to LN in hypoxia.

Conclusions The presented microfluidic system demonstrates a new approach for simultaneous analysis of RBC adhesion and WBV in SCD. The results of this study suggest that WBV is significantly lower in those with HbSS SCD, likely due to severe anemic conditions. Further, WBV inversely associates with RBC adhesion both in normoxic and hypoxic conditions, which has a subject-specific profile. Future studies will aim to tease out the individual as well as synergistic contributions of WBV and RBC adhesion to clinical manifestations of SCD.

Bone Marrow Transplant

B17 NO ASSOCIATION OF TELOMERE LENGTH WITH FRAILTY IN PRE-HEMATOPOIETIC CELL TRANSPLANT POPULATION

[1]Hok Sreng Te, [2]Troy Lund, [2]Bharat Thyagarajan, [2]Todd DeFor, [2]Mukta Arora. *[1]University of Minnesota, Minneapolis, MN; [2]University of Minnesota*

10.1136/jim-2020-MW.2

Introduction/Background Frailty affects about 10% of community dwelling elderly (≥65 years) and is defined as a state of diminished physiological reserve and increased vulnerability to stress associated with aging and decline in function across multiple physiological systems. The hematopoietic cell transplant (HCT) population is unique in that they have already suffered stresses to the hematopoietic cells imposed by prior chemotherapeutic treatments (direct cytotoxicity, DNA damage, and replicative, inflammatory or oxidative stress), which may result in altered leukocyte telomere dynamics even before HCT. These stressors are also known physiological correlates of aging and may also impact frailty. We hence evaluated the prevalence of frailty and its impact on survival and the predictive capability of mean leukocyte telomere length on frailty in a HCT population.
Objective(s) The objective of this study is to determine the prevalence of pre-HCT frailty, the impact of pre-HCT frailty on overall survival at 1-year post-HCT, and the association between pre-HCT frailty and pre-HCT recipient telomere length.
Methods We conducted a prospective, longitudinal study of 117 patients undergoing HCT at age ≥40 years in 2014 and 2015 at the University of Minnesota. Pre-HCT frailty phenotype was constructed based on patient performance to the following criteria: unintentional weight loss, self-reported exhaustion, weakness, slow walking speed, and low physical activity. Frailty was defined as a clinical syndrome meeting ≥3 of the criteria, while pre-frailty was defined as meeting 1 or 2 of the criteria. The study population was analyzed in 2 groups: 40–59 years and ≥60 years. Average telomere length was estimated by Southern Blot analysis. Recipients were grouped by age and quartiles of telomere length into four groups (age 40–59 years and first two quartiles (n=23), age 40–59 years and upper two quartiles (n=23); age 60+ and first two quartiles (n=24), and age 60+ and upper two quartiles (n=24)) and evaluated for subsequent association with frailty. The proportion of patients in each telomere group (1st two quartiles versus 3rd and 4th quartile) in younger (40–59 years) and older (60+ years) groups were compared across frailty score (0, 1–2, 3+).
Results The prevalence of frailty and pre-frailty was 21% and 53% pre-HCT, respectively. The probability of overall survival at one year was 48% (95% CI: 63–94%) for frail recipients as compared to 79% (95% CI: 65–88%) for pre-frail recipients, and 84% (95% CI: 63%–94%) for non-frail recipients (p=0.01). In regression analysis, recipients with frailty had 2.6 times (95% CI: 1.2–5.8) the risk of death as compared to non-frail recipients (p=0.02). The median recipient telomere length was 7065.5 kilobase (kb) (interquartile range: 5894–8848.5 kb) in the younger group (40–59 years) and 6047 kb (interquartile range: 5500–7074 kb) in the older group (>60 years) (p=0.02). We did not see any association of recipient telomere length with pre-HCT frailty (figure 1). A trend towards a higher proportion of patients with shorter telomere length (first two quartiles) was seen in those with unintentional weight loss (58% versus 42%), weakness (53% versus 47%), and low energy expenditure (52% versus 48%), but this did not attain statistical significance.

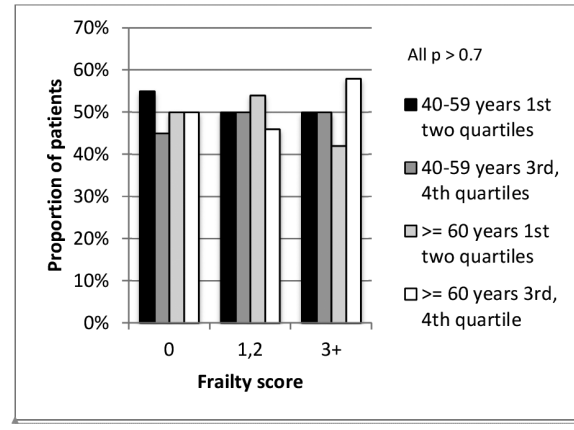

Abstract B17 Figure 1
Proportion of patients with frailty score of 0 (not-frail), 1–2 (pre-frail) and 3+ (frail) across each group of telomere length and age group

Conclusions Independent of comorbidities and age, pre-HCT frailty was noted in 21% of our HCT population. A higher mortality at 1-year post HCT was noted in frail HCT recipients, indicating the need to monitor these patients closely and plan personalized interventions in these patients. We did not find an association between frailty and telomere length. Future studies need to evaluate underlying pathophysiology in frail patients to help identify mechanisms of frailty.

Cardiology/Cardiovascular Disease

B21 CARDIAC HEMODYNAMIC AND REMODELING PATTERNS FOLLOWING TRANSCATHETER AORTIC VALVE REPLACEMENT

[1]Julien Feghaly, [2]Zachary Oman, [2]Debapria Das, [2]Steven Smart. *[1]St Louis University School of Medicine, St Louis, MO; [2]St Louis University School of Medicine*

10.1136/jim-2020-MW.3

Introduction/Background Transcatheter aortic valve replacement (TAVR) has emerged as an alternative to surgical aortic valve replacement for aortic stenosis, associated with a reduction of the aortic valve gradients, improved hemodynamics, and regression of left ventricle (LV) hypertrophy.
Objective(s) We performed a retrospective observational study to examine cardiac remodeling and valvular flow patterns post-TAVR.
Methods Echocardiographic measurements were collected and organized into three distinct time points to evaluate for cardiac remodeling and valvular flow patterns: pre-TAVR, post-TAVR first and post-TAVR follow-up echocardiograms (Echo). Once the data was compiled, statistical evaluation using paired t-test was performed, using R statistical software, to evaluate changes amongst the various time points.
Results The majority of statistically significant changes seen at post-TAVR first and follow-up Echo involved the aortic valve area, velocities, and gradients, as was expected following TAVR. Significant LV outflow tract gradient and velocity changes were noted on long term follow-up about 336 days

Abstract B21 Table 1 Baseline patient characteristics

(total: n=50)			
	Mean ± SD		n (%)
Age, years	74 ± 13	NYHA class:	
		I	2 (4)
	n (%)	II	21 (42)
Sex:		III	23 (46)
Male	26 (52)	IV	4 (8)
Female	24 (48)	CAD	30 (60)
Tobacco use:		ACS	14 (28)
Current	5 (10)	Coronary stent	10 (20)
Former	28 (56)	CABG	10 (20)
Never	17 (34)	Afib or Aflut	12 (24)
Alcohol use	14 (28)	PM or ICD	7 (14)
HTN	45 (90)	CVA/TIA	4 (8)
HLD	26 (52)	COPD	14 (28)
DM	21 (42)	Pulm HTN	6 (12)
CKD	4 (8)	OSA	13 (26)
PVD	3 (6)		

ACS: acute coronary syndrome, Afib or Aflut: atrial fibrillation or atrial flutter, CABG: coronary artery bypass grafting, NYHA: New York Heart Association, CAD: coronary artery disease, CKD: chronic kidney disease, COPD: chronic obstructive pulmonary disease, CVA/TIA: cerebrovascular accident/transient ischemic attack, DM: diabetes mellitus, HLD: hyperlipidemia, HTN: hypertension, OSA: obstructive sleep apnea, PM or ICD: pacemaker or implantable cardioverter-defibrillator, Pulm HTN: pulmonary hypertension, PVD: peripheral vascular disease, SD: standard deviation

post-TAVR. Doppler velocity index changes were significant on post-TAVR first and follow-up Echo. No significant changes were seen for LV mass index or ejection fraction (table 1).

Conclusions TAVR is significantly associated with modification of valvular flow patterns, however, longer-term and a larger sample size evaluation is needed to further appreciate cardiac hemodynamic and remodeling patterns.

B22 INTERVENTIONS FOR REDUCING SURGICAL SITE INFECTION RATES FOR PM/ICD PROCEDURES

[1]Akash P Patel, [2]Sagar Patel, [2]Paul Volansky, [2]Ketan Koranne. *[1]Northwestern University's Feinberg School of Medicine, Chicago, IL; [2]MercyOne North Iowa Medical Center*

10.1136/jim-2020-MW.4

Introduction/Background In 2014, MercyOne North Iowa Medical Center had a rate of around 2% for surgical site infection rates following PM/ICD procedures. The aim of this study was to meet the national mean of surgical site infection rates for PM/ICD procedures, which was 0.44%, by the end of 2019. This would be achieved by implementing Betasept Surgical Scrub, or topical chlorhexidine gluconate, which is a solution used by patients to clean their skin prior to the surgery. Lowering surgical site infection rates can and has led to higher reimbursement rates.

Abstract B21 Table 2 Study findings

	Pre-TAVR echocardiogram (n=50)	Post-TAVR first echocardiogram (mean: 32 days) (n=47)			Post-TAVR follow-up echocardiogram (mean: 336 days) (n=22)			Change from post-TAVR first to follow-up echocardiogram	
	Mean ± SD	Mean ± SD	95% CI	p-value	Mean ± SD	95% CI	p-value	Mean [95% CI]	p-value
LV mass, g	259.1 ± 108	243.4 ± 94.0	[-22.8,66.8]	0.32	236.7 ± 83.3	[-36.0,141.0]	0.22	6.7 [-12.3, 65.9]	0.16
LV mass index, g/m²	126.1 ± 49.6	118.2 ± 41.1	[-13.8,26.9]	0.51	118.2 ± 34.6	[-20.4,60.1]	0.3	0 [-8.18, 154.2]	0.073
LV ejection fraction,%	57.5 ± 14	56.7 ± 13.8	[-3.38, 3.92]	0.88	56.6 ± 16.2	[-6.50, 6.04]	0.94	0.1 [-9.52, 8.99]	0.95
AV mean gradient, mmHg	36.1 ± 18.2	9.0 ± 4.8	[21.7, 33.2]	$*1.78 \times 10^{-12}$	12.2 ± 6.5	[13.5, 28.0]	$*8.91 \times 10^{-6}$	-3.2 [-3.41, 2.26]	0.67
AV peak gradient, mmHg	61.7 ± 29.9	17.5 ± 9.3	[36.3, 55.1]	$*1.3 \times 10^{-12}$	20.9 ± 10.3	[21.0, 47.2]	$*2.96 \times 10^{-5}$	-3.4 [-3.88, 5.17]	0.77
AV peak velocity, cm/s	357.8 ± 96.3	199.9 ± 60.9	[141.9, 211.5]	$*3.26 \times 10^{-13}$	223.4 ± 48.6	[95.8, 177.7]	$*9.29 \times 10^{-7}$	-23.5 [-33.6, 19.8]	0.59
AV VTI, cm	88.8 ± 29.7	34.6 ± 7.7	[14.4, 68.0]	*0.011	51.5 ± 15.0	[12.0, 55.0]	*0.006	-16.9 [-41.6, 35.9]	0.52
AV area, cm²	0.77 ± 0.24	1.83 ± 0.52	[-1.18, -0.75]	$*1.93 \times 10^{-9}$	1.64 ± 0.45	[-1.03, -0.49]	$*2.20 \times 10^{-5}$	0.19 [-0.18, 0.55]	0.28
AV area index, cm²/m²	0.4 ± 0.13	0.93 ± 0.3	[-0.61, -0.39]	$*8.63 \times 10^{-10}$	0.82 ± 0.25	[-0.52, -0.24]	$*3.62 \times 10^{-5}$	0.11 [-0.07, 0.35]	0.17
Aortic root diameter, cm	3.14 ± 0.49	3.17 ± 0.43	[-0.20, 0.23]	0.87	2.89 ± 0.47	[-0.033, 0.57]	0.076	0.28 [-0.18, 0.51]	0.31
LVOT diameter, cm	2.14 ± 0.55	2.08 ± 0.19	[-0.088, 0.066]	0.77	2.1 ± 0.26	[-0.29, 0.62]	0.46	-0.02 [-0.21, 0.11]	0.51
LVOT peak velocity, cm/s	91.9 ± 26.3	96.8 ± 25	[-11.8, 4.62]	0.38	112.9 ± 33.2	[-35.4, -1.52]	*0.034	-16.1 [-38.3, 2.51]	0.081
LVOT peak gradient, mmHg	4.88 ± 7.91	4.99 ± 2.52	[-3.25, 2.91]	0.88	6.0 ± 3.11	[-4.33, 0.33]	0.085	-1.01	/
LVOT mean velocity, cm/s	76 ± 49.7	73.0 ± 19.9	[-119.1, 141.8]	0.74	68.9 ± 26.4	[-24.9, -1.60]	*0.036	4.1	/
LVOT mean gradient, mmHg	3.24 ± 6.11	2.72 ± 1.47	[-5.04, 5.09]	0.98	2.97 ± 1.50	[-1.46, 0.058]	0.06	-0.25	/
LVOT VTI, cm	20.9 ± 6.0	19.2 ± 5.51	[-5.25, 5.51]	0.95	24.6 ± 6.56	[-5.28, 4.38]	0.84	-5.4 [-12.8, 12.6]	0.94
LVOT stroke volume, ml	78.1 ± 29.7	71.4 ± 18.2	[-294.2, 296.7]	0.97	86.1 ± 47.6	[-98.7, 108.4]	0.66	-14.7	/
LVOT stroke volume index, ml/m²	39.6 ± 14.4	37.3 ± 9.9	[-156.1, 157.1]	0.98	43.3 ± 20.4	[-45.1, 49.2]	0.68	-6	/
LVOT cardiac output, ml/min	5852 ± 2443	5456 ± 1771	[-1829, 1250]	0.25	6123 ± 2422	[-1088, 1338]	0.42	-667	/
LVOT cardiac index, ml/min·m²	2904 ± 1015	2821 ± 948	[-9519, 6487]	0.25	3065 ± 1068	[-431, 730]	0.19	-244	/
DVI with LVOT VTI	0.25 ± 0.069	0.64 ± 0.21	[-0.57, -0.09]	*0.018	0.51 ± 0.16	[-0.38, -0.11]	*0.0031	0.13 [-0.77, 0.82]	0.74

*statistically significant, p-value <0.05
AV: aortic valve, CI: confidence interval, DVI: doppler velocity index, LV: left ventricle, LVOT: left ventricular outflow tract, SD: standard deviation, TAVR: transcatheter aortic valve replacement, VTI: velocity time integral,/: no statistical data available

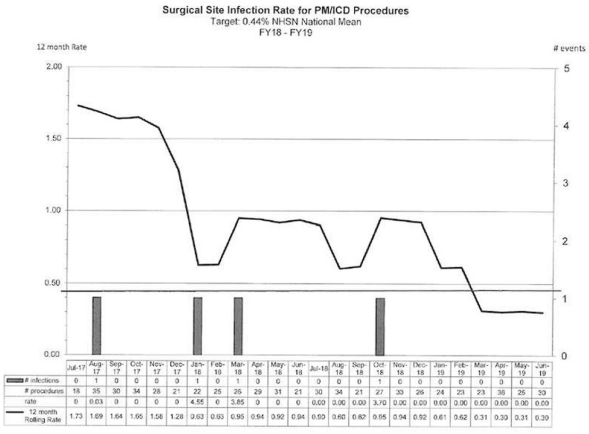

Abstract B22 Figure 1

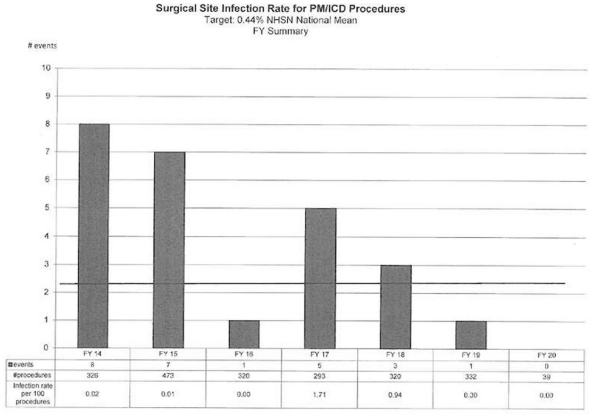

Abstract B22 Figure 2

Objective(s) The objective was to lower surgical site infection rates for PM/ICD procedures to improve reimbursement rates that diminish from these avoidable complications.
Methods This longitudinal study was between 2014–2019 that specifically looked at surgical site infections in patients undergoing PM/ICD procedures. Patients were given Betasept surgical scrub and instructed to clean themselves according to the instructions the day before and the morning of their procedure. Surgical site infections were diagnosed and measured through typical signs and symptoms such as discharge of pus or discoloration. The infectious disease team, nursing staff, and cardiovascular clinicians were part of a multi-disciplinary team to enact this project.
Results Results are attached.
Conclusions This method, along with action by the multidisciplinary team, lowered the rate of surgical infection rates following PM/ICD procedures to below the national mean. We can conclude that Betasept Surgical Scrub has shown to be effective in reducing surgical site infections in this patient population and has an important purpose in the delivery of care.

B01 ABCC9 IS NECESSARY FOR NORMAL CARDIAC MITOCHONDRIA STRUCTURE AND FUNCTION

[1]Chelsea White, [2]David Barefield, [2]Elizabeth McNally, [3]Gregory Aubert. *[1]Loyola University Chicago; [2]Northwestern; [3]Loyola University Chicago, Maywood, IL*

10.1136/jim-2020-MW.5

Introduction/Background Despite recent advances in the treatment of cardiovascular disease, the prevalence of heart failure (HF) continues to grow, affecting about 5.7 million adults in the United States. Accordingly, there is a compelling need for new drugs that could improve clinical outcomes. HF is associated with profound changes in cardiac metabolism characterized by a decrease in cardiac energy production that results from progressive impairments in substrate utilization and mitochondrial structure and function. Therefore, modulating cardiac metabolism may prevent or treat HF. Nevertheless, the exact molecular mechanisms linking metabolic changes to HF development are still poorly understood. We propose that the sulfonylurea receptor 2 (SUR2) contributes to this metabolic derangement during HF. Notably, human mutations in the ABCC9 gene, which encodes SUR2, are known to cause diverse cardiac phenotypes including dilated cardiomyopathy.
Objective(s) To study the role of SUR2 in mitochondrial structure and function in response to cardiac stress.
Methods We have previously shown that cardiac specific SUR2 KO mice have increased glycolysis. Despite a baseline reduced ejection fraction, the cardiac SUR2 KO mice showed a cardioprotective metabolic phenotype in response to ischemia reperfusion injury. To investigate the role of SUR2 in cardiac metabolism and more specifically on mitochondrial structure and function, we 1. examined the mitochondrial structure and function of cardiac specific SUR2 KO mice. 2. Study mitochondrial respiration in hIPSC derived cardiomyocytes from patients with ABCC9 mutations.
Results Adult cardiomyocyte-SUR2 deleted mice displayed smaller mitochondria compared to littermate controls using electron microscopy (EM). Adult isolated cardiomyocytes from SUR2 KO mice show increase reactive oxygen species measured by fluorescence. Adult isolated cardiomyocytes from cardiomyocyte-SUR2 deleted mice have increase maximal oxygen consumption capacity. hIPSC derived cardiomyocytes from two patients with ABCC9 variant confirm increase mitochondrial oxygen consumption. This finding correlated with an altered mitochondrial structure and function in the SUR2 deleted heart.
Conclusions Together, these data highlight SUR2 as a mediator of mitochondrial structure and function in the mature mouse heart. In the adult myocardium, modulating cardiac metabolism by reducing SUR2 leads to increased maximal mitochondrial capacity. These findings suggest a novel mechanism for modulating cardiomyocyte metabolism to protect the myocardium.

A07 B7–33 NORMALIZES BLOOD PRESSURE IN THE REDUCED UTERINE PERFUSION PRESSURE RAT MODEL OF PREECLAMPSIA

[1]Syeda H Afroze, [1]Ahmed F Pantho, [1]Thomas J Kuehl, [2]Lorena Amaral, [3]Babette LaMarca, [4]David C Zawieja, [5]Ross Bathgate, [6]Mohammed Hossain, [7]M Nasir Uddin. *[1]Orion Institute for Translational Medicine, Temple, TX; [2]The University of Mississippi Medical Center; [3]University of Mississippi Medical Center; [4]Texas A&M University College of Medicine; [5]Florey Institute of Neuroscience and Mental; [6]Florey Institute of Neuroscience and Mental Health; [7]Texas AandM University College of Medicine, Orion Institute for Transnational Medicine, Emergent Biotechnologies*

10.1136/jim-2020-MW.6

Introduction/Background Background: Preeclampsia (preE) is a serious complication of pregnancy manifested by high blood pressure, proteinuria, and edema, sometimes with encephalopathy, seizures, and hepatic failure. PreE complicates 5–10% of

pregnancies and is a major cause of maternal and fetal morbidity and mortality worldwide. Nevertheless, an effective therapy for this disorder does not exist. There is no known specific treatment, although palliative measures such as antihypertensive drugs, magnesium, and steroids, and early delivery improve outcomes. Human relaxin 2 (H2 relaxin) acts on the G protein-coupled receptor (GPCR) known as Relaxin Family Peptide Receptor 1 (RXFP1) to mediate vasodilatory and organ-protective effects. Recent data strongly suggest that H2 relaxin will be a promising treatment for preE (Conrad, 2016). Data from our lab suggest that the H2 relaxin-derived peptide B7-33 (Hossain, 2017) attenuates the preE syndrome in vitro.

Objective(s) In this study, we tested B7-33 in a preclinical rat model of preE, the reduced uterine perfusion pressure (RUPP) model (Santiago-Font, 2016).

Methods Experimental Design: Normal pregnant (NP) or RUPP rats assigned to the control peptide or B7-33 treatment groups received intra-abdominal implantation of Alzet mini-osmotic pumps (Model 2001) filled with control peptide or B7-33 diluted to provide concentrations of 4 mg/h (N=10 per group). This dose is chosen as it is the level of relaxin required to mimic normal pregnancy concentrations in the rat (Danielson, 2003). The rats were sacrificed after measurements on GD18, and the mean number of pups and any developmental or histological abnormalities in the pups were assessed. On GD 18, rats were anesthetized with isoflurane, and carotid arterial catheters (V3 tubing, SCI) were inserted into the carotid artery, tunneled under the skin, and externalized at the back of the neck. On the following day, mean arterial pressure was monitored with a pressure transducer (Cobe III Tranducer CDX Sema) and recorded continuously for 30 min. after 30-min. stabilization. Subsequently, rats were anesthetized, blood and urine samples were collected, kidneys, placentas, and spleens were harvested, and litter size and pup weights were recorded. We analyzed terminal blood samples from the rats for NO, TNF-α, and sFlt-s1. Comparisons of control with experimental groups were analyzed by ANOVA with Bonferroni's multiple comparisons test as post hoc analysis with a value of $P<0.05$ considered statistically significant.

Results Mean arterial pressure (MAP) was increased in RUPP compared with NP rats. No significant difference was seen between NP and NP+B7-33. A significant ($p<0.05$) decrease in MAP in the RUPP rats was observed with B7-33 treatment. No significant effects of B7-33 were observed for UAR, body weight, left or right kidney weight, placenta weight, pup weight, or litter size. Treatment with B7-33 increases plasma NO, reduces TNF-α, and normalizes sFlt-1.

Conclusions Based on these extensive preliminary data, both in vitro and in vivo, we conclude that B7-33 is an ideal template for further development as a cost-effective therapeutic for preE. Like H2 relaxin, B7-33 improves the pathophysiology of placental ischemia, including mean arterial pressure (MAP) in the RUPP model.

A10 METABOLIC SYNDROME IMPAIRS MITOCHONDRIAL STRUCTURE AND FUNCTION IN SWINE MESENCHYMAL STEM CELLS

[1]Rahele Farahani, [2]Mohamed Farah, [2]Xiangyang Zhu, [2]Hui Tang, [2]Lilach O Lerman, [2]Alfonso Eirin. [1]*Mayo Clinic Rochester, Rochester, MN*; [2]*Mayo Clinic*

10.1136/jim-2020-MW.7

Introduction/Background Transplantation of autologous mesenchymal stem cells (MSCs) is an effective therapy for several diseases. Mitochondria modulate several important aspects of MSC function, but might be damaged by comorbidities and cardiovascular risk factors. Metabolic syndrome (MetS) alters the fat microenvironment, but whether damages MSC mitochondria remains unknown.

Objective(s) We hypothesized that MetS compromised adipose tissue-derived MSC mitochondrial structure and function in swine.

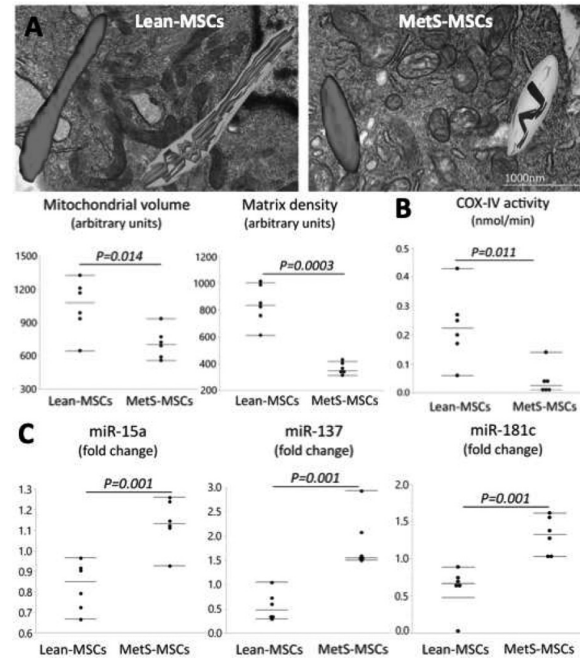

Abstract A10 Figure 1 A: Representative transmission electron microscopy images and 3D reconstruction of Lean-and MetS MSC mitochondria. Images from ~50 consecutive serial sections 0.09μm thick were stacked, aligned, and reconstructed using the 3D reconstruction software Reconstruct (Synapse Web), and mitochondrial volume and matrix density quantified. B: Cytochromec oxidase (COX)-IV activity decreased in Mets-MSCs compared to Lean-MSCs. C. Expression of miR15a, miR-137, and miR-181C was higher in Mets-MSCs versus Lean-MSCs.

Abstract A10 Table 1 Systemic characteristics in experimental groups (n=6, each) at 16 weeks

Parameter	Lean	MetS
Body Weight (Kg)	73.7±10.6	91.3±1.8*
Mean blood pressure (mmHg)	97.3±10.0	122.7±6.2*
Total cholesterol (mg/dl)	84.1±6.3	393.5±66.3*
LDL cholesterol (mg/dl)	34.6±4.9	384.9±153.2*
Triglycerides (mg/dl)	7.9±1.1	16.6±4.6*
Fasting glucose (mg/dl)	136.5±6.0	122.0±18.6
Fasting insulin (μU/ml)	0.4±0.1	0.7±0.0*
HOMA-IR score	0.7±0.0	1.7±0.3*

*p≤0.05 vs. Lean. MetS: metabolic syndrome, LDL: Low-density lipoprotein, HOMA-IR: Homeostasis model assessment of insulin resistance

Methods Domestic pigs were fed a Lean or MetS diet (n=6 each) for 16 weeks. MSCs were collected from subcutaneous abdominal fat and their mitochondria analyzed using state-of-the-art Serial Block Face Electron Microscopy and 3D reconstruction. Mitochondrial function was assessed by cytochrome-c oxidase (COX)-IV activity, and expression of mitochondria-associated microRNAs (mitomiRs) by quantitative polymerase chain reaction (qPCR).

Results MetS pigs developed obesity, hypertension, insulin resistance, and hyperlipidemia (table 1). Mitochondrial density was similar between the groups, but mitochondrial volume and matrix density were lower in MetS-MSCs versus Lean-MSCs (figure 1A), as were COX-IV activity (figure 1B). Contrarily, expression of the mitomiRs miR15a, miR-137, and miR-181c, which target mitochondrial structural (e.g. TOMM20, TFAM, MINOS1) and functional proteins (e.g. UCP2, ATPAF1, MCUR1), was higher in MetS-MSCs compared to Lean-MSCs (figure 1C), suggesting a potential to modulate their expression.

Conclusions MetS damages MSC mitochondrial structure and function, and may modulate genes encoding for mitochondrial proteins. These observations support development of mitoprotective strategies to preserve the regenerative potency of MSCs and their suitability for autologous transplantation in patients with MetS.

A11 RIGHT VENTRICULAR DYSFUNCTION ON CARDIOVASCULAR MAGNETIC RESONANCE IMAGING IN CANCER SURVIVORS TREATED WITH ANTHRACYCLINE-BASED CHEMOTHERAPY

Andrew Hughes, Matthew Hooks, Stephanie Joppa, Kalpit Modi, Ko-Hsuan Amy Chen, Osama Okasha, Pratik S Velangi, Anne H Blaes, Chetan Shenoy. *University of Minnesota Medical School*

10.1136/jim-2020-MW.8

Introduction/Background Cancer survivors treated with anthracycline-based chemotherapy are at risk for long-term adverse cardiovascular outcomes. Clinical and imaging risk factors for these outcomes are unknown. Right ventricular (RV) systolic dysfunction has been described in small series to have prognostic relevance in these patients.

Objective(s) We aimed to determine the prevalence on cardiovascular magnetic resonance (CMR) of right ventricular (RV) systolic dysfunction, its determinants, and its influence on long-term adverse outcomes in a large cohort of cancer survivors treated with anthracycline-based chemotherapy.

Methods Consecutive cancer survivors treated with anthracycline-based chemotherapy who underwent clinical CMRs for known or suspected anthracycline-related cardiomyopathy were studied. The primary endpoint was a composite of death or major adverse cardiac events: aborted cardiac arrest, heart transplantation, left ventricular assist device implantation, or heart failure hospitalization.

Results Among 237 survivors who underwent CMR at a median of 3.0 years after cancer treatment, RV systolic dysfunction - defined as an RV ejection fraction (RVEF) <51% - was present in 57 (24.1%). Of these, 52 (91.2%) were in survivors with an abnormal left ventricular ejection fraction (LVEF), defined as <57%. On logistic regression analyses, factors associated with RV systolic dysfunction were dyslipidemia (odds ratio [OR] 0.53; 95% confidence interval (CI) 0.29–0.98; p=0.045), heart failure at the time of CMR (OR 2.47; 95% CI 1.31–4.63; p=0.005), and decreased LVEF (OR for every 1% decrease in LVEF 1.09; 1.05–1.11; p<0.001). At a median follow-up time after the CMR of 2.5 [interquartile range (IQR) 0.75, 5.1] years, 98 (41.4%) survivors reached the composite endpoint. On Kaplan-Meier analyses, an abnormal RVEF was associated with the composite endpoint compared with normal RVEF (log rank p<0.001). On Cox proportional hazards regression multivariable analyses, RVEF was independently associated with the composite endpoint (hazard ratio [HR] 1.02 for every 1% decrease; 95% CI 1.00–1.05; p=0.032) after adjustment for age, sex, body mass index at the time of CMR, time since cancer treatment, cumulative anthracycline dose, radiation therapy involving the chest, trastuzumab treatment, coronary artery disease at the time of CMR, heart failure at the time of CMR, and LVEF.

Conclusions In cancer survivors treated with anthracycline-based chemotherapy undergoing CMR for clinical indications, RV systolic dysfunction was independently associated with the long-term incidence of death or major adverse cardiac events.

A12 LEFT VENTRICULAR FUNCTION ASSESSMENT IN TWO INBRED MOUSE STRAINS FOLLOWING MYOCARDIAL INFARCTION

[1]Ayman Isbatan, [2]Aayushi Daji, [3]Ming Tang, [2]Haibin Li, [2]Maricela Castellon, [2]Zhigang Hong, [2]Sang Ging On, [2]Jalees Rehman, [2]Jiwang Chen. *[1]University of Illinois at Chicago, Oak Lawn, IL; [2]University of Illinois at Chicago; [3]Univesity of Illinois at Chicago, Chicago, IL*

10.1136/jim-2020-MW.9

Introduction/Background The mouse model of myocardial infarction (MI) has been widely used to study disease mechanisms and therapeutics. Different mouse strains with different ligation times have been traditionally used in cardiac infarct studies.

Objective(s) In this study, we aim to examine left ventricular function in two different mouse strains (C57BL6 and the immunodeficient NOD-SCID strain) using two injury modalities (30 min ischemia/reperfusion versus permanent coronary ligation).

Methods All the procedures were approved by the Ethics/Animal Care Committee of the University of Illinois at Chicago. Myocardial infraction (MI): Adult mice weighing 25–30 g were anesthetized and ventilated. A left thoracotomy was performed via the fourth intercostal space to expose the heart. The left anterior descending coronary artery (LAD) was identified and ligated. For 30 min ligation, the ligation was released after 30 minutes. In permanent ligation, the ligation was left intact. The lungs were inflated by increasing positive end-expiratory pressure and the thoracotomy site closed. Animals that had sham surgery underwent the same procedure with the exception of LAD ligation. The animals were observed and studied for six weeks post-surgery.

Echocardiography was performed with the VEVO2100 (VisualSonic Inc) using a 550Hz transducer.

Results Our data demonstrates that 30 min transient ligation to induce ischemia/reperfusion injury results in significantly lower ejection fraction (EF) and fraction shortening (FS)

values at Day 2 and Day 7 after MI surgeries in C57BL6, when compared to pre-MI baseline values. Similarly, left ventricular function was significantly decreased in C57BL6 mice following permanent ligation. In contrast, NOD-SCID mice did not demonstrate any significant difference of EF and FS values at 48 hrs after transient coronary ligation. Left ventricular function significantly decreased at Day 7 after the transient ligation MI in NOD-SCID mice. However, following permanent coronary ligation, left ventricular function significantly decreased as early as Day 2 in NOD-SCID mice.

Conclusions These data indicate that there is a rapid drop in left ventricular function within 48 hours of inducing myocardial infarction in C57BL6 mice, irrespective of whether the transient ligation or permanent ligation model is used. In immune deficient NOD-SCID mice, which are routinely used to assess the regenerative efficacy of transplanting human cells, only permanent ligation induces an early decrease in cardiac function. This could be due to the importance of intact immune mechanisms involved in the cardiac function decrease during ischemia reperfusion injury.

A13 A VARIED DATA SHAPE AND FIDELITY PROBING APPROACH FOR ASSESSING AUTOMATED DEEP NEURAL NETWORK-BASED CARDIAC MAGNETIC RESONANCE IMAGE SORTING PIPELINES

[1]Keigo Kawaji, [2]Tsubasa Maeda, [3]Daksh Chauhan, [4]Jacob Goes, [4]Blessing Obioma, [5]Marcella K Vaicik, [2]Satoshi Tamura, [3]Amit Patel. *[1]The University of Chicago/Illinois Institute of Technology, Chicago, IL; [2]Gifu University; [3]The University of Chicago; [4]Illinois Institute of Technology; [5]Illinois Institute of Technology, Chicago, IL*

10.1136/jim-2020-MW.10

Introduction/Background Artificial intelligence (AI)-based technologies based on highly parallelized computations and data-driven modeling known as convolutional or deep neural network (CNN, DNN) have recently emerged to rapidly complete what is typically manual and cumbersome clinical tasks. Such emerging methods thereby allow full and/or semi-automated clinical data processing, including anatomy/disease segmentation, image-based classification, and natural language processing of critical patient meta-data. However, for full clinical adaption of such technologies, challenges still remain due to the inherently opaque nature of such DNN-based tools, for which computer-trained bias is not only difficult to detect by the physician users, but is also non-trivial to safely design around by the software method developers. Accordingly, recent works by us and others have explored approaches that fully account for the presence of such biases in the employed training data, as well as human error introduced in the DNN design steps. Specifically, we have emphasized greater attention to the data shape and fidelity over the conventionally emphasized algorithmic design of newly developed AI-based tools, yielding preliminary works that employs mathematical techniques to even outperform the prepared error-embedded training data[1] (Suzuki *et al*. SCMR 2019) in terms of resultant data fidelity. In this work, we examine one such application in cardiac magnetic resonance (CMR) using a straightforward automated image classification task, and thereby propose an AI safeguard framework design and use case based on a physician's differential diagnosis thinking paradigm that dually achieves both: a) mechanistic uncovering of how AI algorithms can be interpreted by physicians, and b) systematically derive additional contexts of the black-box DNN via carefully prepared input data with shape/fidelity variations to probe system responses to these variations.

Objective(s) We demonstrate a specific use case of a generalizable AI safeguard systems framework that replicates a physician's differential diagnosis thinking cascade with the goals of providing additional context of such AI-based tools (which are otherwise opaque), and insights into where in the clinical post-processing cascade that it can most effectively be used. This is achieved through the joint and deliberate manipulation of data shape and fidelity of the handled input data to yield additional context of the DNN algorithm by means analogous to a physician's differential diagnosis cascade, and thereby delineating how we may probe such algorithms in intuitive ways for the assessing physicians.

Methods This specific work chose to further employ a recently examined DNN method based on VGG19 (known as Visual Geometric Group Network with 19 weighted layers[2]; Simonyan *et al*. ICLR 2015) in the design of this specific neural network for CMR image sorting by acquired imaging view[3] (Chauhan *et al*. SCMR 2020). In brief, this approach previously labeled the heart image orientations across four different chamber views (2-chamber, 3-chamber, 4-chamber, and short-axis) obtained from 50,000 cardiac MRI datasets with 99.1% accuracy (figure 1a; 30,000 for training, 10,000 for intermediate validation, and 8200 for final testing). For this specific study, two additional variant DNN models were further developed, benchmarked, and assessed for algorithm performance comparisons. The first variant (Referred as Method 2) was a tuned implementation[3] that generalized for input sizes without accounting for changes in the layer structure from our initial VGG19 approach (figure 1a), and the second variant (i.e. Method 3) was a custom VGG implementation that was developed in a fully independent manner from the baseline approach[3] and its Method 2 variant. This latter Method 3 network architecture incorporated a custom adjustment to the specific number of layers with respect to image input size, leading to fewer layers for smaller thumbnail images, while matching the neural network layer depth as[3] and that of Method 2 for the larger, native resolution images. Experiments were performed using varied input sizes and shapes corresponding to different locations in the clinical post-processing pipeline (e.g. the PACS system) where the DNN implementations can be implemented (figure 1b). The following two metrics were examined in this experiment set: a) Sample image resolution subsampling – varied from 100% (256 × 256), 50% (128 × 128), 25% (64 × 64), 12.5% (32 × 32), and 6.25% (16 × 16); and b) 90 degree rotations in three increments applied to the test dataset. Output accuracy, as well as compute performance benchmarks were examined in this study; computing hardware was performed on two Desktop systems with comparable hardware specifications to that of our cardiologist's clinical workstation at our site. These specifications were: GeForce RTX 2080 TI GPU with 11GB, and a 32/64GB CPU RAM that met sufficient memory requirements for all DNN training for this study.

Results Table 1 summarizes our experiments. We note here that Method 1 (i.e. baseline approach from[3]) was not inherently designed to accommodate the specific input data shape variations as described in this study.

In Experiment a) i.e. spatial resolution adjustment, we observe the extent of the developed DNN algorithm's sensitivity to the finer details at native resolutions, versus to the bulk structural shape at lower image resolutions. The VGG19 variant algorithm (Method 2) yielded gradually lower accuracy from 99.5% (at native 256 × 256) to 97.4% (at 16 × 16) as the input image size was reduced from 256 × 256 to 16 × 16 (table elements in Blue). We additionally note obtaining equivalent performance between 64 × 64 and 32 × 32 (in purple), which may be due to our VGG19 algorithm's design, which required an embedded image interpolation steps for reading in image resolutions below 64 × 64.

On the other hand, Method 3 yielded a consistently high accuracy (in green) across all examined resolutions (~99–99.9%); this can be interpreted as follows: a relatively high and consistent performance across both high and lower resolutions suggests that the gross shape of the heart and vasculature preserved across the lower resolutions contain sufficient information for highly accurate classification without absolute reliance to the finer details only exhibited in the native/high resolution images.

In Experiment b) (i.e. rotations) we note that the 256 × 256 input yielded notably lower accuracy (in orange, ~70%) when compared to assessments at lower spatial resolutions (in yellow; ~99%); we thus observe that subsampled images with deliberate information loss may in fact outperform DNN methods trained at native resolution images. This is consistent with observations by others that also report improved performance gained via deliberate use of low-resolution images in DNN training[4 5] (Miyazaki *et al*. ACPR 2015; Chou *et al*. NeurIPS 2018).

The gained insights from Experiments a) and b) further suggest that: while a single DNN may suggest insights on what image-based features may be necessary for machines to train what humans/physicians do (i.e. image classification based on chamber view orientation in this context), a *combination* of algorithm tests using varied input data shape can yield key observations that allow the users to better understand what each DNN method may potentially weigh favorably in its decision-making.

Lastly, for the DNN training computation time benchmarking, we note significant improvements in total training time (13–25 folds) by employing the Method 3 approach (in sec-

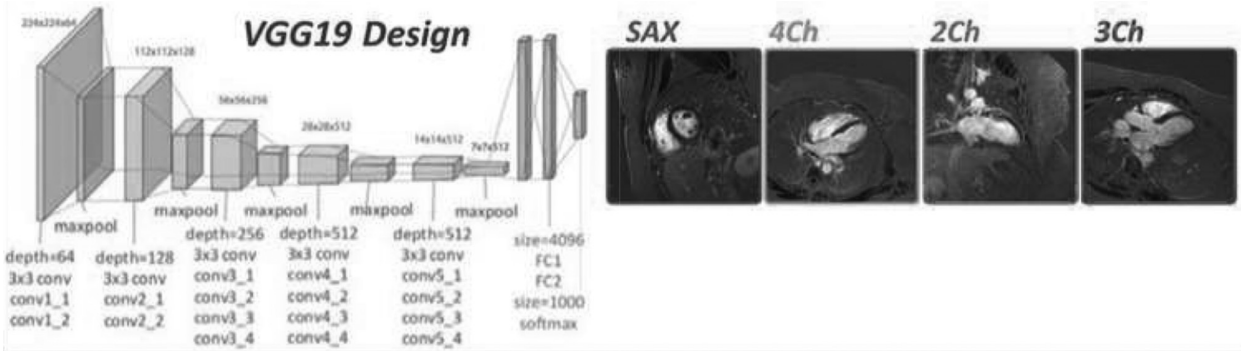

Abstract A13 Figure 1a VGG19 classifier (Chauhan *et al*. SCMR 2020 [3]) to sort four cardiac MR chamber views

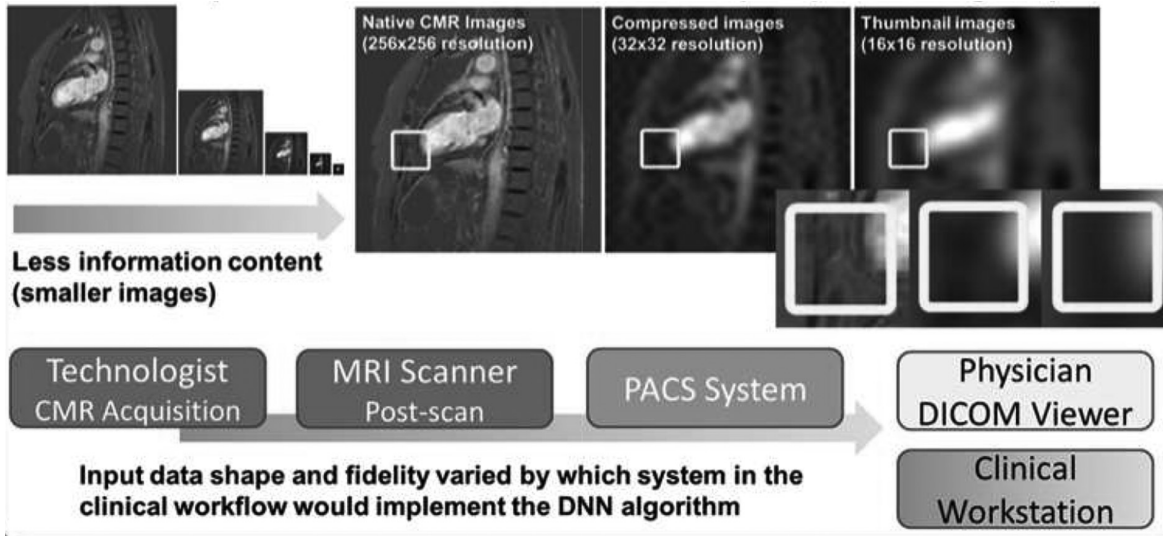

Abstract A13 Figure 1b Image size/resolution (from Native to Thumbnails) better suited for implementation at different clinical postprocessing steps

Abstract A13 Table 1a Experiment results on algorithm performance across baseline and two variants

Two DNN Variants Accuracy Experiments (out of 8193 examined images in test dataset)						
Experiment a) Accuracy in presence of variations in Input Resolution	256x256	128x128	64x64	32x32	16x16	224x224*
Baseline (fixed 224x224 input size)	--	--	--	--	--	99.1%
Variant from Baseline (Method 2)	99.51%	98.12%	97.69%	97.69%	97.40%	
Proposed Variant (Method 3)	99.93%	98.87%	99.86%	99.34%	99.25%	
Experiment b) Accuracy in presence of image rotations with Proposed Variant	70.28%	98.63%	99.85%	99.41%	99.08%	

Abstract A13 Table 1b Experiment results on training performance benchmarks

Training Performance Benchmarks (across 30603 training datasets)						
Variant from Baseline (Method 2)	5.5 h	1.7 h	47 min	45 min	40 min	
Proposed Variant (Method 3)	845 s	507 s	209 s	107 s	111 s	
Benchmark Ratio of Training Time (Baseline Variant vs Proposed Variant)	23.4	12.7	13.5	25.2	20.6	

onds-minutes) over Method 2 (in minutes-hours); where highly accurate DNN algorithm preparation can be easily achieved in non-time-critical cascade steps including background tasks.

This further suggests the feasibility of employing this algorithm (and its routine systems re-training) for completing the CMR image classification task using both low-resolution thumbnail files (e.g. 64 × 64 yielded best trade-off between performance and training speed) as opposed to upstream with native resolution files, which would be computationally more involved and therefore both resource and time-consuming. We further note here that the combination of these alternate DNN algorithms can be jointly run to yield a confidence score beyond that of a single binary classifier (i.e. 0 or 1) from use of a single DNN method alone.

Conclusion This study successfully demonstrated the specific use case of extracting clinically relevant context to both physicians who utilize emerging AI-based tools, and to clinical software architects who deploy these within the clinical infrastructure. More specifically, the full process from data shape/fidelity manipulation to the systematic characterization assessment approach that is accessible to physician users was clearly shown in this CMR image sorting task. Of note, this specific work demonstrates one example of how input data shape/fidelity may give both physician users and clinical systems administrators further insights into means of probing DNN methods, and better position its implementation within the clinical computing workflow (e.g. scanner vs PACS system server vs physician workstation). One example is to support CMR technologist upstream in rapid and correct planning during patient scan acquisition. Future works include systems integration for prospective use across the full clinical workflow.

Acknowledgements This work was supported by the following grants: NIH K25 Award (Kawaji K25 HL141634), AHA AIREA Research and Education Award (Vaicik AIREA34450209), and 2020 ITM Pilot Award (Patel CTSA UL1 TR002389).

REFERENCES

1. Suzuki Y, *et al*. A deep-neural-network-based signal invariance approach to overcome unresolved cardiac MR artifacts exhibited in training data. SCMR 2019.
2. Simonyan K, *et al*. Very deep convolutional networks for large-scale image recognition. ICLR 2015.
3. Chauhan D, *et al*. Artificial intelligence techniques for automatic classification of cardiac magnetic resonance images: is deep learning necessary? SCMR 2020.
4. Miyazaki N, *et al*. Privacy-conscious human detection using low-resolution video. ACPR 2015.
5. Chou E, *et al*. Privacy-preserving action recognition for smart hospitals using low-resolution depth images. arXiv: Computer Vision and Pattern Recognition 2018.

A15 CLINICAL FAK/PYK2 INHIBITOR PROTECTS CARDIOMYOCYTES FROM ROS OVERPRODUCTION AND APOPTOTIC CELL DEATH UNDER ADRENERGIC STIMULATION

[1]Jin O-Uchi, [2]Bong Sook Jhun. [1]*University of Minnesota, Minneapolis, MN*; [2]*University of Minnesota*

10.1136/jim-2020-MW.11

Introduction/Background Mitochondrial Ca^{2+} ($mtCa^{2+}$) overload is associated with reactive oxygen species (ROS) generation, cardiomyocyte apoptosis, and cardiac dysfunction under the pathological condition such as myocardial infarction and heart failure. We previously showed that stimulation of G_q-protein coupled a_1-adrenoceptor (a_1-AR), concomitantly promotes 1) activation of a Ca^{2+}- and ROS-dependent protein tyrosine kinase, proline-rich tyrosine kinase 2 (Pyk2) in the mitochondrial matrix, 2) increased tyrosine phosphorylation of a pore forming subunit of a main $mtCa^{2+}$-uptake channel MCU, and 3) $mtCa^{2+}$ overload in the cardiomyocytes. The focal adhesion kinase (FAK) family, including Pyk2 and FAK, are overexpressed during various cancers, and are potent therapeutic targets for cancer treatment. Currently several selective FAK/Pyk2 inhibitors including PF-431396 are in clinical trials in clinical trials in Europe. Although, Pyk2 is also highly overexpressed and significantly activated in the

cardiac tissues from during human heart failure patients, pathological role of Pyk2 in cardiac dysfunction has not been well studied.

Objective(s) Pyk2 inhibition by a FAK/PyK2 inhibitor which is already approved for a clinical trial in cancer treatment provides strong antioxidative, and anti-apoptotic (pro-survival) in the cardiomyocytes under stress conditions.

Methods Rat cardiac myoblasts (H9c2 cells), primary neonatal and adult rat cardiomycoytes were used for the experiments. The $mtCa^{2+}$ and mitochondrial ROS were measured using mitochondrial matrix-targeted Ca^{2+}-biosensor and mitochondrial ROS-sensitive dye MitoSOX, respectively. Mitochondrial permeability transition pore (mPTP) activity was observed by measuring the amount of cytochrome c in cytosol by Western blotting or by monitoring the release of GFP-tagged mitochondrial protein, Smac-GFP using confocal microscopy.

Results Stimulation by an a_1-AR agonist phenylephrine activated mitochondrial Pyk2 and enhanced $mtCa^{2+}$ uptake via MCU phosphorylation, followed by increased mitochondrial ROS and mPTP opening. These effects were abolished by co-expression of kinase-dead Pyk2 or pretreatment of a potent FAK/Pyk2 inhibitor PF, suggesting that Pyk2-dependent MCU activation followed by $mtCa^{2+}$ overload are critical for this mechanism. Frthermore, pretreatment of PF-431396 inhibited the apoptotic cell signaling activation and increase of apoptotic cell death induced by persistent a_1-AR stimulation in the primary cardiomyocytes.

Conclusion Inhibition of the Pyk2-mediated MCU activation a clinical FAK/Pyk2 inhibitor is capable of protecting cardiomyocytes from the mROS overproduction and cell death under persistent adrenergic stimulation. Thus, Pyk2 may become a novel potent therapeutic target for preventing cardiac cell injury and death during heart failure.

A16 ANTI-MARINOBUFAGENIN ANTIBODY ATTENUATES THE PREECLAMPSIA SYNDROME IN DOCA MODEL OF PREECLAMPSIA

[1]Ahmed F Pantho, [1]Syeda H Afroze, [2]James Larrick, [3]Vikram Sharma, [3]Bo Yu, [3]John Wages, [3]Andrew Mendelson, [1]Thomas J Kuehl, [4]David C Zawieja, [5]M Nasir Uddin. *[1]Orion Institute for Translational Medicine, Temple, TX; [2]Panorama Research, Inc., CA; [3]Panorama Research, Inc; [4]Texas A&M University College of Medicine; [5]Texas A&M University College of Medicine, Orion Institute for Transnational Medicine, Emergent Biotechnologies*

10.1136/jim-2020-MW.12

Introduction/Background A substantial body of data supports the hypothesis that increased circulating marinobufagenin (MBG) is a key factor in the pathogenesis of preeclampsia (PE) (Puschett, 2010b). Plasma MBG is elevated in PE relative to uncomplicated pregnancy (Lopatin, 1999; Averina, 2006; Agunanne, 2011). In a rat model of PE, a rise in MBG levels precedes hypertension (Vu, 2005), and MBG alone can produce hypertension, proteinuria, and fetal abnormalities in a rat model, suggesting that MBG is at least a potential biomarker of the later development of PE and possibly a pathogenetic factor (Puschett, 2008). Digibind, a polyclonal, anti-digoxin Fab with some cross-reactivity to MBG, reverses the PE syndrome in a rat model, alleviates inhibition of Na^+/K^+ ATPase by MBG, and normalizes blood pressure in PE patients (Adair, 2009ab). These studies validate MBG as a therapeutic target. Our collaborators at Panorama Research have identified high-affinity anti-MBG human monoclonal antibodies (humAbs) both from a phagemid library and by humanization of a murine antibody (3E9; Fedorova, 2008). We have demonstrated their effects on angiogenic factors in a cytotrophoblast cell model (Uddin, 2008ab, 2009ab, 2010; Ehrig, 2014; Afroze, 2016; Pantho, 2016). Data from animal models demonstrate an early role for MBG in the development of PE. Considering the 40–50% gain in extracellular fluid (ECF) volume during pregnancy, and data indicating that volume expansion triggers MBG secretion, Puschett and colleagues developed a model of PE in the pregnant rat (Ianosi-Irimie, 2005). Replacement of drinking water with saline, together with injections of the aldosterone precursor desoxycorticosterone acetate (DOCA), result in a syndrome with many of the phenotypic characteristics of human PE: hypertension, proteinuria, intrauterine growth restriction, excessive weight gain, and increased urinary excretion of MBG. In addition, the diameters of decidual blood vessels of PE animals are narrower than those from normal pregnant animals. Perfusion with an MBG solution caused a further constriction of 36%, whereas the vessels from normal pregnant animals did not respond to MBG. These observations indicate sensitization of the arterioles to MBG in this PE model. Antibodies to MBG resolved the hypertension (Vu, 2005). Federova *et al.*, have reported similar data in which a monoclonal antibody to MBG lowered blood pressure in pregnant rats rendered hypertensive by treatment with high salt diets (Federova, 2005; Federova, 2008). Resibufogenin, an MBG antagonist, when given early in pregnancy, prevented development of the phenotypic characteristics of PE in this rat model (Horvat, 2010). In a rat model of PE, a rise in MBG (but not endogenous ouabain) levels precedes the development of hypertension (Vu, 2005). Notably, administration of MBG in normal pregnant rats caused an elevation in blood pressure equivalent to the rise in DOCA- and saline-treated pregnant rats (Vu, 2005).

Objective(s) In this study, we evaluated the anti-MBG human monoclonal antibody (humAb) from Panorama in the DOCA rat model of PE.

Methods The DOCA model is a volume-expansion model of PE in pregnant rats first described by Puschett and colleagues (Vu, 2005; Puschett, 2010b), in which substitution of saline for normal drinking water and injection of deoxycorticosterone acetate (DOCA) induces volume expansion and elevated plasma and urine MBG levels, and results in a syndrome with many of the phenotypic characteristics of human PE: hypertension, proteinuria, and intrauterine growth restriction (IUGR) (reduced pup number and litter weight) (Vu, 2005; Ianosi-Irimie, 2005; Horvat, 2010). Female Sprague-Dawley rats (200–250 g, Charles River Laboratories; Wilmington, MA, USA) were acclimatized for 1 week, and mated with male Sprague-Dawley rats (275–300 g). Pregnancy was confirmed by the presence of vaginal plugs or by examination of vaginal smears. Each rat was housed separately. Five groups of rats were studied (n=10 per group): Group 1 (NP): normal pregnant rats; Group 2 (PDS): pregnant rats injected i.p. initially with 12.5 mg of DOCA in a depot form, followed by a weekly i.p. injection of 6.5 mg of DOCA, and whose drinking water is replaced with 0.9% saline; Group 3 (NPM): Normal pregnant rats given daily injections of MBG (7.65 μg/kg/day) once pregnancy was established on day four of the experiment; Group 4 (PDS-3E9): rats administered DOCA and saline as for Group 2, and also given the murine anti-MBG antibody

3E9 (2.2 mg/kg/day) on GD16, GD17, and GD18; and Group 5 (PDS-H3L2): rats administered DOCA and saline as for Group 2, and also given the humanized anti-MBG antibody H3L2 (2.2 mg/kg/day) on GD16, GD17, and GD18. Systolic blood pressure (BP) was measured by tail-cuff (IITC Inc., Life Science Instruments, Model 59) at GD17–19. For each BP value reported, 3 to 4 readings were performed, and the mean and standard deviation of these values were calculated. Measurements were obtained at the baseline (initial) time point and at the time of sacrifice. The reported BP values are the mean of the daily measurements. At 18–20 days of pregnancy, 24-hour urine was collected in the absence of food to avoid contamination of the urine by any fallen food particles. Each rat was housed separately in a metabolic cage during this portion of the study. The 24-hour protein excretion was measured and was normalized to creatinine. The rats were sacrificed after the last measurement on GD18–20, and blood samples were taken. The number of pups and any developmental or histological abnormalities in the pups were assessed. Statistical analysis was performed using analysis of variance and Tukey's post hoc test. A p value ≤ 0.05 was considered statistically significant. The Baylor Scott & White/TAMU IACUC Federal wide assurance no. is FWA00003358 and registration no IACUC00000706. The Texas A&M IBC permit no. is IBC2016–016 (Project ID: 110500).

Results Table 1. Anti-MBG normalizes preeclampsia symptoms in a rat model. Groups Blood Pressure-Initial (mm Hg) * Blood Pressure-Final (mm Hg) * Urine Protein (mg/24h) ** No. Pups% Malformed Pups NP 103 + 5 98 + 7 2.8 + 1.1 14 + 1.8 0 PDS 101 + 8 141 + 9 # 5.7 + 1.6 # 10.2 + 1.5# 16 # NPM 104 + 4 137 + 5 # 6.4 + 1.8 # 9.5 + 1.3 # 18 # PDS-3E9 102 + 8 100.8 + 8 3.1 + 0.9 13.6 + 2.1 0 PDS-H3L2 104 + 5 109.4 + 11 3.5 + 0.7 12.9 + 3.2 0 NP: normal pregnant PDS: NP + saline drinking water (DOCA model of PE) NPM: NP + MBG (Normal pregnant rats given daily injections of MBG (7.65 μg/kg/d) once pregnancy was established on day four of the experiment.) PDS-3E9: PDS + anti-MBG murine antibody (PDS rats injected i.p. with anti-MBG antibody 3E9, 2.2 mg/kg/d; on GD16, GD17, and GD18.) PDS-H3L2: PDS + anti-MBG humanized antibody (PDS rats injected i.p. with anti-MBG antibody H3L2, 2.2 mg/kg/d; on GD16, GD17, and GD18.) N=10 for all treatment groups. PDS-MAB: PDS rats receiving either anti-MBG antibody. The final (GD17-GD19 of gestation) BP of PDS and NPM rats was higher compared to initial BP. However, there was no BP change in NP and PDS-MAB rats. The 24h urinary protein was significantly higher in PDS and NPM rats compared to NP and PDS-MAB. Number of pups decreased in PDS and NPM rats. The percentage of malformed pups was higher in PDS and NPM rats; there were no malformed pups in NP or PDS-MAB rats (# $p<0.05$). Either administration of exogenous MBG or saline drinking water results in significant increases in blood pressure (BP) and urinary protein, together with a reduction in litter size and an increase in malformed pups. Anti-MBG antibody rescues the normal phenotype in pregnant rats on saline water. * Blood pressure measured by tail cuff. ** Urine protein normalized to creatinine.

Conclusion DOCA and saline treatment increased blood pressure and resulted in proteinuria, an overall reduction in litter size, and fetal malformations in pregnant rats.The administration of MBG alone had similar effects, as previously reported (Vu, 2005). Anti-MBG murine antibody 3E9 prevented this increase in blood pressure, proteinuria, and fetal malformations. Humanized anti-MBG antibody H3L2 produced a similar effect as the parent murine antibody 3E9. Baseline (initial) blood pressure and urine protein were not significantly different among treatment groups. Animals treated with DOCA and saline (NPS) showed statistically significant increases in blood pressure over control pregnant animals (NP) ($p<0.05$). Animals treated with DOCA and saline (NPS) showed statistically significant increases in proteinuria over control pregnant animals (NP) ($p<0.05$). Animals treated with DOCA and saline (NPS) showed statistically significant increases in both number of pups and the percentage of malformed pups over control pregnant animals (NP) ($p<0.05$). Animals treated with MBG (NPM) showed statistically significant increases in blood pressure over control pregnant animals (NP) ($p<0.05$). Animals treated with MBG (NPM) showed statistically significant increases in proteinuria over control pregnant animals (NP) ($p<0.05$). Animals treated with MBG (NPM) showed statistically significant increases in both number of pups and the percentage of malformed pups over control pregnant animals (NP) ($p<0.05$). Animals treated with anti-MBG murine antibody 3E9 (Panorama) did not show a statistically significant increase in blood pressure or proteinuria or any decreased litter size or malformed pups relative to control DOCA-saline-treated animals (PDS). Animals treated with anti-MBG human antibody H3L2 (Panorama) did not show a statistically significant increase in blood pressure or proteinuria or any decreased litter size or malformed pups relative to control DOCA-saline-treated animals (PDS).

A18 TRANSCATHETER AORTIC VALVE REPLACEMENT IN NATIVE PURE AORTIC REGURGITATION: PERIPROCEDURAL AND 30-DAYS OUTCOMES

[1]Shilpkumar Arora, [2]Sopan Lahewala, [3]Samarthkumar Thakkar, [4]Chinmay Jani, [5]Harsh P Patel, [6]Aanandita Singh, [7]Sidakpal S Panaich, [8]Brian D Hoit. *[1]Harrington Heart and Vascular Institute/University Hospitals Cleveland Medical Center/Case western Reserve University,Cleveland,OH; [2]Saint Francis Hospital and Medical center,CT,USA; [3]Rochester General Hospital, NY; [4]Mount Auburn Hospital, Boston; [5]Louis A Weiss Memorial Hospital, Chicago,IL,USA, Chicago, IL; [6]Sri Guru Ram Das institute of Medical Sciences and research, Punjab, India; [7]University of Iowa, Iowa; [8]Harrington Heart and Vascular Institute/University Hospitals Cleveland Medical Center/Case Western Reserve University, Cleveland, OH*

10.1136/jim-2020-MW.13

Introduction/Background Although patients with severe aortic regurgitation (AR) with reduced systolic function have an annual mortality rate of 20%, only 5% of these patients are offered surgical repair. Transcatheter aortic valve replacement (TAVR) may be an effective option for these high-risk patients, although European and Asian experiences of TAVR for NPAR (Native Pure Aortic Regurgitation) are published in the past 6 years. The American experience is still lacking.

Objective(s) To explore the american experience of TAVR in patients with NPAR.

Methods The study cohorts were derived from HCUP's Nationwide Readmissions Database (NRD) and Nationwide inpatient Sample (NIS) 2016. TAVR and NPAR were identified using appropriate ICD-10-CM codes. Patients with aortic stenosis, missing data (age, gender, and mortality) were excluded. A composite of outcomes stated in the figure 1 was a primary outcome. Individual components of the primary outcome were evaluated as secondary outcomes. Predictors

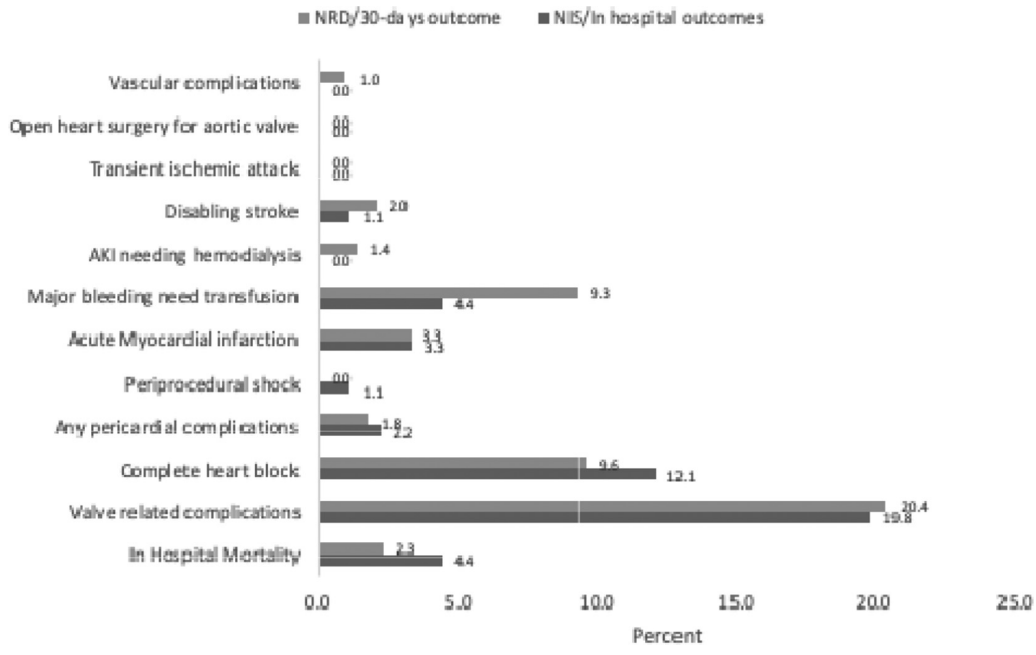

Abstract A18 Figure 1 Complications associated with TAVR in NPAR

included all routine clinical, demographic and hospital-level variables. Multivariate logistic regression models were used to evaluate study outcomes.

Results In total, 353 patients from the NRD (male-68.0%, age³65–79.7%) and 455 patients from the NIS (male-68.1%, age³65–84.7%) underwent TAVR for native pure AR (NPAR). Hypertension (85–88%), CAD (66–71%) and Atrial Fibrillation (42–45%) were the most common comorbidities. The median LOS in both databases was 4 days; 30-day mortality was 2.3% in NRD, while in-hospital mortality was 4.4% in NIS. Valve-related complications occurred in ~ 20% for both NIS and NRD, with a paravalvular leak (5.5–8%) being most common. Other complications are listed in the figure 1. No patient from either cohort required open-heart surgery. Predictors of the primary outcome were peripheral vascular disease (PVD) and anemia. Predictors of increased valvular complications over 30-days were age, chronic obstructive lung disease, and anemia, while the history of PVD was a significant predictor of increased complete heart block over 30-days.

Conclusions With technical advancements and increased operator expertise, TAVR is a promising primary treatment for patients with NPAR; expansion of TAVR utilization in patients with NPAR warrant further study.

A19 TRANSCRIPT VARIANT OF MCU PROTECTS MITOCHONDRIA FROM CA^{2+} OVERLOAD AND ROS OVERPRODUCTION IN CARDIAC MYOCYTES

[1]Iuliia Polina, [2]Jyotsna Mishra, [3]An Xie, [3]Neeta Adhikari, [3]Bong Sook Jhun, [3]Samuel Dudley, [1]Jin O-Uchi. [1]*University of Minnesota, Minneapolis, MN*; [2]*Medical College of Wisconsin*; [3]*University of Minnesota*

10.1136/jim-2020-MW.14

Introduction/Background Recent clinical and basic studies suggest that mitochondrial dysfunction caused by excessive mitochondrial Ca^{2+} ($mtCa^{2+}$) uptake is one of the major determinants for the development of life-threatening human diseases associated with apoptotic cell death, such as heart failure (HF) and neurodegenerative diseases. The $mtCa^{2+}$ uptake is mainly regulated by mitochondrial calcium uniporter (MCU) encoded by CCDC109A gene. The MCU channel function is likely to be hyperactivated under pathological conditions, leading to decreased ATP production, overproduction of reactive oxygen species (ROS), and apoptotic signaling activation. However, to date, there have been no clinical trials designed to combat $mtCa^{2+}$ overload via MCU, possibly, due to the lack of potent and specific pharmacological and genetic tools, which can directly inhibit MCU function. In addition to originally reported MCU (renamed as longest variant of MCU: MCU-L), we recently found that CCDC109A gene produces a transcript variant shorter than MCU-L (named short-form MCU: MCU-S) that lacks the mitochondria-targeted sequence (MTS) at N-terminal. However, the biological function of MCU-S is completely unknown.

Objective(s) To determine whether novel MCU variant MCU-S can use as a therapeutic tool for protecting the cardiac myocytes from apoptotic cell death under stress condition.

Methods Biochemical (cell surface protein biotinylation and mitochondrial fractionation), cell biological (live cell imaging of GFP-tagged MCU-L and -S), and physiological assays (live cell Ca^{2+} imaging and whole cell patch-clamp) were applied to HEK293T cells and primary cardiomyocytes isolated from 1–2 day old neonatal rat hearts in ordered to assess MCU-S expression and function.

Results We found that MCU-S maintains a similar channel structure with MCU-L, despite of lacking MTS at N-terminal. Indeed, we confirmed that MCU-S is preferentially expressed in the plasma membrane (PM), and forms Ca^{2+}-permeable channels on the PM in HEK293T cells. Importantly, we also found that overexpression of MCU-S significantly blocks $mtCa^{2+}$uptake by inhibiting the MCU-L trafficking into mitochondria in both HEK293T cell and primary cardiomyocytes.

Finally, using primary cardiomyocytes, we found that overexpression of MCU-S significantly inhibits mCa^{2+} overload, ROS overproduction and activation of apoptotic signaling in primary cardiomyocytes under cytosolic Ca^{2+} elevation induced by G_q protein-coupled receptor stimulation compared to the GFP overexpression as a control.

Conclusions These results indicate that strategy of increased MCU transcript variant (i.e., MCU-S) provides strong antioxidative and anti-apoptotic effects by decreased number of mitochondrial MCU channels via inhibition of MCU-L trafficking into mitochondria. Further study of the splicing machinery for CCDC109A opens a possibility to develop new therapies for of various life-threatening human diseases associated mitochondrial dysfunction and apoptosis including heart failure.

A20 MYOCARDIAL DAMAGE ASSESSED BY LATE GADOLINIUM ENHANCEMENT ON CARDIOVASCULAR MAGNETIC RESONANCE IMAGING IN CANCER PATIENTS TREATED WITH ANTHRACYCLINES AND/OR TRASTUZUMAB

[1]Chetan Shenoy, [1]Kalpit Modi, [1]Stephanie Joppa, [1]Ko-Hsuan Chen, [1]Osama Okasha, [1]Pratik S Velangi, [1]Matthew Hooks, [2]Prabhjot Nijjar, [1]Anne H Blaes, [3]Afshin Farzaneh-Far, [2]Mehmet Akcakaya. *[1]University of Minnesota Medical School; [2]University of Minnesota; [3]University of Illinois*

10.1136/jim-2020-MW.15

Introduction/Background In cancer patients treated with anthracyclines and/or trastuzumab, available data on the prevalence of late gadolinium enhancement (LGE) on cardiovascular magnetic resonance (CMR) are conflicting and range from 0% to 100%. The patterns of LGE are poorly described.

Objective(s) We aimed to investigate the prevalence and the patterns of LGE in a large cohort of consecutive cancer patients treated with anthracyclines and/or trastuzumab.

Methods We studied 298 patients in whom the most prevalent cancers were breast cancer, lymphoma, and leukemia. We analyzed the prevalence, patterns, and correlates of LGE, and identified their causes.

Results Overall, 31 (10.4%) patients had LGE. The prevalence of LGE did not differ between patients who received anthracyclines only and those who received trastuzumab only (11.3% vs. 17.7%; p=0.43). An ischemic pattern LGE was seen in 20 (6.7%) and non-ischemic pattern LGE was seen in 11 (3.7%) patients. Among the 11 patients with non-ischemic LGE, 3 were attributed to myocarditis, 2 to cardiac sarcoidosis, 1 to acute myocardial calcification, 1 to lymphoma infiltration of the LV, and 4 could not be attributed to a specific cause.

Conclusions LGE was present in 10% of cancer patients treated with anthracyclines and/or trastuzumab who had clinical CMRs. The most common cause was myocardial infarction. Most cases of non-ischemic LGE were attributable to causes unrelated to the cancer treatments, demonstrating that cardiomyopathy associated with anthracyclines and/or trastuzumab is not associated with LGE. CMR imaging could be used to reliably identify the cause of cardiomyopathy and guide disease-specific management in these patients.

A21 SINGING IMPROVES VASCULAR FUNCTION ACUTELY

[1]Kamila Somayaji, [2]Morgan Frenkel, [3]Tanya Ruck, [4]Luai Tabaza, [5]Michael Widlansky, [5]Jacquelyn Kulinski. *[1]Medical College of Wisconsin; [2]MCW; [3]University of Wisconsin-Milwaukee; [4]Albert Einstein- Philadelphia; [5]MCWAH*

10.1136/jim-2020-MW.16

Introduction/Background Cardiac rehabilitation participation after a cardiovascular event improves health outcomes, including reductions in cardiac events, cardiovascular and all-cause mortality, hospitalizations, and symptoms. Older adults are less likely to be referred for cardiac rehabilitation and are also less likely to participate even when referred. Limited mobility and/or difficulty with physical exercise contribute to low participation rates. This unveils the need to incorporate beneficial, non-exercise interventions for secondary prevention in this population. Singing is a physical activity involving components of the vagal nerves manifested as changes in cardiac autonomic regulation. Unlike traditional exercise, the effects of singing on cardiovascular health have not been well-studied. To our knowledge, no studies have evaluated the impact of singing on endothelial function, an important marker of cardiovascular health and future cardiac risk.

Objective(s) The primary objective of this study was to assess the acute effects of singing on peripheral vascular endothelial function. The secondary objective was to measure cardiac hemodynamics before, during, and after a 10- minute period of singing.

Methods Fifty adults ≥18 years were recruited from our cardiology clinics to participate in a single, 90-minute study visit. Subjects with a permanent pacemaker or implantable cardioverter defibrillator (ICD) and known atrial arrhythmias were excluded. Vascular function was measured at the fingertips with pneumatic probes and a peripheral arterial tonometry (PAT) device. Heart rate variability (HRV) was measured with a chest strap sensor. While seated, subjects watched and sang to a 10-minute coaching video led by a voice expert. The video included a warm-up with vocal exercises and lyrics to the Star-Spangled Banner. PAT measurements were obtained before and after singing and expressed as reactive hyperemia index (RHI) and Framingham reactive hyperemia index (fRHI). Measures of HRV included root mean square of successive RR interval differences(RMSSD) and standard deviation of NN (or RR) intervals (SDNN).

Results Fifty subjects completed the study (68% female, mean age 60±13 years, mean BMI 33±8). There was a significant increase in fRHI (1.88±1.05 to 2.10±1.01, p=0.034) after singing with no significant change in the RHI (2.00±0.73 to 2.11±0.67, p=0.22). There was a significant decrease in HRV during singing (compared to baseline) (RMSSD: 44.9±39.0 to 35.2±31.7, p=0.009 and SDNN: 55.7±37.5 to 35.4±22.4, p=0.035). HRV measures trended back towards baseline in the post-singing (recovery) period.

Conclusions Following a brief singing intervention, there was a significant improvement in PAT-derived endothelial function that was more substantial in subjects with worse baseline endothelial function. Moreover, HRV decreased during singing, similar to what happens with traditional exercise. This may prove beneficial for patients who would benefit from cardiac rehabilitation yet have physical limitations to exercise. Future studies should focus on subjects with established coronary

disease (endothelial dysfunction) and explore additional mechanisms by which singing may impact cardiovascular health in both the short- and long-term.

A22 STIFFNESS OF AORTIC ARCH AND CAORTID ARTERY INCREASES IN HIGH FAT-FED APOE DEFICIENT MICE: EVIDENCE FROM ECHOCARDIOGRAPHY

[1]Ming Tang, [2]Liang Hong, [2]Haibin Li, [3]Wei Huang, [3]Jiwang Chen. *[1]Univesity of Illinois at Chicago, Chicago, IL; [2]Univesity of Illinois at Chicago; [3]The First Affiliated Hospital of Chongqing Medical University*

10.1136/jim-2020-MW.17

Introduction/Background Atherosclerosis is a chronic inflammatory disorder that is the underlying cause of most cardiovascular disease (CVD). ApoE-knockout (ApoE $^{-/-}$) mice after deposition of high-fat diet develop phenotypes similar to atherosclerosis. Arterial stiffness, the expression of reduced arterial elasticity, is an effective predictor of atherosclerosis. Measurement of pulse-wave velocity (PWV) is a gold-standard approach to study the arterial stiffness.
Objective(s) In this study, we aimed to use high-resolution ultrasound (echo) to measure stiffness of aortic arch and carotid arteries and heart functions in ApoE knockout mice and their WT siblings.
Methods Animals: A mouse model of atherosclerosis was used. Male Apoe deficient mice and C57Bl6 mice (7-week old) and wild type mice were fed with high fat and normal diets for over two months respectively. The atherosclerosis phenotypes will be further examined by oil red O and elastin staining. PWV measurement: The ascending and descending aortic peak velocities were measured from the pulse wave (PW) Doppler-mode aortic arch view. On the same image plane, the time (T1) was measured from the onset of the QRS complex to the onset of the ascending aortic Doppler waveform in the ascending aorta, while the time (T2) was measured from the onset of the QRS complex to the onset of the descending aortic Doppler waveform as distal as possible in the descending aorta. Pulse wave velocity (PWV) was obtained from the B-mode and Doppler-mode aortic arch view, calculated as PWV = aortic arch distance/[T2 - T1(cm/s)]. The similar method was used to measure carotid artery stiffness, calculated as PWV = carotid artery distance/[T4 – T3(cm/s)]. Left ventricular diastolic function was examined by measuring mitral inflow velocity and tissue Doppler in apical 4-chamber views; Left ventricular systolic function was obtained from parasternal long-axis views under M-mode; MV E velocity, E/A, E/e, IVRT, EF%, CO, SV and FS were calculated respectively.
Results Compared with WT group, PWV values in both aorta and carotid arteries of mice were significantly increased in ApoE $^{-/-}$ group, (aorta arch PWV: 469.15±201.51 cm/s vs. 170.67±87.88 cm/s; Carotid artery PWV: 496.87±263.90 cm/s vs. 193.18±103.36 cm/s, respectively; both $P<0.01$). In addition, left ventricular diastolic function according to E/A ratios and left ventricular ejection fraction values significantly decreased in ApoE $^{-/-}$ mice. This was consistent with the changes in PWV.
Conclusions Stiffness of aortic arch and carotid artery was significantly increased in ApoE-knockout mice fed with high-fat diet. All the evidences indicate that echocardiography could be a potential diagnostic strategy for early detection of atherosclerosis.

A23 BUPROPION IN THE TREATMENT OF POSTURAL TACHYCARDIA SYNDROME (POTS): A SINGLE CENTER EXPERIENCE

[1]Rohit Vyas, [2]Zeid Nesheiwat, [3]Rahul Vyas, [4]Mohammed Ruzieh, [4]Blair Grubb. *[1]University of Toledo, Toledo, OH; [2]The University of Toledo Medical Center, Maumee, OH; [3]Wayne State University; [4]n/a*

10.1136/jim-2020-MW.18

Introduction/Background Postural Tachycardia Syndrome (POTS) is estimated to impact millions of people each year. However, there is no established gold standard for its treatment. Bupropion is a norepinephrine and dopamine reuptake inhibitor and has been implicated as a potential treatment for POTS.
Objective(s) The objective of this study is to investigate bupropion and its utility in the treatment of POTS.
Methods Retrospective chart review was performed for 47 patients with POTS with a mean age of 42±13. Comorbidities and prior medications were documented and analyzed. Orthostatic vital signs along with symptoms were measured before and after Bupropion initiation. Statistical analysis was performed to evaluate for significant findings including reduced orthostasis and improvement of symptoms.
Results Bupropion was not associated with a statistically significant improvement in orthostatic vitals but there was an overall reduction in reported syncope.
Conclusions While the use of bupropion does not show a statistically significant impact on orthostatic vitals in POTS patients, it did show a degree of improvement in syncope and as such might be useful in patients with syncope-predominant POTS.

A24 PULMONARY VESSEL CASTING IN RODENT MODELS OF PULMONARY HYPERTENSION

[1]Yifan Wang, [2]Zhongkai Zhu, [2]Ayako Makino, [2]Richard Mishall, [2]Jiwang Chen. *[1]UIC College of Pharmacy, Chicago, IL; [2]University of Illinois at Chicago*

10.1136/jim-2020-MW.19

Introduction/Background Pulmonary hypertension (PH) is a severe and progressive disease characterized by sustained elevations in pulmonary artery (PA) pressure, defined as a mean pulmonary artery pressure (mPAP) ≥25 mmHg at rest, measured by right heart catheterization, leading to an elevation of increased pulmonary vascular resistance and right heart failure. Pulmonary vascular network structure and blood flow have been found to be different between patients with PH and healthy controls. Adventitial fibrosis, medial hypertrophy and intimal thickening contributes to the progression of pulmonary vascular remodeling (PVR). PVR is mainly due to small pulmonary arterial wall thickening and lumen occlusion. Plexiform lesions are a typical phenotype for several PH. Thus, high quality visualization and quantification of vascular changes in the development of experimental PH may aid the detection and understanding of disease pathogenesis. Many imaging techniques including computed tomography, vessel angiography and vessel casting have been developed to help visualizing pulmonary vascular network. Among these methods, the vessel casting is the simplest and most effective method to examine the angioarchitecture of normal and pathological tissues. Vascular casting precisely reflects the structure of blood

vessels and also allow observing the microangioarchitecture of capillaries that create the terminal ways of functional and nourishing blood circulation. For the rodent models of PH, acquisition of high-quality pulmonary vessel images and image analysis are still challengeable. Up to now, no reports show holistic pulmonary vasculature patterns in rat models of PH.

Objective(s) In this study, we have developed a simple reproducible procedure to image the whole pulmonary vasculature and quantify its change in mouse hypoxia mediated PH model, rat monocrotaline (MCT) model, and rat hypoxia sugen mediated PH model.

Methods All experiments were approved by the Ethics/Animal Care Committee of the University of Illinois at Chicago. Male Sprague Dawley® rats (200 g) were used in this study. In the MCT-induced PH model, one dose of MCT (60 mg/kg body weight) was subcutaneously injected to rats. Phenotypic characterization studies were performed 4 weeks after MCT injection. In the hypoxia+sugen PH model, one dose of Sugen (20 mg/kg body weight) was given subcutaneously at day 1 of

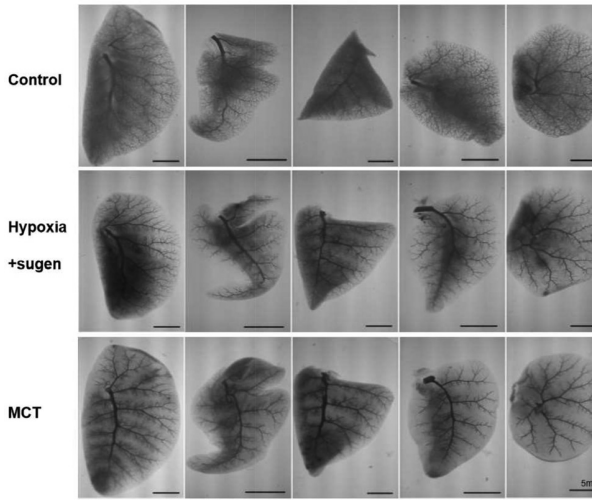

Abstract A24 Figure 1 Rats Models of PH
Representative holistic pulmonary vessel images of five pulmonary lobes in rat models of pulmonary hypertension

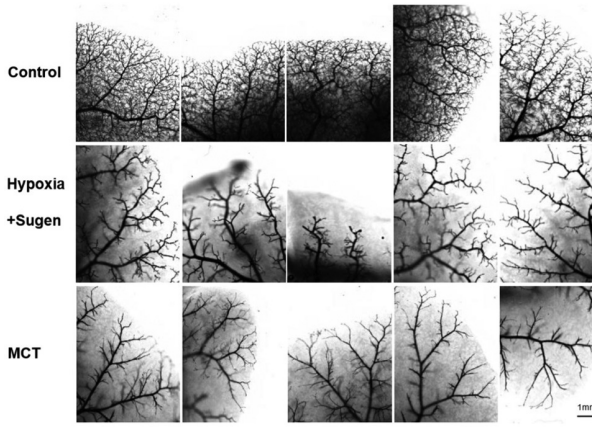

Abstract A24 Figure 2 Rats models of PH close up
Representative distal pulmonary vessel images and quantification of five pulmonary lobes in rat models of pulmonary hypertension

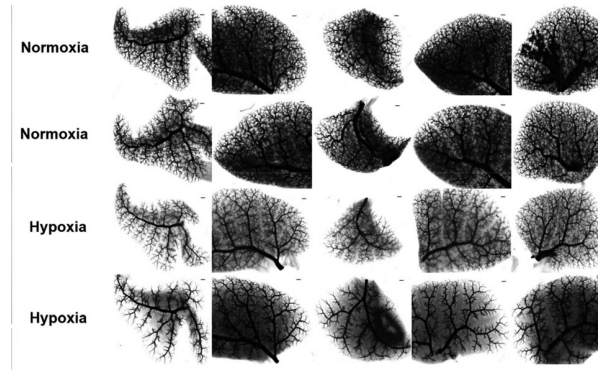

Abstract A24 Figure 3 Mouse Models of PH
Representative holistic pulmonary vessel images of five pulmonary lobes in a mouse model of hypoxia mediated pulmonary hypertension. Size bar: 300 μm

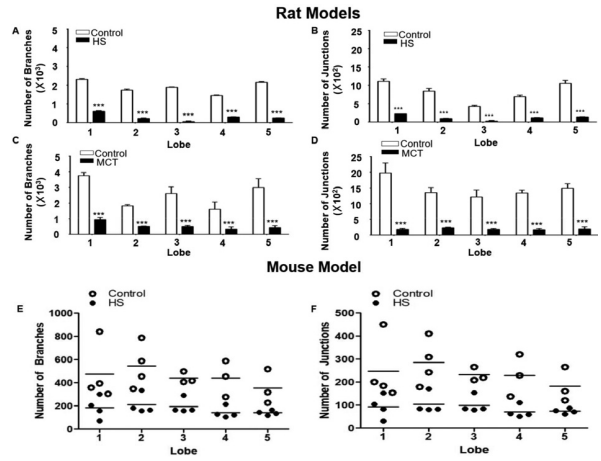

Abstract A24 Figure 4 Image quantification
Image quantification of five pulmonary lobes in rat models of pulmonary hypertension mediated by hypoxia sugen (HS) or monocrotaline and mouse model of pulmonary hypertension mediated by HS. MCT: monocrotaline group. N=3–6 in each group for panels A-F, ***, p<0.0001

hypoxia exposure (10% O2). After three-week chronic hypoxia exposure, the rats were placed back into room air. Phenotypic characterization studies were performed 4 weeks after reoxygenation. In mouse hypoxia mediated PH model, 8-week old male mice (C57BL6) were exposed to 10% O2 for 4 weeks. Heparin (1000 UI/kg) was injected IP 10 minutes before administration of ketamine and xylazine. After removal of the anterior chest wall from fully anesthetized rodents, the PA was perfused with saline. After the perfusion, Microfil polymer mixture (350 μl/300 g for rats and 100 μl/25 g for mouse) freshly made was infused to PA via the apex of the right ventricle under a dissecting microscope until it reached to the end branch of PA. At the end of the experiment, lungs and hearts were removed from the rats and transferred to saline solution. The organs were dehydrated using a series of ethanol solution (50%, 70%, 80%, 95%, and 100%), and then soaked with Methyl Salicylate solution. The translucent lungs were then photographed using a Stereo microscope (SKU: SM-7B-FRL, AMScope) with a camera (SKU: WF200, AMScope) and a transilluminator (TW-43 white light) for the

holistic view of each single lobe. A fluorescent microscope (BZ-X700, KEYENCE) was then used for end-branch views of each lobe. The end-branch pulmonary vessel images were quantified by Image J to calculate numbers of branches and junctions of pulmonary vessels.

Results The holistic views of pulmonary vessels and distal PA branches' image analysis we presented clearly show the significant decrease in branches and junctions of distal pulmonary arteries in the pulmonary hypertensive groups. The data well matches their mPAP values and number of occlusive pulmonary vessels in these rodent PH models.

Conclusions In conclusion, we are the first one to show holistic patterns of pulmonary vasculature in rat models of PH mediated MCT or mouse hypoxia sugen exposure. The distal pulmonary artery images clearly demonstrate pulmonary vascular remodeling in the rats with high mPAP and occlusive pulmonary vessels. The innovative protocol and image quantification we presented here are important for us to understand the vasculature with PH or other vascular diseases.

A25 ACTIVATION OF AUTOPHAGIC FLUX INDUCES MITOCHONDRIAL BIOGENESIS DURING CARDIAC ISCHEMIA/REPERFUSION INJURY

[1]Jing Yang, [2]Geoffrey Cho, [1]Lihao He, [1]Yuxin Chu, [1]Jin He, [1]scott Ballinger, [1]martin Young, [1]Sumanth Prabhu, [2]Joseph Hill, [3]Min Xie. *[1]University of Alabama at Birmingham; [2]UT Southwestern Medical Center; [3]University of Alabama at Birmingham, Birmingham, AL*

10.1136/jim-2020-MW.20

Introduction/Background Reperfusion injury accounts for ~50% of myocardial infarct size, and meaningful clinical therapies targeting this do not exist. We have shown that HDAC inhibition-enhanced cardiomyocyte autophagy, with concurrent PGC1α-mediated mitochondrial biogenesis, blunts ischemia/reperfusion (I/R) injury when intervention is imposed at the time of reperfusion.

Objective(s) However, as HDAC inhibition may have a pleiotropic effect, we set out to test whether augmentation of autophagy by a specific autophagy-inducing peptide, Tat-Beclin (TB), protects myocardium through maintenance of mitochondrial homeostasis.

Methods 8–12-week-old, wild-type, C57BL6 mice were randomized into three groups: vehicle control, exposed to a Tat-Scrambled (TS) peptide, or exposed a Tat-Beclin (TB) peptide. Each group was subjected to I/R surgery (45 min coronary ligation, 24h reperfusion). Infarct size, systolic function, and mitochondrial dynamics were assayed. Cultured neonatal rat ventricular myocytes (NRVMs) were exposed to TB during simulated I/R injury. ATG7 knockout (ATG7 KO) mice and ATG7 knockdown by siRNA in NRVMs were used to evaluate the role of autophagy.

Results TB treatment at reperfusion reduced infarct size by 20.1% (n=23, p<0.05) and improved systolic function (n=11, p<0.05). Improvement correlated with increased autophagic flux in the border zone with less oxidative stress. ATG7 KO mice did not manifest TB-promoted cardioprotection during I/R. TB increased mtDNA content in the border zone (n=10, p<0.05). In NRVMs subjected to I/R, TB reduced cell death by 41% (n=12, p<0.001), reduced I/R-induced reactive oxygen species (ROS) production I/R-induced mtDNA damage, and increased mtDNA content by ~50% (n=3, p<0.05). Moreover, TB promoted expression of the gene coding for PGC-1a which controls mitochondrial biogenesis, in the border zone (n=9, p=0.02) and NRVMs subjected to I/R (n=5, p<0.05), along with expression of the mitochondrial dynamics genes Drp1, Fis1, and MFN1/2 (n=9, p<0.05). Conversely, ATG7 knockdown in NRVMs and inducible cardiomyocyte-specific knockout of ATG7 abolished these beneficial effects of TB on mitochondria (n=5–8, P<0.05).TB treatment at reperfusion reduced infarct size by 20.1% (n=23, p<0.05) and improved systolic function (n=11, p<0.05). Improvement correlated with increased autophagic flux in the border zone with less oxidative stress. ATG7 KO mice did not manifest TB-promoted cardioprotection during I/R. TB increased mtDNA content in the border zone (n=10, p<0.05). In NRVMs subjected to I/R, TB reduced cell death by 41% (n=12, p<0.001), reduced I/R-induced reactive oxygen species (ROS) production I/R-induced mtDNA damage, and increased mtDNA content by ~50% (n=3, p<0.05). Moreover, TB promoted expression of the gene coding for PGC-1a, which controls mitochondrial biogenesis, in the border zone (n=9, p=0.02) and NRVMs subjected to I/R (n=5, p<0.05), along with expression of the mitochondrial dynamics genes Drp1, Fis1, and MFN1/2 (n=9, p<0.05). Conversely, ATG7 knockdown in NRVMs and inducible cardiomyocyte-specific knockout of ATG7 abolished these beneficial effects of TB on mitochondria (n=5–8, P<0.05).

Conclusions Autophagy is a sufficient and essential process to mitigate myocardial reperfusion injury through maintenance of mitochondrial homeostasis and partly through inducing PGC1α-mediated mitochondrial biogenesis. Augmentation of autophagic flux may emerge as a viable clinical therapy to reduce reperfusion injury in myocardial infarction.

Diagnosis or Treatment of a Disease Process or Clinical Syndromes

B18 APPROACH TO SEVERE PULMONARY STENOSIS FOLLOWING TETRALOGY OF FALLOT REPAIR

[1]Julien Feghaly, [2]James Ampadu, [3]Piotr Horbal, [4]Abdul Rahman Al Hout. *[1]St Louis University School of Medicine, St Louis, MO; [2]University of California San Diego School of Medicine; [3]St Louis University School of Medicine; [4]St Elizabeth Hospital*

10.1136/jim-2020-MW.21

Introduction/Background Tetralogy of Fallot (ToF) is the most common cyanotic congenital heart disease and continues to increase in prevalence. Treatments to relieve the pathognomonic right ventricular outflow tract (RVOT) obstruction have evolved and can be variable. With advancements in therapy for ToF, these patients continue to age into adulthood and degenerative valvular complications are inevitable.

Case Presentation A 29-year-old female with a history of ToF, repaired as a child with a RVOT conduit and bioprosthetic pulmonic valve (bPV) presented with chest pain. She was evaluated with echocardiogram, which showed severe pulmonary stenosis (PS), a peak gradient of 64 mmHg and an area index 0.6 cm^2/m^2. Currently, the standard treatment for PS in ToF is reoperation of the PV. Considering the patient's age and history of two prior sternotomies, percutaneous treatment options were favored to surgical intervention. Percutaneous

options discussed were balloon valvuloplasty, although there is a scarcity of data in bPV, and percutaneous valve in valve replacement. For bioprosthetic PS, valve in valve therapy has been shown to be beneficial in patients with favorable anatomy. Ultimately, the decision was made for balloon valvuloplasty as a bridge to reoperation.

Discussion Within ten years, at least 80% of ToF patients with bPV require reoperation or have significant valvular dysfunction. Treatment strategy of PS in adults with ToF must be tailored to the individual patient with consideration of previous treatments, current anatomy, PS peak gradient, and patient preference. The goal of such interventions ultimately is the symptomatic improvement and the aversion of irreversible cardiac dysfunction.

B19 YOUR HEART KNOWS THINGS YOUR MIND CAN'T EXPLAIN

[1]Julien Feghaly, [2]Ariana Mooradian. [1]*St Louis University School of Medicine, St Louis, MO*; [2]*St Louis University School of Medicine*

10.1136/jim-2020-MW.22

Introduction/Background Takotsubo cardiomyopathy (TTC) was first described in 1990, named after the shape of the left ventricle appearing like a tako-tsubo (Japanese: 'octopus,' 'trap'). It has often been linked to emotional stress, however, since then other associations have emerged such as cerebrovascular disease with takotsubo like myocardial dysfunction.

Case Presentation A 69-year-old female with a history significant for hypertension and cerebrovascular accident (CVA), 2 years prior, with no residual deficit, presented with confusion, dysarthria and right-sided facial & limb weakness. On presentation, she was found to have a minimally elevated troponin level without ST changes on electrocardiography. CT & MRI scans did not show any acute intracranial abnormality and the impression was that of a transient ischemic attack. Echocardiography went on to show a small (0.5 × 0.6 cm) left ventricle (LV) thrombus adjacent to the distal anterolateral wall; in addition to akinesia of the inferior, septal, anteroseptal and apical walls, with hyperdynamic wall motion in keeping with takotsubo cardiomyopathy (figure 1).

Abstract B19 Figure 1
Apical 4 chamber view demonstrating left ventricular apical ballooning

Discussion An association between CVA and TTC is evident in the literature. An investigation of 569 patients with acute ischemic stroke discovered TCC in 7 patients (1.2%), all of whom were females above the age of 75 years and had suffered a prior CVA. Several pathophysiological associations have been proposed linking the two events, even though their succession is uncertain: CVA leading to stress-mediated catecholamine surge inducing TCC, LV thrombus dissipation in the setting of TTC leading to a CVA, vasospasm of a large left anterior descending (LAD) artery or multi-vessel coronary vasospasm. Nevertheless, despite unclear pathogenesis, anticoagulation is recommended for CVA prevention in patients with sizable LV akinesia or the presence of a thrombus.

B24 NON-TYPEABLE HAEMOPHILUS INFLUENZA ENDOCARDITIS IN A PATIENT WITH HYPOCOMPLEMENTEMIA

[1]Suha Abu Khalaf, [1]Sachin Patil, [2]Abdallah Mansour, [1]Dima Dandachi. [1]*University of Missouri-Columbia*; [2]*University of Missouri- Columbia, columbia, MO*

10.1136/jim-2020-MW.23

Introduction/Background Haemophilus influenza (H.influenzae) is a pleomorphic gram-negative coccobacillus that can be either encapsulated (typeable) or unencapsulated (non-typeable). H. influenzae type b (Hib) used to be one of the most common causes of invasive infections until the introduction of the vaccine in the late 80s of the last century. Nontypeable H.influenza (NTHi) causes the majority of invasive H. Influenza cases nowadays with an incidence of two cases per 100,000 in adults who are 65 years or older. Immunocompromised people, due to asplenia, hypocomplementemia, or HIV, are at higher risk of developing more devastating infections. Currently, there is no effective vaccine against NTHi. The majority of the reported H. influenzae endocarditis cases are due to Hib; cases of NTHi endocarditis are extremely rare and underreported.

Case Presentation A 49-year-old male with a medical history of tobacco, methamphetamine abuse, and meningococcal meningitis, who presented with nausea, vomiting, watery diarrhea, and hemoptysis of a few days duration. Vitals were remarkable for a blood pressure of 85/40 mmHg, pulse rate of 58 beats/min, temperature of 37 C, respiratory rate of 18 breaths/min. Physical exam was remarkable for diffuse abdominal tenderness, decreased breath sounds bilaterally, and muffled heart sounds with a faint 2/6 apical systolic murmur. Initial workup was notable for leukocytosis, normocytic anemia, thrombocytopenia, and acute kidney injury (AKI), procalcitonin was elevated, total and alternative complement pathway levels were deficient as well as C3 and C4 (table 1). Stool polymerase chain reaction was positive for Chlostridoids difficile (C.diff) toxin. A computed tomography (CT) of the chest, abdomen, and pelvis were significant for colitis and multifocal innumerable upper lobe predominant ground glass and nodular opacities in bronchioalveolar distribution (figure 1). The patient was initially treated for multifocal pneumonia with fluid resuscitation, intravenous vancomycin, and piperacillin-tazobactam, as well as oral vancomycin for C.diff colitis. Subsequently, blood cultures grew beta-lactamase negative H.

influenzae. A transthoracic echocardiogram revealed a 1.5 cm vegetation over the anterior mitral valve leaflet. A Transesophageal echocardiogram showed a large (1.73 × 0.55 cm) mobile vegetation visualized on the atrial aspect of the anterior leaflet of the mitral valve and protrudes to the left ventricle during diastole with severe mitral regurgitation. The patient underwent a bioprosthetic mitral valve replacement, and antibiotics were narrowed down to intravenous ceftriaxone for a total of 6 weeks from the surgery. The valve culture also grew beta-lactamase negative H. influenzae. The patient's condition improved after discharge and was free of symptoms on six months follow up.

Discussion NTHi is an extremely rare cause of endocarditis and usually carries a good prognosis once treated promptly. Hematogenous spread secondary to bacteremia from a different infection is the most common source of seeding into the heart valves in immunocompromised patients. Our patient is immunocompromised secondary to hypocomplementemia and presented with bronchoalveolar pneumonia that is likely secondary to NTHi infection, which is the source of the bacteremia and subsequent endocarditis. The absence of an effective vaccine against NTHi, as well as the developing of virulence factors (such as enhanced adhesion ability, increased mucin production, and evasion of host defenses via immunoglobulin A proteases, epithelial cell entry, and antigenic variation), resulted in increasing invasive infections such as endocarditis. Clinicians should be aware of this possible complication in patients presenting with seemingly uncomplicated NTHi sinopulmonary infection. Hence, evaluation for endocarditis in patients with blood cultures positive for H. influenzae is essential to obtain an early diagnosis and avoid complications.

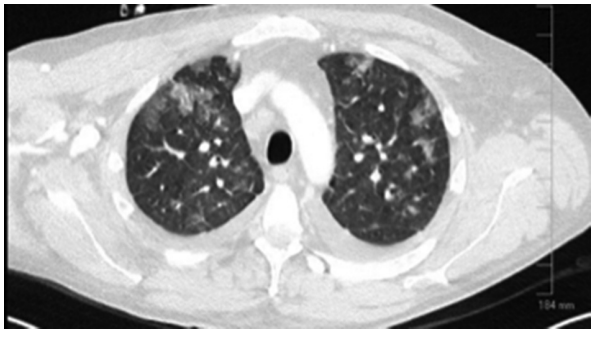

Abstract B24 Figure 1

Abstract B24 Table 1

Lab test (unit)	Result	Reference value
Blood count		
Hemoglobin (g/dl)	8.9	12–15.5
Hematocrit (%)	26.7	34.9–44.5
MCV (fl)	85	81.6–98.3
WBC (× 10^9/l)	35.4	3.5–10.5
ANC (× 10^9/l)	30	1.7–7
Platelets count (x10^9/l)	65	150–450
Others		
Creatinine (mg/dl)	2.13	0.5–1.2
BUN (mg/dl)	35	6.0–20
Procalcitonin (ng/ml)	27.5	<0.05
Total complement level (U/ml)	<3	30–75
Complement alternative pathway (U/ml)	<10	>46
C3 (mg/dl)	65	82–185
C4 (mg/dl)	11	15–53

B25 BRADYCARDIA AS THE ONLY PRESENTING SIGN FOR SEVERE HYPERKALEMIA

[1]Abdallah Mansour, [2]Tushar Tarun, [2]Tanvi Nandani, [2]Brian Bostick, [2]Mary Dohrmann. *[1]University of Missouri- Columbia, columbia, MO; [2]University of Missouri-Columbia*

10.1136/jim-2020-MW.24

Introduction/Background Severe hyperkalemia is known to be life-threatening and manifest by electrocardiographic (ECG) abnormalities that prompt emergent management to prevent cardiac catastrophe. We present a case of bradycardia as the only ECG manifestation of severe hyperkalemia.

Case Presentation A 63-year-old male with chronic kidney disease stage (CKD) 5, not on dialysis, presented with symptoms of dizziness and feeling unwell. His ECG showed junctional bradycardia with a heart rate of 43 beats per minute. There were no significant changes in T waves or QRS duration. His serum potassium (K+) at presentation was 7.3 mmol/L. Urgent hemodialysis resulted in the improvement of serum K+ and in the resolution of bradycardia and junctional rhythm. This patient had three additional hospitalizations with hyperkalemia with his ECG showing sinus bradycardia or junctional rhythm. Given his multiple hospitalizations with advanced CKD, chronic hemodialysis was initiated. The patient had no further hospital admissions for bradycardia caused by hyperkalemia.

Discussion Usual ECG changes noted with hyperkalemia are PR prolongation, P wave flattening, peaked T wave, widening of QRS, high grade atrioventricular (AV) block, and sinusoidal wave pattern. However, symptomatic bradycardia, in this case, was the only manifestation of the patient's severe hyperkalemia. The sinus node is known to be less sensitive to changes in K+ because of low resting K+ conductance and because of sinus node dependence on the calcium-dependent slow response. However, the conduction through the atrioventricular node can be impaired in hyperkalemia, which is attributed to the potentiation of adenosine sensitive inward rectifier K+ channel. In our patient, hyperkalemia likely affected the AVN with no significant effect on the Purkinje system and ventricular muscle resulting in junctional bradycardia with no significant T wave and QRS changes.

B36 VARENICLINE FOR TREATMENT OF RESISTANT FECAL INCONTINENCE

[1]Peter Z Abaskhroun, [2]Madeline Stecy, [3]Amulya Prakash, [3]Muhammad Asif, [4]Ben Terrany, [4]Ahmad Sharayah, [4]Hamzah Qudah. *[1]Monmouth Medical Center, Rutgers University, Long Branch, NJ; [2]Rutgers Medical school; [3]Monmouth Medical Center, Rutgers University; [4]Monmouth Medical Center*

10.1136/jim-2020-MW.25

Introduction/Background Fecal incontinence (FI) affects more than 5 million Americans, or about 7.7% of the population.[1] Management of this condition begins conservatively, with dietary changes such as avoiding non-easily absorbed food, and application of barrier creams. If these supportive measures

fail, bulking agents and anti-diarrheal medications are added. Finally, more invasive measures can be considered, ranging from Sacral nerve stimulator placement to sphincteroplasty, or even colostomy.[2] If a patient fails more aggressive treatment measures, the remaining options available are unfortunately limited. Here, we present a case of a patient with FI resistant to Sacral nerve stimulator placement. The patient was concurrently taking the medication Varenicline for smoking cessation and noticed immediate improvement in her FI. Given Varenicline's pharmacologic activity, this suggests a possible mechanism by which the medication may improve fecal incontinence.

Case Presentation The patient Is a 59-year-old woman with a 30-pack-year smoking history and 9-year history of FI who presented with the chief complaint of acutely worsening FI. Her FI occurred spontaneously throughout the day and was not related to exertion. She had continuous leakage of non-bloody liquid stools and complete absence of the urge to defecate. She denied any trauma to her perineal region, denied history of rectocele, and denied urinary incontinence or constipation. She had 2 uncomplicated vaginal deliveries. On assessment at the gastroenterology clinic, her vital signs were unremarkable. On physical exam, no pelvic organ prolapses, or mucosal tears were grossly visible. Sensation around the perineal area was intact. On digital rectal exam, the patient was found to have weak anal sphincter tone. Considering these findings and her age, a colonoscopy was recommended. The colonoscopy was performed and was found to be unremarkable. Anal manometer was offered, however the patient declined. The patient was treated with the submucosal injectable gel dextranomer microspheres 50 mg/mL + sodium hyaluronate 15 mg/mL (Solesta), a tissue bulking agent, but this failed to improve her symptoms. Subsequently, a Sacral nerve stimulator was placed but did not improve the patient's FI. Two to three years after the Sacral nerve stimulator placement, the patient still did not see improvement in her FI. Concurrently, the patient's primary care physician started her on Varenicline 1 mg oral twice daily for smoking cessation. She found her fecal incontinence improved significantly after the initiation of Varenicline. She regained the urge to defecate, she had formed stools, and her stool leakage almost completely resolved. When the patient successfully quit smoking 2 months later, she decided to stop the Varenicline. She noticed an immediate resumption of her FI symptoms, including the loss of the urge to defecate and leakage of non-bloody stool. The patient decided to resume the Varenicline 1 mg oral once daily because of its effect on her FI and elected to have the Sacral stimulator removed. She again found an improvement of FI symptoms. Two months later, the patient stopped Varenicline due to limited insurance coverage and her FI returned. Given the patient's report of the temporal relationship between starting Varenicline and cessation of FI, we decided to place the patient on Varenicline 1 mg oral daily for treatment of FI. She had almost complete resolution of her symptoms and will continue taking Varenicline.

Discussion Here we present a case of FI refractory to standard medical therapy and to Sacral nerve stimulator placement that resolved when the patient began Varenicline treatment for smoking cessation. The patient's incontinence had no clear etiology and was therefore described as idiopathic. However, one mechanism that may underlie this patient's fecal incontinence is a stretch nerve injury to the Pudendal nerve secondary to prolonged straining during defecation and weakness of muscles on the pelvic floor with aging. This could account for her poor rectal sphincter tone and absence of urge to defecate, given the Pudendal nerve's action in maintaining voluntary fecal continence. The temporal relationship between the resolution of her symptoms with starting Varenicline, the resumption of her symptoms with stopping the drug, and the absence of other lifestyle or medication changes suggests that Varenicline may have had a causal effect on the improvement of her incontinence. Varenicline is a partial agonist of $\alpha4\beta2$ nicotinic acetylcholine receptors (nAChR) is indicated as a treatment for smoking cessation.[3] The drug binds $\alpha4\beta2$ nAChR in the mesolimbic dopaminergic pathway to increase the tonic dopamine response, subsequently decreasing nicotine craving. It also has antagonist effects via reducing dopamine release induced by nicotine binding at the $\alpha4\beta2$ nAChR.[3] In addition to binding receptors in the central nervous system, Varenicline exerts effects peripherally in enteric nervous system.[4] Gastrointestinal symptoms, including constipation, nausea, and flatulence are common side effects of Varenicline taken at therapeutic doses for smoking cessation (1 mg oral twice daily for more than 6 weeks). A meta-analysis of randomized-controlled trials found number needed to harm for constipation was 24.[5] Varenicline's effects on gut motility may be due to modulation in Cholinergic response at the $\alpha3$, $\alpha4$, $\alpha7$, and $\beta4$ nACh R subunits in the myenteric and submucosal plexus.[6] Adding to the complexity of pharmacologic targets is the genetic variability of nAChR subunits, which may account for individual patient susceptibility to gastrointestinal adverse effects.[4] We hypothesize that our patient was able to achieve continence through Varenicline's modulatory effects on the colonic motor response via its partial agonist activity at nAChRs. As a partial agonist, Varenicline's stimulating or inhibiting actions depend on the availability of acetylcholine.[7] We therefore cannot assume Varenicline simply activates nAChR on colonic smooth muscle as a pure agonist. In fact, in vitro studies in mice and rat models demonstrate the opposite: Varenicline was found to decrease distal colonic contractions.[7] These findings suggest that Varenicline may decrease gut motility and restore disrupted cholinergic responses in vivo, which may explain the drug's effects on our patient's FI. Although the exact mechanism of action on this patient's idiopathic FI is unclear, our patient's success with Varenicline is encouraging. After failing first-line medical and invasive management strategies, her symptoms apparently resolved with Varenicline. The peripheral effect of Varenicline on the enteric nervous system and the underlying pathophysiology of FI warrants further study. In the future, Varenicline may prove to be a promising option for treatment-resistant FI.

REFERENCES

1. Bharucha A. Fecal incontinence. *Gastroenterology* 2003;124:1672–1685.
2. Bharucha, A. Management of fecal Incontinence. *Gastroenterology & Hepatology* 2008;4(11):807–817.
3. Fagerstrom K, Hughes J. Varenicline in the treatment of tobacco dependence. *Neuropsychiatric Disease and Treatment* 2008;4(2):353–363.
4. Swan GE, Javitz HS, Jack LM, Wessel J, Michel M, Hinds DA, *et al*. Varenicline for smoking cessation: nausea severity and variation in nicotinic receptor genes. *Pharmacogenom J* 2012;12:349–358.
5. Leung LK, PatafioFM, Rosser WW. Gastrointestinal adverse effects of varenicline at maintenance dose: a meta-analysis. *BMC Clinical Pharmacology* 2011;11:15.
6. Mandl P, Kiss JP. Role of presynaptic nicotinic acetylcholine receptors in the regulation of gastrointestinal motility. *Brain Research Bulletin* 2007;72(4-6):194–200.

7. Temiz TK, Demir, Omer Keskin Arslan, Elif Acar, Selin Karadaş, Barış Köylüoğlu, Gökhan. Effect of varenicline on colonic motility in a rat model of experimental irritable bowel. 2017;28(6):2743–2748.

B38 DOXYCYCLINE-INDUCED HEPATIC FAILURE: A CASE REPORT

[1]Ahish Chitneni, [2]Andrew G Birkhead, [3]Krista Santilli, [3]Silvia Plascencia. *[1]A.T Still University (SOMA), Chicago, IL; [2]Cook County Health, Chicago, IL; [3]John Stroger Hospital*

10.1136/jim-2020-MW.26

Introduction/Background Drug-induced liver injury (DILI) is known to be one of the most common causes of liver failure in the United States and accounts for 10 percent of the cases of acute hepatitis.[1] Cases of drug-induced liver injury can be labeled as idiosyncratic or nonidiosyncratic, the latter most commonly caused by acetaminophen overdose. Due to a lack of specific markers or tests for DILI, it is typically a diagnosis of exclusion and clinical judgment is necessary to halt the use of the offending agent.[2] Doxycycline is a tetracycline antibiotic that has been shown to be used as an effective alternative therapy for levofloxacin in the treatment of community-acquired pneumonia (CAP).[3] Though hepatotoxicity with the use of doxycycline is a reported adverse effect, very few cases of doxycycline induced acute liver failure have been reported in literature.[4] The following presents a case of acute necrotic liver disease from chronic hepatitis B activated by a 7-day course of doxycycline.

Case Presentation A 61-year-old Bulgarian female with past medical history of hysterectomy 2/2 cervical dysplasia 15 years prior presented to the emergency department with painless jaundice. Her jaundice started on her face and upper chest two days prior, after completing a 7-day course of doxycycline 100 mg for treatment of CAP. Patient had not had any previous episodes of jaundice. Of note, she experienced 1 week of dark urine, decreased appetite for 1 month, and 10 lb weight loss over 2 months. The patient suspects that she had a blood transfusion during her hysterectomy 15 years prior in Bulgaria, and this is thought to be the origin of her hepatitis. However, she does not have her medical records available. Her last travel outside the country was approximately one year ago to Bulgaria. The patient denies alcohol use, IV drug use, tobacco use, abdominal pain, nausea, vomiting, fever, chills, hematochezia, or hematuria. On presentation, patient was hemodynamically stable with labs showing AST 2099, ALT 1167, alkaline phosphatase 273, total bilirubin 13.4, and direct bilirubin 8.4. Five days prior to the start of the course of doxycycline, the patient had an AST of 764 and ALT of 936. One year prior her liver function was within the normal laboratory limits. Ultrasound of the gallbladder showed no biliary dilatation. CT abdomen demonstrated cholelithiasis with surrounding pericholecystic fluid and dilation of the intrahepatic biliary ducts with no concern for malignancy. Liver ultrasound showed unremarkable findings. Patient was nonreactive for HIV, hepatitis C, and hepatitis A but was positive for hepatitis B core antibody and surface antigen indicating chronic untreated hepatitis B infection. Her hepatitis B E-Antibody was positive, suggesting a control of replication state and low virus transmissibility. On the second day of hospitalization, given the prolonging INR and bilirubin the patient was started on tenofovir 300 mg and 3-day course of Vitamin K. Despite treatment, the patient continued to have up-trending total bilirubin, direct bilirubin, INR, AST >1000, and ALT >700. On the fifth day of hospitalization, given the continued progression of her disease, she was transferred to outside hospital for rescue liver transplant.

Discussion Given that the AST and ALT values on presentation were in the 1000s, the top differential diagnoses for this case include ischemic hepatitis, acute viral hepatitis, and drug induced liver injury. Given unremarkable findings on imaging, malignancy can be ruled out as a potential cause of liver injury in this scenario. In this patient, the findings of hepatitis B core antibody and surface antigen and the elevated AST and ALT values prior to the receiving the course of doxycycline suggest an untreated chronic hepatitis B infection that may have already been in the process of activation. The intake of doxycycline caused a 2-fold increase of AST and ALT and a 3-fold increase in bilirubin which leads us to believe a causal relationship exists between the doxycycline and liver failure for this patient. An objective causality assessment scale, the Maria and Victorino (M&V) system, suggested that in this case the doxycycline was the 'possible' (Score=12) cause of the drug induced liver injury.[5] Cases of doxycycline induced hepatic failure have been rarely reported in literature with less than 5 cases found during a preliminary literature search. A similar case was reported with a 36-year old female who was prescribed doxycycline for ureaplasma urealyticum genitourinary infection.[6] Within a week after beginning doxycycline, the patient had levels of AST 2620 IU/L, ALT 1990 IU/L, ALP 143 mg/dL. A complete inpatient work up was conducted for the patient and all other potential differentials were ruled out. In this case, a transjugular liver biopsy was conducted which revealed massive hepatocellular necrosis. Another objective causality assessment scale, the Roussel Uclaf Causality Assessment Method (RUCAM) score, suggested that in this case the doxycycline was the 'probable' (score=8) cause of liver injury. Similar to the patient discussed in our case, the patient was taken for rescue liver transplantation. Another case of doxycycline-induced hepatic failure was reported in a 17-year old female who began a prescription of doxycycline for acne.[7] Within five days of beginning the course, the patient presented to the emergency department with jaundice, scleral icterus, and hepatomegaly. A transjugular liver biopsy conducted on hospital day 2 showed pericellular fibrosis and parenchymal necrosis and liver transplant was performed successfully on hospital day 4. Given that the hepatotoxic effects of doxycycline have been reported in the past, doxycycline should be prescribed with caution in all patients with potential underlying untreated hepatitis infection or other sources of liver injury.[8]Patients with risk factors may find benefit with undergoing LFTs monitoring or hepatitis panel prior to starting a course of doxycycline.

REFERENCES

1. Zimmerman, *et al*. Drug-induced liver disease. *Clinical Liver Disease*. February 2000.
2. Kleiner, *et al*. Hepatic histological findings in suspected drug-induced liver injury: systematic evaluation and clinical associations. *Hepatology* February 2014.
3. Makabberi, *et al*. Doxycycline vs. levofloxacin in the treatment of community-acquired pneumonia. *Journal of Clinical Pharmacy and Therapeutics* April 2010;**35** (2).
4. LiverTox: Clinical and Research Information on Drug-Induced Liver Injury [Internet]. Bethesda (MD): National Institute of Diabetes and Digestive and Kidney Diseases; 2012-. Doxycycline.
5. LiverTox: Clinical and Research Information on Drug-Induced Liver Injury [Internet]. Bethesda (MD): National Institute of Diabetes and Digestive and Kidney Diseases;

2012. Maria and Victorino (M & V) System of Causality Assessment in Drug Induced Liver Injury.
6. Salehpour, *et al*. Fulminant liver failure secondary to doxycycline requiring rescue liver transplantation. Program No. P640. World Congress of Gastroenterology at ACG2017 Meeting Abstracts. Orlando, FL: American College of Gastroenterology.
7. Fish J, Ingram D, & Walkiewicz-Jedrzejczak D. Fulminant liver failure presenting shortly after initiation of doxycycline: A Case Report. *Clinical Pediatrics* 2015;**54** (9):904–906.
8. Heaton, *et al*. Association between tetracycline or doxycycline and hepatotoxicity: a population-based case-control study. *Journal of Clinical Pharmacy and Therapeutics* October 2007;**32**(5).

B39 A RARE CASE OF ADALIMUMAB-INDUCED ANGIOEDEMA IN A MAN WITH ULCERATIVE COLITIS AND RHEUMATOID ARTHRITIS

[1]Arabelle Abellard, [2]Shahnur Saiyad, [3]Halley Sullivan, [3]Arya Nikamal, [3]Mohammed Omari. *[1]University of Illinois At Chicago – ACMC, Oak Lawn, IL; [2]University of Illinois at Chicago – ACMC; [3]Advocate Christ Medical Center*

10.1136/jim-2020-MW.27

Introduction/Background Adalimumab is a recombinant human-derived, anti-tumor necrosis factor-alpha, monoclonal antibody that is used in the treatment of various autoimmune diseases. While there are known adverse events that can occur with adalimumab therapy (including malignancy, infections and skin reactions), the development of angioedema/edema is very rare. We present a rare case of angioedema that we believe was associated with adalimumab therapy.

Case Presentation A 49-year-old male with a medical history of rheumatoid arthritis (RA), ulcerative colitis (UC), hemochromatosis and allergic rhinitis presented to the Emergency Department (ED) for worsening neck swelling and bilateral periorbital swelling with conjunctival chemosis. A few days before presentation, he noted neck swelling that worsened after his Gastroenterologist recommended that he double his adalimumab dose from 40 mg every other week to 80 mg that week, followed by 40 mg weekly for 4 weeks. This new regimen was started because he had been having recurrent, persistent UC flares for the past 8 weeks, with up to 15 bloody bowel movements per day. He had been on adalimumab maintenance therapy for at least 1 year. After receiving this loading dose, he woke up the next day with photophobia, blurry vision, eye pain, and worsening neck swelling. He presented to the ED two days later. On exam, no injection site reaction or generalized urticaria was noted. Eye exam showed conjunctival chemosis with mild pemphigoid-like reaction. Neck CT showed diffuse enlargement of the soft palate and uvula, concerning for angioedema. He was given epinephrine and started on IV diphenhydramine and methylprednisolone. However, within a few hours of presentation, he developed tachypnea and respiratory distress with progressive throat swelling and had to be intubated for airway protection. He was extubated 3 days later and was discharged home on day 5 with mild residual neck swelling and on oral prednisone, 40 mg once daily for a few days. However, he was readmitted within 6 hours of discharge for reoccurring, progressive neck and throat swelling. Repeat neck CT re-demonstrated oropharyngeal and parapharyngeal soft tissue swelling, concerning for persistent angioedema. He was restarted on high dose IV corticosteroids and diphenhydramine and was re-intubated. Immunology workup showed elevated CRP of 6.9 mg/dl and normal levels of IgE, C3, C4, CH50 (total complement activity), C1q, C1INH total and C1INH functional. Radioallergosorbent test (RAST) for common food allergens, environmental allergens and Penicillin G were unremarkable; anti-adalimumab antibodies were positive. He was extubated on day 4 and received IV steroids for a total of 10 days, followed by an oral steroid taper. The angioedema resolved and did not recur. Adalimumab therapy was discontinued, and he agreed to have a colectomy several weeks later.

Discussion We believe that our patient's angioedema, periorbital swelling, and conjunctival chemosis were most likely secondary to adalimumab therapy; however, no skin testing and biopsies were performed. Our immunology workup as noted above was unremarkable and no localized erythema and edema were noted at the injection site. The pathophysiology of adalimumab-induced edema is not fully clear at this time as reactions to adalimumab can be localized or systemic, immediate or delayed, with or without urticaria. The absence of urticaria in our patient and the fact that he had been on adalimumab maintenance therapy for at least one year, suggest that his reaction to adalimumab was most likely, not primarily mediated by histamine. His symptoms did not recur after discontinuation of adalimumab. Although very rare, it is important to keep in mind the possibility of adalimumab-induced edema in patients who present with persistent body part swelling, not explained by other variables or etiologies.

B42 CONFUSING CASE OF DELIRIUM

[1]Matthew Cormier, [2]Ariana Mooradian, [3]Jennifer Schmidt. *[1]Saint Louis University, St. Louis, MO; [2]St Louis University School of Medicine; [3]Saint Louis University School of Medicine*

10.1136/jim-2020-MW.28

Introduction/Background Delirium is common in hospitalized patients, but can be difficult to identify and treat, especially in the elderly. It is a significant burden on society associated with increased risk for cognitive and function decline as well as increased cost of health care. While delirium is common in elderly hospitalized patients with a prevalence of 25%, it still poses a challenge for clinicians to recognize. Up to 70% of new cases of delirium are missed by clinicians and, even in recognized cases of delirium, the exact etiology often goes uncovered. This is in part because most cases of delirium have multifactorial causes and a wide range of presentations. Among all causes of delirium, polypharmacy and medication effects continue to be the number one reason for reversible delirium. Psychoactive drugs and multidrug interactions increase the risk of delirium in elderly patients 4.5-fold and 2.9-fold, respectively. Complicating the matter, changes in the patient's health status, such as infection or even dehydration, can trigger drug-induced delirium even without changes to patient's home medication doses. There has been increased attention to develop tools to better identify delirium such as the Confusion Assessment Method. There also has been increased effort to implement medication reconciliation for patients being admitted and discharged to ensure their medications are appropriate both in and out of the hospital, and minimize any associated adverse events such as delirium. Delirium continues to be difficult to diagnose and treat especially due to its many causes, but documenting mental status and reconciling medications early are easy steps to help reduce the prevalence of delirium and chances of poor outcomes from it.

Case Presentation A 68-year-old male with history of paraplegia on the Medicine service with sepsis secondary to pyelonephritis and aspiration pneumonia has worsening confusion for 1 day. Due to a switch day, the entire Medicine team was new and had not previously examined the patient; mental status was not documented. Patient was increasingly somnolent on exam, requiring sternal rub for arousal. On chart review, patient's last bowel movement was 2 days ago. Straight catheterization revealed >700cc of urine in bladder. Medication review showed patient received diazepam 10 mg the day prior due to concern for benzodiazepine withdrawal (listed as home medication but had not received for 3 days in hospital). Oxybutynin was also restarted one day prior; patient received 15 mg (home dose 5 mg TID) due to dosing confusion. Team contacted patient's daughter who managed home medications. Confirmed all medications patient was actively receiving at home and compared to medication list. Patient was receiving baclofen 40 mg QID in hospital but taking 20 mg TID at home and patient not currently taking diazepam at home. Bowel regimen and routine bladder scans/straight caths were initiated in addition to medication adjustments to correct dosing. Overnight patient had a bowel movement, 1.2L urine output via catheterization. Baclofen and oxybutynin doses were adjusted and diazepam was discontinued. Patient's mental status returned to baseline (oriented x4) approximately 48 hours later. Patient and family received medication education at discharge including updated medication list in the EMR.

Discussion This case demonstrates the difficulty of diagnosing and treating delirium. It illustrates potential improvements that could prevent future cases of delirium such as establishing baseline mental status and reconciling medications early.

B46 RARE CASE OF COWDEN SYNDROME

[1]Mansi Singapori, [2]Yasir Farah, [2]Harmesh Naik. *[1]St. Mary Mercy Hospital Livonia, MI, Northville, MI; [2]St Mary Mercy Hospital, Livonia, MI*

10.1136/jim-2020-MW.29

Introduction/Background Cowden syndrome is a rare autosomal dominant inherited complex disorder with a prevalence of 1 in 250,000. It manifests with various hamartomatous growths of multiple organs. In 80% cases, the human tumor suppressor gene, phosphatase and tensin homolog (PTEN) is mutated.

Case Presentation A 39-year-old female with past medical history of Cowden syndrome and PTEN-related breast cancer status post chemotherapy, radical mastectomy, and radiation presented with vision changes for one week. She described her visual changes as bilateral 'tornadoes'. It was associated with a constant sensation of the room spinning. She also had a one-day old headache in the bifrontal area in a bandlike distribution with pressure like pain that fluctuated from mild to severe. She denied any fever, floaters, flashes, diplopia, and weight changes. Family history consisted of mother diagnosed with breast cancer. Both vitals and labs were unremarkable. Physical exam was significant for left homonymous hemianopsia. MRI Brain was obtained which confirmed widespread metastatic disease throughout the brain causing significant cerebral edema. Her symptoms were secondary to brain metastasis. Patient was started on Decadron and Keppra. Upon discharge, her treatment plan consisted of radiation.

Discussion Cowden syndrome is a cancer predisposition syndrome with an increased risk of developing malignancy in many tissues but especially breast, thyroid, and endometrium. The greatest cancer risk for a woman with CS is breast cancer. The lifetime risk for a woman with CS to develop breast cancer is estimate to be in the range of 50 to 85%. Therefore, it is extremely important for clinicians to recognize this rare syndrome due to its high risk for multiple of malignancies. These patients need to have extensive malignancy screening recommendations with strict surveillances. Hence, the importance for clinicians to recognize this rare syndrome.

B47 RARE CASE OF LATE RELAPSE OF TESTICULAR CANCER AFTER 20 YEARS

[1]Mansi Singapori, [2]Ramesh Mohindra, [2]Amit Mohindra, [2]John Harb, [2]Cheryl VandeWege. *[1]St. Mary Mercy Hospital Livonia, MI, Northville, MI; [2]St Mary Mercy Hospital, Livonia, MI*

10.1136/jim-2020-MW.30

Introduction/Background Late relapse of testicular cancer (LRTC) is commonly defined as recurrence atleast 2 years after successful initial treatment. It is rare, with an incidence of 2.6% in testicular cancer patients.

Case Presentation A 47-year-old male with past medical history of left testicle orchiopexy, successfully treated non-seminomatous testicular cancer diagnosed in 1999 presented to an outpatient office for evaluation of hematuria of 2 weeks. He denied any weight loss, abdominal pain and fever. His family history is significant for brother who expired due to testicular cancer. Vitals were stable. Physical exam was pertinent for absent left testis. Labs were remarkable for elevated creatinine (2.1 mg/dl) and BUN (17 m mg/dl). Urinalysis showed blood with RBCs with no casts. CT Abdomen and Pelvis showed enlargement of the left seminal vesicle and prostate with left common and external iliac lymphadenopathy. PSA and testicular cancer tumor markers (LDH, AFP, B-HCG) were elevated. Biopsies of the left common iliac lymph node and prostate revealed metastatic non-seminomatous germ cell tumor. Final diagnosis made was stage IIIB non-seminoma testicular cancer. The patient treatment plan is to complete 4 cycles of Bleomycin, Etoposide and Cisplatin.

Discussion LRTC is characterized by slow growth, high AFP production, chemoresistance and poor prognosis in contrast to primary testicular cancer. Our patient had recurrence of testicular cancer after 20 years. Current guidelines for non-seminoma testicular cancer follow up includes up to five years. Therefore, our case emphasizes the importance of a life-time surveillance of testicular cancer patients to allow for early recurrence detection.

B51 A CASE REPORT OF ESOPHAGEAL TUBERCULOSIS IN A PATIENT FROM UNITED STATES

[1]Greta M Josephson, [2]Saira Ajmal. *[1]University of Illinois Chicago/Advocate Christ Medical Center, Chicago, IL; [2]Advocate Christ Medical Center*

10.1136/jim-2020-MW.31

Introduction/Background Gastrointestinal (GI) tuberculosis (TB) is rare in the United States and is the sixth most frequent site of extra pulmonary involvement of TB overall. It can involve any site along the GI tract, however, esophageal TB is

uncommon. Dysphagia is the most common presenting symptom of esophageal TB and misdiagnosis is frequent given its rarity. We present a unique case of a 57-year-old male with progressive dysphagia, found to have presumed esophageal TB.

Case Presentation A 57-year-old Hispanic male, employed as factory worker, with past medical history of newly diagnosed diabetes mellitus (HbA1c of 10.5), presented with two-week history of subjective fever, chills, headache, nasal congestion, sore throat and twelve-pound weight loss. Patient was originally from Mexico, but has resided in the United States for the past 20 years. Computed tomography scan of the neck was obtained at outside hospital, revealing a 4.9 × 3.3 × 4.2 cm superior mediastinal mass with lateral esophageal displacement; necessitating transfer to our facility for further evaluation. Initial laboratory work-up was notable only for leukocyte count of 16.9 thou/mcL. During admission patient's symptoms advanced to dysphagia and odynophagia, initially with solids then progressing to liquids, and ultimately difficulty with secretions. Patient was started on empiric antibiotic therapy and underwent laryngoscopy, which was negative for any mass. Upper gastrointestinal endoscopy (EGD) was then performed, which revealed an extrinsic high-grade compression/mass lesion in the cervical esophagus that appeared submucosal, with significant purulent drainage from esophageal wall. Pathology report from EGD demonstrated extensively ulcerated squamous mucosa with acute inflammatory exudate, with immunostains for CMV and HSV negative and GMS stain negative for fungal organisms. A whole-blood interferon-gamma assay (QuantiFERON) was obtained and returned positive, although review of esophageal biopsy did not show any evidence of granulomas. AFB stain and TB-polymerase chain reaction (TB-PCR) of esophageal biopsy were negative, along with stool TB-PCR. Patient continued to clinically improve and completed a total three-week course of antibiotic therapy with piperacillin-tazobactam for presumed abscess. However, on subsequent follow-up visit, repeat computed tomography imaging of the chest, abdomen, and pelvis with contrast was obtained demonstrating gastroesophageal wall thickening and punctate calcifications in the medial right lung base, anterior wall of proximal esophagus, and anterior to C7 vertebral body, highly concerning for TB in setting of positive QuantiFERON. Work-up is currently ongoing for patient to undergo repeat EGD and possible endoscopic ultrasound for definitive diagnosis and ultimately treatment of presumed esophageal TB.

Discussion Esophageal TB is rare, accounting for only 0.2–1% of all reported gastrointestinal TB cases overall, with majority of published case reports documented from developing countries. It is typically secondary to tuberculosis from another site in the body, most commonly pulmonary. Typically, esophageal involvement occurs from direct extension from mediastinal lymph nodes or lung cavity, although it may also spread via blood, lymphatic drainage, or from swallowed sputum. In our patient, it is postulated that he had a paraesophegal lymph node from TB that reactivated and subsequently affected the esophagus. Furthermore, the diagnosis of esophageal TB is difficult, as sensitivity of tests including AFB and PCR are variable and radiographic/biopsy results can be ill defined. In the case of our patient, positive QuantiFERON is concerning for possibility of esophageal TB in setting of suspicious punctate calcifications noted on repeat imaging. While initial esophageal AFB and TB-PCR were negative, as noted in Dahale *et al*., initial esophageal biopsies were diagnostic only 57% of the time. Repeat EGD with biopsy or endoscopic ultrasound is oftentimes necessary for definitive diagnosis, as is planned with our patient. If left untreated, esophageal TB can lead to numerous complications, including bleeding, fistula formation, and esophageal strictures.

B53 EXPECT THE UNEXPECTED, A CASE OF PROTEUS MIRABILIS PERICARDITIS

[1]Manikandan Seralathan, [1]Ridham Patel, [2]Narayana Gandham, [3]Preeti Misra. *[1]St.Mary Mercy Hospital, Westland, MI; [2]St Mary Mercy Hospital, Livonia; [3]St Mary Mercy Hospital*

10.1136/jim-2020-MW.32

Introduction/Background In the United States, from 2000 to 2011, the rate of pericarditis-related hospitalizations due to infections was 11 to 15 cases per 100,000 admissions. Virtually any infectious organism can infect the pericardium and can cause pericarditis and effusion. However, etiologies of pericarditis have changed significantly in the post-antibiotic era. Particularly making purulent (bacterial) pericarditis relatively uncommon. A few studies reported that Gram-positive organisms were found in 40% to 45% cases of bacterial pericarditis, with staphylococcal species being the most common among them. Gram-negative species like Proteus mirabilis causing purulent pericarditis is extremely rare. We present such a case of primary bacterial pericarditis caused by Proteus mirabilis.

Case Presentation A 78-year-old female with a history of rheumatoid arthritis (not on immunosuppressive therapy) and hypothyroidism presented to the hospital with complaints of right-sided sharp non-radiating chest and progressive shortness of breath for 10 days. On subsequent evaluation, CT imaging showed a large pericardial effusion with features of early tamponade and left-sided pleural effusion. The cardiothoracic surgeon was consulted, who subsequently drained 700 ml of bloody fluid from the pericardial space along with 950 ml of clear fluid from the left pleural space. The pericardium had a gross characteristic 'bread and butter appearance' as described by the cardiothoracic surgeon. The pericardial fluid and pericardial tissue samples were sent for microbiology testing. The patient was transferred to ICU with a pericardial window and left chest drain in place. Cultures from the pericardium and left chest drain grew Proteus mirabilis and rare diphtheroids. The pathology exam showed organizing fibrinous pericarditis with no signs of malignancy. Upon extensive work up no focus of infection was identified suggesting that it could have been a primary infection of the pericardium. The patient was treated with IV ceftriaxone for 10 days followed by PO cefuroxime for 4 days with complete clinical recovery.

Discussion Gram-positive organisms are the most common causes of purulent pericardial effusions. Gram-negative organisms causing purulent pericardial effusion is uncommon and can be seen rarely in immunocompromised individuals. Previously two cases were described with a similar presentation where polymicrobial gram-negative species including Proteus mirabilis were isolated. The other finding of classic 'bread-and-butter' appearance of fibrinous pericarditis has been described in rheumatic disease and other immunologic diseases such as systemic lupus erythematosus, post-myocardial infarct, uremia, tuberculosis, radiation

effects, bacterial, and viral etiology. Our case, to the best of our knowledge, is an extremely rare presentation of primary purulent pericarditis secondary to Proteus species. It emphasizes the need to consider gram-negative species in the empiric treatment of purulent pericardial effusions. Early recognition and prompt intervention are paramount for a favorable outcome in these cases.

B70 PERINEURAL NON-CASEATING GRANULOMA: RED FLAG OR RED HERRING?

[1]Matthew J Mandell, [2]Alysia V Kwiatkowski, [3]Meredith Morse, [3]Brittany Cody, [4]Mark Hoffman, [3]Meenakshi Jolly, [3]Wenlu W Xiong. *[1]University of Illinois at Chicago College of Medicine/Advocate Christ Medical Center, Chicago, IL; [2]University at Buffalo; [3]Rush University; [4]The University of Chicago*

10.1136/jim-2020-MW.33

Introduction/Background Sarcoidosis can affect just about any organ—although it most commonly affects the lungs and hilar lymph nodes—and is histologically characterized by non-caseating granulomas. The most commonly affected extra-thoracic site is the skin—either as an isolated phenomenon or in association with systemic disease. Leprosy is also characterized by non-caseating granulomas. India has the greatest number of cases worldwide. With a predilection for cooler environments, it most commonly affects skin and superficial nerves. Cardinal signs include hypopigmented or reddish skin lesions with loss of sensation, peripheral nerve involvement, and AFB positive skin smear. Differentiating between cutaneous sarcoidosis and tuberculoid leprosy can be difficult.

Case Presentation A 45-year-old Indian male—with 3 month history of fatigue, 15 lb weight loss, and asymptomatic bilateral lower extremity rash—presented with progressive weakness and worsening fatigue. He had recently been diagnosed with vitamin D deficiency (25-OH vitamin D level 6 nmol/l), for which 50,000 units of ergocalciferol (vitamin D2) once weekly was started, and two doses were taken by the time of presentation. On admission, he was found to have severe hypercalcemia (Ca 15.8 mg/dL). Serum calcium had been normal five weeks prior (corrected Ca 9.8 mg/dL). He denied numbness, tingling, pain, or pruritis associated with the rash. General exam was notable for cachexia (weight 61.2 kg, BMI 19.93 kg/m^2). Skin exam revealed scattered red to brown macules and minimally raised plaques with thin overlying scale on the lower extremities. There were no enlarged or tender peripheral nerves. Severe hypercalcemia was initially treated with aggressive IV hydration, IV bisphosphonate, and loop diuretics with improvement but not resolution of hypercalcemia. Intact PTH was appropriately suppressed (5.3; normal 8.0–85.0 pg/mL). Further work-up disclosed low PTHrP (12; normal 14–27 pg/mL), low 25-OH vitamin D3 (10 ng/mL), and markedly elevated total 1,25-(OH)2 vitamin D (244; normal 18–72 pg/mL). Vitamin A level and thyroid function tests were normal. Potential infectious causes for hypercalcemia were excluded, including negative blood cultures, QuantiFERON-TB Gold, histoplasma urine antigen, and HIV antigen/antibody. SPEP, UPEP, and serum free light chain analysis were normal, with no identifiable monoclonal protein. Serum angiotensin converting enzyme (ACE) returned markedly elevated (625, normal 9–67 U/L). CT-chest/abdomen/pelvis was negative for lung consolidation, mediastinal lymphadenopathy, or mass. Skin biopsy of the rash revealed well-formed non-caseating granulomas scattered throughout the dermis, some of which were associated with nerve fascicles. PAS, GMS, and Fite stains were all negative for microorganisms and no polarizable foreign body material was identified. Given perineural localization of granulomas on biopsy, absence of pulmonary involvement, and patient demographics, the possibility of borderline (paucibacillary) leprosy was entertained, and the patient was referred to an infectious diseases specialist who concluded that while paucibacillary leprosy could have false negative Fite stain, the absence of neuropathy and anesthesia of skin lesions would be unusual, and marked improvement in skin lesions with steroids alone without directed antimycobacterial therapy would be unlikely in leprosy. Oral prednisone 30 mg daily and topical clobetasol 0.05% were prescribed, with a working diagnosis of isolated cutaneous sarcoidosis. At follow-up three months after initial hospitalization, the patient was doing quite well. His low energy, imbalance, and generalized fatigue resolved, and his weight normalized (68.5 kg, BMI 22.96 kg/m^2). There was 95% improvement of the rash. His dose of oral prednisone was weaned to 5 mg once every other day with maintenance of normocalcemia. Interestingly, an ophthalmologic exam revealed unilateral uveitis, for which corticosteroid eye drops were started.

Discussion As demonstrated by our case, differentiating between cutaneous sarcoidosis and tuberculoid leprosy can pose a diagnostic dilemma. There have been numerous reports of patients originally misdiagnosed with sarcoidosis only later to be diagnosed with leprosy. In some of these cases, initial biopsies showed epithelioid histiocytes forming granulomas, but staining for AFB and PCR was not performed; when these patients later returned with new symptoms, subsequent biopsies and PCR were positive for AFB. All of these patients who were later diagnosed with leprosy experienced associated loss of sensation, anesthesia to light touch, and/or inability to distinguish between hot and cold. Peripheral nerve involvement is very common in leprosy, whereas it is quite rare in sarcoidosis. Just as there are reported cases of leprosy being misdiagnosed as cutaneous sarcoidosis, there are also cases of the opposite. A red flag is that these patients had intact sensation and no peripheral nerve thickening. In one study of 76 patients with cutaneous sarcoidosis, 23% of biopsies demonstrated perineural granulomas. None of these patients had clinical features to suggest leprosy; no nerve damage was identified, and Fite stain was negative. An additional finding that may lend support to the diagnosis of sarcoidosis over leprosy is the presence of uveitis. Eye lesions are present in 50–70% of sarcoidosis versus 15–20% of leprosy. Uveitis is the most common eye lesion in sarcoidosis, but is rare in leprosy. Hypercalcemia is found in 10% of sarcoidosis. Hypercalcemia can be unmasked or exacerbated by exogenous vitamin D intake in sarcoidosis. On the other hand, hypercalcemia is very rare in leprosy. Hypercalcemia in sarcoidosis is caused by extra-renal 1-hydroxylase hydroxylation of calcidiol to calcitriol in granulomatous macrophages. This peripheral activation of vitamin D explains our patient's profound hypercalcemia, which manifested shortly after consuming exogenous vitamin D2. Elevated serum ACE level is historically thought to be a non-specific finding in granulomatous disease. While it can be seen in both sarcoidosis and leprosy, the degree of elevation is higher in sarcoidosis compared leprosy. In one case-series of 51 patients with sarcoidosis, an ACE level >100 IU/L was found to have 93.4% specificity for sarcoidosis. In summary,

the presence of intact sensation and lack of peripheral nerve thickening suggests against a diagnosis of leprosy. The histopathologic spectrum of cutaneous sarcoidosis should be expanded to include perineural granulomas. The histological finding of non-caseating granulomas in a patient with skin lesions, corresponding sensory loss, and enlarged nerves warrants consideration of leprosy. Finally, hypercalcemia is more common in sarcoidosis than leprosy and may manifest to great degree after ingestion of supplemental vitamin D.

B71 ACUTE HYPOXEMIC RESPIRATORY FAILURE IN NON-VAPING TETRAHYDROCANNABINOL (THC) INHALATION

Yeohan Song. *Columbus Regional Hospital*

10.1136/jim-2020-MW.34

Introduction/Background The increased use of e-cigarettes, or vaping, has been associated with a recently reported outbreak of severe acute inhalational pulmonary disease termed vaping-associated lung injury (VALI) that has been cause of great public health concern.[1–2] Of particular importance, the affected patients have included teenagers and young adults, many without previously known pulmonology disease, with reported median patient ages of <25 years from recently reported cohorts of cases spanning multiple states.[2–3] These cases have been associated with heterogeneous presentations and radiographic patterns of lung injury, including those seen with acute eosinophilic pneumonia, organizing pneumonia, lipoid pneumonia, diffuse alveolar hemorrhage, and hypersensitivity pneumonitis,[4–5] with up to 80% of patients reporting inhalation of tetrahydrocannabinol (THC)-containing products.[3 6] This report describes the successful management of a 21-year-old female without previously known chronic pulmonary disease who presented with acute hypoxemic respiratory failure in the setting of non-vaping THC inhalation.

Case Presentation A 21-year-old Caucasian female previously in good health presented to a regional hospital with a 5-day history of progressively worsening dyspnea with cough productive of white sputum. She denied exposure to other individuals with respiratory illness prior to the onset of her symptoms, and also denied hospitalizations, outpatient antibiotic use, and international travel within the previous 3 months. She initially denied recreational and illicit drug use, including e-cigarette and tobacco use, but later admitted to inhalational use of marijuana. On initial assessment in the emergency room, the patient was found to be febrile to 38.1 degrees Celsius, with blood pressure of 133/84 mm Hg, heart rate of 128 beats per minute, respiratory rate of 15 breaths per minute, and oxygen saturation of 92% on 3 L/m of oxygen by nasal cannula. She was noted to have neutrophilic leukocytosis with white blood cell count of 15.8 thousand/μL and neutrophil count of 14.7 thousand/μL, with lactic acid of 1.6 mmol/L and pro-calcitonin of 1.04 ng/mL. Hemoglobin was 11.9 g/dL, and platelets were 356 thousand/μL. Sodium was 131 mmol/L, potassium was 2.9 mmol/L, and creatinine was 0.71 mg/dL. Electrocardiogram showed resolution of tachycardia, with normal sinus rhythm and no T wave flattening. Serum pregnancy test was negative. As the patient also reported abdominal discomfort with non-bloody diarrhea, a CT scan of the abdomen and pelvis was obtained in the emergency room and showed no acute abdominal pathology, but did demonstrate bilateral lower lobe alveolar infiltrates, also observed on chest x-ray (figure 1). Electrolytes were replaced, blood and sputum cultures were ordered, levofloxacin was empirically started, and the patient was admitted to the medical floor with a presumptive diagnosis

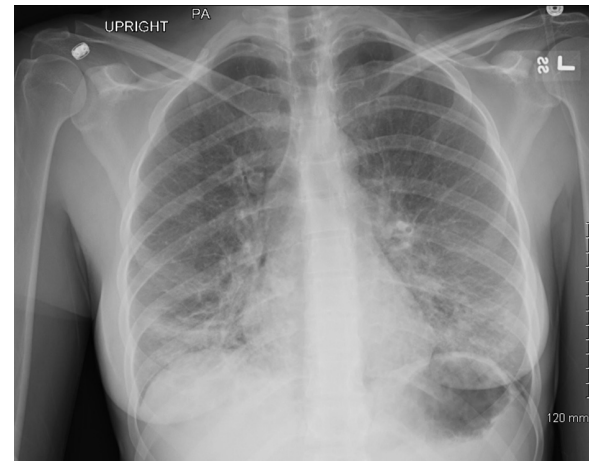

Abstract B71 Figure 1

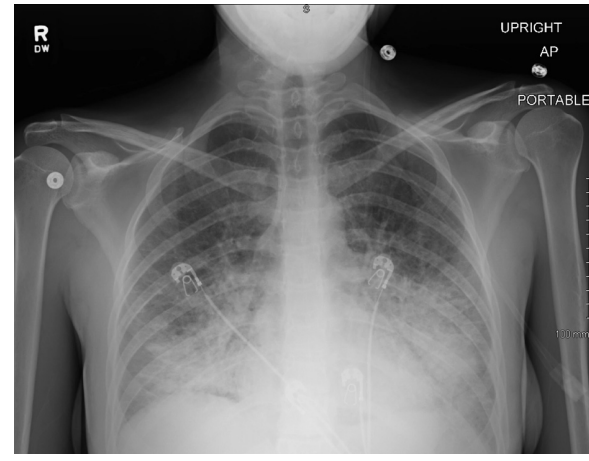

Abstract B71 Figure 2

Abstract B71 Figure 3

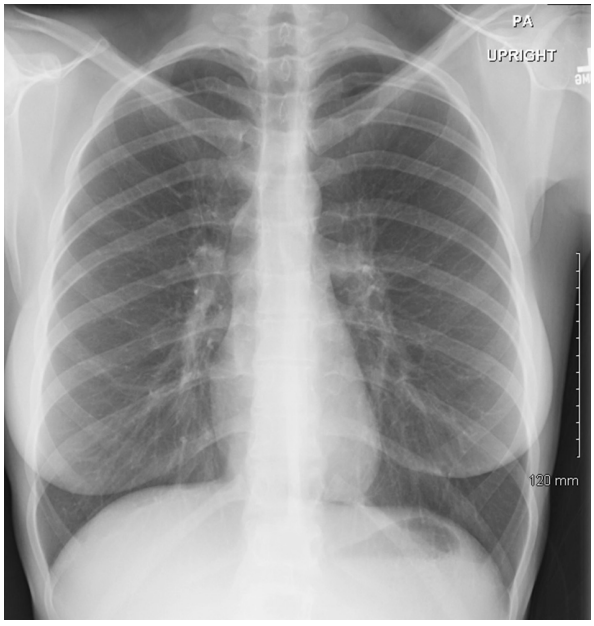

Abstract B71 Figure 4

of bilateral community acquired pneumonia. The next morning, the patient defervesced, with resolution of leukocytosis, but continued to require supplemental oxygen of 5 L/m by nasal cannula. Further laboratory investigations resulted with negative respiratory viral panel and Streptococcal and Legionella urine antigens, but positive urine drug screen for cannabinoids, with confirmatory THC testing later resulting positive. In the afternoon, the patient developed further worsening of acute hypoxemia requiring high flow nasal cannula. Repeat chest radiograph showed increasing bilateral infiltrates (figure 2), and given concern for acute respiratory distress syndrome (ARDS) physiology with P/F ratio of 143, empiric antibiotics were escalated to piperacillin/tazobactam and vancomycin, and the patient was started on methylprednisolone, initially at 1 mg/kg/day and escalated to 40 mg every 6 hours upon transfer to the intensive care unit. CT thorax without contrast was obtained, which confirmed progression of extensive bilateral ground-glass infiltrates with lower lobe predominance (figure 3). The patient experienced gradual improvement in hypoxemia on the same dose of methylprednisolone over the next 2 days and did not require intubation. Blood and sputum cultures showed no growth of pathogens, antibiotics were de-escalated to amoxicillin/clavulanic acid, and the patient was transferred back to the medical floor, after which methylprednisolone dose frequency was decreased to twice daily the following day, then once daily for the following 3 days. Patient was weaned off oxygen requirement and discharged on an abbreviated prednisone taper of 20 mg daily for 2 days followed by 10 mg daily for 2 days. On re-assessment by primary care provider the following week, the patient remained without oxygen requirement, and no further glucocorticoids were required. Repeat chest radiograph 2 weeks after discharge showed complete resolution of bilateral infiltrates (figure. 4).

Discussion This case describes the identification of a case of non-vaping THC inhalation associated with acute respiratory failure in a pattern previous seen with VALI,[7] supporting the association of inhaled THC with pulmonary toxicity in the absence of vaping. Further studies confirming this link may lead to important public health and policy regulations for non-vaping use of THC-containing marijuana products.

REFERENCES

1. Centers for Disease Control and Prevention. Outbreak of severe pulmonary disease associated with using e-cigarette products: investigation notice. 2019 Aug. (https://www.cdc.gov/tobacco/basic_information/e-cigarettes/severe-lung-disease.html).
2. Centers for Disease Control and Prevention. Evaluation of bronchoalveolar lavage fluid from patients in an outbreak of e-cigarette, or vaping, product use-associated lung injury – 10 states, August- October 2019. MMWR. 2019 Nov. 68 (45);1040–1041. (https://www.cdc.gov/mmwr/volumes/68/wr/mm6845e2.html).
3. Layden JE, Ghinai I, Pray I, *et al*. Pulmonary illness related to e-cigarette use in Illinois and Wisconsin — preliminary report. *N Engl J Med* DOI: 10.1056/NEJMoa1911614.
4. Henry TS, Kanne JP, Kligerman SJ. Imaging of vaping-associated lung disease. *N Engl J Med* 2019 Oct;381:1486–1487.
5. Henry TS, Kligerman SJ, Raptis CA, *et al*. Imaging findings of vaping-associated lung injury. *Am J Roentgenol* 2019 Sept; 1–8. [Epub ahead of print]
6. Christiani D. Vaping-induced lung injury. *N Engl J Med* 2019 Sept. DOI: 10.1056/NEJMe1912032
7. Maddock SD, Cirulis MM, Callahan SJ, *et al*. Pulmonary lipid-laden macrophages and vaping. *N Engl J Med* DOI: 10.1056/NEJMc1912038.

B72 PNEUMATOSIS INTESTINALIS SECONDARY TO SCLERODERMA

Alyssa Kwok, Shiva Arami. *University of Illinois at Chicago*

10.1136/jim-2020-MW.35

Introduction/Background Pneumatosis intestinalis—or the presence of gas within the bowel wall—is a radiographic sign that can be idiopathic (15%) or secondary to a known cause. It can occur anywhere along the GI tract. Whereas in neonates, pneumatosis intestinalis is pathognomonic for necrotizing enterocolitis, in adults there can be various associated diagnoses, such as COPD, scleroderma, or acute mesenteric ischemia. In the latter, pneumatosis intestinalis and air in the portal vein are harbingers of advanced disease and poor prognosis. The management depends upon the etiology: If there is concern for ischemia or perforation, an exploratory laparotomy is indicated. Otherwise, supportive care and serial imaging are recommended.

Case Presentation We present a case of a 65-year-old Asian female with a history of systemic sclerosis complicated by interstitial lung disease and Raynaud phenomenon requiring digital amputations who developed post-prandial diffuse abdominal pain and 5–6 dark stools over several hours. This was associated with nausea and non-bloody, non-bilious vomiting. She denied sick contacts and had eaten the same food as her family that day. None were ill. In the ED, she was febrile to 39C, hypotensive to 91/47, and had a heart rate of 97, respiratory rate of 22, and O2 saturation of 97% on room air. Exam was notable for hyperactive bowel sounds and mild tenderness to palpation with no rebound, rigidity, or guarding. A CT of the abdomen and pelvis with IV contrast showed gastric pneumatosis with portal venous gas, heavy atherosclerotic calcifications at the superior mesenteric artery and celiac origins, patulous air-filled distal esophagus, and pancolitis. The patient was started on IV vancomycin and piperacillin-tazobactam. After resuscitation with crystalloid, vital signs improved, but her lactate increased from 3.2 to 4.5. Surgery was consulted, and due to the worsening lactate, they recommended emergent exploratory laparotomy. Despite being informed of the risks, the patient refused surgery given her life-limiting

illness, recent amputations, significant weight loss, and fear of complications. The patient was admitted to the medical intensive care unit for supportive care. A nasogastric tube was placed for decompression and ultimately removed due to minimal output. As fluid resuscitation continued, the patient's lactate decreased to 0.9 by the evening of admission. Antibiotics were transitioned to IV levofloxacin and metronidazole for intraabdominal coverage and PO vancomycin for C.diff diarrhea, which was diagnosed by stool sample. The patient's diet was advanced from NPO to liquid diet, and diarrhea continued to improve. The patient was successfully transferred to the general medical floor after 48 hours in the ICU and continued to improve after levofloxacin and metronidazole were discontinued. She was discharged to home to finish a 14-day course of PO vancomycin. Subsequent outpatient CT of the abdomen 6 months after discharge showed resolution of gastric pneumatosis and portal venous gas. The patient lived for a year after this hospitalization, ultimately passing in home hospice from end-stage scleroderma-related ILD.

Discussion This case is unique because the presentation—hemodynamic instability, elevated lactate, and signs on CT—suggested possible acute mesenteric ischemia. However, this patient was febrile, and C.diff diarrhea was a more likely explanation of her hemodynamic status and elevated lactate. Most notably, in the setting of a patient with systemic sclerosis, pneumatosis intestinalis is a known incidental radiographic finding that occasionally ruptures to cause benign pneumoperitoneum. The patient was successfully managed with conservative therapies and avoided unnecessary surgery and its complications.

A02 TORTURE BY A TORTUOUS ARTERY: A RARE CASE OF FIBROMUSCULAR DYSPLASIA IN A YOUNG MALE COMPLICATED BY ACUTE RENAL INFARCTION

Munis Mahboob Ahmed, Syeda Ramsha Zaidi, Steven Kirby, Sophia Kumar. *St Mary Mercy Hospital, Livonia, Westland, MI*

10.1136/jim-2020-MW.36

Introduction/Background Fibro-muscular dysplasia (FMD) is an uncommon idiopathic, systemic disease of medium to small sized arteries presenting as non-inflammatory and non-atherosclerotic segmental lesions, which results in arterial stenosis, dissection, aneurysm or tortuosity. It is a multifactorial disease with a prevalence of 3.34% and diagnosed predominantly in young females (90%). The disease can affect any part of the arterial wall resulting in localized or multifocal lesions. Renal arteries are most commonly affected followed by other arterial beds including extra-cranial cerebral arteries and mesenteric arteries. FMD is complicated by fatal conditions including renal infarct, subarachnoid hemorrhage, cerebral artery dissection and others.

Case Presentation We are presenting a case of 31-year-old male with a past medical history of ADHD, vitamin B12 deficiency who presented with left lower quadrant abdominal pain radiating to left flank and back. He described it as an intermittent dull to sharp pain of varying intensity, not responsive to over-the-counter NSAIDS. He denied any fevers, chills, dysuria, increased frequency or urgency, hematuria, sick contacts' exposure, nausea, vomiting, diarrhea, antibiotic use, or recent travel history. He endorsed daily marijuana use and cigarette smoking for 10 years. A few days prior to this presentation, he was discharged from the hospital after being treated for progressive paresthesia due to vitamin B-12 deficiency. His initial vitals showed hypertension & tachycardia. Physical exam was remarkable for left lower quadrant tenderness, but no CVA tenderness. Labs including CBC, BMP, Urinalysis, LFTs, lipase, CRP, ESR, TSH, ANA, Anti-Cardiolipin Antibody, Anti-glycoprotein Antibody, and lipid profile were unremarkable. CT abdomen and pelvis showed well-defined areas of low density in upper and mid pole of left kidney suggestive of multifocal renal infarcts which were absent on lumbosacral MRI done a week ago. Repeat CT scan was done due to worsening of pain which showed a new infarct in inferior pole and renal scarring on right hence IV heparin was started. He was also started on enalapril as his blood pressure continued to be high in the range of 140–150/80–90. Low levels of Anti-thrombin gene and positive lupus anticoagulant were found. CTA of renal artery performed showed multifocal vascular abnormalities involving the bilateral renal artery branches, right common iliac artery and left external iliac artery where there were areas of vascular dilatation and stenosis with beaded appearance suggestive of fibromuscular dysplasia/FMD along with focal vascular dissection (and thrombosis) involving left renal artery likely renal infarction. Focal non-occlusive vascular dissection of the left external iliac artery, affecting bilateral renal arteries. Vascular surgery was consulted who recommended renal angiogram which was followed by balloon angioplasty on left renal artery but no stent was placed and the patient was resumed on anticoagulation for 6 months and discharged home with outpatient follow up for whole body imaging.

Discussion Acute renal infarction secondary to total occlusion of renal artery is a rare complication of FMD, which usually has a slow progression of arterial stenosis and almost never leads up to complete obstruction. It is also uncommon to diagnose FMD in a male patient with initial presentation of renal infarct at a young age in the absence of causative risk factors such as coagulopathy, arrhythmias or endocarditis. An association of FMD with antiphospholipid antibody (APLA) syndrome has been reported previously. The fact that luminal narrowing and fibrodysplasia of arterial intima can expose endothelial cells to APLA antibody, such as lupus antibody in our case, suggests a possible mechanism of platelet aggregation and thrombotic occlusion of renal artery.

B11 WHEN AFIB GOES BAD...THE DANGERS OF ATRIAL FIBRILLATION ABLATIONS

[1]Ali Hasnie, [2]Ammar Hasnie, [3]Ragheb Assaly. *[1]University of Toledo, Toledo, OH; [2]University of Missouri Kansas City School of Medicine; [3]University of Toledo*

10.1136/jim-2020-MW.37

Introduction/Background Atrio-Esophageal fistula creation is the most feared complication following an Atrial Fibrillation ablation. Despite the rarity of the complication, the mortality rate is high. The optimal management strategy is still debated and can be compounded with concurrent comorbidities.

Case Presentation A 65 y/o M with past medical history of Atrial Fibrillation (AF), TIA, & CHFrEF presented to his cardiologist for continued complaints of symptomatic atrial fibrillation despite maximized medical therapy. The patient chose to undergo pulmonary vein isolation (PVI) of AF for symptomatic control. He tolerated the procedure well and was discharged home. Four weeks following the AF ablation he

presented with complaints of fatigue, chills, weakness and lethargy. Initial laboratory workup showed a WBC count of 12.9K and Procalcitonin of 64.43. Outside hospital blood cultures were positive for gram positive cocci. CT brain showed evidence of a new subarachnoid hemorrhage. Follow up MRI demonstrated multiple infarcts throughout the brain. Possible septic emboli was the suspected cause of the numerous acute small infarctions throughout the cerebral hemispheres with endocarditis as the source. TTE was negative for manifestations of endocarditis. Blood cultures returned positive for streptococcus mitis, a common oral flora. Atrio-esophageal fistula (AEF) was suspected and gated CTA was performed. A tract out of the left atrium in proximity to the esophagus was noted, consistent with an AEF. The following evening the patient complained of melanotic stools and his hemoglobin dropped from 11 to approximately 7 g/dL. The patient was deemed to require surgical intervention for repair of the AEF. However, evidence of recent SAH on initial CT Head prevented the possibility of cardiopulmonary bypass surgery due to need for heparin. In addition, the numerous infarctions in his brain were concerning for mycotic aneurysms. He was temporarily stabilized with an esophageal stent. A cerebral angiogram was performed which demonstrated no evidence of mycotic aneurysms. Due to risk of further decompensation the benefit of definitive repair outweighed the risk of operative intervention. He underwent successful pericardial patching of his atria as well as primary closure of his esophageal defect. He was discharged on six weeks of antibiotic therapy to a rehabilitation facility.

Discussion Non-pharmacologic therapy is an alternative management strategy for AF which has been increasing in popularity. Most commonly this is via catheter-based ablation around the culprit pulmonary veins. AF ablation carries a small (<0.1% risk) but significant (fatality 67–100%) risk of AEF. Symptoms can appear in as short as two weeks following the ablation to nearly two months after. Management includes surgical repair of the fistula or esophageal stenting. Management of the fistula creation can be compounded with concurrent SAH as in this case, delaying definitive surgical intervention.

B15 MASSIVE PROTEINURIA IN A YOUNG MALE WITH A DIFFUSE RASH

[1]Ayham Alagha, [2]Roger Rodby, [3]Khaleel Sayeed. *[1]West Suburban Medical Center, Palatine, IL; [2]RUSH University; [3]NANI*

10.1136/jim-2020-MW.38

Introduction/Background Proteinuria in non-diabetic adults is most often secondary to focal segmental glomerular sclerosis (FSGS), membranous glomerulonephritis (MGN) and minimal change disease (MCD) in addition to a number of systemic diseases with glomerular involvement. FSGS, MGN and MCD have primary idiopathic forms but 'secondary' forms can also be seen related to a number of disease conditions. While the pathologic diagnosis is made by renal biopsy, a clinical diagnosis also requires a history and physical exam (PE) in addition to a series of blood tests. We present a case of massive proteinuria in a patient with a diffuse rash in which the diagnosis was strongly suggested by the PE alone.

Case Presentation A 28-year-old male with a PMH of anxiety and depression presented to the clinic with fever and a progressive diffuse pink maculopapular rash initially on his palms which had spread to other extremities including his trunk. He denied any sick contacts, no recent outdoor activities, and has no recent travel history. He is sexually active with multiple partners and takes emtricitabine/tenofovir disoproxil fumarate for pre-exposure prophylaxis. He had fever, tender lymphadenopathy, and anorexia but denied headache, visual changes, hair loss, chest pain, shortness of breath, musculoskeletal complaints, changes in his urinary or bowel habits or weight loss. Routine labs showed a serum (SCr) creatinine of 1.1 mg/dl, a urinalysis (U/A) was not done. Further workup by his PCP demonstrated a 1:64 RPR titer with negative hepatitis B, C and HIV serologies. He was started on IV penicillin G. After the first injection, the patient developed chills, fevers, headache, and myalgias, consistent with a Jarisch- Herxheimer reaction requiring a hospital admission treated with ibuprofen. Upon follow up with PCP 3 weeks later the patient complained of frothy urine. A urine protein to creatinine ratio (UP/C) was 7.3 g/g with a SCr 1.3 mg/dl. He was referred to a nephrologist and SCr was 1.6 mg/dl, a UP/C too high to calculate, serum albumin 1.6 g/dl and total cholesterol 401 mg/dl. His PE was unremarkable except for cervical lymphadenopathy, diffuse maculopapular rash, and minimal peripheral edema. A renal biopsy was performed which showed normal glomeruli on light microscopy, however the immunofluorescence demonstrated glomerular basement membranes containing diffuse finely granular deposits of IgG with subepithelial electron dense deposits on electron microscopy consistent with MGN.

Discussion MGN is a rare but well described complication of secondary syphilis. This patient's history of recent ibuprofen use increased the differential diagnosis to NSAID related MCD. The diagnosis of MGN was confirmed on renal biopsy and that in conjunction with his rash and positive syphilis serology confirmed the diagnosis of syphilis related MGN. Resolution usually occurs with antibiotics.

A08 MYOCARDIAL INFARCTION WITH NON-OBSTRUCTIVE CORONARY ARTERIES

[1]Sabaa Ahmed, [2]Sheraz Hussain, [2]Luay Rifai. *[1]Advocate Christ Medical Center, IL; [2]Advocate Christ Medical Center*

10.1136/jim-2020-MW.39

Introduction/Background When thinking about myocardial infarctions, one typically thinks of obstructed coronary arteries leading to lack of perfusion to the myocardial tissue. However, this particular patient's presentation and ultimate findings served as a paradigm shift in modern-day cardiology. This case outlines the clinical trajectory of a 67-year old female with past medical history of diabetes, hypertension, and CKD who presented to the hospital with atypical symptoms in the setting of acute coronary syndrome. She complained of back pain and headaches upon arrival. She did not report any chest discomfort or shortness of breath. Initial vitals were normal including blood pressure in both arms. Initial EKG in the emergency room revealed mild ST elevations in lateral leads I and aVL, concerning for an acute ST elevation myocardial infarction.

Case Presentation After obtaining the initial EKG concerning for ST elevation myocardial infarction, repeat EKG was done and revealed worsening of ST elevation. Initial labs showed serial elevations of troponin up to 81. The patient was

urgently taken to cardiac Cath lab and underwent coronary angiogram. Coronary angiography did not reveal any evidence of coronary artery disease with TIMI-3 flow in all vessels. Left ventriculogram was then done, showing an ejection fraction of 60%. Thereafter, another repeat EKG was done which showed persistent lateral ST elevations. The patient underwent a ventilation perfusion scan which deemed patient to be of low probability for pulmonary thromboembolic disease. A transthoracic echocardiogram showed left ventricular ejection fraction 45 to 50%, anterolateral and inferoposterior lateral wall hypokinesis with grade 2 diastolic dysfunction. CTA of the chest was negative for aortic aneurysm or dissection. The patient was briefly started on a calcium channel blocker for presumptive vasospasm of the coronary arteries, pending further test results. Rheumatologic workup including an ANA panel and inflammatory markers was negative. A transesophageal echocardiogram ruled out a thrombus as a possible cardioembolic source as well as a patent foramen ovale. The patient was scheduled for a cardiac biopsy and abdominal fat pad biopsy to rule out systemic amyloidosis, which both came back negative. Myocardial biopsy however did show concern for lymphoplasmacytic interstitial infiltrate and serology came back positive for coxsackie B virus.

Discussion The patient was deemed to have had myocardial infarction with nonobstructive coronary arteries, MINOCA. Secondary to residual cardiac dysfunction, the patient was referred to advanced heart failure to be started on guideline directed medical therapy. MINOCA occurs in approximately 5–6% of all diagnosed cases of acute myocardial infarction. It typically occurs in females without history of hyperlipidemia, and tends to be present in younger age groups. By definition, MINOCA must occur in patients without obstructive coronary lesions greater than 50%, which is determined by coronary angiography. It is of utmost importance that other overt causes for elevated troponin and nonischemic causes for myocyte injury are further investigated as well. Although it is understood that there have been no randomized trials or prospective studies conducted on MINOCA thus far, it is still recommended that if there is evidence of atherosclerosis in these patients, it should be treated aggressively. The underlying cause of MINOCA also plays a vital role in directing treatment. As with our patient, who was treated with calcium channel blockers, this class of medication has been deemed the best treatment of MINOCA secondary to coronary vasospasm. Additional research about MINOCA is still needed in order to determine the efficacy of medications aimed at secondary prevention of acute myocardial infarction.

A09 CHIARI MALFORMATION OF RIGHT ATRIUM DISGUISED AS INFECTIVE ENDOCARDITIS

[1]Khawaja Akhtar, [2]Maham Khan, [2]Usman Bhatti, [2]Ali Jafry, [2]Mark Allee. *[1]University of Oklahoma Health Sciences Center, Oklahoma City, OK; [2]University of Oklahoma Health Sciences Center*

10.1136/jim-2020-MW.40

Introduction/Background The Chiari Network is a sieve-like membrane consisting of strands in the right Atrium. It is a congenital remnant resulting from incomplete resorption of the right valve of Sinus Venosus. Chiari formation is extremely rare and is usually diagnosed incidentally on echocardiogram. We present a case of Chiari network in a young pregnant female who was referred to our hospital for workup of Infective Endocarditis.

Case Presentation A 33 year old, 11-week-pregnant female with past medical history of intravenous drug abuse was referred to our hospital from high risk clinic for evaluation of Infective Endocarditis (IE) after a transthoracic echocardiogram (TTE) revealed an 'Irregular mass' in the right atrium. On presentation the patient was hemodynamically stable, afebrile and initial lab work-up was unremarkable. Physical exam was unremarkable without any immunologic or embolic phenomena suggestive of IE. Electrocardiogram revealed normal sinus rhythm; urine toxicology screen was negative for any recent recreational drug use. Modified Duke's criteria was suggestive of moderate risk for IE. The patient was started on IV Vancomycin and Ampicillin-Sulbactam along with therapeutic anticoagulation with Enoxaparin after consultation with Cardiology and Gynaecology. Lower extremity and abdominal Doppler scans were negative for thromboembolic phenomena. Patient received a repeat TTE along with trans-esophageal echocardiogram for further evaluation; these showed a hypermobile linear mass in the right atrium (figure 1), diagnosed as a right atrial Chiari network. Blood cultures were negative, following which antibiotics and enoxaparin were discontinued. Patient was discharged home with scheduled follow-up appointments.

Discussion The Chiari network is an embryonic remnant from persistence of right valve of the sinus venosus and is reported to occur in 2% of the population. Echocardiography is an excellent tool for the diagnosis and echocardiographic findings of a Chiari network include a highly mobile fenestrated structure attached to the right atrium, in close proximity with the junction of the inferior and superior venae cavae. Presence of Chiari network may be confused with Ebstein anamoly and flail leaflets of the tricuspid valve. In addition to its role as a risk factor for arterial embolic events, it has been suggested that Chiari network may act as a nidus for Infective Endocarditis. During invasive procedures, catheters, guidewires and pacemaker leads may get entrapped within the network. Potentially fatal massive pulmonary embolism may be seen in association with Chiari formations. The Chiari network remains an important differential to be considered in the finding of a right atrial abnormality and should be distinguished from masses such as thrombi, flail tricuspid leaflets and tricuspid valve vegetations.

A14 EXPLORING FAMILIAL RESTRICTIVE CARDIOMYOPATHY – A CASE REPORT

[1]Zeid Nesheiwat, [2]Paul Harnish, [2]Muhammad Mangi. *[1]The University of Toledo Medical Center, Maumee, OH; [2]The University of Toledo Medical Center*

10.1136/jim-2020-MW.41

Introduction/Background Familial restrictive cardiomyopathy is an extremely rare and progressive genetic disorder with only a few documented cases, thus its true prevalence, as well as optimal management, remains unknown. There are several unique but typical constellations of clinical, radiographic, and invasive findings of familial restrictive cardiomyopathy.

Case Presentation A 37-year-old male with a significant family history of restrictive cardiomyopathy presented for abdominal distension and weight gain. Initial examination revealed jugular venous distension and abdominal ascites. A full workup including an echocardiogram, cardiac magnetic resonance

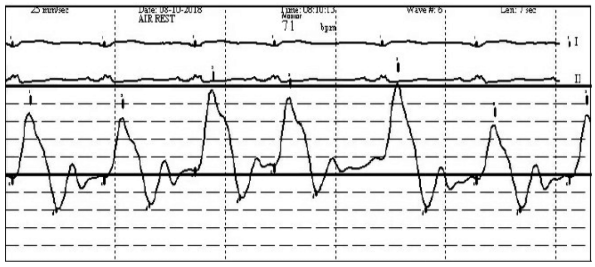

Abstract A14 Figure 1
Right heart catheterization showing the dip and plateau sign or 'square root' sign which is consistent with restrictive cardiomyopathy

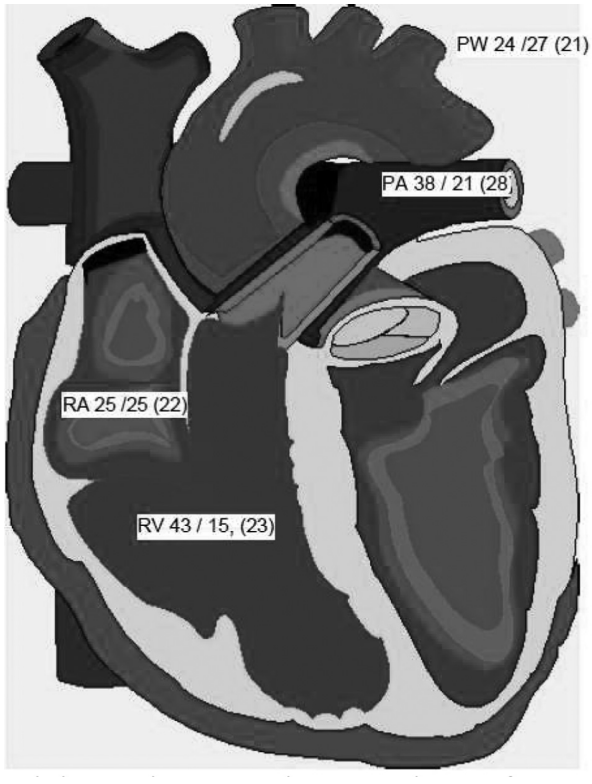

Abstract A14 Figure 2
Right heart catheterization showing equalization of pressures in all four chambers of the heart

imaging, and right-sided cardiac catheterization proved consistent with restrictive cardiomyopathy (figure 1,2). The patient was treated with ongoing inotropic therapy as well as high dose diuretics and was ultimately transferred for cardiac transplantation.

Discussion Clinicians should be aware of the unique findings of restrictive cardiomyopathy including bi-atrial enlargement, diastolic dysfunction, and most notably, equalization of pressures in all four chambers, including the dip and plateau or 'square root' sign. Unfortunately, due to its low prevalence, the optimal management remains unknown. Current treatment regimens are empiric and aim to reduce pulmonary and systemic congestion. The prognosis remains poor with reduced survival. The ultimate treatment modality is patients are eligible is cardiac transplantation. In conclusion, familial restrictive cardiomyopathy is a rare genetic disorder affecting less that one per one million people. Although rare, clinicians must be aware of the clinical, radiographic, and invasive findings of restrictive cardiomyopathy. This case demonstrates the unique clinical, radiographic, and invasive findings to confirm the diagnosis of restrictive cardiomyopathy in a patient with a significant family history of the disease.

A17 A TOUGH DECISION TO MAKE: EMBOLIC OR HEMORRHAGIC STROKE?

[1]Akash P Patel, [2]Sagar Patel, [3]Denisa L Hagau. *[1]Northwestern University's Feinberg School of Medicine, Chicago, IL; [2]MercyOne North Iowa Medical Center; [3]Mason City Clinic*

10.1136/jim-2020-MW.42

Introduction/Background Cerebral amyloid angiopathy is an important cause of primary lobar intracerebral hemorrhage in older adults. Because of the high recurrence rate, providers typically avoid anticoagulant and antiplatelet agents in this population. This becomes an issue when compounded with atrial arrhythmia that recommends anticoagulation as part of the management.

Case Presentation A 58-year-old patient with a past medical history of uncontrolled hypertension and traumatic subdural hematoma in 2018 was admitted after presenting with facial droop and right-sided weakness. MRI of the brain revealed an acute multifocal, bilateral cerebrovascular accident, suspicious for embolic origin, and amyloid angiopathy of the brain. Carotid dopplers did not reveal any significant stenosis. Echocardiogram did not reveal any valvular pathology, but focal apical left ventricular hypertrophy was noted. The Technetium pyrophosphate scan did not reveal any amyloid deposition in the LV myocardium. On telemetry, atrial flutter was discovered. A transesophageal echocardiogram was performed and did not show any intracardiac thrombus. For the atrial flutter, the patient was started on metoprolol. Cardiology recommended anticoagulation due to elevated CHA_2DS_2-VASc of 3 for preventing any embolic stroke. However, neurology recommended against the use of anticoagulation due to the high risk of intracranial hemorrhage in the setting of intracranial amyloid angiopathy. At this point, the patient was given the option of anticoagulation or not. The decision to not anticoagulate was chosen by the patient.

Discussion Anticoagulant and antiplatelet agents are avoided in patients diagnosed with cerebral amyloid angiopathy due to the high recurrence rate of intracerebral hemorrhage. Warfarin increases the frequency by 7-to-10-fold and severity with a 60% mortality[1]. The direct oral anticoagulants (DOACs) have been shown to be as effective as warfarin prevention of ischemic strokes in patients with atrial fibrillation and confer lower risks for intracranial hemorrhage. Therefore, these are typically used for patients with atrial fibrillation and CAA who are at high risk for both ischemic and hemorrhagic stroke. In a prospective cohort of patients with primary lobar intracerebral hemorrhage (ICH), aspirin was associated with an increased risk of ICH recurrence when controlling for other hemorrhage risk factors.[2] This represents a lower risk of ICH than DOACs, but less effective anticoagulation for this patient's atrial flutter. In comparison, there is an increased risk for clinical thromboembolism in patients with persistent atrial flutter compared to the general population without atrial arrhythmias.[3] The long-term embolic risk in patients with sustained atrial flutter was estimated at 3% per year but increases with

an increasing CHA2DS2-VASc score. Overall, when presented with a patient with cerebral amyloid angiopathy and a need for anticoagulation such as atrial flutter, it is important to balance the risk between thromboembolism and the risk of a cerebral hemorrhage.

REFERENCES

1. Rosand J, Hylek EM, O'Donnell HC, Greenberg SM. Warfarin-associated hemorrhage and cerebral amyloid angiopathy: a genetic and pathologic study. *Neurology* 2000;**55**(7):947.
2. Biffi A, Halpin A, Towfighi A, Gilson A, Busl K, Rost N, Smith EE, Greenberg MS, Rosand J, Viswanathan A. Aspirin and recurrent intracerebral hemorrhage in cerebral amyloid angiopathy. *Neurology*. 2010;**75**(8):693.
3. Ghali WA, Wasil BI, Brant R, Exner DV, Cornuz J. Atrial flutter and the risk of thromboembolism: a systematic review and meta-analysis. *Am J Med*. 2005;**118**(2):101.

A26 DIAGNOSING HEARTLESS ENDOCARDITIS

[1]Jaya Bommireddipally, [2]Jennifer Schmidt. *[1]Saint Louis University, St. Louis, MO; [2]Saint Louis University School of Medicine*

10.1136/jim-2020-MW.43

Introduction/Background Streptococcus intermedius is a member of the Streptococcus anginosus group, which is found as normal flora in the oropharynx, gastrointestinal tract, and the genitourinary tract.[7] This group of bacteria has been known to form abscesses and infections in several parts of the body, including the brain, heart, lungs, liver, and the spleen .[5 6 10] Specifically, S. intermedius is associated with the development of brain and liver abscesses.[11] This bacterium has also been reported to cause infective endocarditis.[8 12] Infective endocarditis (IE) is diagnosed using the modified Duke criteria.[4] An important teaching point from our case is that endocardial involvement is not a requirement to diagnose IE. We report a unique case of S. intermedius infection, complicated by hepatic and brain abscesses, with the diagnosis of IE despite the lack of evidence of endocardial involvement.

Case Presentation We discuss a 57-year-old male with a distant history of IV drug use (IVDU) who initially presents in clinic with worsening productive cough, chest and abdominal pain, fever, and 30-lb weight loss. Labs are remarkable for WBC of 17.9. He is started on levofloxacin for ten days. Four months later, the patient presents to the ED with worsening symptoms. Imaging shows multiple pulmonary and hepatic abscesses. Blood cultures are positive for Streptococcus intermedius. Hepatic drain is placed, and the patient is started on ceftriaxone and metronidazole. TEE is negative for vegetations. The patient receives an MRI brain due to confusion and hallucinations. This shows multiple intraparenchymal abscesses. The patient is treated with 6 weeks of IV antibiotics for presumed IE based on the modified Duke criteria.

Discussion Our case is unique due to the S. intermedius causing IE without evidence of endocardial involvement, complicated by brain and liver abscesses. IE is diagnosed by the modified Duke criteria.[4] Duke criteria for diagnosing IE has been established since 1994.[1] Slight modifications to these criteria have been made in the year 2000 to produce the modified Duke criteria.[4] Although it has been over twenty years since the creation of the criteria, studies have confirmed its importance in diagnosing IE.[9] The modified Duke criteria include major and minor criteria for diagnosing definite, possible, or rejected IE.[4] Major criteria include 1) two positive blood cultures for typical IE organisms, 2) Coxiella burnetii positive blood culture, or 3) echocardiogram evidence. Minor criteria include 1) IVDU or a predisposing heart condition, 2) fever (>38°C), 3) vascular/immunologic phenomenon, 4) other microbiologic evidence. Definite IE diagnosis meets 2 major criteria OR 1 major and 3 minor criteria. Possible diagnosis meets 1 major and 1 minor criterion OR 3 minor criteria. Rejected diagnosis is when 1) a clear alternate diagnosis is made, 2) symptoms resolve with <5 days of antibiotic therapy, 3) surgery or autopsy shows no IE evidence after <5 days of antibiotic therapy, or 4) criteria for definite or possible IE are not met.[4] Based on the modified Duke criteria, it is important to reiterate that the diagnosis of IE does not require endocardial involvement. Studies have confirmed TTE sensitivity/specificity in detecting vegetations is 44–63%/91–98%. TEE sensitivity/specificity is 87–100%/91–100%.[3] In patients with positive blood cultures, TEE found vegetations in 82% and TTE in 69% of patients.[2] Therefore, patients that meet the criteria should be treated for IE despite a lack of echocardiogram evidence. Our patient meets 3 minor criteria for possible IE: a history of IVDU, fever, and S. intermedius positive blood cultures. He was treated with 6 weeks of IV antibiotics as no other clear source of infection was identified.

REFERENCES

1. Durack DT, Lukes AS, & Bright DK. New criteria for diagnosis of infective endocarditis: utilization of specific echocardiographic findings. Duke Endocarditis Service. (1994, March).
2. Erbel R, Rohmann S, Drexler M. Mohr-Kahaly S, Gerharz CD, Iversen S, … Meyer, J. Improved diagnostic value of echocardiography in patients with infective endocarditis by transoesophageal approach. A prospective study. (1988, January) Retrieved from
3. Evangelista A, & Gonzalez-Alujas MT. Echocardiography in infective endocarditis. (2004, June).
4. Li JS, Sexton DJ, Mick N, Nettles R, Fowler VG, Ryan T, … Corey GR. Proposed modifications to the duke criteria for the diagnosis of infective endocarditis. (2000, April).
5. Livingston LV, & Perez-Colon E. Streptococcus intermedius bacteremia and liver abscess following a routine dental cleaning. (2014, August).
6. Maliyil J, Caire W, Nair R, & Bridges D. Splenic abscess and multiple brain abscesses caused by Streptococcus intermedius in a young healthy man. (2011, July).
7. Mejàre B, & Edwardsson S. Streptococcus milleri (Guthof); an indigenous organism of the human oral cavity. (1975, November).
8. Rashid RM, Salah W, & Parada JP. 'Streptococcus milleri' aortic valve endocarditis and hepatic abscess. (2007, February).
9. Topan A, Carstina D, Slavcovici A, Rancea R, Capalneanu R, & Lupse M. Assessment of the Duke criteria for the diagnosis of infective endocarditis after twenty-years. An analysis of 241 cases. (2015, July).
10. Tran MAP, Caldwell-McMillan M, Khalife W, & Young VB. Streptococcus intermedius causing infective endocarditis and abscesses: a report of three cases and review of the literature. (2008, November 10).
11. Whiley RA, Beighton D, Winstanley TG, Fraser HY, & Hardie JM. Streptococcus intermedius, Streptococcus constellatus, and Streptococcus anginosus (the Streptococcus milleri group): association with different body sites and clinical infections. (1992, January).
12. Woo PCY, Tse H, Chan K-ming, Lau SKP, Fung AMY, Yip K-tong, … Yuen K-yung. 'Streptococcus milleri' endocarditis caused by Streptococcus anginosus. (2004, February).

A27 MANTLE CELL LYMPHOMA COMPLICATED BY CARDIAC TAMPONADE

[1]Julien Feghaly, [2]Ariana Mooradian. *[1]St Louis University School of Medicine, St Louis, MO; [2]St Louis University School of Medicine*

10.1136/jim-2020-MW.44

Introduction/Background Malignant pericardial effusion is a common but serious complication of solid tumors & hematological malignancies. Rarely these effusions exhibit life-

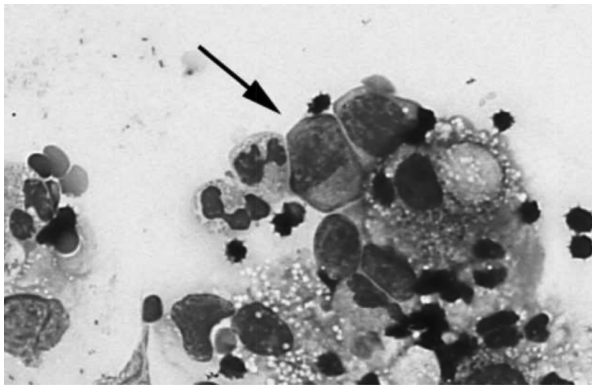

Abstract A27 Figure 1
Cells consisting of large lymphocytes (arrow), moderate macrophages & eosinophils, and few neutrophils, small lymphocytes & mesothelial cells

threatening cardiac tamponade physiology leading to circulatory & respiratory compromise, requiring prompt evaluation & treatment.

Case Presentation A 65-year-old male with a history of mantle cell lymphoma presented with shortness of breath worse on exertion. He denied orthopnea, chest pain, fevers, chills, and had not required oxygen. He was diagnosed one year prior by bone marrow biopsy, status post four cycles of bendamustine and rituximab with complete remission on PET CT after cycle three. Six months following initial diagnosis, he presented with abdominal pain and CT at that time showed multiple soft tissue masses in the mediastinum, left upper quadrant and both cutaneous and subcutaneous tissues concerning for progression of the disease. He underwent Hyper CVAD the following month and two months later underwent autologous stem cell transplantation. Along with shortness of breath, he reported cold intolerance, dysuria, and worsening abdominal distension. Imaging from an outside hospital showed pleural effusion and pericardial effusion. On arrival, he was afebrile, tachycardic, with normal respiratory rate saturating 100% on room air. He had coarse sounds bilaterally, regular heart rhythm, distended abdomen, 2+ peripheral edema. Due to his shortness of breath, a transthoracic echocardiogram was ordered which showed new large pericardial effusion with tamponade physiology. He was taken for emergency catheterization and pericardiocentesis. Flow cytometry of fluid consistent with lymphomatous cells. Due to repeated relapse and progression of his lymphoma, the patient ultimately decided to transition to comfort care and expired.

Discussion Pericardial disease may develop through various mechanisms: direct or metastatic spread via the bloodstream or lymphatics to the pericardium, radiation toxicity, chemotherapy toxicity or opportunistic infections. In certain malignancies, pericardial effusion may be the first presentation, often rapidly progressing and recurrent. As such, prompt diagnosis, therapeutic management & a multi-disciplinary approach play an important role in maintaining hemodynamic stability & improving prognostic outcomes. Patients with pericardial tamponade often present with shortness of breath, dyspnea, chest pain, palpitations, dizziness, fatigue, and syncope; associated with Beck's triad of hypotension, tachycardia, and muffled heart sounds. Prompt pericardiocentesis is highly recommended for pericardial effusions exhibiting cardiac tamponade physiology especially in the setting of circulatory & respiratory compromise.

A28 CODE STROKE! A CASE OF NONBACTERIAL THROMBOTIC ENDOCARDITIS

[1]Julien Feghaly, [2]James Ampadu, [3]Debapria Das. *[1]St Louis University School of Medicine, St Louis, MO; [2]University of California San Diego School of Medicine; [3]St Louis University School of Medicine*

10.1136/jim-2020-MW.45

Introduction/Background Mitral valve masses are at an increased risk for embolic events due to their location, instability, and interaction with the dynamic movement of the heart. Thus, given their high-risk prompt identification and treatment is essential to reduce the threat of permanent neurological deficit.

Case Presentation A 73-year-old female with a history of diabetes mellitus type II presented with acute confusion and dysarthria. 'Code stroke' was initiated. Due to favorable circumstances & lack of contraindications, tissue plasminogen activator was administered with the resolution of her symptoms. Imaging for the stroke displayed acute lacunar infarctions of the right thalamus and occipital lobe. Transthoracic echocardiogram went on to show normal left ventricular function without a cardioembolic source. Due to a persistent

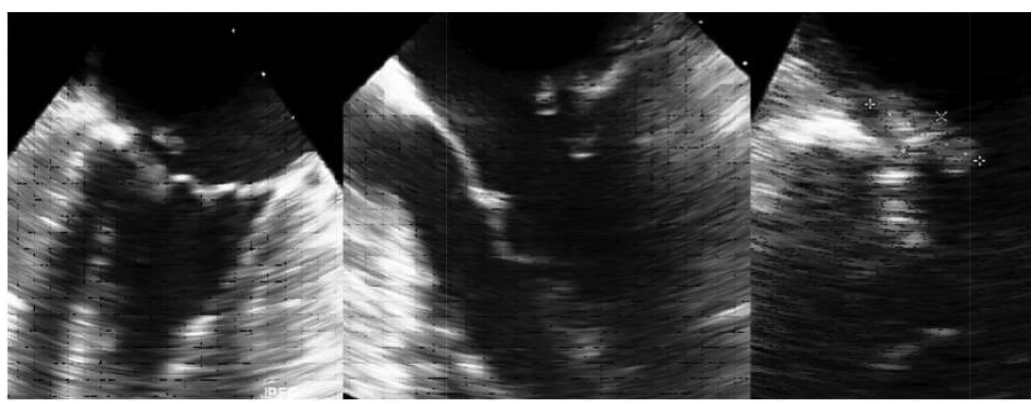

Abstract A28 Figure 1
Transesophageal echocardiogram revealing a mobile hyperechoic density on the posterior mitral valve annulus, measuring 1.1 × 0.5 cm (far right)

heightened suspicion for an embolic phenomenon, a transesophageal echocardiogram was obtained revealing a mobile hyperechoic density on the posterior mitral valve annulus, measuring 1.1 × 0.5 cm, thought to be a vegetation versus annular calcification (figure 1). Given the mobility, size of the lesion, and location, there was a concern for recurrent embolization. Multiple specialty teams decided the best approach to prevent a potentially catastrophic event was surgical resection. This intervention carried its risks however it served to definitively prevent further embolization and characterize the mass. Favorably, the patient tolerated the surgery well and was discharged on postoperative day four, following negative malignancy & hypercoagulable workup. The pathology later resulted in a calcified thrombotic vegetation, keeping with nonbacterial thrombotic endocarditis (NBTE).

Discussion To date, no medical management has been identified to reverse valvular vegetations seen in NBTE. Current therapeutic options for NBTE focus on anticoagulation and surgical resection, while managing the risk for systemic embolization. Anticoagulation is often favored due to concern for recurrent embolization, however, it increases the risk of life-threatening bleed such as central nervous system hemorrhage. The American College of Chest Physician recommends long-term anticoagulation regardless of the evidence for emboli. Whereas, surgical resection offers a definitive treatment option for left-sided masses (>1 cm), as anticoagulation alone is not entirely protective due to the risk of fragment embolization.

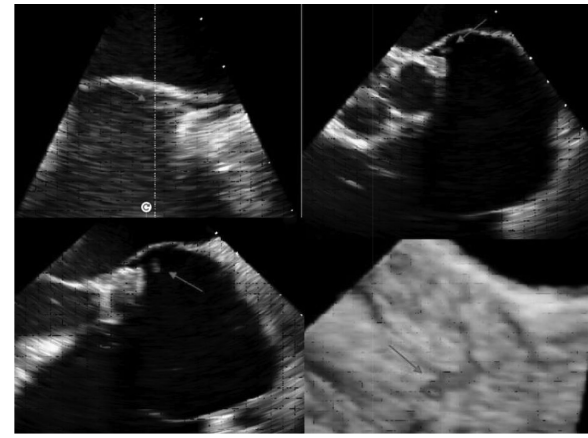

Abstract A29 Figure 1
Transesophageal echocardiogram demonstrating thrombus lodged in a patent foramen ovale, with approximately 5–7 mm of thrombus in the right atria

A29 SORRY, YOUR TRIP HAS BEEN DELAYED: THROMBUS IN TRANSIT

[1]Julien Feghaly, [2]James Ampadu, [3]Steven Smart. *[1]St Louis University School of Medicine, St Louis, MO; [2]University of California San Diego School of Medicine; [3]St Louis University School of Medicine*

10.1136/jim-2020-MW.46

Introduction/Background Thrombus in transit (TT) is a rare phenomenon, reported to be seen in 4% of acute pulmonary emboli (PE). In combination, TT and PE carry a high mortality rate of 28% and 80–100% if left untreated. Hence once diagnosed, immediate treatment is required. Yet, no clear consensus on the optimal treatment approach is present.

Case Presentation A 66-year-old male with a history of hypertension presented with shortness of breath. Imaging revealed acute PE. Echocardiogram supported this with evidence of right ventricular strain. There was also a mobile mass seen near the tricuspid valve, concerning for TT. Transesophageal echocardiogram confirmed TT that was lodged in a small patent foramen ovale. There was 5–7 mm of thrombus on the right atrial side of the septum and no thrombus seen on the left atrial side of the septum (figure 1). Given the risk for embolization, multiple specialty teams were involved in making a clinical decision. Medical therapy, surgical embolectomy, thrombolysis, and percutaneous thrombus aspiration were all considered as potential treatment options. The decision was made that percutaneous or open surgical intervention was a prohibitively higher risk to this patient. Systemic anticoagulation was chosen, and the patient was discharged from the hospital. A repeat echocardiogram at three months showed resolution of the thrombus and, more importantly, the patient did not have complications from the thrombus in the interim.

Discussion TT is a medical emergency requiring prompt recognition and treatment to reduce mortality. The several treatment options available need to be evaluated on a case-by-case basis. Yet, patients who are deemed high surgical risk or are found to have a small patent foramen ovale, are to further benefit from anticoagulation versus surgical intervention.

A30 STAPHYLOCOCCUS PSEUDINTERMEDIUS, AN UNPLEASANT GIFT FROM A DOG TO ITS OWNER

[1]Suha Abu Khalaf, [2]Abdallah Mansour, [1]Dima Dandachi. *[1]University of Missouri-Columbia; [2]University of Missouri- Columbia, columbia, MO*

10.1136/jim-2020-MW.47

Introduction/Background Staphylococci are considered common pathogens in dogs with soft tissue infections. Staphylococcus pseudintermedius (S. pseudintermedius), which is viewed as a part of the normal flora of cats and dogs, are known to cause otitis externa and other soft tissue infections in dogs. Recent reports have raised concern for developing multiple antimicrobial resistance and violence factors, including the ability to form biofilms and cause debilitating canine infections. It is rarely reported for a human to develop an infection secondary to S. pseudintermedius, and the reported cases were mostly immunocompromised, dog owners who present with soft tissue infections. We present a case of S. pseudintermedius infection in an immunocompromised patient to add our case to the growing literature and consider it as a potential organism when dealing with recurrent skin and soft tissue infections in immunocompromised dog owners.

Case Presentation A 37-year-old female who presented to the emergency department complaining of right ear pain, redness, swelling, with purulent, foul-smelling discharge, and intermittent chills for the previous six months. Her medical history was remarkable for sarcoidosis treated with methotrexate, splenectomy in 2014, thrombocytosis treated with hydroxyurea, uncontrolled diabetes mellitus (hemoglobin A1C 9.4), recurrent otitis externa since 2001. Over the years, the patient has been treated with different antibiotics for her recurrent otitis

externa, treatment was frequently interrupted by her developing allergies to multiple antibiotics, and no causative organism was detected. Of note, the patient reports having two dogs at home. Upon presentation, the patient was afebrile with stable vital signs. Physical exam was remarkable for tender, swollen, and erythematous right external ear canal with crusted yellowish discharge. Labs were notable for a mild leukocytosis with a white count of 12 × 109/L and 93% neutrophils. Computed tomography (CT) of the head didn't show an underlying abscess or fluid collection. The patient was admitted for further workup and treatment and was empirically started on intravenous vancomycin and aztreonam, in addition to ciprofloxacin/dexamethasone ear drops. The ear discharge was swabbed, and the culture grew heavy penicillin-resistant, methicillin-sensitive S. pseudintermedius. The patient was allergic to penicillin (difficulty breathing) and hence was started on trimethoprim-sulfamethoxazole and continued ciprofloxacin/dexamethasone ear drops for a total of 14 days of antibiotics, the patient was advised to avoid contact with her pets to prevent further recurrence. The patient improved significantly on follow up one month after discharge with no residual symptoms.

Discussion S. pseudintermedius is the most common microorganism of the skin and mucosa flora of dogs and cats. It was described in 2005 and was found to be a major bacterial pathogen causing skin and ear infections in these animals. S. pseudintermedius was also reported initially in 2010 to cause human soft tissue and wound infections in owners of infected pets. Even though it is rare, it might be underreported and missed in patients who are immunocompromised and present with recurrent skin and soft tissue infections despite treatment. Clinicians should be aware of the possibility of zoonotic transmission of this infection, especially in immunocompromised patients, making avoiding contact with such pets essential to prevent further recurrence.

A31 SULFASALAZINE INDUCED LUNG DISEASE, A DIAGNOSTIC CHALLENGE

[1]Suha Abu Khalaf, [2]Abdallah Mansour, [1]Beenish Zulfiqar. [1]*University of Missouri-Columbia*; [2]*University of Missouri- Columbia, Columbia, MO*

10.1136/jim-2020-MW.48

Introduction/Background Sulfasalazine-induced lung disease (SILD) is a rarely reported entity that presents with various presentations that mimic eosinophilic pneumonitis, pulmonary vasculitis, Interstitial lung disease, and pulmonary fibrosis. The typical manifestations of SILD include dyspnea, pleuritic chest pain, cough, and fever. Chest imaging could show nonspecific infiltrates that will blur the diagnosis and make it more challenging for the clinicians. The majority of the patients improved with discontinuation of Sulfasalazine. We present a case of a 22-year-old female who presented with pulmonary symptoms three weeks after starting sulfasalazine. Clinical thinking, detailed workup, management, and follow up are discussed to highlight the importance of keeping SILD under our radar in such cases, to reduce time to diagnosis and facilitate prompt treatment.

Case Presentation The patient is a 22-year-old female who presented to our hospital complaining of three weeks history of right-sided pleuritic chest pain and nausea. She has a past medical history of ulcerative colitis (UC) for which she was started on sulfasalazine six weeks before the presentation and a history of recent nicotine vaping. On presentation, the patient was afebrile, tachycardic with a heart rate of 110 beats/min, tachypneic with a respiratory rate of 25 breaths/min, and had an oxygen saturation of 95% on ambient air. The initial laboratory workup is summarized in table 1. Infections workup was also negative for bacterial, viral, and fungal infections, blood and urine cultures, respiratory pathogen panel, urine streptococcus pneumonia, legionella, and

Abstract A31 Table 1 Initial laboratory workup

Lab test (unit)	Result	Reference value
Complete blood count		
Hemoglobin (g/dl)	10.3	12-15.5
Hematocrit (%)	31	34.9-44.5
MCV (fl)	87	81.6-98.3
WBC (× 10^9/l)	7.79	3.5-10.5
ANC (× 10^9/l)	7	1.7-7
Platelets count (x10^9/l)	320	150-450
Complete metabolic panel and miscellaneous		
Creatinine (mg/dl)	0.59	0.5-1.2
BUN (mg/dl)	8	6.0-20
Na^+ (mmol/l)	137	136-145
K^+ (mmol/l)	3.9	3.5-5.1
Cl^- (mmol/l)	103	92-107
HCO_3^- (mmol/l)	24	22-29
Total bilirubin (mg/dl)	0.24	0.0-1.6
INR	1	0.9-1.1
PTT (seconds)	28.7	25.7-35.2
AST (units/L)	10	<32
ALT (units/L)	8	<35
ESR (mm/hour)	22	0-20
CRP	9.15	0.0-0.5

ANC: absolute neutrophil count; BUN: blood urea nitrogen; Cl-: chloride; HCO3-: bicarbonate; INR: international normalized ratio; K+: potassium; MCV: mean corpuscular volume; Na+: sodium; PTT: partial thromboplastin time; WBC: white blood cell; AST: aspartate aminotransferase; ALT: alanine transaminase; ESR: erythrocyte sedimentation rate; CRP: C-reactive protein

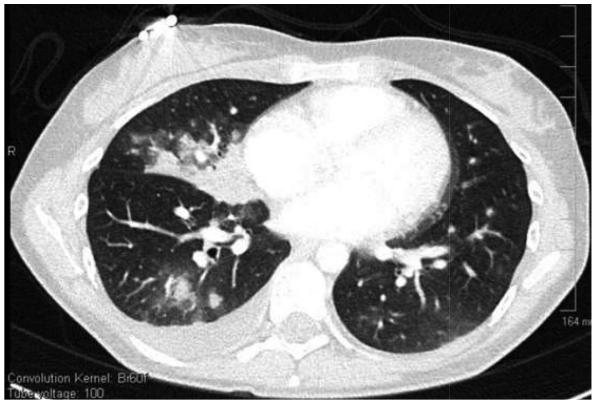

Abstract A31 Figure 1 Chest CT scan upon presentation
Bilateral patchy infiltrates with moderate right pleural effusion

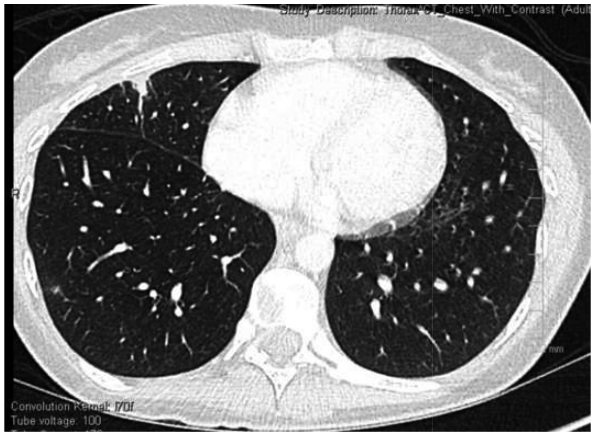

Abstract A31 Figure 2 Chest CT scan three weeks after discharge
Resolution of the pleural effusion and infiltrates a few weeks after holding the sulfasalazine

Histoplasma antigens, coccidiomycosis antibodies, Blastomyces antigen were unremarkable. Urine analysis was negative for blood or protein. X-ray and computed tomography (CT) of the chest (figures 1,2) revealed multifocal lower lung predominant pulmonary consolidations with no evidence of pulmonary embolism (PE). Differential diagnoses initially included multifocal pneumonia, malignancy, vasculitis, embolic phenomenon, and vaping-induced lung disease (VILD). CT of the abdomen ruled out UC flare and pancreatitis. Sulfasalazine was held until further evaluation. Transthoracic echocardiography was done and was unremarkable for valvular vegetations or intrachambers thrombi to explain a source of embolization. Over the subsequent days, the patient's symptoms worsened, and she was found to have interval development of right pleural effusion on a follow-up CT scan of the chest. She underwent thoracentesis, which revealed a sanguineous exudative effusion, 13000 WBCs with 69% polymorphonuclear cells, and no malignant cells were found on cytology. After that, she underwent bronchoscopy with bronchoalveolar lavage (BAL), transbronchial biopsy, and micro brushing of the right lower lobe; This has returned negative for malignant cells and no significant findings on microbiological testing. Lipid laden macrophages staining with Oil Red O to rule out VILD was negative as well. Cardiothoracic surgery was consulted to perform a video-assisted thoracoscopic surgery (VATS) guided right upper lobe lung wedge resection to obtain a better histological specimen. A week after, the pathology results came back, showing coagulative necrosis with acute and granulomatous inflammation and vasculitis suggestive of granulomatosis with polyangiitis (GPA). The pathology specimens were sent to Mayo Clinic labs for a second opinion, which also confirmed the diagnosis. Her antinuclear antibodies (ANA) titers were 1/1280. Anti-neutrophil cytoplasmic antibodies (ANCAs) levels were negative. Follow up CT chest three weeks after discharge (figure 2) showed marked improvement in the bilateral opacities and right pleural effusion with significant improvement in symptoms.

Discussion The patient's presentation carries a very high suspicion for SILD due to the temporal association between the symptoms' development and the initiation of sulfasalazine therapy. Also, the discontinuation of sulfasalazine was sufficient to result in the resolution of symptoms and radiological findings. Primary vasculitis, such as GPA, is a possible diagnosis given the pathological findings; however, a negative ANCAs, normal kidney function and absence of hematuria favor the diagnosis of SILD over primary GPA. Limited GPA with negative ANCAs was reported in the setting of SILD. Clinicians should be vigilant when evaluating patients who present with pulmonary symptoms shortly after starting sulfasalazine therapy.

A35 A CASE OF RECURRENT DIABETIC MYONECROSIS

[1]Arabelle Abellard, [2]Shahnur Saiyad, [3]Mihaela Mihailescu. *[1]University of Illinois At Chicago – ACMC, Oak Lawn, IL; [2]University of Illinois at Chicago – ACMC; [3]Advocate Christ Medical Center*

10.1136/jim-2020-MW.49

Introduction/Background Diabetic myonecrosis, which is also referred to as diabetic muscle infarction, is a rare, unusual microvascular complication of diabetes mellitus that is not always recognized initially. The pathophysiology of diabetic muscle infarction is also not well understood at this time. This case highlights diabetic myonecrosis as a distinctive myopathy that should be considered in the differential diagnosis of any patient with long-standing, poorly controlled diabetes mellitus who presents with sudden, atraumatic muscle pain. With uncontrolled diabetes, there is a high rate of recurrent diabetic myonecrosis, usually involving the contralateral side.

Case Presentation A 35-year-old African American woman with a history of hypertension, poorly controlled type 2 diabetes mellitus, peripheral neuropathy, chronic kidney disease (stage 3) presented to the emergency department (ED) for sudden, left thigh pain that started three weeks prior. She was already seen in a clinic and in the ED for this pain and was prescribed analgesics, but the pain persisted. She reported muscle spasms in her left thigh and described a throbbing and constant pain that radiated to her left hip. She was able to walk and bear weight, but her thigh pain worsened with movement and palpation. She denied any history of trauma, insect bites, fever, or chills. Examination revealed diffuse tenderness over the anterior lateral aspect of her left thigh. No redness, discoloration, induration, soft tissue fullness or fluctuance were noted, but the left thigh was warm to the touch. Her BMI was 50. Bloodwork included CK 387 units/L, CRP 5.5 mg/dL, ESR 96 mm/hr, WBCC 12300 cells/mm3, platelet count 458000 cells/mcL, and hemoglobin A1c 14%. MRI revealed extensive subcutaneous superficial perifascial edema throughout the left thigh with significant intramuscular edema within the

vastus lateralis and an area of non-enhancing necrotic tissue in this muscle. The patient underwent irrigation and debridement. No gross purulence was seen intraoperatively, but diffuse edema of the vastus lateralis was found, with clear fluid. Cultures were unremarkable. She improved quickly after the procedure and was discharged home three days later on milder analgesics and insulin, and compliance was emphasized. This intervention was however, complicated several days later by an infection in the wound and required a course of antibiotics and superficial debridement. She presented back to the ED one year later for worsening right calf pain, with cramps and swelling that started four weeks ago. She also complained of polyuria and was found to have very high serum glucose and hemoglobin A1c. She denied fevers, chills and acute trauma to her right calf. Doppler study showed no evidence of deep venous thrombosis and radiographs showed no fracture. MRI of the right lower extremity showed diffuse muscular edema in the gastrocnemius muscle medially, with moderate enhancement. A non-enhancing area in the gastrocnemius muscle, consistent with necrosis, was observed. This time, the patient was treated conservatively, with non-operative management. She was educated again about nutrition and the complications of uncontrolled diabetes with strong emphasis on compliance and follow-ups.

Discussion Diabetic myonecrosis usually occurs as a late complication of diabetes mellitus and there is a high recurrence rate, typically on the contralateral side, in those with uncontrolled disease. It is more commonly seen in women. Diabetic muscle infarction should be considered in the differential diagnosis of any patient with long-standing, poorly controlled diabetes mellitus who presents with sudden, atraumatic muscle pain, especially in the thigh or calf muscles. In general, MRI is considered the diagnostic tool of choice, over muscle biopsy or surgical exploration when evaluating stable patients with suspected diabetic myonecrosis. Characteristic features on MRI include hyperintense signals on T2-weighted sequences. The areas of high signal are due to edema and inflammation. T1-weighted images usually appear isointense or hypointense. To minimize complications, conservative management of diabetic myonecrosis, with good glycemic and pain control, is usually recommended over surgical intervention; progressive improvement is noted over several weeks.

A41 IT'S APPENDAGITIS, NOT APPENDICITIS!

[1]Zarak Khan, [2]Mohammad Alam, [2]Danekka Loganathan, [2]Randa T Alsayed, [2]Narayana Gandham, [2]Ryan Wolok. *[1]St Mary Mercy Hospital, Livonia, MI, West Bloomfield, MI; [2]St Mary Mercy Hospital, Livonia*

10.1136/jim-2020-MW.50

Introduction/Background Epiploic appendages are small peritoneal fat pouches located around the colon. Although they serve no specific function, they are known to get occasionally inflamed, a condition known as 'epiploic appendagitis'. This inflammation is due to either ischemia from spontaneous torsion leading to gangrenous necrosis or by thrombosis of the associated vein and inflammation. Although, they are found spread all over the serosal surface of the colon, they are much more abundant and larger on the sigmoid and transverse colon walls. Due to the location of the appendages, acute appendagitis can involve the sigmoid colon, descending colon and cecum, thus having equivocal presentation to more serious conditions including diverticulitis and appendicitis. This imitation of symptoms can lead to misdiagnosis and mistreatment of this condition.

Case Presentation 66-year-old gentleman with past medical history of hypertension, type 2 diabetes mellitus and hyperlipidemia presented to the outpatient clinic with 1-day history of right lower quadrant pain. Pain was gradual in onset, 6/10 in intensity, throbbing in quality, non-radiating and associated with some nausea and four episodes of non-bloody vomiting. He denied fever, chills, back pain, bloating, heartburn, malena or hematochezia, constipation or diarrhea. Complete blood count, comprehensive metabolic panel, lipase, and urinalysis were done which were only significant for a white blood cell count of 11,100 with 9,210 neutrophils. CT scan of the abdomen and pelvis demonstrated epiploic appendagitis involving the sigmoid colon. Patient was advised to continue diet and manage pain with ibuprofen as needed. He was also advised to go to the emergency department if his condition worsens. Patient's symptoms resolved in the next 2 days and he was back to baseline.

Discussion Epiploic appendagitis has been reported in 2–7% of patients with a presumed clinical diagnosis of acute diverticulitis and 0.3–1% of those suspected of having acute appendicitis. Owing to the nonspecific nature of presenting symptoms, physical signs, and laboratory findings, it is extremely difficult to make the correct diagnosis without radiological investigations. Therefore, most cases are detected incidentally on CT scans while ruling out other intra-abdominal pathologies. CT scan is the gold standard of diagnosis. It requires only conservative management in most cases. Only cases with persistent symptoms require laparoscopic appendagectomy. Therefore, it is pivotal to correctly diagnose and treat this condition to avoid unnecessary hospitalizations, antibiotic use and surgical interventions. Our case report is meant to shed light on the diagnosis and management of the condition.

A46 CASE REPORT: ELEVATED CREATININE AS AN INITIAL PRESENTATION OF STAGE IV UROTHELIAL CARCINOMA

[1]Salah D Dajani, [2]Suresh Kumar, [3]Nfn Shakuntulla. *[1]Amita St. Joseph's Hospital, CHICAGO, IL; [2]Saint Joseph Hospital, Chicago, Chicago, IL; [3]OSF Heart of Mary Medical Center, Chicago, IL*

10.1136/jim-2020-MW.51

Introduction/Background Urothelial carcinoma is the predominant form of bladder cancer, accounting for almost 90% of all bladder cancers. Patients typically present with gross or microscopic hematuria, symptoms of obstruction, retention, dysuria, or increased frequency. Typically patients are over the age of 40 upon presentation. After initial presentation of symptoms, patients typically undergo cystoscopy for further evaluation of the urinary tract and bladder as cystoscopy combined with urine cytology is considered the gold standard. The addition of urine cytology is critical to detect lesions that may be missed by cystoscopy alone. At the time of cystoscopy, if a mass is noted, biopsy of the mass is performed. Additionally, at the time of cystoscopy the normal-appearing urothelium, bladder wall, and prostatic urethra may also be biopsied. The bladder is the source of positive cytology in roughly 80% of patients. Initial evaluation typically includes transurethral resection of bladder tumor which allows for further grading and staging after evaluating how extensive the invasion is.

Subsequently patients typically obtain a PET-CT for further workup. Treatment is then based on the staging of the cancer.
Case Presentation Patient is an 82 y.o. male with a PMHx of HTN, HLD, CAD S/P stenting in 2011, and Dementia, sent to the hospital in 09/2019 by his PCP as labs showed elevated creatinine of 4.0. His last creatinine was 1.8 in 08/2019. Patient's spouse reported that the patient has been experiencing urgency and incontinence that has been worsening over the past few months and associated with decreased frequency. Patient's spouse also reports the patient has had a 25 lb weight loss over the summer. He was treated for suspected UTI in 05/2019. The patient was diagnosed in 08/2019 with a bladder polyp and was planned to have a possible resection of the polyp in 09/2019. After presenting to the hospital and being found to have a significantly elevated creatinine, he was then admitted for further workup. CT-Abdomen & Pelvis showed bilateral hydronephrosis and hydroureter secondary to marked urinary bladder wall thickening. Patient was also noted to have uncomplicated cholelithiasis. Per urology recs patient placed on foley catheter and nephrotoxic agents were avoided. Urology performed cystoscopy on and found a large invasive bladder tumor. Patient is subsequently underwent nephrostomy tube placement. Pathology on bladder tumor biopsy showed invasive bladder carcinoma. Patient was then discharged and followed up with Oncology for further evaluation. Subsequent PET-CT showed para-aortic lymphadenopathy indicative of Stage IV Urothelial Carcinoma. The patient was deemed a poor candidate for cystectomy or chemotherapy. Given the patients poor performance status and advanced dementia, palliative care was consulted and the family decided to focus on comfort care.
Discussion As noted, there are multiple ways Urothelial Carcinoma may be detected. Typically, we note the presence of gross or microscopic hematuria. In this case, our patient was noted to have a bladder polyp at an earlier date and was simply being planned for polyp resection. It was only prior to the planned polyp resection that the patient underwent typical preoperative laboratory testing that revealed a markedly elevated creatinine. At this point, the patient's tumor had grown so large that it was impinging on the bilateral ureters, causing urinary retention and creatinine elevation. Obstruction is commonly relieved with ureteral stent placement or nephrostomy tubes. Our patient required nephrostomy tubes. This is a prime example of how tumor growth can present with atypical symptoms.

A47 THINK OUTSIDE THE BOX A NOVEL THERAPEUTIC OPTION FOR SECONDARY CNS LYMPHOMA

[1]Sayan Mullick Chowdury, [2]Joshua Palmer, [2]Narendranath Epperla. *[1]Ohio State University, Columbus, OH; [2]The Ohio State University*

10.1136/jim-2020-MW.52

Introduction/Background Secondary central nervous system lymphomas (SCNSL) are rare forms of lymphoma that originate from CNS involvement of a systemic lymphoma either at presentation or relapse. The majority of these cases (~90%) are diffuse large B-cell lymphoma (DLBCL). SCNSL are highly resistant to current treatment options with poor prognosis overall. There are no guidelines for the treatment of SCNSL, however, in general, these patients are treated with agents that have CNS penetration such as high dose (HD) intravenous (IV) methotrexate (MTX) or cytarabine. Here we report a case of relapsed SCNSL that showed sustained response with fractionated stereotactic radiosurgery (FSRS) followed by R2 (Rituximab and Revlimid) indicating a possibly novel treatment option for this aggressive disease.
Case Presentation A 72-year-old male with stage IV DLBCL (GCB subtype without c-myc rearrangement) involving multiple nodal and extranodal sites including, liver, bone and bone marrow was treated with R-CHOPx3 and R-miniCHOPx3 (due to cytopenias) and intrathecal MTXx4 (high CNS IPI and epidural involvement). End of treatment PET scan showed excellent systemic response but with a new right caudate nucleus lesion confirmed on MRI brain (which showed a new enhancing right-sided brain lesion involving the ependyma and extending from the caudate nucleus into the septum pellucidum near the foramen of Monroe). The biopsy of the brain lesion came back consistent with DLBCL. He received 2 cycles of rituximab and IV HD MTX with a very good partial response (PR). He could only receive one additional cycle of HD MTX (of the planned 6 cycles) due to significant fatigue and prolonged cytopenias. Bone marrow biopsy showed a hypocellular marrow with minimal tri-lineage hematopoiesis possibly secondary to the myelosuppression from HD chemotherapy precluding treatment with cytarabine and autologous stem cell transplantation. Restaging MRI brain 6 weeks following the third cycle showed progression of disease in the brain, while PET scan was negative for systemic relapse. He underwent FSRS (to frontal mass, foramen of Monroe, 24 Gy in 3 fractions) followed by R2 therapy (lenalidomide dose of 20 mg). The first cycle of R2 was complicated by neutropenic fever secondary to central line associated infection (pantoea septica) necessitating a dose reduction of lenalidomide to 10 mg/day. Restaging MRI brain after 2 cycles of R2 showed excellent response to therapy (near-complete remission). The patient remains on R2 therapy and is currently on cycle 7 with no new clinical or radiographic findings.
Discussion SCNSL lymphoma is an aggressive disease that is refractory to current therapeutic options. IV HD MTX is an effective therapeutic option in those who did not receive this previously. Even in these patients, administration of IV HD MTX may not be possible due to poor performance status or multiple co-morbidities especially renal insufficiency. Hence, there is an urgent unmet need for novel therapeutic options for the management of SCNSL. We show for the first time that SRS followed by R2 could be an effective and well-tolerated therapeutic option for treatment of SCNSL. This approach needs to be explored in a systematic fashion in larger cohort to validate our findings.

A49 THE TALE OF TWO TUMORS: MIXED NEUROENDOCRINE AND NON-NEUROENDOCRINE NEOPLASM MASQUERADING AS GASTRIC OUTET OBSTRUCTION

[1]Yousaf Zafar, [2]Anas Al Bawaliz, [3]Adnan Zafar. *[1]Naples Community Healthcare, FL; [2]University of Missouri- Kansas City; [3]CMH Lahore Medical College*

10.1136/jim-2020-MW.53

Introduction/Background Mixed neuroendocrine-non-neuroendocrine neoplasms (MiNEN) are tumors with two distinct neuroendocrine and non-neuroendocrine cell origins with each component comprising at least 30% of the entire neoplasm. These are rare tumors that have been reported in different

parts of the digestive tract. We report the case of MiNEN identified in the duodenum of a patient who presented with gastric outlet obstruction.

Case Presentation A 61-year-old African American male with past medical history significant for stage 2 prostate adenocarcinoma (in remission) and alcohol induced cirrhosis who presented with abdominal pain, intractable nausea and vomiting for one week and concomitant weight loss over the past few months. He was tachycardic and normotensive on presentation. Physical examination was remarkable for gastric splash without notable abdominal distention. A Computed Tomography of the abdomen showed focal thickening in the duodenum near the ampulla. An esophagogastroduodenoscopy was remarkable for a periampullary, protruding and fungating mass in the second part of the duodenum that was biopsied and confirmed to be adenocarcinoma. The endoscope could not traverse beyond the identified lesion. Patient underwent Whipple procedure and intra-operative biopsy revealed invasive well-differentiated intra-ampullary adenocarcinoma, arising in intraductal papillary mucinous neoplasm, in addition to a well-differentiated neuroendocrine tumor in the second part of the duodenum. Post-operative course was complicated by upper gastrointestinal bleeding from anastomotic site, hepatorenal syndrome, abdominal compartment syndrome and acute hypoxic respiratory failure. Due to poor prognosis and worsening condition family elected to pursue comfort care and the patient passed away.

Discussion The occurrence of MiNEN is rare and to our knowledge this is the first case to present as gastric outlet obstruction. Biopsies are needed to confirm diagnosis and surgical intervention is mainstay for management.

A50 A RARE MANIFESTATION OF A COMMON DISEASE: TENOSYNOVITIS ASSOCIATED WITH CLOSTRIDIUM DIFFICILE: A CASE REPORT AND REVIEW OF THE LITERATURE

[1]Greta M Josephson, [2]Saira Ajmal. *[1]University of Illinois Chicago/Advocate Christ Medical Center, Chicago, IL; [2]Advocate Christ Medical Center*

10.1136/jim-2020-MW.54

Introduction/Background Reactive arthritis is an aseptic, painful inflammatory arthritis that most commonly affects the large joints of the lower extremities. It typically develops following an enteric or genitourinary infection and the most well documented offending pathogens are Chlamydia, Salmonella, Shigella, Yersinia, and Campylobacter. We report a unique case of a young, healthy patient with tenosynovitis attributed to Clostridium difficile (C. difficile), and subsequent review of the literature. This case report outlines the clinical presentation and treatment course of an 18-year-old African American male with C. difficile colitis complicated by tenosynovitis of the bilateral hands. In addition, review of literature was performed yielding 53 available case reports. The search terms 'reactive arthritis' and 'C. difficile' were searched in PubMed. Two additional cases were excluded as they were published in French.

Case Presentation An 18-year-old healthy African American male with no significant past medical history presented with a nine day history of diffuse, severe abdominal pain and profuse diarrhea. In addition, two days prior to presentation to hospital, patient developed pain and swelling to the bilateral digits, as well as an erythematous/ecchymotic rash primarily localized over the second and third digits. Approximately four weeks prior to symptom onset patient was treated for strep pharyngitis with a course of antibiotics. On arrival, patient had a temperature of 38.0, mild tachycardia, and otherwise stable vital signs. He was noted to have diffuse abdominal tenderness and edema of the PIP/DIP joints with tenderness throughout the phalangeal soft tissue, consistent with tenosynovitis. Laboratory examination revealed a leukocyte count of 33.0 thou/mcL, with 23.8% neutrophils and 6.3% monocytes, C-reactive protein of 12.0 mg/dL (normal <1.0 mg/dL); otherwise hemoglobin, platelet, and erythrocyte sedimentation rate were within normal ranges. Results of blood culture and stool culture for Salmonella, Shigella, Campylobacter, Shiga toxin, E. coli, and Vibrio cholera were all negative, along with HIV testing. C. difficile toxin PCR returned positive, although C. difficile toxin EIA was negative. CT scan of the abdomen and pelvis with contrast demonstrated mural thickening and pericolonic stranding, consistent with extensive, severe colitis. Patient was started on treatment with oral vancomycin 125 mg every six hours and within approximately forty eight hours of treatment, he had significant improvement of symptoms, notably of the synovitis. Patient was discharged to home on hospital day seven to complete a total course of fourteen days of oral vancomycin. On follow-up appointment on day twelve, patient was noted to have complete resolution of the tenosynovitis.

Discussion Putterman and Rubinow outlined clinical criteria for the diagnosis of C. difficile reactive arthritis including: sterile inflammatory arthritis preceding diarrhea with previous antibiotic exposure, stool test positive for C. difficile toxin, and no acceptable alternative diagnosis for either diarrhea or arthritis; all of which our patient fulfilled (5). Our literature review revealed 22.6% (12/53) of cases had involvement of hands, although all also had involvement of other joints. Our patient's isolated tenosynovitis of bilateral hands is unique, and has only been reported once prior to our knowledge, in Wright *et al*. in 1976 (6). Literature suggests treatment of the underlying C. difficile infection should result in rapid clinical improvement of tenosynovitis symptoms, as in our patient. C. difficile continues to pose a significant threat to health and burden on the healthcare system. The association of reactive arthritis and C. difficile was first reported in 1976 by Rollins and Moeller, with only 53 subsequent cases reported (1, 3, 4, 6). Reactive arthritis classically presents as an asymmetrical oligio or polyarthritis most commonly involving the lower extremities or large joints (4). Our case demonstrates isolated tenosynovitis of the hands may also be a possible presentation. Given the continued rise of C. difficile infections, it is imperative that this pathogen be considered in such cases.

A51 PSOAS ABSCESS, PARASPINAL ABSCESS, EPIDURAL ABSCESS, CONTIGUOUS ABSCESSES IN A RARE PRESENTATION

Mohsin S Mughal, Wahab J Khan. *Monmouth Medical Center, Long Branch, NJ*

10.1136/jim-2020-MW.55

Introduction/Background Psoas abscess, paraspinal abscess and epidural abscess share risk factors and symptoms. Rarely these entities present together creating a medical dilemma of

medical management versus surgical management of the condition. We present a rare presentation of psoas abscess, paraspinal abscess that is contiguous with epidural abscess with severe cord compression in a 56 years old man after a fall without any skin laceration or hematoma formation. Psoas/Iliopsoas abscess can be classified into Primary and Secondary but sometimes it is hard to classify into one of those categories, especially in a scenario where involvement of contiguous structures can be a source or a consequence. In diabetics, trauma is considered a risk factor leading to the formation of hematoma and later iliopsoas abscess. Presentation can be back pain, flank pain, fever, limp or anorexia but often subtle that it can delay the diagnostic and therapeutic process.[1] In a case series, mortality in treated primary and secondary Psoas Abscess was 2.4% and 19% respectively. Astonishingly, if left untreated can go up to 100%.[1] When bacteria get access to the epidural space hematogenously or via direct extension, the Epidural Abscess develops. It can be either a spinal or an intracranial Epidural Abscess. Incidence of spontaneous Epidural Abscess (SEA) is less than 1% per 10,000 persons per year but it has been rising.[2 3] A case series reported an incidence of 5% per 10,000 persons that is an increase of five-fold.[3 4] Alongside DM, intravenous drug abuse, trauma and contiguous tissue infection can be a risk factor for the development of an epidural abscess. It has a variable presentation from back pain with no sensory-motor deficit to emergent limb paralysis. In case of non-operative treatment failure morbidity accounts for 22% risk of permanent paralysis and significant mortality of 3–25%.[5]

Case Presentation A 56-year-old diabetic male with poor glycemic control had a mechanical fall and started having localized, dull, left flank pain at the L2-L3 level. Initially presented to ED, where X-ray of the back was done that did not show any sign of fracture. He was discharged home on painkillers with a presumptive diagnosis of muscle sprain. Patient returned to ED two days later as he was unable to work. At the time of presentation he was having sharp, constant, left lower back pain at L3 level, 7/10 radiating to thigh, that worsen with the movement. Patient neither reported weakness, numbness, tingling nor he had any bowel or bladder dysfunction.[1] He reported having fever with chills at home but he was afebrile and non-toxic appearing at the time of admission. He did not endorse any lower urinary tract symptoms. In the ED he had leukocytosis WBC 26.2 with 91% neutrophil and one band. Random Blood sugar was 301 mg/dl. CRP was 463.8, urine analysis showed ketonuria 80 mg/dl and glucosuria 500 mg/dl HbA1c of 11. Blood cultures were sent, that came back negative. CT scan showed nonobstructive right-sided kidney stones and some irregular enlargement of left paraspinal muscles but no abscess. Initially patient was watched off the antibiotics in accordance with non toxic appearance. Patient continued to spike fever with inadequate pain control. Repeat blood culture showed MRSA bacteremia and he was started on Vancomycin.[6] MR was done that showed large left multiloculated, heterogeneously enhancing paraspinal abscess, psoas abscess measuring 25.6 × 8.0 × 9.5 cm (figure 1) extending as dorsal epidural abscess L2-L3 level with severe central stenosis (figure 2) and a component of it extending through neural foramina at L3-L4 level shows enhancement with moderate cord compression. Initially, medical management was opted with antibiotics. Interventional radiology attempted ultrasound-guided aspiration of the abscess twice but due to loculations, percutaneous drainage was not successful. They could aspirate only 3cc of it, an attempt to re-aspirate the injected contrast was unsuccessful.[7-] Patient clinically continued to deteriorate as he continued to spike fever and worsening pain. Repeat blood and abscess cultures both were positive for MRSA.[8] Wshile the patient was receiving intravenous antibiotics.[6] Due to the inability to achieve adequate vancomycin trough level, daptomycin was started, and later in course due to persistently positive cultures ceftaroline was added. General surgery and neurosurgery decided to take the patient to OR for drainage of psoas, paraspinal and epidural abscesses.[7] Incision and drainage of left Paraspinal Abscess and retroperitoneal drainage of Psoas Abscess was done.[9] Intraoperative finding showed significant subfascial paraspinal abscess. Patient tolerated the procedure well. Repeat fourth blood culture came back negative. Wound care was done on a daily basis. A follow-up MR of Lumbar and thoracic spine was donethat showed mild cord compression but size of epidural abscess decreased in size. Patient remained afebrile, leukocytosis resolved and his pain improved.

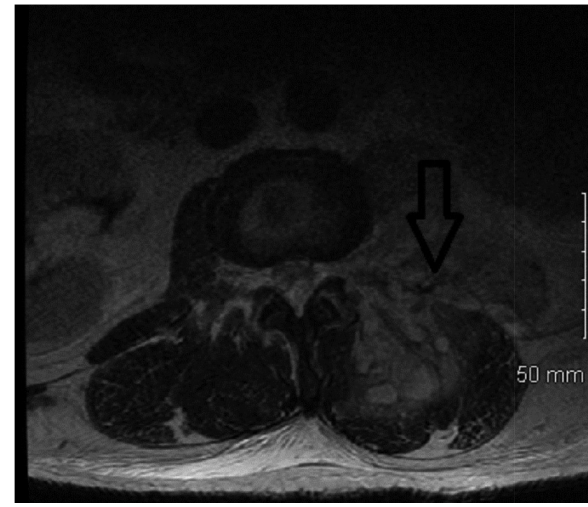

Abstract A51 Figure 1 T2 Axial section
Image shows psoas and paraspinal abscess

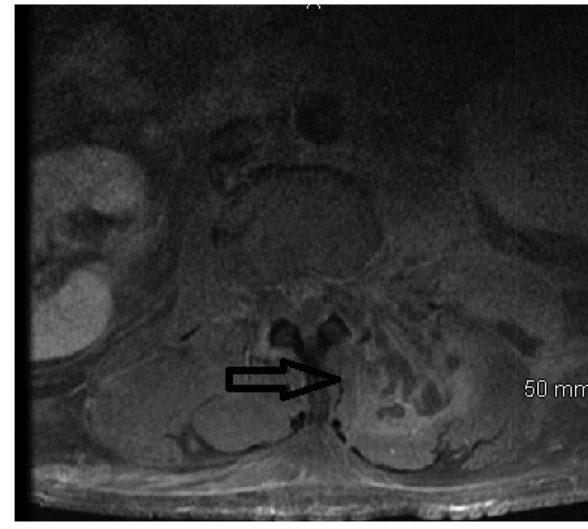

Abstract A51 Figure 2 T1 Axial section
Image shows psoas and paraspinal abscess

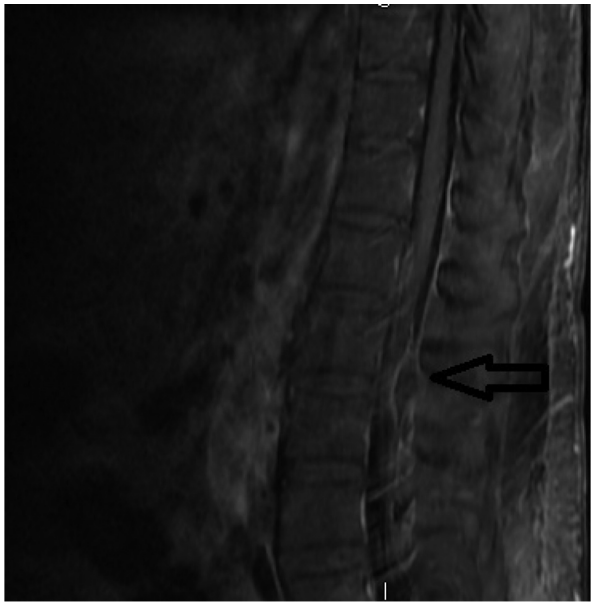

Abstract A51 Figure 3 Epidural abscess

Discussion Rarely, these infectious processes; psoas abscess, paraspinal abscess, and epidural abscess can coexist as they share many risk factors. Being contiguous structures, one process can be a source or a consequence of the other. Epidural abscess with cord compression is a neurosurgical emergency but management of this involves Infectious Disease, General Surgery, Neurosurgery and Interventional Radiology. Morbidity and mortality can be high as many of the patient with epidural abscess have 2–3 mean visits to the ED before medical admission and actual diagnosis. Psoas abscess can develop spontaneously in diabetics after a fall, without obvious skin tear or hematoma formation. It should be in our differentials as timely diagnosis and management either conservatively with antibiotics or surgically, incision and drainage of the abscess with better source control can improve the outcome and decrease the morbidity and mortality.[2 10] Studies are indicative of early surgical management for cervical epidural abscess is superior to conservative or late surgical intervention but insufficient data is available for spinal epidural abscess.[11]

A57 HEMODIALYSIS NEEDED IN IMMUNOGLOBULIN A NEPHROPATHY OR IS IT ALREADY TOO LATE? A CASE OF RAPIDLY PROGRESSIVE IMMUNOGLOBULIN A NEPHROPATHY

[1]Mansi Singapori, [2]Zarak Khan, [3]Kelly Mercier. *[1]St. Mary Mercy Hospital Livonia, MI, Northville, MI; [2]St Mary Mercy Hospital, Livonia, MI, West Bloomfield, MI; [3]St Mary Mercy Hospital, Livonia, MI*

10.1136/jim-2020-MW.56

Introduction/Background Immunoglobulin A nephropathy (IgAN) is the most common cause of primary glomerulonephritis. Most patients present with either one or recurrent episodes of gross hematuria, usually following an upper respiratory tract infection or microscopic hematuria on routine examination. A small percentage of patients present with nephrotic syndrome or acute kidney injury with or without oliguria.

Case Presentation Patient is a 21-year-old male with no significant past medical history who presented to the ED with two days history of fever, chills, headache, nausea, loose stools and dark colored urine. He stated his headache was in the temporal and occipital regions bilateral. He took Ibuprofen which improved the headache. He denied any urgency, frequency, photophobia and sick contact. Vital signs were significant for blood pressure of 173/97 mmHg. Initial lab work was significant for blood urea nitrogen (BUN) of 46.3 mg/dL, creatinine of 4.81 mg/dL, protein level of 6.0 gm/dL and albumin level of 2.8 gm/dL. Ultrasound KUB was within normal limits. Urine drug screen was negative. Urine analysis was significant for cloudy red colored urine with 3+ blood, 3+ protein, 172 RBCs, 1+ bacteria, 2+ granular cast and 2 + hyaline cast. Patient underwent extensive work up. Labs ordered included anti-glomerular basement membrane (GBM), complement C3 and C4 levels, anti-double stranded DNA (dsDNA), rheumatoid factor (RF), antinuclear antibody (ANA) and antistreptolysin O titers, cytoplasmic antineutrophil cytoplasmic antibodies (C-ANCA), Perinuclear antineutrophil cytoplasmic antibody (P-ANCA), HIV and screening tests for hepatitis A, B and C. All work up was negative. Urine protein-creatinine ratio was 5.07 consistent with nephrotic range proteinuria. Renal biopsy reported IgA nephropathy with global and segmental glomerulosclerosis as well as severe interstitial fibrosis and tubular atrophy. Patient was started on IV methylprednisolone with plan to transition to oral prednisone. During his hospital course, his creatinine continued to worsen to a level of 6.61 mg/dL. Within a month of diagnosis, patient was started on hemodialysis (HD) as renal function continued to worsen and he was subsequently put on renal transplantation list.

Discussion Despite IgAN being the most common glomerulonephritis, a case of rapid progression to ESRD is uncommon (<10%). Our case represents a small percentage of patients with IgAN acutely progressing to ERSD requiring HD. The most predictive factors for progression to ESRD are hypertension, severity of proteinuria, and findings of necrosis/fibrosis on the initial renal biopsy. As per treatment, our patient was immediately treated with steroids. However, despite its prevalence and clinical importance, the treatment is uncertain. We share this case to increase awareness about diagnosing and treating crescentic, rapidly progressive IgAN. If clinicians were able to diagnose these patients sooner and effective treatment was available, then there might be an improvement in clinical outcomes.

A58 DIAGNOSTIC DILEMMA: A COMPLICATED CASE OF ANCA VASCULITIS WITH MULTI SYSTEM INVOLVEMENT

[1]Urja Patel, [2]Muaataz Azawi, [3]Ismail Omran, [4]Anand Amin, [3]George Coritsidis. *[1]Icahn School Medicine at Mount Sinai, Elmhurst, NY; [2]Icahn School of Medicine at Mount Sinai, Astoria, NY; [3]Icahn School of Medicine at Mount Sinai; [4]Gmers medical college, Vadodara India*

10.1136/jim-2020-MW.57

Introduction/Background ANCA-associated vasculitis (AAV) is defined as inflammation of small to medium sized blood vessels. Uncommon presentations of AAV have been demonstrated in extremes of age with a PR3 predominance and are associated with subsequent development of AKI. The clinical manifestations of ANCA-associated vasculitis are broad,

varying from skin rash to multi system disease, which often leads to significant delay in diagnosis. Although AAV is often associated with renal and pulmonary manifestations, it can in fact extend to other organ systems. Despite recent advances in the treatment of AAV, these prove useless if the physician misses the diagnosis until after the disease irreversibly destroys organ systems. We present a complicated case of ANCA vasculitis with PR3 predominance and multi system involvement associated with rapid deterioration in clinical status and fatal outcome.

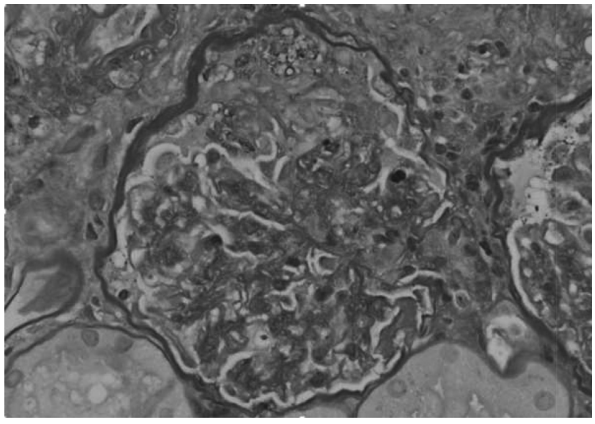

Abstract A58 Figure 1 PAS crescent

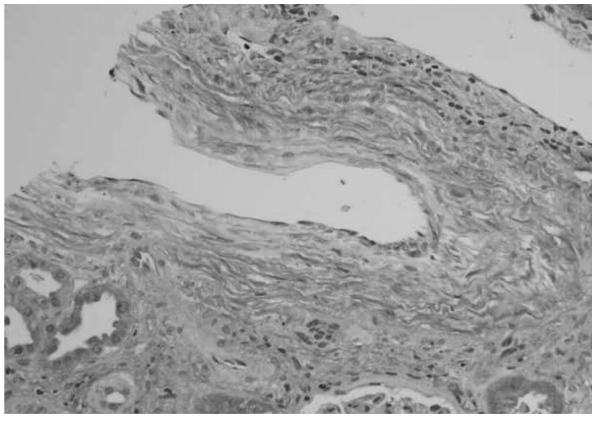

Abstract A58 Figure 2 Trichrome stain

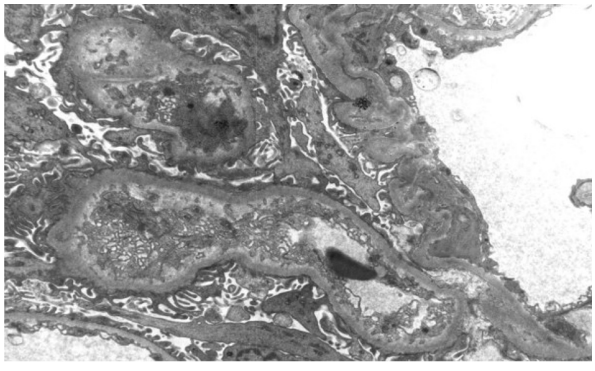

Abstract A58 Figure 3 EM subendothelial expansion

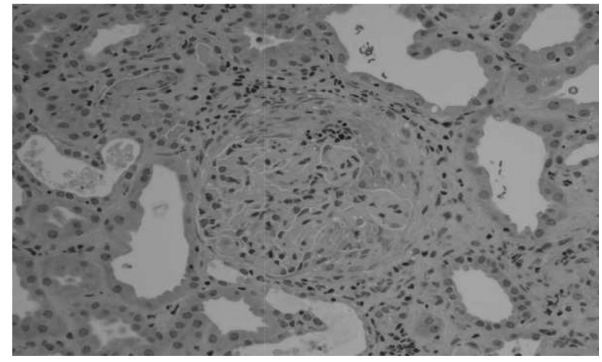

Abstract A58 Figure 4 H&E segmental fibrinoid necrosis

Case Presentation This patient was a 69-year-old female with history of hypertension, hyperlipidemia, hypothyroidism, diabetes, coronary disease and systolic heart failure, who presented with decreased urinary output and right flank pain. The patient was seen 2 months earlier for poly arthralgias and found to have positive serology for p-ANCA and ANA, but was lost to follow up. Laboratory exam indicated acute renal failure with creatinine of 4.28, an anion gap metabolic acidosis with lactate of 9.4 and HCO3–14. Autoimmune work up was again notable for P-ANCA positive at 1:1280, C-ANCA negative, MPO negative, PR3 positive with titer >200, antihistone antibody weakly positive at a titer of 1:11, anti-ds DNA -39 but complements were normal. Urine analysis showed few RBCs, protein 100 mg/dl on dipstick with UPCR-1.0 and granular casts. CXR showed bilateral infiltrates and patient was started on vancomycin and meropenem. CT abdomen and pelvis was negative for stones or obstruction but did however show bilateral pleural effusions. Transthoracic echocardiogram showed severely reduced left ventricular ejection fraction. Despite treatment, the patient continued to have significant electrolyte abnormalities as well as elevated liver enzymes and thrombocytopenia. Hemodialysis was initiated given oliguria and no improvement in renal function. Once platelet count was stable, patient underwent renal biopsy which showed pauci immune crescentic glomerulonephritis with thrombotic microangiopathy. Patient started to experience shortness of breath and worsening hypoxia requiring supplemental oxygen. Her rapid respiratory decline raised concern for diffuse alveolar hemorrhage, but bronchoscopy could not be pursued given the acuity of the condition. The plan was to start immunosuppressive therapy in the form of Rituximab or cyclophosphamide for RPGN secondary to ANCA vasculitis but deteriorated rapidly with worsening of respiratory status and hypoxia suggestive of ARDS. Family decided on comfort care and DNR.

Discussion In this case, the differential diagnosis was broad which included sepsis, ANCA vasculitis, lupus nephritis, drug induced lupus, cardiorenal syndrome and TTP. Diagnostic efforts were made more difficult due to bleeding diathesis. pANCA is typically associated with MPO and not PR3 however in this case the lab results were opposite. Atypical AAV presentations has been seen in the past with a previous case of Churg strauss syndrome and PR3. It has been implied that antibodies to minor antigens could contribute to lab discrepancies and may even contribute to AAV. However, it still remains unclear about the correlation of these ANCA associated minor antigens to a particular disease pattern and warrants further investigation.

A59 A SILENT KILLER: SPONTANEOUS ILIOPSOAS HEMATOMA IN A PATIENT ON ANTICOAGULATION

[1]Randa A Abd Algayoum, [2]Zarak Khan, [3]Mansi Singapori, [4]Narendra Khanchandani. *[1]St Mary Mercy Hospital, Canton, MI; [2]St Mary Mercy Hospital, Livonia, MI, West Bloomfield, MI; [3]St.Mary Mercy Hospital Livonia, MI, Northville, MI; [4]St Mary Mercy Hospital, Livonia*

10.1136/jim-2020-MW.58

Introduction/Background Spontaneous retroperitoneal hemorrhage is a known, but rare complication of anticoagulation therapy associated with high morbidity and a 30% mortality rate. The incidence rate of retroperitoneal haematoma as a complication of anticoagulation is about 1.3–6%.[1 2] Specifically, iliopsoas muscle hematoma is infrequent and is known to be between 0.1 and 0.6. Risk factors for retroperitoneal hematomas include anticoagulation, old age and hemodialysis.[3] Presenting symptoms range from mild groin pain to hypovolemic shock.[4] The exact mechanism is unknown but proposed hypotheses include forceful muscular strain, diffuse small vessel arteriosclerosis, heparin-induced immune microangiopathy, and unrecognized minor trauma. We present the case of a female who developed a spontaneous large retroperitoneal hematoma on intravenous heparin.

Case Presentation A 72-year-old lady with a history of congestive heart failure, chronic lymphedema and hypothyroidism, presented complaining of severe bilateral lower extremity swelling. Upon presentation, the patient was found to be in atrial fibrillation with rapid ventricular response. Physical examination revealed 3+ pitting bilateral lower extremity edema. Initial labs were significant for a an elevated BNP and hemoglobin was 12 g/dl. She was started on heparin and diltiazem drips for management of new onset atrial fibrillation. On the night of admission, rapid response was called due to hypotension. Patient's blood pressure was 64/40. Upon examination, patient had tenderness in the right middle and lower abdominal quadrants. Labs obtained revealed a drop in hemoglobin to 7 g/dl. CT scan of the abdomen and pelvis demonstrated a large right abdominopelvic retroperitoneal hematoma measuring 13.8 × 9.0 × 20.3 cm. Heparin was immediately discontinued and the patient was transfused with 2 units of packed RBCs. She was started on norepinephrine and the decision was made to transfer her to the intensive care unit for further management. Patient was managed conservatively with close monitoring, requiring a total of 4 packed red blood cell transfusions.Vascular surgery was consulted and they recommended conservative management. Patient was gradually weaned off the levophed and remained hemodynamically stable not requiring any surgical intervention. Her symptoms resolved, hemoglobin stabilized at 8.2 g/dl and she was transferred back to the medical floors. Hospital course was complicated with Congestive heart failure exacerbation, Hospital acquired pneumonia and Acinetobacter bacteremia requiring IV antibiotics and Lasix. Patient improved and was eventually discharged to sub-acute rehab on oral Augmentin and diuretics.

Discussion Iliopsoas hematoma has known high mortality, early diagnosis is crucial to avoid its fatal implications. The most sensitive test for diagnosis of small hematomas is a magnetic resonance imaging but since it is time consuming, the most commonly employed test is computed tomography.[5 6 7 8] Treatment modalities range from observation to surgical exploration based upon the overall condition of the patient. Surgical Intervention is indicated when the patient remains hemodynamically unstable despite medical resuscitation, if interventional radiology is unsuccessful or in case of developing abdominal compartment syndrome. Our case highlights the importance of timely recognition in patients on anticoagulation due to its subtle presentation, and management of this relatively uncommon, but in many cases a fatal complication.

REFERENCES

1. Tosun A, Inal E, Keles I, *et al*. Conservative treatment of femoral neuropathy following retroperitoneal hemorrhage: a case report and review of the literature. *Blood Coagul Fibrinolysis* 2014;**25**(7):769–72.
2. White DJ, Lytle FT. Femoral neuropathy following spontaneous retroperitoneal hemorrhage after cardiac surgery: a case report. *A A Case Rep* 2017;**8**(8):203–5.
3. Llitjos JF, Daviaud F, Grimald D, Legriel S, Georges JL, Guerot E, Bedos JP, Fagon JY, Charpentier J, Mira JP. Ilio-psoas hematoma in the intensive care unit: a multicentric study. *Ann Intensive Care* 2016 Dec;6(1):8.
4. Hulley JL, Fitzsimmons PR. Spontaneous iliopsoas hematoma with femoral neuropathy-an unusual complication of anticoagulation. *Clin Geriatrics Case Report* 2010;**18**:27–8.
5. Conesa X, Ares O, Seijas R. Massive psoas haematoma causing lumbar plexus palsy: a case report. *Journal of Orthopaedic Surgery* 2012;**20**(1):94–7.
6. Giuliani G, Poppi M, Acciarri N, Forti A. CT scan and surgical treatment of traumatic iliacus hematoma with femoral neuropathy: case report. *J Trauma* 1990 Feb;**30**(2):229–31.
7. Tamai K, Kuramochi T, Sakai H, Iwami N, Saotome K. Complete paralysis of the quadriceps muscle caused by traumatic iliacus hematoma: a case report. *J Orthop Sci* 2002;**7**(6):713–6.
8. Weiss JM, Tolo V. Femoral nerve palsy following iliacus hematoma. *Orthopedics* 2008 Feb;**31**(2):178.

A62 RIGHT ATRIAL WALL MASS WITH PROLAPSE OF THE TRICUSPID VALVE IN THE SETTING OF A NEWLY DIAGNOSED GASTROINTESTINAL STROMAL TUMOR

Nancy Guirguis, Bassem Chaar. *Advocate Christ Medical Center*

10.1136/jim-2020-MW.59

Introduction/Background Gastrointestinal stromal tumors (GIST) are rare tumors of the gastrointestinal tract that arise predominantly due to a mutation in KIT gene leading to overexpression of the respective receptor tyrosine kinase. This abnormality results in the uncontrolled growth of mesenchymal gastrointestinal cells. Incidence of GIST tumors are 1 out of 100,000 per year.1 More importantly, GIST tumors are usually diagnosed in patients in their 60s, and rarely does it occur in younger adults.2 We present a rare case where the discovery of a right atrial mass prolapsing through the tricuspid valve leads to the diagnosis of gastric GIST in a 26-year-old male.

Case Presentation 26-year-old previously healthy African American male presents with new onset palpitations and three weeks of progressive fatigue, weakness, and decreased appetite. Initial evaluation identified the following abnormalities: heart rate at 156 bpm, hemoglobin 8.0, hematocrit 24, WBC 46.4, and lactate venous 1.5. TTE/CT imaging noted a large, multilobulated mass originating from IVC/RA junction and extending through the right atrium prolapsing in and out of the tricuspid valve (figure 1). Shortly thereafter, the patient developed numbness of the right upper extremity, right facial droop and MRI of brain revealed a left parietal CVA, felt to be likely ischemic vs thrombotic in nature. No PFO was identified. Persistent tachycardia led to a CT angiogram which revealed pulmonary emboli. Concurrently, CT abdomen/pelvis revealed a large abdominal mass arising from the posterior aspect of the stomach. Endoscopic ultrasound guided biopsy of the mass confirmed a GIST tumor. The patient underwent surgery with excision of the right atrial mass, determined to be a thrombus, consistent with the

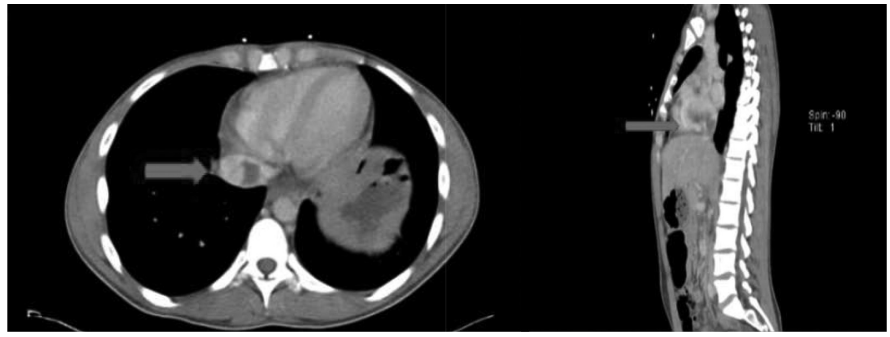

Abstract A62 Figure 1 Right atrial mass
Coronal and sagittal views of the right atrial mass (red arrows) seen on CT imaging

setting of a malignancy induced hypercoagulable state. The plan was to start neoadjuvant Imatinib to be followed by surgical resection. However, the clinical course was complicated by a GI hemorrhage. EGD revealed a large necrotic friable gastric mass, that had fungated through the gastric mucosa with diffuse bleeding that was not amenable to endoscopic management. The patient underwent an urgent enblock resection with a partial gastrectomy and splenectomy. The patient recovered well post-operatively. Imatinib was initiated on an outpatient basis.

Discussion GISTs are rare mesenchymal tumors of the GI tract. Current literature suggests less than 5000 cases are diagnosed annually.3 Often, initial symptomatology includes abdominal pain, nausea or vomiting. We present a rare incidence where a symptomatic atrial mass lead to the diagnosis of a GIST in a young patient. A review of the literature revealed a handful of cases where GIST tumors were associated with atrial thrombosis after diagnosis, but never as the presenting initial finding at the time of diagnosis. To the best of our knowledge, this is the first report of a concomitant atrial thrombus at the time of initial diagnosis of a GIST in a previously healthy young male.

A72 UNUSUAL PRESENTATION OF RETROPERITONEAL FIBROSIS

[1]Suresh Kumar, [2]Salah D Dajani, [3]Nfn Shakuntulla, [4]Chandur Bhan. *[1]Saint Joseph Hospital, Chicago, Chicago, IL; [2]Amita St. Joseph's Hospital, CHICAGO, IL; [3]OSF Heart of Mary Medical Center, Chicago, IL; [4]Amitahealth Saint Joseph Hospital Chicago, Chicago, IL*

10.1136/jim-2020-MW.60

Introduction/Background Background: Idiopathic Retroperitoneal fibrosis is a rare condition with annual incidence of 1–2 per 100,000 people. It is characterized by the presence of a fibro-inflammatory tissue, which usually surrounds the abdominal aorta and the iliac arteries and extends laterally into the retro peritoneum to envelop adjacent structures. The symptoms and signs associated with RPF are nonspecific; it can present with dull, poorly localized, noncolicky pain in the flank, back, scrotum, or lower, DVT, hydronephrosis or lower extremity edema.

Case Presentation A 73-year-old male was admitted to hospital due to recurrent lower abdomen and left groin pain, aggravated by sitting and weight bearing and relieved by lying flat. He had experienced similar left groin pain in past, each time managed conservatively. Work up included MRI hips to evaluate possible etiology which showed mild to moderate degenerative joint disease; A testicular ultrasound with doppler which showed normal testicles size and echogenicity and bilateral testicular microlithiasis, normal symmetrical vascularity in both testicles. Subsequently, he underwent CT abdomen and pelvis which showed severe bilateral perinephric edema and inflammatory changes enlarging retroperitoneum, extending into the renal hila bilaterally distorting the intrarenal collecting systems, abnormalities were worse on left compared to right. There was no hydronephrosis noticed on imaging. Laboratory studies revealed elevated ESR to 39, CRP, IgG-4 and IL 6 were all with in normal limits. ANA was positive and DsDNA was slightly elevated to 26 but rest of autoantibodies work up was unremarkable including normal Myeloperoxidase Abs and ANCA Proteinase -3. CT guided biopsy of perinephric tissue was performed and pathology revealed fragments of fibrous tissue consistent with retroperitoneal fibrosis. He was subsequently started on steroids. Upon follow up patient reported improvement in symptoms.

Discussion

Conclusion Our patient presented with left inguinal pain and imaging revealed severe bilateral perinephric edema and inflammatory changes enlarging the retroperitoneum and extending into the renal hila bilaterally distorting the intrarenal collecting systems, abnormalities worse on left compared to right. Biopsy findings revealed retroperitoneal fibrosis. This case reports add to the medical literature how testicular/inguinal pain can be caused by an underlying disease entity not related to the usual causes.

A74 HYDROXYCHLOROQUINE-RELATED NEUROMYOPATHIC AND CARDIAC TOXICITY

[1]Michael Manansala, [2]Jacqueline Kannan, [2]Pooja Patel, [2]Anjali Mehta, [2]Manuel Utset, [3]Peter Pytel, [2]Tibor Valyi-Nagy, [2]Shiva Arami. *[1]University of Illinois at Chicago, Chicago, IL; [2]University of Illinois at Chicago; [3]University of Chicago*

10.1136/jim-2020-MW.61

Introduction/Background Hydroxychloroquine (HCQ) is an antimalarial drug that is commonly used for treatment of autoimmune diseases. Side effects are rare and the drug is generally well tolerated with the exception of retinopathy, hyperpigmentation and GI upset.[1] However, there are few case reports of HCQ neuromyopathy[2 3] and cardiomyopathy[3 4] after prolonged use of the drug. Here, we present a case of a patient with RA who developed multiple HCQ related toxicities, including cardiotoxicity and neuromyopathy.

Case Presentation A 69 year old female with a history of RA developed several months of worsening dysphagia, generalized weakness, and new decompensated heart failure with reduced ejection fraction (HFrEF). She reported difficulty in swallowing liquids and solids for two months, but denied odynophagia. She had been very functional at home until 1 year prior to admission. However, she became bed bound due to progressive diffuse weakness. She was not on any medications associated with myopathy besides HCQ. With regard to her rheumatologic history, she was maintained on HCQ 400 mg daily for 5 years by a rheumatologist outside our hospital system. On physical exam, the patient demonstrated moderate dysarthria and profound weakness, greater proximally than distally (+2/5 on bilateral upper extremities and shoulders, +3/5 bilateral elbow and grip strength), and bilateral leg edema. Swallowing studies demonstrated dysphagia. Flexible laryngoscopy showed normal mobile vocal folds, no masses, and a patent airway. Electromyography demonstrated diffuse myopathy affecting proximal muscles more so than distal muscles as well as length dependent axonal sensorimotor polyneuropathy. Laboratory results were significant for an elevated ESR, LDH and SSA 52 antibody IgG. Biopsy of the left vastus lateralis revealed diffuse atrophy of muscle tissue with myofibers exhibiting abnormal granular cytoplasmic staining and increased acid phosphatase activity consistent with toxic myopathy. Transthoracic echo (TTE) was notable for an ejection fraction (EF) of 30% with diffuse left ventricular hypokinesis and dysfunction. TTE 1 month prior to presentation demonstrated a normal EF of 60–65%. Cardiac catheterization 2 months prior was normal. Serial EKGs during admission were without ischemia or ST changes. BNP on presentation was elevated to 2473 pg/mL. Initial troponin was also elevated but down trended with treatment for HF. Repeat TTE 1 month into her hospitalization redemonstrated a reduced EF of 30%. HCQ was discontinued early during admission given concern for potential toxicities. The patient was started on prednisone 60 mg daily with minimal improvement of her myopathy. She continued to have worsening dysphagia and required G tube placement. For HFrEF, the patient was continued on her home metoprolol 50 mg, placed on a fluid restriction and started on IV diuresis. She continued to decline clinically while awaiting rehab facility placement, developed sepsis secondary to clostridium difficile infection and eventually expired.

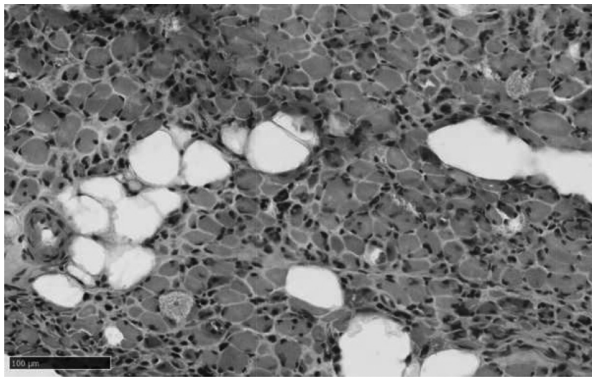

Abstract A74 Figure 1A
H&E stained sections of the skeletal muscle biopsy specimen shows atrophy of muscle fibers with increased adipose tissue and connective tissue. Some myofibers show granular basophilic cytoplasm. Some features of necrosis and regeneration of individual myofibers are seen. Admixed throughout are focal accumulations of brown granular pigment consistent with lipofuscin. No significant inflammatory infiltrates or blood vessel abnormalities are seen (magnification: 200 X)

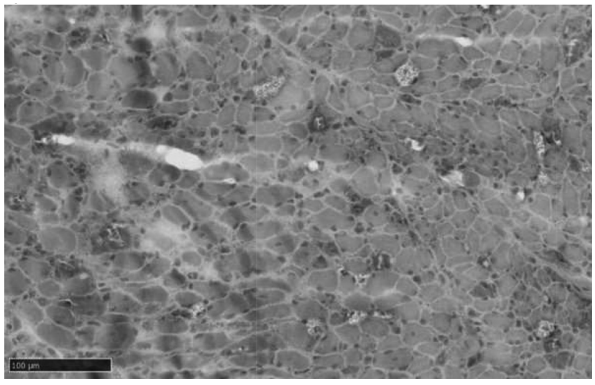

Abstract A74 Figure 1B
Modified Gomori trichrome stain highlights the presence of lipofuscin within myofibers and also the granular changes present in the cytoplasm of some of the myofibers (magnification: 200 X)

Discussion We present a case in which a 69 year old woman with RA who developed biopsy proven neuromyopathy and cardiomyopathy as evidenced by new onset of HFrEF due to prolonged HCQ use. Neuromyopathy and cardiomyopathy are known to be rare side effects of prolonged HCQ use and are likely underrecognized given the insidious onset of symptoms. In a longitudinal prospective study of 119 patients with rheumatic diseases treated with antimalarial drugs such as HCQ, up to 6.2% were found to have clinically significant muscle weakness. Furthermore, 12.6% were found to have some sort of muscle enzyme disturbance, including elevated LDH or CK.[5] Symptoms of myopathy typically start weeks or months after administration and, if recognized early, usually improve after cessation of the drug.[6] A case by Kwon et. al described a patient with similar myotoxicity and cardiomyopathy in which the patient's chest pain and shortness of breath resolved after 18 months of cessation of HCQ.[2] Another case by Mateen and Keegan detailed a case of an 89 year old male who had 3 years of progressive dysphagia while taking antimalarials for 18 years for treatment of morphea profunda. After 7 months of cessation of antimalarials, his dysphagia and muscle weakness resolved.[3] In the case presented here, we were unable to follow if our patient's dysphagia, weakness, and cardiac function improved after long term cessation of HCQ as the patient expired due to sepsis. Mechanism of Toxicity HCQ-myopathy is a form of vacuolar myopathy and is diagnosed via muscle biopsy consistent with increased lysosomal activity and vacuolar changes. The exact mechanism of HCQ-myopathy is unknown but is thought to be related to lysosomal dysfunction. As HCQ infuses into lysosomes, it increases intravacuolar pH, resulting in inhibition of lysosomal enzymes. Lysosomes are vital in the degradation of cytoplasmic proteins and production of other macromolecules. Disruption of lysosomal function leads to an accumulation of vacuoles filled with lipids and other cytosomal proteins.[2 6] Additionally, HCQ can displace calcium in the phospholipid bilayer leading to myofiber necrosis.[6] The mechanism for HCQ-cardiomyopathy is thought to be similar to that for skeletal muscle. The gold standard for diagnosis is endomyocardial biopsy, which will reveal vacuolated cardiac myocytes. When

endomyocardial biopsy in contraindicated, muscle biopsy showing similar findings of vacuolated myocytes can help establish the diagnosis in the appropriate clinical setting.[7]

Conclusion HCQ is a commonly prescribed medication in autoimmune diseases. Although generally very well tolerated, it can have severe side effects and, as in the case presented here, can result in mortality. This patient not only had biopsy proven neuromyopathic toxicity but also likely developed cardiomyopathy due to HCQ. If recognized early, these particular toxicities may be reversible. However, there are currently no guidelines addressing routine lab monitoring for HCQ myopathy or cardiomyopathy. This case highlights the importance of frequent routine monitoring of patients taking antimalarials for a prolonged period with an index of suspicion for neuromyopathy and cardiomyopathy in addition to the known side effect of retinopathy.

REFERENCES

1. Sanofi-Aventis. Product monograph: Plaquenil. http://products.sanofi.ca/en/plaquenil.pdf. Accessed Nov 15, 2019.
2. Kwon JB, Kleiner A, Ishida K, Godown J, Ciafaloni E, & Looney RJ. Hydroxychloroquine-induced myopathy. *JCR: Journal of Clinical Rheumatology* 2010;**16**(1):28–31.
3. Mateen FJ, & Keegan BM. Severe, reversible dysphagia from chloroquine and hydroxychloroquine myopathy. *Canadian Journal of Neurological Sciences* 2007;**34**(3):377–379.
4. Zhao H, Wald J, Palmer M, & Han Y. Hydroxychloroquine-induced cardiomyopathy and heart failure in twins. *Journal of thoracic disease* 2018;**10**(1):E70.
5. Casado E, Gratacos J, Tolosa C, Martínez JM, Ojanguren I, Ariza A,. .. & Larrosa M. Antimalarial myopathy: an underdiagnosed complication? Prospective longitudinal study of 119 patients. *Annals of the rheumatic diseases* 2006.;**65**(3):385–390.
6. Valiyil R, & Christopher-Stine L.. Drug-related myopathies of which the clinician should be aware. *Current rheumatology reports* 2010:**12**(3), 213–220.
7. Costedoat-Chalumeau N, Hulot JS, Amoura Z, Delcourt A, Maisonobe T, Dorent R,. .. & Piette JC. Cardiomyopathy related to antimalarial therapy with illustrative case report. *Cardiology* 2007;**107**(2):73–80.

Endocrinology/Metabolism

B26 GLUCOSE DEPENDENT EXPRESSION OF PAX6 AND HDAC7 IN PANCREATIC BETA CELL REGULATION

Sivasangari Balakrishnan. *Bharathidasan University, Chicago, IL*

10.1136/jim-2020-MW.62

Introduction/Background Glucose regulation of β-cell function depends on a number of complementary mechanisms that include recruitment of transcription factors to regulatory sites, histone modifications and initiation of transcription. Hence, dysregulation of any of the above events can interfere with β-cell function and result in diabetes. Therefore, the investigation of the mechanisms by which glucose controls β-cell-enriched transcription factors and regulates epigenetic modifications will be helpful in the design of novel clinical interventions to prevent and treat diabetes.

Objective(s) To study the effects of glucose mediated expression of PAX6 in regulation of epigenetic modifications in β-cells and its role in insulin gene transcription.

Methods Cell Culture Rat insulinoma-1E (INS-1E) cells were cultured in a humidified atmosphere containing 5% CO2 in complete medium composed of RPMI-1640 supplemented with 10% heat-inactivated fetal bovine serum, 1 mM sodium pyruvate, 50 μM β-mercaptoethanol, 2 mM glutamine, 10 mM Hepes, 100 units/ml penicillin, and 100 μg/ml streptomycin (Merglen *et al*., 2004). For the glucose regulation experiments, cells were grown in complete medium and then washed with 3 × phosphate-buffered saline and transferred to low (1 mM) or high (25 mM) glucose-containing media for indicated times. At the end of the experimental period whole cell lysate or total RNA was prepared and used for further analyses. siRNAs Transfection Transfection with small interfering RNAs (siRNAs) was performed using the Eppendorf Multiporator system under optimized conditions. The siRNAs were transfected at a final concentration of 200 nM. Protein expression studies Protein expression studies confirmed by western blotting. Cell extracts from INS-1E cells were prepared in lysis buffer. Proteins were separated by SDS-PAGE and subsequently electroblotted onto nitrocellulose membranes. Membranes were blocked for 1 h at room temperature After blocking, membranes were incubated overnight at 4°C either with an antibody specific for target protein of interest (Acetylation sites, Pax6,HDAC7,PKD1,Beta Actin). Membranes were washed four times for 10 min in TTBS and subsequently incubated for 1h at room temperature with a secondary horseradish peroxidase-conjugated antibody and proteins were visualized using the 3,3'-Diaminobenzidine (DAB) chromogen system PCR Transcription factor mRNA(Pax 6and HDAC7) family and mRNA expressions carried out and real-time PCR also carried out to confirm the mRNA expressions. Immunocytochemistry Briefly, INS-1E cells were grown in monolayer culture on a sterilized coverslip. Cultured cells were treated with 1 mM or 25 mM glucose in serum-free RPMI medium. After incubation, the cells on the coverslip were washed thoroughly with 1X PBS and then fixed with 4% (v/v) paraformaldehyde in PBS for 20 minutes at room temperature. The cells were washed thoroughly with 1X PBS and then blocked with 1% BSA for 1 h at room temperature. After blocking, the cells were incubated with the primary antibody (HDAC7; Santa Cruz Biotechnology, Inc., Santa Cruz, CA) overnight at 4°C. Then, the cells were washed in 3 times 1XPBS and then incubated in the FITC-labeled secondary antibody (GeNei, India) for 2 h at room temperature in dark. Finally, the Coverslips were washed and mounted using Vectashield containing 4', 6'-diamidino-2-phenylindole to visualize the cell nuclei. Immunostained proteins in cells were visualized by immunofluorescence microscopy. Data Analysis The values are expressed as mean ± standard deviation (SD). Differences between groups were assessed by one-way analysis of variance using the GraphPad Prism 6.0 software package for Windows.

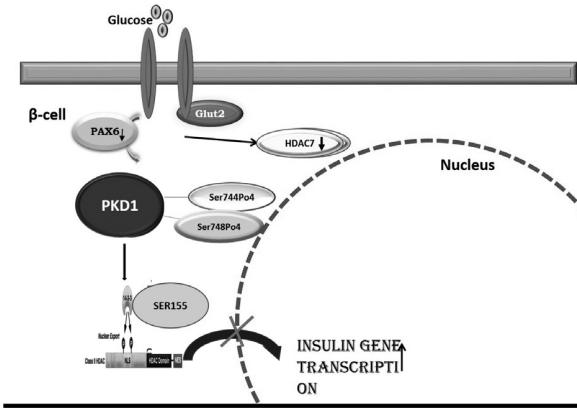

Abstract B26 Figure 1 Graphical abstract

Post hoc testing was performed using Tukey's multiple comparisons test. Values are statistically significant at ***P<0.001, **P<0.01, *P<0.05 and ns- non significant.

Results The experiments from siRNA mediated knockdown suggest that PAX6 regulates HDAC7 expression in response to glucose concentrations. Furthermore, glucose by itself modulates the subcellular localization of HDAC7 phosphorylation of serine 155 through PKD1 serine 744,748 mediated phosphorylation. The siRNA mediated knockdown of HDAC7 significantly increased insulin mRNA levels at low glucose concentrations, suggesting its vital role in the regulation of insulin gene transcription.

Conclusions In conclusion, the present study reveals a novel finding that glucose-mediated suppression of Pax6 results in the down-regulation of HDAC7 and these events regulate cell survival and insulin gene transcription in pancreatic beta-cells.

B27 ABSTRACT WITHDRAWN

B28 REGULATION OF ADIPOSITY AND METABOLIC HEALTH THROUGH DIETARY HISTIDINE RESTRICTION

[1]Victoria Flores, [2]Dudley Lamming. [1]*University of Wisconsin-Madison, Madison, WI*; [2]*University of Wisconsin-Madison*

10.1136/jim-2020-MW.63

Introduction/Background Low protein (LP) diets are associated with a decreased risk of diabetes in humans, and we and others have demonstrated that a low protein diet promotes leanness and glycemic control in lean and obese rodents. In a short-term randomized clinical trial, LP diets also promote leanness and glycemic control in humans. However, the specific dietary components altered in a LP diet that promote metabolic health have not been fully characterized.

Objective(s) The increasing prevalence of obesity is a serious threat to global health, placing humans at increased risk of many diseases, including diabetes, cancer, and Alzheimer's disease. An intervention is urgently needed to put an end to this epidemic.

Methods We utilized 6-week-old C57BL/6J male mice. After placing them on a Western diet (WD) for 12 weeks, we split mice into four groups and intervened by feeding them a Control chow diet, WD Control, WD low protein; WD Low His diet where the only histidine is reduced 67% from WD Control; all diets were isocaloric, with carbohydrates substituted as necessary and identical levels of fat. We characterize the metabolic response by measuring changes in glycemic control, energy expenditure, and transcriptomic profiling.

Results We previously determined that reduced consumption of dietary essential amino acids mediates the metabolic response to a LP diet, with the branched-chain amino acids playing a crucial role. However, we observed that reduced intake of the other six essential dietary amino acids also lead to changes in body composition. Here, we report our finding that dietary histidine plays a key role in the metabolic response to an LP diet. Specific restriction of dietary histidine by 67% reduces weight gain of young, growing C57BL/6J mice, reducing both adipose and lean mass gain; and improving glucose metabolism. Specifically restricting histidine promotes rapid weight loss with reduction of both adipose and lean mass, but with an overall reduction in adiposity. This effect is not mediated by decreased food consumption, but instead is associated with increased energy expenditure. Conversely, when we took young male C57BL/6J mice and placed them on a supplemented histidine diet, we observed supplementation of histidine to increase adipose and lean mass. To determine the potential relevance of our findings to the human obesity epidemic, we analyzed population health and nutrition data gathered from over 600 Wisconsin residents. Surprisingly, we find that the variation in dietary histidine levels helps to explain differences in body mass index (BMI) in humans living in Wisconsin.

Conclusions Overall, our data suggest that dietary histidine is an important regulator of body weight and composition in both mice and humans and suggests that dietary guidelines and clinical interventions based on reduced levels of histidine may be an effective means to intervene in the obesity epidemic.

B29 PROGESTERONE RECEPTOR DEPENDENT REGULATION OF ^{18}F-FLUORODEOXYGLUCOSE UPTAKE IN BREAST CANCER

Kelley Salem, Amy M Fowler. *University of Wisconsin-Madison*

10.1136/jim-2020-MW.64

Introduction/Background Positron emission tomography (PET) imaging with ^{18}F-fluorodeoxyglucose (^{18}F-FDG) is used clinically for staging, restaging, and assessing therapy response in breast cancer. Tumor accumulation of ^{18}F-FDG reflects the underlying cancer hallmark of increased glucose metabolism. Various steroid hormones, including progesterone, have been shown to influence key metabolic pathways such as glycolysis and the pentose phosphate pathway. The direct role progesterone receptor (PR) plays in tumor glucose metabolism and ^{18}F-FDG uptake by breast cancer cells has not been determined.

Objective(s) The aim of this study was to determine the role PR has in regulating ^{18}F-FDG uptake in breast cancer cells via pharmacologic and genomic-based approaches.

Methods Six established breast cancer cell lines were studied; two were ER-/PR- (MDA-MB-231, MDA-MB-468) and four were ER+/PR+ (T47D, MCF-7, ZR-75-1, CAMA-1). T47D cells with CRISPR/Cas9 PGR gene knock out (T47D PR KO) and their scrambled control were also used as matched isogenic cell lines without or with PR protein expression, respectively [Davaadelger B *et al* Endocrinology 2018;159:3581–3595]. Expression of select facilitative glucose transporter gene superfamily members (GLUT isoforms 1, 2, 3, 4, and 12) was measured using quantitative polymerase chain reaction in cells lines and normal mammary tissue. Glucose utilization was measured using ^{18}F-FDG cell uptake assays in response to 24 h treatment with various PR agonists (promegestone/R5020, medroxyprogesterone acetate/MPA, or megestrol acetate/MA), PR antagonists (mifepristone/RU486, or ulipristal acetate/UPA), or ethanol vehicle control. Agonist and antagonist function of PR ligands were confirmed using a progesterone-response-element luciferase reporter gene assay as a positive control.

Results The ER-/PR- cell lines tested had greater avidity for ^{18}F-FDG compared to the ER+/PR+ cell lines. GLUT1 and

GLUT3 mRNA were overexpressed in all six breast cancer cell lines compared to normal mammary tissue. GLUT4 expression was decreased in all six cell lines compared to normal mammary tissue. GLUT12 had variable expression whereas GLUT2 was not detectable in any of the samples. T47D cells treated for 24 h with PR agonist drugs (R5020, MPA, or MA at 100 nM) had approximately two-fold increase in ^{18}F-FDG uptake compared to cells treated with ethanol control. This induction was not observed in the ER-/PR- cell lines. A dose titration curve for R5020 in T47D cells yielded an EC50 of 0.2 nM for ^{18}F-FDG uptake and an EC50 of 0.07 nM for PR transcriptional activation. Treatment with the PR antagonists, RU486 or UPA, at 100 nM were each able to mitigate progestin-induced ^{18}F-FDG uptake ($9.9\pm0.5 \times 105$ CPM/mg protein and $7.3\pm0.3 \times 105$ CPM/mg protein, respectively, vs $12.7\pm0.9 \times 105$ CPM/mg protein). Inhibition of PR transcriptional function by these antagonist compounds was confirmed using a reporter gene assay. In the genomically-edited T47D cells lacking PR protein (T47D PR KO), ^{18}F-FDG uptake was not increased after treatment with R5020, MPA, or MA (0.83 ± 0.14 fold, 0.98 ± 0.12 fold, or 1.0 ± 0.08 fold, respectively). For comparison, treating the isogenic scrambled control cell line which retains PR expression with R5020, MPA, or MA increased ^{18}F-FDG uptake by 2.02 ± 0.11 fold ($p=0.0002$), 1.88 ± 0.10 fold ($p=0.0006$), and 1.84 ± 0.13 fold ($p=0.0008$) compared to ethanol control. Appropriate PR protein expression and transcriptional function were confirmed in the genomically-edited T47D cell lines.

Conclusions PR mediates changes in ^{18}F-FDG uptake by breast cancer cells in response to progestins and anti-progestins.

B30 DIETARY BRANCHED-CHAIN AMINO ACID RESTRICTION EXTENDS LIFESPAN AND PROMOTES HEALTHSPAN IN MICE

[1]Nicole Richardson, [2]Elizabeth Konon, [2]Alexis Mitchell, [2]Colin Boyle, [2]Megan Finke, [2]Haley Schuster, [2]Soha Ahmad, [2]Allison Rodgers, [2]Lexington Haider, [3]Victoria Flores, [3]Heidi Pak, [2]Sareyah Ahmed, [2]Abigail Radcliff, [2]Jessica Wu, [2]Dawn Sherman, [2]Elizabeth Williams, [2]Timothy Hacker, [1]Dudley Lamming. *[1]University of Wisconsin-Madison; [2]UW-Madison; [3]University of Wisconsin-Madison, Madison, WI*

10.1136/jim-2020-MW.65

Introduction/Background Reduced caloric intake without malnutrition, or calorie restriction (CR), is often referred to as the 'gold standard' of nutritional interventions known to robustly extend mammalian lifespan and improve metabolic health. CR is a difficult diet to adhere to, however, especially as developed societies have access to many cheap and calorie dense foods. Recently, it has been discovered that restricting dietary protein alone is sufficient to recapitulate many benefits of a CR diet, extending the lifespan of flies and mice, and improving metabolic health in mammals as well as humans. The precise amino acid balance in dietary protein also appears to play a role in metabolic health and longevity; it has been previously shown that restricting dietary methionine, or eliminating certain essential amino acids from the diet rapidly improves health. Our lab has previously shown that restricting, not eliminating, dietary branched-chain amino acids (BCAAs; leucine, isoleucine, and valine) by two-thirds improves metabolic health in both lean and diet-induced obese young male mice. These data led us to believe that a Low BCAA diet would influence longevity.

Objective(s) We hypothesized that a Low BCAA diet would improve metabolic health in male and female mice, increasing healthspan with age. We predicted that Low BCAA diet feeding would extend lifespan in short-lived mutant mice and well as wild-type mice.

Methods Amino acid defined diets restricted in BCAAs were fed to two short-lived mouse models: LMNA $^{-/-}$ and LMNA$^{G609G/G609G}$ mice of both sexes. Additionally, this dietary intervention was fed to aged wild-type male and female mice from 16 months of age onwards, as well as to male and female wild-type mice from weaning. Where possible, longitudinal metabolic health and overall fitness was recorded, as well as lifespan data. To uncover mechanisms of action in improving mouse fitness with age, we performed transcriptional profiling of quadriceps muscle tissue from 16 month old male and female wild-type mice fed either Control or Low BCAA diets from weaning.

Results Low BCAA diet feeding extended median female LMNA $^{-/-}$ lifespan by up to 85%, and also extends the maximum lifespan of LMNA$^{G609G/G609G}$ mice. In wild-type mice, we find that BCAA restriction improves healthspan and metabolic health in both young and aged life. When a Low BCAA diet is implemented at weaning, it robustly extends male lifespan, increasing median lifespan by 30%. We find that male and female quadriceps transcriptional profiles are similar under Control diet feeding, but diverge upon BCAA restriction. Kegg overrepresentation analysis identified multiple pathways implicated in longevity were altered in male mice, including the mechanistic Target of Rapamycin (mTOR) pathway. Indeed, western blotting of these muscles showed that mTORC1 signaling to downstream substrates was selectively reduced in male Low BCAA fed mice.

Conclusions Our results suggest that protein quality can be just as important as protein quantity when dictating health and lifespan. Furthermore, BCAA intake regulates healthspan in male and female mice, and we show for the first time that reduced BCAA intake is sufficient to extend male lifespan. These data indicate that reducing dietary BCAA intake may be highly translatable in promoting metabolic health, promoting healthspan, and treating age-related disease.

B31 EXPRESSION LEVELS OF LAMININ α4 IN SUBCUTANEOUS WHITE ADIPOSE TISSUE BEFORE AND AFTER BARIATRIC SURGERY

[1]Liesl M Schroedl, [2]Anna Goddi, [3]Alanis Carmona, [4]Matthew J Piron, [2]Jeremy White, [3]Isabel Casimiro, [5]Matthew J Brady, [3]Ronald N Cohen. *[1]University of Chicago Pritzker School of Medicine, Chicago, IL; [2]University of Chicago, Committee on Molecular Metabolism and Nutrition; [3]University of Chicago Medicine Department of Medicine, Section of Endocrinology, Diabetes, and Metabolism; [4]University of Chicago; [5]University of Chicago Medicine Department of Medicine, Section of Endocrinology, Diabetes, and Metabolism, Committee on Molecular Metabolism and Nutrition*

10.1136/jim-2020-MW.66

Introduction/Background Obesity is a condition with major global burden, affecting approximately 500 million people worldwide. It is associated with significant morbidity and mortality, but there are few effective medical treatments. Therefore, it is crucial to elucidate the mechanisms that contribute to and protect against obesity, in hopes of eventually creating novel therapies for this condition. In working to

understand mechanisms underlying obesity, our lab has identified a class of extracellular matrix proteins called laminins that play a role in regulating adipose tissue function. In particular, when one of the laminin chains, laminin α4 (LAMA4), was knocked out in a mouse model, mice were resistant to obesity, exhibiting reduced weight gain and increased energy expenditure. However, it is unknown whether humans also exhibit changes in LAMA4 expression relative to adiposity.

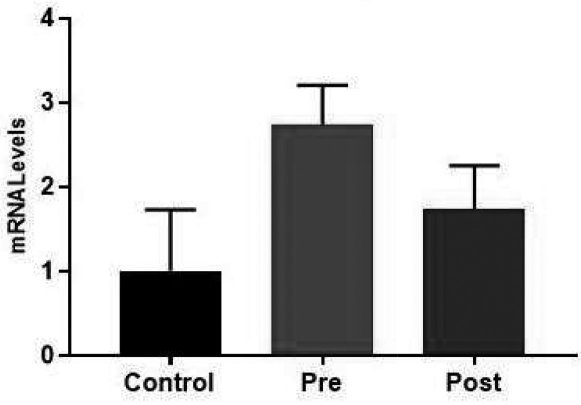

Abstract B31 Figure 1 Laminin α4 mRNA expression levels
Expression of laminin α4, defined as fold change in mRNA levels, in sWAT of controls (control), obese patients before surgery (pre), and obese patients 3 months post-surgery (post)

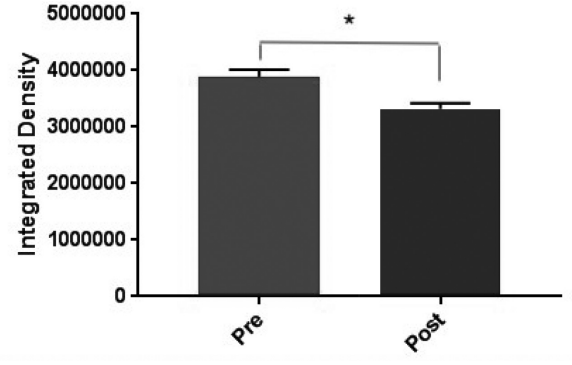

Abstract B31 Figure 2 Laminin α4 protein expression levels
LAMA4 protein expression, defined as average integrated density, in sWAT of obese patients before surgery (pre) and obese patients 3 months post-surgery (post) (*p=0.007)

Abstract B31 Figure 3 LAMA4 IHC
Representative images of immunohistochemical staining for LAMA4 in sWAT of obese patients before surgery (left) and obese patients 3 months post-surgery (right)

Objective(s) The objective of this study is to determine whether LAMA4 expression in subcutaneous white adipose tissue (sWAT) of obese patients was increased compared to non-obese control patients, and whether LAMA4 expression decreased in obese patients 3 months after bariatric surgery.
Methods This study used samples of sWAT from six obese female patients taken two weeks prior to bariatric surgery (n=6) and three months after surgery (n=5), as well as samples from non-obese controls (n=3), for a total of 9 participants. Of note, one patient did not have a post-surgery sample. Quantitative RT-PCR for laminin α4 mRNA levels was performed on the samples, and output data was analyzed with the ΔΔ threshold cycle (Ct) method. Immunohistochemistry (IHC) was performed to analyze LAMA4 protein expression. Density quantification was performed to measure signal on microscopy images using Fiji.
Results sWAT of obese patients before bariatric surgery exhibited a trend towards increased levels of laminin α4 mRNA compared with both control patients and also 3 months after surgery, though these changes were not statistically significant. However, the sWAT of obese patients before surgery exhibited significantly higher levels of LAMA4 protein expression compared with after surgery (p=0.007).
Conclusions The results of this study suggest that humans exhibit increased levels of LAMA4 protein expression, similar to what occurs in mouse models, in the setting of increased adipose tissue. Therefore, it is reasonable to pursue further studies of these extracellular matrix proteins and their associated intracellular signaling pathways in human samples as potential novel targets in the treatment of obesity. Limitations of this study include small sample size and lack of post-surgery data for one patient.

B32 SERUM METABOLOMIC PROFILES IDENTIFY ALTERATIONS IN LIPID METABOLISM IN PREMENARCHAL GIRLS AT INCREASED RISK FOR PCOS

[1]Laura Torchen, [2]Warwick Dunn, [2]Wiebke Arlt, [3]Andrea Dunaif. *[1]Ann and Robert H Lurie Children's Hospital of Chicago, Northwestern University Feinberg School of Medicine, Chicago, IL; [2]University of Birmingham; [3]Icahn School of Medicine at Mount Sinai*

10.1136/jim-2020-MW.67

Introduction/Background Daughters of women with PCOS (PCOS-d) and girls with obesity (OB-g) have unique risk factors for PCOS. We have previously reported distinct early reproductive phenotypes in premenarchal PCOS-d and OB-g, characterized by similar degrees of hyperandrogenemia, but elevated anti-Mullerian hormone (AMH) levels only in PCOS-d. Differences in early metabolic phenotypes in PCOS-d compared with OB-g have not been investigated. Metabolomic studies in these at-risk populations may identify novel metabolic pathways involved in the early pathogenesis of PCOS.
Objective(s) We performed non-targeted metabolomic analyses in premenarchal PCOS-d, OB-g, and lean control girls (L-g) to identify metabolic differences characteristic of PCOS or diabetes risk in these distinct risk groups.
Methods Twenty-seven premenarchal PCOS-d, 30 OB-g, and 22 L-g of comparable age were studied at an academic medical center. A fasting morning blood sample was obtained for hormone levels and non-targeted metabolomics analysis.

Results Thirty metabolites were significantly different in OB-g and PCOS-d compared with L-g. These metabolites were enriched for differences in the ether glycerophospholipid and ceramide and sphingolipid classes, which have been associated increased metabolic risk. Only 6 metabolites were significantly different in PCOS-d compared with both OB-g and L-g, again enriched for differences in ether glycerophospholipids. These differences were largely independent of body mass index. Glycerophospholipids were highly correlated with testosterone and AMH levels.
Conclusions We found evidence for a common early metabolomic signature in premenarchal PCOS-d and OB-g through non-targeted metabolomics analyses, suggestive of increased metabolic risk.

B33 FEASIBILITY OF A 1 HOUR ORAL GLUCOSE TOLERANCE TEST (OGTT) TO SCREEN FOR CYSTIC FIBROSIS-RELATED DIABETES

[1]Collin R Walentine, [2]Christine L Chan, [3]Joon Ha, [3]Arthur Sherman, [2]Melanie Cree-Green, [2]Kristen J Nadeau. *[1]University of Colorado Anschutz Medical Campus, Oakland University William Beaumont School of Medicine, Auburn Hills, MI; [2]University of Colorado Anschutz Medical Campus; [3]National Institutes of Health*

10.1136/jim-2020-MW.68

Introduction/Background Cystic fibrosis-related diabetes (CFRD) and prediabetes (CFRPD) predispose youth to nutritional decline and early mortality. Screening with a yearly OGTT, including fasting and 2h glucose (2hG), is the standard of care for patients with CF ≥10 years of age. Nationally, screening OGTT's are performed in only ~60% of youth and ≤30% of adults. OGTT's are costly and patient intensive, so strategies are needed to improve screening rates.
Objective(s) We evaluated if a 1h glucose (1hG) cutoff predicts subsequent CFRD development in youth.
Methods This was a retrospective chart review of patients from a tertiary care regional pediatric CF center. Inclusion criteria: CF, age ≥6 years at first OGTT, absence of CFRD at first OGTT, multiple OGTT visits between 2/2010–6/2019, and at least one visit with a 1hG. Linear mixed effect model fits were performed to identify 1hG cutpoints that predict CFRD. Model Disposition Index (mDI), a surrogate of relative β-cell function, was calculated from the product of insulin sensitivity and secretion derived by mathematical modeling of glucose measurements during the OGTT.
Results 192 patients age 12±2.6 years at initial screening were identified with a mean of 3.7±1.9 years of follow-up, 27 of whom developed CFRD per current criteria. All who developed CFRD crossed the 1hG CFRPD cutpoint (155 mg/dL) earlier than the 2hG CFRPD cutpoint (140 mg/dL). The average 1hG was 166 mg/dL when the 2hG crossed 140 mg/dL. mDI was significantly higher in those with lower 1hG (<166 mg/dL) + normal glucose tolerance (NGT) vs. high 1hG (≥166 mg/dL) + NGT ($p<0.00001$). mDI was similar in those with high 1hG NGT vs. 2hG≥140 mg/dL ($p=0.89$). Those with CFRD, i.e. 2hG≥200 mg/dL, had a 1hG of 267 mg/dL. mDI was similar in those with 1hG≥267 vs. 2hG≥200 mg/dL ($p=0.94$).
Conclusions Despite a normal 2hG, abnormalities in β-cell function were demonstrated in youth with CF via higher 1hG that were similar to patients with prediabetes by current 2hG criteria. This suggests elevated 1hG is a condition that may need to be treated in CF. Furthermore, we were able to establish a 1hG cutpoint in CF that correlates with a 2hG≥200 and could reduce the time and cost of a 2hr OGTT.

101 EMC10, A NOVEL CIRCULATING FACTOR, PROMOTES DIET-INDUCED OBESITY VIA SUPPRESSION OF ADIPOCYTE THERMOGENESIS

[1]Yanliang Li, [2]Xuanchun Wang, [3]Guifen Qiang, [3]Maximilian McCann, [3]Victoria Gil, [4]Matthias Blüher, [3]Chong Wee Liew. *[1]University of Illinois at Chicago, Chicago, IL; [2]Fudan University; [3]University of Illinois at Chicago; [4]University of Leipzig, Leipzig*

10.1136/jim-2020-MW.69

Introduction/Background Activation of brown and subcutaneous adipose tissues could reduce obesity and improve glucose homeostasis through adaptive thermogenesis. Secreted factors from adipose tissues play an important role in the regulation of energy homeostasis. However, such factors are still not available for the treatment of obesity and metabolic diseases.
Objective(s) Here we describe a novel, adipose-enriched secreted regulator of adiposity and energy metabolism, scEmc10 (secreted-isoform of endoplasmic reticulum membrane complex subunit 10), which is associated with obesity both in rodents and humans, regulating systemic energy and metabolic homeostasis.
Methods The role of scEmc10 was investigated in EMC10 $^{-/-}$ mice and B6 mice with enhanced circulating scEmc10 by expression of secretable AAV-hscEmc10 in the liver with both chow diet and high-fat diet (HFD). In humans, using an in-house-developed chemiluminescent immunoassay, serum scEmc10 were evaluated in lean (BMI≤25) overweight (25<BMI≤29.9) and obese (BMI >29.9) groups. Finally, the effect of monoclonal anti-scEmc10 was evaluated in B6 mice challenged with 8 weeks of HFD.
Results We found that serum scEmc10 levels are significantly upregulated in overweight and obese patients and can be normalized by bariatric surgery-induced weight loss. Gain- and loss-of-function studies in mice demonstrated that scEmc10 promotes susceptibility to diet-induced obesity and obesity-induced metabolic dysfunction. Subsequent metabolic analysis revealed that Emc10 KO mice on HFD have elevated whole-body energy expenditure compared to WT controls via an increase in oxygen consumption in both the brown and inguinal subcutaneous fat. Our mechanistic analysis demonstrated that ablation of scEmc10 promotes adaptive thermogenesis in adipocytes via activation of the PKA signaling pathway and its downstream targets, particularly CREB and p38MAPK. Furthermore, neutralization of scEmc10 in the circulation reduced body weight and improved diet-induced metabolic dysfunction in obese mice.
Conclusions Together, our data suggest that scEmc10, as a novel secreted factor, dysregulation is a conserved feature of obesity in humans and mice and the scEmc10/PKA axis regulates body weight and metabolic homeostasis by suppressing adaptive thermogenesis in brown and white adipose tissues, which establish scEmc10 with therapeutic potential for the treatment of obesity and obesity-associated disorders.

104 IMPAIRED INSULIN SENSITIVITY IS RELATED TO INCREASED SKELETAL MUSCLE MITOCHONDRIAL RESPIRATORY CAPACITY DURING INSUFFICIENT SLEEP

[1]Sarah Morton, [2]Kenneth P Wright, [3]Irene E Schauer, [4]Michael J Jurczak, [3]Bryan C Bergman, [5]Josiane Broussard. [1]*Colorado State University*; [2]*University of Colorado Boulder*; [3]*University of Colorado Anschutz Medical Campus*; [4]*University of Pittsburgh*; [5]*Colorado State University, Arvada, CO*

10.1136/jim-2020-MW.70

Introduction/Background Insufficient sleep induces metabolic dysfunction, however, the mechanism(s) by which this occurs are unknown. In the context of type 2 diabetes, impaired insulin sensitivity is associated with reduced mitochondrial respiratory capacity.[1] [2] However, whether insufficient sleep affects mitochondrial function is not known.

Objective(s) We therefore sought to determine whether mitochondrial respiration is impacted by approximately one work-week of insufficient sleep.

Methods Eleven sedentary, healthy lean adults (26+1y; 23 +1 kg/m^2; 8M) participated in a 6-day in-laboratory protocol with 9h in bed (habitual sleep) followed by 4 nights of 5h in bed (insufficient sleep). For one week prior to the study, participants maintained a 9h sleep schedule, confirmed by actigraphy. For 3 days prior to the study and throughout the in-laboratory protocol, participants consumed a diet designed to meet daily energy requirements. Insulin sensitivity (glucose infusion rate) was assessed using a hyperinsulinemic euglycemic clamp before and after insufficient sleep. Muscle biopsies of the vastus lateralis were taken immediately before each clamp and mitochondrial respiration was examined using high-resolution respirometry (Oxygraph-2K, Oroboros).

Results Insulin sensitivity was significantly decreased during insufficient sleep (11.2+1.8 v 10.0+1.4 mg/kg/min; $p<0.05$). In contrast, ADP-stimulated mitochondrial respiration (state 3) and maximal uncoupled respiration (state U) were significantly elevated in isolated permeabilized ex vivo muscle fibers using pyruvate/malate as substrates. In vivo insulin sensitivity was negatively associated with mitochondrial respiration, such that lower insulin sensitivity was associated with higher mitochondrial respiration during state 3 ($r=-0.611$; $p<0.05$) and state U ($r=-0.672$; $p<0.05$).

Conclusions These findings are consistent with another study that reported circadian misalignment impairs insulin sensitivity and leads to increased mitochondrial respiration.[3] The implications of elevated mitochondrial respiration in this context are unclear, but may represent an acute compensatory response to insufficient sleep, implicating sleep as a regulator of mitochondrial function.

REFERENCES

1. Chomentowski P, Coen PM, Radikova Z, Goodpaster BH, Toledo FG. Skeletal muscle mitochondria in insulin resistance: differences in intermyofibrillar versus subsarcolemmal subpopulations and relationship to metabolic flexibility. *J Clin Endocrinol Metab* 2011;96(2):494–503.
2. Kelley DE, He J, Menshikova EV, Ritov VB. Dysfunction of mitochondria in human skeletal muscle in type 2 diabetes. *Diabetes* 2002;51(10):2944–50.
3. Wefers J, van Moorsel D, Hansen J, Connell NJ, Havekes B, Hoeks J, *et al*. Circadian misalignment induces fatty acid metabolism gene profiles and compromises insulin sensitivity in human skeletal muscle. *Proc Natl Acad Sci USA* 2018;115 (30):7789–94.

A03 SEX AND STRAIN DETERMINE THE METABOLIC RESPONSE TO DIETARY PROTEIN LEVEL

[1]Cara L Green, [1]Heidi Pak, [2]Nicole Richardson, [1]Victoria Flores, [2]Katherine Kredell, [2]Shany Yang, [2]Michelle Sonsalla, [2]Deyang Yu, [2]Jay Tomasiewicz, [2]Jesse Fan, [2]Juan Juarez, [2]Sabrina Dumas, [3]Cholsoon Jang, [3]Joshua Rabinowitz, [2]Dudley Lamming. [1]*University of Wisconsin- Madison, Madison, WI*; [2]*University of Wisconsin-Madison*; [3]*Princeton University*

10.1136/jim-2020-MW.71

Introduction/Background Low protein-high carbohydrate diets promote improved metabolic health in both rodents and humans, and have been shown to increase the lifespan of mice. However, the vast majority of research on protein restriction (PR) has been completed in male C57BL/6 mice. Recent work in the calorie restriction (CR) field has highlighted that sex, genetic background (strain), and the level of restriction are crucial factors to consider in nutritional intervention studies.

Objective(s) To characterize the impact of sex and genetic background on the metabolic response of mice to different levels of protein in the diet.

Methods We utilized male and female mice from three different genetic backgrounds, C57BL/6J, DBA/2J, and HET3 (the F2 progeny of 4 different inbred lines, including C57BL/6J and DBA/2J). C57BL/6J and DBA/2J mice are traditionally good and poor responders, respectively, to dietary interventions, while HET3 mice provide a heterogeneous population which more accurately reflects the genetic diversity of humans. We placed these mice on diets in which either 21% (control), 14% (medium protein, MP), or 7% (low protein, LP) of calories were provided by protein; all diets were isocaloric, with carbohydrates substituted as necessary and identical levels of fat. We characterized the metabolic and molecular responses to different protein intakes by measuring changes in body weight, food intake, glycemic control, energy expenditure, respiratory exchange ratio (RER), activity levels, the transcriptome and the metabolome.

Results We found that male C57 mice robustly respond to PR, with improved glucose tolerance, insulin sensitivity, and increased energy expenditure, with the majority of these metabolic responses only occurring on a LP diet, not on the MP diet. This speaks to the existence of a protein threshold effect, where metabolic effects are only observed once dietary protein drops below a certain level. In contrast, male DBA/2J mice were resistant to virtually all of the effects of PR, and did not demonstrate improved glucose homeostasis or altered energy balance. The ability of PR to induce metabolic changes was correlated with the ability of PR to induce fibroblast growth factor 21 (FGF21), a hormone previously associated with increased insulin sensitivity and energy expenditure, as Fgf21 liver expression increased in C57 but not DBA male mice on the LP diet. Whilst female C57 mice responded to the LP diets in a similar, though blunted fashion to that of their male counterparts, female DBA mice showed a pronounced response to the LP diet relative to the DBA males. Female C57 mice showed improvements in glucose tolerance, independent of changes in insulin sensitivity and body weight. However, whilst no improvements in glycemic control were seen in DBA females, a LP diet did result in reduced weight gain, in addition to, and contrasting with C57 males, a reduction in circulating FGF21. In HET3 mice the response to decreased protein intake was much more

variable, though it followed a similar but weaker pattern to that of C57 mice, and PR had some significant benefits, particularly in males. In an effort to understand the molecular basis for these results we performed transcriptional and metabolomics profiling of livers from C57 and DBA male and female mice. Hepatic metabolomics analysis indicated that on a LP diet acyl-carnitines were increased in C57 females and DBA male mice, whereas they were low in C57 males. Furthermore, DBA female mice showed changes in free fatty acids. Transcriptomic analysis of the liver indicated that fatty acid degradation and peroxisome proliferator-activated receptor (PPAR) signaling were increased in C57 male and female mice and oxidative phosphorylation was decreased in males on LP diets. However, female DBA mice showed no significant changes in PPAR signaling and fatty acid degradation on an LP diet, but did see increased changes in oxidative phosphorylation, carbon metabolism and the TCA cycle. This suggests that, whilst the molecular responses are clearly sexually dimorphic and strain-dependent, they center around alteration of changes in lipid and carbohydrate signaling and metabolism pathways.

Conclusions We have determined that there are both sex and strain specific effects of a PR diet on both phenotypic (body weight, food intake, glycemic control, energy expenditure, activity and RER) and molecular (hepatic transcriptome and metabolome) signatures. This suggests that humans may also respond differently to LP diets, which may be the result of allelic variants that impact energy sensing and metabolism genes. This highlights the importance of robustly testing the effects of dietary interventions in studies that seek to improve metabolic health. This will be key for future initiatives that utilize personalized medicine to treat pathologies associated with metabolic health disorders.

106 CONTRIBUTION OF HEPATOCYTE-SPECIFIC PPAR GAMMA TO THE DEVELOPMENT OF NON-ALCOHOLIC STEATOHEPATITIS (NASH), INSULIN RESISTANCE AND OBESITY

[1]Samuel Lee, [1]Jose Muratalla, [2]Alberto Diaz-Ruiz, [3]Jose Cordoba-Chacon. *[1]University of Illinois at Chicago; [2]IMDEA Food; [3]University of Illinois at Chicago, Chicago, IL*

10.1136/jim-2020-MW.72

Introduction/Background Non-alcoholic steatohepatitis (NASH) is a hepatic disease characterized by severe hepatic steatosis, inflammation, ballooning degeneration, fibrosis, and it is strongly associated with type 2 diabetes. While there is no FDA-approved pharmacological therapies for NASH yet, specific treatments for diabetes may reduce and reverse this disease. For instance, insulin sensitizers such as thiazolidinediones (TZDs) have been considered as a potential therapy for NASH. Positive results from the use of TZD in NASH patients were reported, but some mixed and modest outcomes questioned their therapeutic effects. TZDs are agonists of peroxisome proliferator-activated receptor gamma (PPARG) which is a well-known steatogenic factor in mice. Although the expression of PPARG is low in healthy livers, it has been positively associated with the progression of NASH.

Objective(s) We assessed the specific contribution of hepatocyte Pparg expression in the progression of NASH, insulin resistance, and obesity in a mouse model of diet-induced NASH.

Methods Control and adult-onset hepatocyte-specific Pparg knockout ($Pparg^{\Delta Hep}$) mice were fed either a low fat (LFCF) or a high fat, cholesterol, and fructose (HFCF) diet to induce NASH for up to 24 weeks. NMR-spectroscopy was used to track changes in body composition induced by $Pparg^{\Delta Hep}$ or the diet. Alterations in hepatic gene expression were assessed with RNAseq. After 8 and 24 weeks of HFCF diet, glucose homeostasis was assessed with glucose (GTT), insulin (ITT), and pyruvate (PTT) tolerance tests. In addition, metabolic rate, activity, and food intake were measured with metabolic cages.

Results HFCF-fed control mice developed NASH with a NASH Activity Score (NAS) of 6.78 ± 0.36. HFCF-fed $Pparg^{DHep}$ mice showed reduced NAS (5.0 ± 0.3), hepatic steatosis, inflammation, plasma ALT, liver weight, liver triglyceride levels and reduced bridging fibrosis (F3, 61% in controls vs 25% in $Pparg^{DHep}$), compared to HFCF-fed controls. Gene expression profiling by RNAseq identified 2273 differentially expressed genes in HFCF-fed $Pparg^{DHep}$ mice vs HFCF-fed controls (1055 upregulated, and 1218 downregulated). Interestingly, gene ontology analysis revealed an enrichment of >100 upregulated genes associated with inflammation and fibrogenesis in HFCF-fed mice and from these, $Pparg^{DHep}$ downregulated 71 and 82 genes, respectively. These findings suggest that hepatocyte-specific Pparg contributes to the progression of NASH in mice fed a HFCF diet. However, our study revealed additional interesting observations. First, independent of hepatic Pparg expression, HFCF feeding for 8 weeks induced insulin resistance, and increased food intake and energy expenditure (EE). Increased EE may have prevented increased body weight gain and/or adiposity in HFCF-fed mice. Second, 24 weeks of HFCF-diet induced NASH and hepatic insulin resistance, but did not induce severe obesity or whole-body insulin resistance. In fact, control mice fed a HFCF diet tended to have reduced adiposity and EE associated with increased activity, which might be indicative of additional effects of this diet in peripheral tissues. Nonetheless, although $Pparg^{DHep}$ ameliorated the progression of NASH, the knockout of hepatocyte Pparg expression increased adiposity and impaired glucose clearance during a GTT in mice fed a HFCF diet for 24 weeks.

Conclusions Hepatocyte-specific Pparg contributes to the progression of NASH. In addition, hepatocyte Pparg may protect against metabolic dysfunction and adiposity in peripheral tissues.

B02 OBESITY-ASSOCIATED HYPOXIA CONTRIBUTES TO ABERRANT METHYLATION OF GENES IMPLICATED IN INFLAMMATION AND VASCULAR FUNCTION

[1]Mohamed Ali, [2]Chandra Hassan, [2]Mario Masrur, [2]Francesco Bianco, [2]Patrice Frederick, [2]Giulianotti Cristoforo, [2]Antonio Gangemi, [2]Shane Phillips, [1]Abeer M Mahmoud. *[1]University of Illinois at Chicago, Chicago, IL; [2]University of Illinois at Chicago*

10.1136/jim-2020-MW.73

Introduction/Background Obesity is a significant risk factor for cardiovascular disease. It is characterized by a large accumulation of dysfunctional adipose tissue, which is now recognized as an endocrine organ that secretes numerous hormones and inflammatory cytokines generating a systemic proinflammatory state. We previously demonstrated an impaired vascular function in obese adults (OB). We now hypothesize a role of

obesity-associated hypoxia in disturbing the methylation/expression of genes involved in inflammation/vascular function. We also propose a mediating role of the hypoxia-inducible factor, HIF1α and the DNA hydroxymethylase, TET1.

Objective(s) This study is expected to elucidate DNA hypomethylation as an underlying epigenetic mechanism for the uncontrolled production of inflammatory adipocytokines in obesity and identify the intracellular signal, HIF1α/TET1, as an upstream target that initiates DNA hypomethylation.

Methods We obtained subcutaneous and visceral adipose tissue (AT) biopsies from bariatric patients (n=60; age: 36±7 yrs; BMI: 50.7±8.7 kg/m^2) and non-obese (NOB) adults having elective surgeries (n=30; age: 36±2 yrs; BMI: 25.8±1 kg/m^2). AT-isolated arterioles were tested for vasoreactivity in response to pressure gradients of Δ10-Δ100 cmH2O. Arteriolar nitric oxide (NO) and reactive oxygen species (ROS) were measured. Protein expression of HIF1α and TET1 and methylation/expression of leptin, IL1β, IL6, IL8, IL17, CXCL5, TNF-α, and IFNγ were measured in the AT.

Results Flow-induced dilation (FID) was 40–50% higher in NOB than OB adults across all pressure gradients ($p<0.05$). NO production was higher, and ROS generation was lower in OB arterioles compared to NOB. HIF1α and TET1 proteins were 2–4-fold higher in OB compared to NOB adults and correlated negatively with arteriolar FID, NO, and brachial artery FID (r=0.82, 0.64, 0.91, respectively; $p<0.001$) and positively with ROS (r=-0.71, $p<0.01$). Global hydroxymethylation and adipocytokine promoter hypomethylation and increased expression were observed in OB compared to NOB.

Conclusions Our results suggest that vascular dysfunction in OB adults may be attributed to aberrant DNA methylation and increased expression of adipocytokines. This conclusion was also supported by invitro mechanistic studies.

B03 FASTING, NOT REDUCED CALORIC INTAKE, MEDIATES THE EFFECTS OF A CALORIE RESTRICTED DIET ON SYSTEMIC INSULIN SENSITIVITY AND THE LIVER METABOLOME AND EPIGENOME

[1]Heidi Pak, [2]Spencer Haws, [2]Mikaela Koller, [2]Cara L Green, [2]Nicole Richardson, [2]Shany Yang, [2]Sabrina Dumas, [2]Lindsey Bray, [2]Michelle Sonsalla, [2]John Denu, [2]Dudley Lamming. [1]*University of Wisconsin, Madison, Madison, WI*; [2]*University of Wisconsin-Madison*

10.1136/jim-2020-MW.74

Introduction/Background It has been over a century since the discovery of life and health extension properties of calorie restriction (CR), defined as the reduction of energy intake without malnutrition. While effective in rodents and other mammalian species, an abstemious CR diet is too difficult for most people to maintain. Understanding the mechanisms by which CR promotes healthspan and developing effective CR-mimicking dietary regimens or pharmaceuticals is therefore essential to harnessing the benefits of CR. Recently, it has become apparent that when we eat may be just as important as what and how much we eat. Research into feeding paradigms have found that time-restricted feeding and intermittent fasting has metabolic benefits, protecting mice and perhaps humans from the negative metabolic effects of a high-fat, high-sucrose 'Western' diet. Similarly, meal-fed mice, which are fed a nearly ad libitum portion of food but consume it over ~12–15 hours, live longer than truly ad libitum fed animals. These findings significantly complicate the interpretation of CR studies done in a laboratory setting, as CR-fed animals are typically fed only once per day, consuming their food in ~2 hours, and are subjected to fasting for the remaining 22 hours per day. A largely overlooked question is whether the metabolic health benefits of CR arise solely from the reduction in calories, or if this enforced period of daily fasting is also required.

Objective(s) Here, we distinguish fasting dependent and independent effects by utilizing multiple feeding paradigms to determine if the metabolic effects of CR are mediated by reduced caloric intake, or also require prolonged fasting.

Methods We randomized male and female C57BL/6J and DBA/2J mice to four groups: 1) ad libitum diet or to one of three CR regimens in which calories were restricted by 30%: 2) animals fed once per day during the light period; 3) animals fed three equal meals during the course of the 12 hour dark period; and 4) animals provided with ad libitum access to a low energy diet diluted with indigestible cellulose, which reduced calorie intake by ~30%. Additionally, to fully address the impact of fasting duration from energy intake we used a 5) fifth feeding paradigm where mice were entrained to rapidly consume an ad libitum portion of food, and were fasted for the remaining ~22 hours per day.

Results We observed that all three CR regimens had similar effects on weight and body composition, fasting blood glucose levels and glucose tolerance for all strains and sexes. Intriguingly, we found that only male and female C57BL/6J mice on a traditional CR regimen, fed once daily, had improved sensitivity to insulin, a phenotype of CR that has been suggested to mediate many of CR's beneficial effects on longevity. This was also observed in the fifth feeding group, demonstrating that fasting, not caloric intake, is responsible for the improved insulin sensitivity of CR-fed mice. We examined the effects of CR at the molecular level by measuring metabolites and performing epigenetic profiling of the liver. As expected, we observed a distinct metabolomic signature associated with once-a-day CR compared to the ad libitum control. However, surprisingly, the metabolomic signature of the diluted diet group resembled closely that of the ad libitum control. This was also true with the acetylation profiles of histones, which suggest fasting, not reduced calorie intake, mediates the metabolomic and epigenetic profile typically shown in calorie restriction studies.

Conclusions We conclude that while many of the metabolic benefits of a CR diet are mediated by reduced caloric intake, the prolonged fasting induced in CR mice fed once a day mediates the effects of CR on systemic insulin sensitivity, as well as the metabolomic and epigenetic profiles observed in calorie restriction studies.

A33 ABLATION OF ADIPOSE CREB3L3 PREVENTS BROWNING AND PROMOTES INFLAMMATION

[1]Maximilian Mccann, [1]Marcos Muñoz, [1]Victoria Gil, [2]Kezhong Zhang, [1]Chong Wee Liew. [1]*University of Illinois at Chicago*; [2]*Wayne State University*

10.1136/jim-2020-MW.75

Introduction/Background The body contains two kinds of fat: white fat, which acts as an energy storage organ, and brown fat, which utilizes energy to generate heat. White fat consists

of the subcutaneous and the visceral fat. Accumulation of visceral fat contributes more to metabolic dysfunction due to its increased rate of lipolysis, reduced ability to form brown-like adipocytes known as 'beige' cells, and its more inflammatory nature.

Objective(s) In this study, we investigated the role that cyclic-AMP Responsive Element Binding Protein 3-like-3 (CREB3L3) plays in adipose tissue.

Methods Upon discovering that CREB3L3 is not only expressed in adipose tissue, but selectively downregulated in the more 'metabolically healthy' subcutaneous fat in both obese mice and humans, we investigated how ablating this transcription factor would affect adipose biology. To study this, we created a CREB3L3 fat-specific knockout (fKO) mouse. The fKO and floxed controls were fed high-fat diet for 10 weeks to induce obesity.

Results When challenged with high-fat diet, the fKO mice became 18% heavier than floxed controls. They had significant expansion of their epididymal and inguinal adipose depots, due to a reduction in whole-body energy expenditure and oxygen consumption as measured by indirect calorimetry. The fKO mice are also more resistant to browning during cold exposure and treatment with the B3-adrenergic receptor agonist CL316,243, suggesting impairment of adaptive thermogenesis in the subcutaneous fat. Expansion of the visceral epididymal fat caused the tissue to become more inflammatory as evidenced by an increase in the number of crown-like structures and expression of the macrophage marker F/480 in the fKO tissue. This led to the fKO mice becoming more insulin resistant following high-fat feeding.

Conclusions Together, ablation of CREB3L3 enhances adiposity and insulin resistance during obesity due to a reduction in browning potential and amplified visceral inflammation.

A34 A HUMAN GPR17 VARIANT ASSOCIATED WITH METABOLIC DISEASES HAS IMPAIRED SIGNALING FUNCTION

[1]Jason Conley, [2]Kristin Ayers, [2]Rong Chen, [3]Hongxia Ren. [1]*Indiana University School of Medicine*; [2]*Icahn School of Medicine at Mount Sinai*; [3]*Indiana University School of Medicine, Indianapolis, IN*

10.1136/jim-2020-MW.76

Introduction/Background Metabolic diseases, such as obesity and type 2 diabetes, affect millions of individuals in the United States and are associated with cardiovascular and other comorbidities. Considering the increasing prevalence, poor health outcomes, and high economic cost of these chronic diseases, there is a critical need to identify novel safe and effective therapeutic strategies. G protein-coupled receptors (GPCRs) expressed in the endocrine system contribute to the regulation of feeding, glucose homeostasis, and energy balance and thereby represent rich sources of potential novel pharmacological targets for metabolic diseases. We previously identified an orphan GPCR, GPR17, as an effector of the transcription factor FoxO1. We recently reported that Gpr17 deficiency in POMC neurons ameliorated the metabolic derangements caused by long-term high-fat diet feeding in rodent models (Reilly AM *et al*. 2019). We hypothesize that GPR17 is a promising therapeutic target for metabolic diseases, however our understanding of the role of GPR17 in human metabolism is limited. Major impediments of translating our rodent physiology findings to therapeutic strategies include the species difference of the GPR17 transcripts and incomplete understanding of GPR17 signaling pathways in key endocrine tissues.

Objective(s) The objective of this study was to identify human GPR17 genetic variants associated with metabolic diseases and investigate the impact of such mutations on receptor protein expression, plasma membrane localization, and intracellular signaling pathways.

Methods We mined genomic sequences of control and metabolic disease cohorts from UK10K data sets for GPR17 genetic variants in human patient populations. Site-directed mutagenesis was used to generate plasmids that encode GPR17 variants associated with metabolic diseases for in vitro evaluation of protein expression level, subcellular localization, and functional downstream signaling.

Results We report the identification of four non-synonymous GPR17 variants that were associated with adverse metabolic phenotypes in human patients. These human GPR17 variants have mutations in the conserved amino acid residues, which could have impact on cellular signaling by affecting ligand binding and G protein coupling. We generated the corresponding mutations in expression vectors with coding sequences for human short and long GPR17 isoforms. Subsequent in vitro characterization of the GPR17 variants suggested that receptor protein expression levels and subcellular localization were similar to wild type GPR17. We used a synthetic small molecule agonist to elicit GPR17-mediated calcium and cAMP signaling activities in cultured cells expressing GPR17 variants. While three of the GPR17 variants displayed signaling activities comparable to wild type GPR17, one of the variants displayed drastically altered calcium and cAMP signaling profiles.

Conclusions Here we report a specific GPR17 variant with altered downstream signaling function that was identified in human populations with adverse metabolic phenotypes. Elucidating the detailed mechanisms of how mutations in the critical residues impact cellular signaling will provide insight in the GPR17-mediated G protein-coupled signaling pathways. Knowledge gained from studying human genetic variants will ultimately provide a basis for future translational studies to target GPR17 for metabolic disease treatment.

Epidemiology/Health Outcomes/Quality Improvement/Bio-informatics

B34 IMPROVING THE OBJECTIVITY OF DIAGNOSIS OF URINARY TRACT INFECTION AFTER SPINAL CORD INJURY

[1]Felicia Skelton-Dudley, [2]Sarah May, [3]Annette Walder, [2]Larissa Grigoryan, [2]Barbara Trautner. [1]*Baylor College of Medicine, Houston, TX*; [2]*Baylor College of Medicine*; [3]*Michael E. DeBakey VA Medical Center*

10.1136/jim-2020-MW.77

Introduction/Background Urinary tract infection (UTI), including catheter-associated UTI, has been a salient topic in recent years due to its economic and health burden to the patient. UTI is especially burdensome after spinal cord injury (SCI). Our own work using the Healthcare Cost and Utilization Project database demonstrates that UTI is consistently amongst the top three reasons for emergency room visits and inpatient admissions, with a yearly cost of over $4 billion. While the

importance of recognizing and treating true UTI is evident, distinguishing this condition from asymptomatic bacteriuria (ASB, a positive urine culture without clinical signs or symptoms of infection) is particularly challenging after SCI, as we have described. Previous studies have shown that persons with SCI have difficulty accurately attributing their signs and symptoms to an UTI. We have recently interviewed 12 SCI providers, finding that even they struggle with which clinical signs and symptoms to use to guide bacteriuria management (manuscript in progress). Thus, the need to make the diagnosis criteria of UTI after SCI more objective and tailored to this patient population is clear. The hypothesis that underlies the development of the Acute Physiology and Chronic Health Evaluation-II (APACHE-II) tool provides a helpful framework: '..the severity of acute disease can be measured by quantifying the degree of abnormality of multiple physiology variables.'To calculate the degree of abnormality, however, we must have a better sense of the normal values for the SCI patient population, rather than the non-SCI population. The pathophysiology of autonomic nervous system changes leading to cardiovascular abnormalities after SCI have been well described, but there is little data quantifying the degree of change or expected values for vital sign readings in the SCI population, nor other common laboratory values.

Objective(s) Establish physiologic baselines for vital sign and lab measurements that may be used in the of diagnosis UTI after chronic SCI using national Veterans Health Administration (VHA) data sources.

Methods Case-control retrospective database study. Approach: We utilized VHA Corporate Data Warehouse (CDW), a national repository that includes clinical and administrative data from VHA. Data are stored in a relational database (i.e. data are grouped into several domains that are structured to recognize relations among the stored information) and are updated on a continual basis. Participants include Veterans with SCI (cases) as well as Veterans without SCI matched for age and Deyo co-morbidity index (controls), seen in the outpatient clinic setting in 2018 and 2019, based on frequency matching. Data from several domains within CDW to obtain participant demographics (age, gender, race/ethnicity); diagnoses (including level of SCI), outpatient vital signs (temperature, heart rate, blood pressure, respiratory rate); laboratory data (albumin, creatinine, total white blood cell count, urea, glucose, hemoglobin, electrolyte panels, and urinalysis results [urine pH, urine white blood cells and urine red blood cells]). Data analysis: Descriptive statistics for each group will be calculated, including mean and standard deviation (continuous variables) and frequency counts and percentages (categorical variables). T-tests will compare the means of the lab values of the cases to those of the controls. Chi-square tests will be used to compare categorical variables between cases and controls. Logistic regression will be used to study the associations between each factor (temperature, heart rate, systolic blood pressure, levels of pyuria and serum leukocytes) and SCI. The analyses will be adjusted for potential confounding variables, including age, gender, race/ethnicity, level of SCI and Deyo co-morbidity index.

Results The SCI cohort includes 4,560 participants. Demographically, median age is 60 (interquartile range 21–84); the sample is predominantly male (95%) and white (60%). The mean pulse was 73 beats per minute (SD 14), the mean temperature was 97.9 degrees Fahrenheit (SD 0.96), mean systolic blood pressure was 126 mm Hg (SD 16) and mean diastolic blood pressure was 74 (SD 11).

Conclusions This data will help address the gaps in knowledge of physiologic baselines for cardiovascular parameters for persons with SCI to develop a diagnostic tool to aid in the diagnosis of UTI. This tool will help make the diagnosis of UTI after SCI more objective and evidence-based. Improving the diagnostic accuracy of UTI in turn minimizes the inappropriate use of antibiotics for ASB and thus reduces the downstream harms of antibiotic overuse for persons with SCI.

B35 UTILIZING ETDQ-7 AS A TOOL TO PREDICT THE BETTER MEDICAL INTERVENTION FOR EUSTACHIAN TUBE DYSFUNCTION

[1]Sarah Toti, [2]Lazaro Peraza, [3]Anthony Zamboni. *[1]University of Nevada, Reno School of Medicine, Reno, NV; [2]University of Nevada, Reno School of Medicine; [3]Silver State ENT*

10.1136/jim-2020-MW.78

Introduction/Background A diagnosis of Eustachian Tube Dysfunction (ETD) is commonly treated with either oral steroids or tympanostomy tube insertion. Many patients suffer from a myriad of symptoms with varying severities and degrees of improvement from these interventions. This brings to question the best approach to treating ETD.

Objective(s) The objective of this study is to utilize the ETDQ-7 questionnaire to quantify initial symptom severity and the subsequent improvement of multiple symptoms following a medical intervention in patients diagnosed with ETD. Tracking this data could ultimately determine whether the questionnaire has the ability to accurately predict the best treatment option based on initial symptom severity.

Methods Patients referred to Silver State ENT with a diagnosis of Eustachian tube dysfunction, who had previously failed medical treatment with their primary care physician, were administered the Eustachian Tube Dysfunction Questionnaire-7 (ETDQ-7) before and after further medical intervention by the ENT. The survey assesses the severity of several symptoms such as pressure in ears, pain in ears, muffled hearing, popping sounds in ears, and others using a numerical sliding scale. Medical interventions included oral and nasal steroids first, followed by tympanostomy tube insertion if the steroids failed to improve their symptoms. Patients either completed 2 or 3 surveys depending on ETD improvement. Data was separated by symptom and analyzed for significance between surveys via t-test. Surveys were administered from November 2017 to September 2019.

Results A total of 153 surveys were completed by patients. The pre and post averages for the symptoms of pressure in the ears, ear problems during cold or sinusitis, and crackling or popping sounds in ear were significant for every medical intervention. If patients rated these symptoms in the moderate category on the ETDQ-7 scale, then oral and nasal steroids were sufficient in improving symptoms. However, if patients rated these symptoms in the severe category, tympanostomy tube insertion became the more successful medical intervention for improving symptoms. The pre and post averages for the symptoms of feeling that ears are clogged or 'underwater' and feeling that hearing is muffled were not significant for patients successfully treated with oral and nasal steroids. However, for patients who failed oral and nasal steroids and went on to have tympanostomy tube insertion, their pre and post averages for feeling that ears are clogged or 'underwater' and feeling that hearing is muffled were significant. The symptoms of

Abstract B35 Table 1 ETDQ-7

During the past 1 month, how much of a problem was each of the following?	No Problem				Moderate Problem	
1. Pressure in the ears?	1	2	3	4	5	
2. Pain in the ears?	1	2	3	4	5	
3. A feeling that your ears are clogged or "underwater"?	1	2	3	4	5	
4. Ear problems when you have a cold or sinusitis?	1	2	3	4	5	
5. Crackling or popping sounds in the ears?	1	2	3	4	5	
6. Ringing in the ears?	1	2	3	4	5	
7. A feeling that your hearing is muffled?	1	2	3	4	5	

The seven item Eustachian tube dysfunction questionnaire

Abstract B35 Table 2 ETDQ-7 pre and post medical intervention averages

The initial symptom averages versus the post steroid averages of patients who improved with oral and nasal steroids

	Pressure in Ears	Pain in the Ears	Ears clogged/underwater	Ear Problems when cold/sinusitis	Crackling or popping sounds in ears	Ringing in ears	A feel
Pre-med average	4.9	3.6	4.7	4.33	4.5	3.1	
Post-med average	2.5	1.6	2.2	1.44	1.3	1.3	
P-Value	0.04	1.00	0.10	0.01	0.01	0.73	

The initial symptom averages versus the post tympanostomy tube insertion averages of patients who improved with tubes

	Pressure in Ears	Pain in Ears	Ears clogged/underwater	Ear Problems When Cold/Sinusitis	Crackling or Popping Sounds in Ear	Ringing in Ears	A fe
Pre-med Average	6.20	3.98	6.27	6.12	6.05	3.84	
Post-tube Average	1.93	1.47	1.95	1.72	1.72	1.57	
P-Value	<0.01	0.17	<0.01	<0.01	<0.01	0.45	

Questions analyzed separately utilizing a t-test to determine significance

pain in the ears and ringing in the ears were not significant for any medical intervention.

Conclusions The ETDQ-7 is currently used as a diagnostic tool and symptom tracker of ETD. Our data suggests that the ETDQ-7 can also be used as a tool to predict the best treatment option for patients with ETD. Since there is no definitive consensus in the field of otolaryngology about the best management for adult ETD, this could lay the foundation for an algorithm of treatment for ETD. The symptoms of pressure in the ears, ear problems during cold or sinusitis, and crackling or popping sounds in ear were the strongest determinants for anticipating success with either oral and nasal steroids or tympanostomy tube insertion. The symptoms that showed no significant improvement with these two medical interventions should be investigated further with ETD medical interventions different from this study (i.e. myringotomy, balloon dilation) or by challenging their validity in assessing true ETD.

B12 DESCRIBING AND ASSESSING A NEW METHOD OF APPROXIMATING INDIVIDUAL-LEVEL INCOME IN CANCER REGISTRIES

[1]Uriel Kim, [2]Siran Koroukian, [2]Johnie Rose. *[1]Case Western Reserve University, Cleveland, OH; [2]Case Western Reserve University*

10.1136/jim-2020-MW.79

Introduction/Background Because income is rarely directly captured in cancer registries, individual patient-level income is often approximated using community-level income data from the US census. The traditional approach estimates income deterministically (for example, setting patients' incomes equal to the median income of their community of residence), which can lead to substantial income misclassification.

Objective(s) To describe and assess a new method of approximating individual-level income for patients in cancer registries using community-level data from the US census, in a process coined 'probability weighting.'

Methods In probability weighting, patient income is approximated probabilistically. First, data from the US census is used to calculate the probability of having a certain user-defined income in each census tract; for example, in census tract A, the probabilities of having an income of 0–149% of the federal poverty level (FPL), 150–299% FPL, 300–499% FPL, and 500%+ FPL might be 0.20, 0.25, 0.30, and 0.25, respectively. These probabilities are the probability weights. Next, patients are assigned the probability weights of their census tracts of residence. Finally, the probability weights are used as observation weights in calculations, allowing for a broad range of income-stratified cancer statistics. As a demonstration of this probability weighting approach, we calculated the age-adjusted, income-specific incidence rates of colorectal cancer in Ohio from 2014–2015, stratified by Non-Hispanic White (NHW) and Non-Hispanic Black (NHB) individuals, along with the percentage of metastatic cases at diagnosis.

Results There are 2,952 census tracts in Ohio. The median probability weights of these census tracts for incomes between 0–149% FPL, 150–299% FPL, 300–499% FPL, and 500%+ FPL are 0.19, 0.27, 0.27, and 0.21, respectively. The probability weighting approach estimates that age-adjusted incidence

rates are similar across income categories for both NHW and NHB Ohioans. Among NHW Ohioans with incomes of 0–149% FPL, 150–299% FPL, 300–499% FPL, and 500%+ FPL, the percentages of metastatic cases at diagnosis are 20.7% (95% CI: 18.8–22.7), 20.2% (95% CI: 18.8–21.7), 20.6% (95% CI: 19.2–22.2) and 21.2% (95% CI: 19.7–22.9), respectively. There is a stronger association between income and the percentage of metastatic cases at diagnosis in NHB Ohioans; the figures for the same income categories mentioned previously are 26.9% (95% CI: 22.4–31.7), 25.6% (95% CI: 21.1–30.6), 23.9% (95% CI: 18.9–29.6), and 22.6% (17.1–28.9), respectively. The estimates generated from this probability weighting exercise suggest that disparities in colorectal cancer burden are concentrated in low income (0–149%) NHB individuals, who experience the highest proportion of metastatic disease at diagnosis.

Conclusions Probability weighting is a method of individual-level income approximation that has the potential to generate more accurate income-specific cancer statistics using cancer registries than traditional approaches. The approach can scale across registries, and is useful for a broad range of cancer epidemiology and disparities studies. Most importantly, the granular information that probability weighting provides about the relationship between income and cancer burden can better inform, evaluate, and drive interventions and policies that aim to eliminate income-based cancer disparities.

B13 PREOPERATIVE GOAL-SETTING BY PATIENTS IS CORRELATED WITH BASELINE AND NOT 6-WEEK OUTCOMES FOLLOWING TOTAL KNEE ARTHROPLASTY (TKA)

[1]Vesta Nwankwo, [1]Janet Bettger, [2]Green Cindy,, [1]Thomas Risoli. [1]*Duke University School of Medicine*; [2]*Department of Biostatistics and Bioinformatics*

10.1136/jim-2020-MW.80

Introduction/Background Patient beliefs and goals can facilitate discussion of recovery expectations, patient-provider collaboration and maximization of goal achievement. Patients with specific activity/lifestyle goals may differ functionally preoperatively, and patient counseling should incorporate tailored expectation management for recovery. Given the importance and extensive implementation of physical rehabilitation during the subacute perioperative setting, it is necessary to better characterize which aspects of patient goal setting contribute to outcomes in the postoperative period.

Objective(s) In this study, we sought to address an evidence gap and examine the association of preoperative self-assessment of goals with preoperative and 6-week knee function and gait speed among total knee arthroplasty (TKA) patients.

Methods We conducted a secondary analysis of data from the VERITAS randomized, controlled trial conducted from 11/2016–03/2018 that included adults age ≥18 years with scheduled and completed unilateral TKA followed by post-surgical physical therapy. Patients rated their ability to perform various activities of daily living goals scaled from 0 (unable to perform) to 10 (full performance). Patients were categorized by pre-surgical (baseline) goal rating: low=0–2, intermediate=3–4, and high=5–10. Outcomes including gait speed and the KOOS were assessed within 10 days prior to surgery and 6-weeks post-surgery. Descriptive statistics and outcomes were compared for patients by preoperative goal rating using Chi-square or Fisher's exact tests and ANOVA or Kruskal-Wallis tests as appropriate.

Results Of 288 patients (mean age 65±8; 62.5% women; 82% white), 102 had a low goal rating (GR), 86 intermediate, and 99 high. Patients with low GR preoperatively generally had lower baseline mean scores than intermediate and high GR patients, respectively, on the KOOS (33.9/35.6/39.8; $p<0.001$) and lower gait speed (m/s) compared to intermediate and high GR patients at baseline (0.9/1.1/1.0; $p=0.009$). The low, intermediate, and high GR groups, respectively, showed no difference across mean KOOS scores (61.0/61.2/61.9; $p=0.63$) or gait speed (m/s) (1.0/1.0/1.0, $p=0.33$) at 6 weeks postoperative.

Conclusions In this study, adults who perceived greater difficulty with a pre-selected activity goal, exhibited lower function prior to TKA but showed no differences in function 6-weeks after surgery. Follow-up studies will describe the association between goal-setting preoperatively and patient goal attainment and satisfaction following surgery.

B14 BARRIERS TO FITBIT USE AMONG LOW-INCOME MINORITY WOMEN WITH ASTHMA

[1]Darshil Patel, [2]Guilherme Balbim, [2]Spyros Kitsiou, [2]David Marquez, [2]Lisa Sharp, [1]Sharmilee M Nyenhuis. [1]*University of Illinois at Chicago, Chicago, IL*; [2]*University of Illinois at Chicago*

10.1136/jim-2020-MW.81

Introduction/Background Fitbit activity trackers are increasingly used in physical activity (PA) interventions to promote self-monitoring of PA and assessing adherence to PA goals. While findings show that Fitbit activity trackers are reliable and feasible to use in a variety of research studies targeting PA, barriers may exist to their use especially in low-income minority populations. No current studies have explored the barriers that occur when using Fitbit activity trackers in PA interventions which may impact intervention adherence.

Objective(s) The aim of this study is to identify barriers to using activity trackers in a physical activity (PA) intervention designed for African American women with asthma (ACTION intervention).

Methods Fifty-three African American women with uncontrolled asthma (age 18–70) were enrolled in the 36-week study. Participants were randomized into enhanced usual care or the ACTION intervention, a behavioral walking program designed for African American women with asthma. All participants (control and intervention) received a Fitbit Charge HR or Fitbit Charge 2 and were invited to participate in an in-person Fitbit education session. All participants were instructed to report any issues with their Fitbit to the study team by their preferred contact method (phone, text or email). Intervention participants only, attended monthly group sessions for the first 24 weeks. During these group sessions, study staff queried participants about any Fitbit issues. All issues were documented in a Microsoft Excel sheet. At the end of the study, user responses were categorized by the study PI and staff.

Results A total of 183 issues were reported. The issues were categorized into user-related, device-related and app-related issues. User-related issues were the most reported (103 issues) followed by device-related issues (53 issues) and lastly app-related issues (27 issues). The most common user-related issue was navigating the Fitbit app (48 issues). The most common

device-related issue was participants reporting their PA not being recorded accurately (28 issues). The most common app-related issue was unable to sync the device with the app (17 issues).

Conclusions Despite their popularity commercially, there are barriers to implementing the use of Fitbit activity trackers in a PA intervention. Prior to utilizing commercially available fitness trackers in PA interventions, researchers need to prepare and train study staff and participants on potential issues that may arise with these devices and systematically record issues with device utilization. Additional work on investigating the user experience with these devices in PA intervention are needed.

A36 ABSTRACT WITHDRAWN

A37 THE RELATIONSHIP BETWEEN EXPERIENCES OF DISCRIMINATION & SUBSTANCE USE AMONG SEXUAL MINORITY YOUNG ADULTS: A DAILY DIARY STUDY

Cara Exten. *Pennsylvania State University, University Park, PA*

10.1136/jim-2020-MW.82

Introduction/Background Background: Sexual minority (SM) young adults experience significantly elevated rates of substance use behaviors and disorders relative to heterosexuals (Marshal *et al*., 2008; Rice *et al*., 2019). An emerging body of research demonstrates the relationship between discrimination and health among SMs (Hatzenbuehler, 2009; Meyer, 2003; Marshal *et al*., 2008), yet, the mechanism by which discrimination contributes to health disparities is poorly understood.

Objective(s) This study will examine the complex relationship between discrimination and substance use among sexual minority young adults using baseline and daily diary data, providing a unique contribution to the understanding of this understudied association.

Methods Data collection is ongoing and will be completed in December 2019. Data is being collected from sexual minority college students, aged 18–25, at a major public university in the Eastern United States. To date data have been collected from 93 participants, with anticipated enrollment of an additional 157 young adults (for a final expected enrollment of 250 participants). Students were recruited using advertisements and course announcements and screened for eligibility. Eligible participants completed a baseline survey assessing experiences of discrimination, substance use, sexual behaviors, and mental health, and 30 days of daily diary data assessing the same experiences and behaviors. Preliminary baseline data is presented here. Final analyses will use Modified Poisson regression (Zou, 2004) to evaluate the complex relationship between past year discrimination and past year substance use outcomes at baseline. Substance use outcomes include binge drinking, use of illicit drugs, and tobacco use. Key demographic variables, including gender, race, and sexual orientation, will be evaluated as effect modifiers. Further, we will evaluate the potential protective effects of social support and community support on these relationships. Multi-level models will be used to evaluate these same relationships at the day-level.

Results The mean age of participants is 20 years old. Among the 93 participants, 69% are female, 24% are male, 4% are nonbinary, and 3% report another gender. The majority of participants identify as bisexual (55%) or queer (13%), but gay, lesbian, mostly heterosexual, and other orientations are represented in the data. Substance use is common among participants, with 91% reporting past-year alcohol use, 61% reporting past-year marijuana use, and 45% reporting past-year cigarette or e-cigarette use. Thirty seven percent of participants report binge drinking at least monthly. Most commonly reported illicit drug use includes cocaine (11%) and stimulants (18%). Sexual-orientation based discrimination in the past year is reported by 46% of participants. Full results will be available on the complete sample at the time of presentation.

Conclusions In this preliminary data, reports of discrimination and substance use are highly prevalent among sexual minority young adults. As the substance use disparities affecting the sexual minority population continue to be documented, it is critical that we evaluate significant predictors of substance use and identify potential protective factors. This presentation will contribute to a deeper understanding of these relationships, which is crucial for future prevention and intervention programming.

A38 MULTIPLE SCLEROSIS CLUSTER: MYCOTOXIC LEUKOENCEPHALOPATHY UPDATE

[1]Gary J Ordog, [2]Theadora V Ordog. [1]*University of British Columbia, Maple Ridge, BC*; [2]*University of Iowa, Coralville, IA*

10.1136/jim-2020-MW.83

Introduction/Background A cluster of 42 patients was identified, out of 652 who were examined, all of whom were employed at a California courthouse. As previously reported, the worksite was known to have had 20 years of water intrusion, chronic dampness and mold growth, including the toxigenic Stachybotrys chartarum.

Objective(s) Prospective case outcome study.

Methods Environmental testing. Examination, laboratory and imaging studies on all.

Results Environmental testing confirmed the presence of air borne mold amplification in every room tested, distributed by a contaminated HVAC system. Surface and bulk mycotoxin levels were uniformly elevated from micro- to milligram ranges for trichothecenes, satratoxins, and aflatoxins. Corresponding ELISA serology was present in the employees with elevations in a series of mold hypersensitivity pneumonitis panels and ELISA mycotoxin panels for trichothecenes, satratoxins, and aflatoxins in over 95% of the patients. Immune function testing was abnormal in over 95% of the patients, with decreases in Interleukin-2 and Natural Killer Cell (T-lymphocyte) number and function. Forty-two of the employees complained of neurological deficit including memory loss, cognitive dysfunction, dizziness, abnormalities of executive functioning, headaches, visual disturbances, and symptoms of numbness and weakness of the extremities. These patients had signs of memory loss, cognitive dysfunction, executive dysfunction, sensory and motor deficits, positive Romberg Signs and ataxia. These patients had positive

MRI and PET scan findings consistent with areas of demyelination. Forty-two had areas of brain hypo-perfusion on FDG PET Scan. Neurological antibody testing was positive, including for myelin associated glycoprotein, glutamate receptors, myelin basic protein, chondroitin sulfate, and crystalline. These 42 patients were diagnosed with mycotoxic leukoencephalopathy, causing their Multiple Sclerosis (MS)-like syndrome. Treatment including removal of the patient from the building resulting in general improvement, with not further exacerbations of the illness. The areas of demyelination also improved or resolved in 40 of 42 patients, after a year with removal from the building and treatment.

Conclusions The incidence of MS is stated to be 1 per 100,000 in the general population. A cluster of 42 patients out of 600 from a single building known as a site of chronic biotoxin associated illness due to chronic dampness, mold growth and mycotoxin contamination, far exceeds a billion to one probability that it is not due to chance ($p \leq 0.05$). Ruling out all other areas of differential diagnosis, the cause of this cluster is mycotoxin exposure from the indoor dampness. Mycotoxic leukoencephalopathy has been identified as the cause of this cluster of Multiple Sclerosis-like illness. The reason this is called MS-'like' illness, is that when the cause was determined, the patients were treated and removed from the source of exposure. Following these over the next fifteen years, only two of the forty-two had further worsening or exacerbation from re-exposure, thus validating a clinical definition of Multiple Sclerosis. A final phase of the study to prove Koch's Postulate of Medical Toxicology, would have been to re-expose those patients to the source and examine for exacerbation of the illness, but this was neither ethical nor practical as the building was destroyed. Of note, many of the patients reported temporary exacerbation of symptoms when entering other 'musty' or 'moldy' buildings afterwards. Other cases of Multiple Sclerosis (Mycotoxic Leukoencephaloathy) should be investigated for a similar toxicological cause.

A39 ANALGESIC USE IN PATIENTS WITH DRUG-INDUCED, ACUTE DYSTONIA: A DEMOGRAPHIC STUDY

[1]Fahad Qureshi, [2]Eleni Tambassis, [2]John Lin, [2]Anum Chaudhry, [2]Julie Banderas, [2]Suman Sahil, [3]Brian Lee. *[1]University of Missouri School of Medicine, Glenview, IL; [2]UMKC School of Medicine; [3]Children's Mercy Hospital*

10.1136/jim-2020-MW.84

Introduction/Background Dystonia is a movement disorder characterized by painful, abnormal posturing due to agonist and antagonist muscles contracting together. Numerous individuals diagnosed with dystonia receive an analgesic. Drug overdose deaths continue to rise, with ~68% involving a prescription or illicit opioid. Although opioid prescription rates have significantly fallen, overall amounts of opioid prescribed were still 3x higher in 2015 than in 1999.[1] [2] Recently, new CDC guidelines have been established for opioid administration. Prescription rates must be frequently assessed to determine the effectiveness of measures taken.[3]

Objective(s) The goal of this study was to observe the rate at which potentially abusive and non-abusive analgesics are prescribed in the emergency department and identify any bias or other factors that influence the prescription rate.

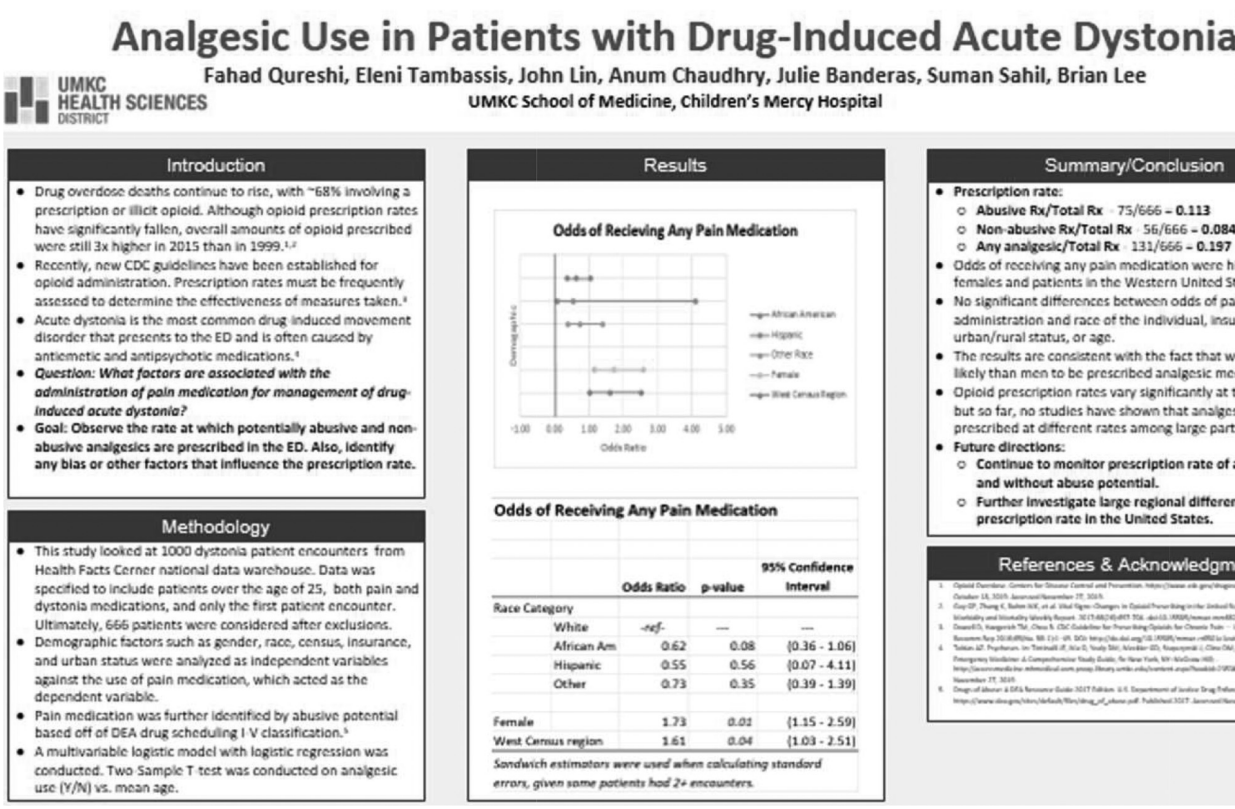

Abstract A39 Figure 1

Methods This study looked at 1000 dystonia patient encounters from Health Facts Cerner national data warehouse. Data was specified to include patients over the age of 25, both pain and dystonia medications, and only the first patient encounter. Ultimately, 666 patients were considered after exclusions. Demographic factors such as gender, race, census, insurance, and urban status were analyzed as independent variables against the use of pain medication, which acted as the dependent variable. Pain medication was further identified by abusive potential based off of DEA drug scheduling I-V classification.[4,5] A multivariable logistic model with logistic regression was conducted. A Two-Sample T-test was conducted on analgesic use (Y/N) vs. mean age.

Results The significant findings were those of females and the west census region with a p-value of 0.01 and 0.04, respectively. The odds ratio was 1.73 and 1.61, respectively. The 95% confidence interval was 1.15–2.59 and 1.03–2.51, respectively. All in all, females and the west census region were shown to have higher odds of receiving pain medications.

Conclusions Odds of receiving any pain medication were higher for females and patients in the Western United States. There were no significant differences between odds of pain medication administration and race of the individual, insurance type, urban/rural status, or age. This is relevant because the opioid epidemic has been a huge blow to our country and across the world, and by better understanding who is more likely to be prescribed pain medications, health professionals can better perform a necessary risk-benefit analysis. This would result in more accurate prescriptions and decreased patient mortality.

REFERENCES

1. Opioid Overdose. Centers for Disease Control and Prevention. https://www.cdc.gov/drugoverdose/index.html. Published October 18, 2019. Accessed November 27, 2019.
2. Guy GP, Zhang K, Bohm MK, *et al*. Vital Signs: Changes in Opioid Prescribing in the United States, 2006–2015. *MMWR Morbidity and Mortality Weekly Report*. 2017;**66**(26):697–704. doi:10.15585/mmwr.mm6626a4.
3. Dowell D, Haegerich TM, Chou R. CDC Guideline for Prescribing Opioids for Chronic Pain — United States, 2016. MMWR Recomm Rep 2016;65(No. RR-1):1–49. DOI: http://dx.doi.org/10.15585/mmwr.rr6501e1external icon.
4. Tobias AZ. Psychoses. In: Tintinalli JE, Ma O, Yealy DM, Meckler GD, Stapczynski J, Cline DM, Thomas SH. eds. Tintinalli's Emergency Medicine: A Comprehensive Study Guide, 9e New York, NY: McGraw-Hill; http://accessmedicine.mhmedical.com.proxy.library.umkc.edu/content.aspx?bookid=2353§ionid=190079424. Accessed November 27, 2019.
5. Drugs of Abuse: A DEA Resource Guide 2017 Edition. U.S. Department of Justice Drug Enforcement Administration. https://www.dea.gov/sites/default/files/drug_of_abuse.pdf. Published 2017. Accessed November 27, 2019.

A40 ASSESSING THE VALIDITY OF THE ETDQ-7 SURVEY QUESTIONS BASED ON EUSTACHIAN TUBE DYSFUNCTION OUTCOMES

[1]Sarah Toti, [2]Lazaro Peraza, [3]Anthony Zamboni. *[1]University of Nevada, Reno School of Medicine, Reno, NV; [2]University of Nevada, Reno School of Medicine; [3]Silver State ENT*

10.1136/jim-2020-MW.85

Introduction/Background The Eustachian Tube Dysfunction Questionnaire-7 (ETDQ-7) was created to assess Eustachian tube dysfunction (ETD) in patients displaying chronic ETD symptoms for >1 month. Since its inception, it has been used as a symptom tracker. However, the ETDQ-7 contains questions that may not correlate with the symptoms of ETD but rather a comorbidity.

Objective(s) The purpose of this study is to analyze each question on the ETDQ-7 and determine the significance of each question following ETD treatments of oral and nasal steroid therapy and/or tympanostomy tube insertion. This analysis will provide a chance to assess the validity of individual questions on the ETDQ-7 and whether modifications should be made to the questionnaire.

Methods 37 patients (54 ears, 151 total surveys) were administered the ETDQ-7 before and after medical intervention by the ENT. Average scores were calculated for each question on the ETDQ-7 before and after each intervention, and then compared against each other for statistical significance via t-test. A p-value of 0.05 determined whether or not the degree of symptom improvement following each intervention was significant. The data was separated into three comparison

Abstract A40 Table 1 Averages for each question on ETDQ-7 before and after medical interventions

The initial symptom averages versus the post steroid averages of patients who improved with oral and nasal steroids

	Pressure in Ears	Pain in the Ears	Ears clogged/underwater	Ear Problems when cold/sinusitis	Crackling or popping sounds in ears	Ringing in ears	A
Pre-med average	4.9	3.6	4.7	4.33	4.5	3.1	
Post-med average	2.5	1.6	2.2	1.44	1.3	1.3	
	Significant	No Significance	No Significance	Significant	Significant	No Significance	

The post steroid averages versus the post tympanostomy tube insertion averages of patients who improved with tubes

	Pressure in Ears	Pain in Ears	Ears clogged/underwater	Ear Problems When Cold/Sinusitis	Crackling or Popping Sounds in Ear	Ringing in Ears	A
Post-med Average	5.95	3.67	6.14	5.86	5.80	3.84	
Post-Tube Average	1.93	1.47	1.95	1.71	1.72	1.58	
	Significant	No Signficance	Significant	Significant	Significant	No Significance	

The initial symptom averages versus the post tympanostomy tube insertion averages of patients who improved with tubes

	Pressure in Ears	Pain in Ears	Ears clogged/underwater	Ear Problems When Cold/Sinusitis	Crackling or Popping Sounds in Ear	Ringing in Ears	A
Pre-med Average	6.20	3.98	6.27	6.12	6.05	3.84	
Post-tube Average	1.93	1.47	1.95	1.72	1.72	1.57	
	Significant	No Significance	Significant	Significant	Significant	No Significance	

The initial symptom averages versus the post steroid averages of patients who improved with oral/nasal steroid showed significance for pressure in the ears, ear symptoms during cold or sinusitis, and crackling or popping sounds in ears. The questions regarding pain in the ears, a feeling that ears are clogged or 'under water', ringing in ears, and a feeling that hearing is muffled were not significant for patients who improved with oral and nasal steroids. The post steroid averages versus the post tympanostomy tube insertion averages of patients who improved with tubes had the same significance outcomes as the last comparison group of initial symptom averages versus the post tympanostomy tube insertion averages of patients who improved with tubes. For these two groups pressure in the ears, a feeling that ears are clogged or 'underwater', ear symptoms during cold or sinusitis, crackling or popping sounds in ears, and a feeling that hearing is muffled were all statistically significant. Pain in ears and ringing in ears were not statistically significant.

Abstract A40 Table 2 ETDQ-7

During the past 1 month, how much of a problem was each of the following?	No Problem				Moderate Problem	
1. Pressure in the ears?	1	2	3	4	5	
2. Pain in the ears?	1	2	3	4	5	
3. A feeling that your ears are clogged or "underwater"?	1	2	3	4	5	
4. Ear problems when you have a cold or sinusitis?	1	2	3	4	5	
5. Crackling or popping sounds in the ears?	1	2	3	4	5	
6. Ringing in the ears?	1	2	3	4	5	
7. A feeling that your hearing is muffled?	1	2	3	4	5	

The seven item Eustachian tube dysfunction questionnaire ETDQ-7, copyright 2012 by McCoul ED, Anand VK and Christos PJ. Weil Cornell Medical College. New York, New York.

groups: 1) the initial symptom averages versus the post steroid averages of patients who improved with oral/nasal steroids, 2) the post steroid averages versus the post tympanostomy tube insertion averages of patients who improved with tubes, 3) the initial symptom averages versus the post tympanostomy tube insertion averages of patients who improved with tubes. Based on the statistical significance pattern of a question, this determined which symptoms of the ETDQ-7 could be improved from ETD interventions. Questions that were not statistically significant following ETD interventions should have their inclusion on ETDQ-7 challenged.

Results The data shows statistical significance in every group for pressure in the ears, ear symptoms during cold or sinusitis, and crackling or popping sounds in ears indicating that these symptoms are highly correlated with true ETD and can be improved by ETD medical interventions. This validates that these 3 questions are assessing ETD and belong on the ETDQ-7. The data shows no statistical significance in every group for pain in the ears and ringing in the ears, indicating that these symptoms cannot be improved by ETD medical interventions. This decreases the validity of these 2 questions accurately assessing ETD, and therefore, raises concerns of their presence on the ETDQ-7. The data showed mixed statistical significance for a feeling that ears are clogged or 'underwater' and a feeling that hearing is muffled, indicating a need for further evaluation or alteration of these 2 questions.

Conclusions Our data suggests removing the questions of pain in the ears and ringing in the ears due to no correlation with outcomes after ETD medical interventions. Given the descriptive terminology used in the ETDQ-7, we are interested in combining questions 3 and 7 seeing as they had mixed statistical significance. This would leave us with an ETDQ-4 which could be more accurate in assessing true ETD and leave out possible comorbidities (i.e. TMJ, presbycusis, hearing loss) that cannot be resolved with ETD medical interventions.

Gastroenterology/Clinical Nutrition

B37 YOUTUBE VIDEOS ON IRRITABLE BOWEL DISEASE: A QUALITATIVE ANALYSIS OF VIEWS AND CONTENT

[1]Muaataz Azawi, [2]Urja Patel, [3]Nassif Marc Ayoub, [4]Manar Alwan, [5]Aaron Walfish. [1]*Icahn School of Medicine at Mount Sinai, Astoria, NY*; [2]*Icahn School Medicine at Mount Sinai, Elmhurst, NY*; [3]*Elmhurst Hospital Center, NY*; [4]*Damascus University – Faculty of Medicine*; [5]*Elmhurst Hospital Center*

10.1136/jim-2020-MW.86

Introduction/Background Irritable bowel syndrome (IBS) is a functional disorder of the GI tract. It accounts for 25–50% of all referrals to gastroenterologists in the US, ranking it as the second highest cause of work absenteeism. Patients tend to use the internet, and particularly social media sites, to learn more about their medical condition. YouTube being one of the largest search engines, has grown its popularity as a go-to health-related source of information.

Objective(s) This study aims to evaluate the quality of material available for IBS patients.

Methods Youtube.com main page was queried for the search term 'Irritable Bowel Disease'. The top 20 videos were evaluated for content, duration, source, and audience interaction: number of views, likes, and dislikes. The content was classified based on the uploader's identity to health care professionals, health care organizations, individuals/patients, clips from TV shows, and non-professional educational groups. These videos were further analyzed for content using the published DISCERN instrument with 16 questions each consists of a 5-point scale for assessing the quality of health information.

Results The search phrase 'Irritable Bowel Disease' recaptured thousands of videos sorted by default filter of 'relevance.' The top 20 videos were analyzed as these are the videos that patients were likely to view by visitor statistics. On average, videos had 5:41 minutes duration, 184892 views, 1471 likes, and 81 dislikes. 50% of videos were from health care professionals, 30% from health care organizations, 10% from individuals/patients, 5% clips from TV shows, and 5% non-professional educational groups. Health care organization videos scored an average of 2.9 out of 5 on the DISCREN scale

Abstract B37 Table 1 Schedule

Duration	0:05:41
Views	184892.2
Likes	1470.75
Dislike	80

The average data of the 20 top 20 videos

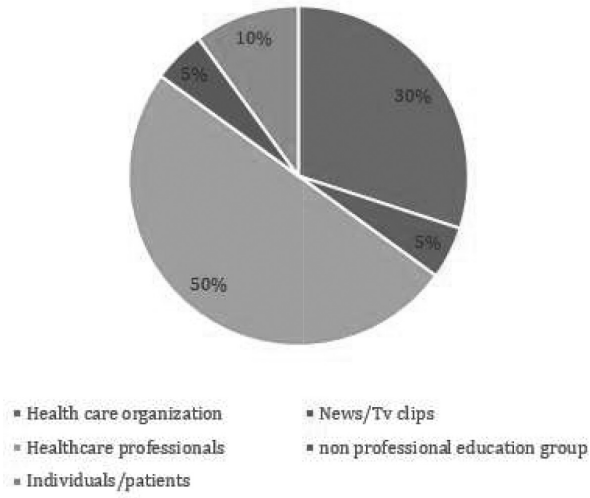

Abstract B37 Figure 1 To 20 videos Uploaders

indicating fair quality. Health care professionals' videos obtained an average DISCERN score of 2.5. On the other hand, new/TV clips obtained a 2 on DISCERN score. Individuals/patients and non-professional educational groups videos recorded 1.5% and 1% respectively.

Conclusions Despite YouTube being the fastest growing shared videos website, it lacks qualitative videos about a very common disease such IBS. As one of the largest online references for many patients, healthcare organizations can utilize this platform to correct misconceptions about the disease. Although the majority of the top 20 videos were created by healthcare professionals, it is advisable to improve their content quality and given the prevalence of misleading videos, patients should exercise extra caution towards this information and verify it directly from a healthcare provider.

A42 ALCOHOL-INDUCED GHRELIN PROMOTES HEPATIC STEATOSIS BY MODULATING HORMONE MEDIATED GUT-PANCREAS-ADIPOSE-LIVER AXIS

[1]Carol Casey, [1]Kusum Kharbanda, [1]Jacy Kubik, [2]Karuna Rasineni. *[1]University of Nebraska Medical Center; [2]University of Nebraska Medical Center, Omaha, NE*

10.1136/jim-2020-MW.87

Introduction/Background Hepatic steatosis, characterized by the fat accumulation in hepatocyes, is one of the earliest pathological changes in the progression of alcoholic liver disease. Pathophysiological mechanisms involved in development of these fatty liver diseases are complex and multifactorial, including gut, pancreas and adipose tissue dysfunctions that promote liver injury and its progression. Accumulating evidence has demonstrated that the interplay between the gut, adipose, pancreas, and liver are regulated by peptide hormones. Thus, there is a growing interest in understanding the role of hormones in organ interactions and in the development of metabolic diseases including alcoholic liver disease. Recently, we showed that ghrelin, a gut hormone significantly increased with chronic alcohol exposure, plays a major role in the development of alcoholic steatosis. We demonstrated that the alcohol-induced increase in ghrelin impaired insulin secretion from pancreatic β-cells. The consequent reduction in the circulating insulin levels promoted adipose lipolysis and mobilization of fatty acids to the liver to ultimately contribute to hepatic steatosis. In addition, we also reported that ghrelin inhibits adiponectin secretion, a hormone which reduces hepatic lipogenesis and promotes lipid oxidation. Further, we also reported that decreased levels of adiponectin, a hormone which reduces hepatic lipogenesis and promotes lipid oxidation. Recently, we observed serum glucagon-like peptide-1 (GLP-) is increased in ethanol-fed rats. GLP-1 is known to stimulate insulin secretion from pancreas and also known to promote hepatic fatty acid oxidation. However, the increased GLP-1 and decreased insulin levels in serum of alcohol-fed rats suggests that GLP-1-mediated signaling may be impaired by ethanol administration.

Objective(s) In this study we investigate the role of ghrelin in GLP-1 mediated hepatic metabolism and development of fatty liver.

Methods Primary rat hepatocytes were cultured in presence of 500 μM oleic acid overnight and then incubated the cells for 4h in serum-free media in the presence or absence of ghrelin (5 nM) and/or GLP-1 analog exendin-4 (20 nM). After treatment, cellular triglycerides were measured. For in vivo studies, adult male Wistar ghrelin receptor knockout (KO) rats and wild type (WT) rats were pair-fed for 6 weeks with Lieber-DeCarli liquid control and ethanol diets. After 6 weeks, rats were sacrificed, the blood and tissues were collected for analysis.

Results Treatment of hepatocytes with exendin-4 reduces triglyceride content, whereas treatment with exendin-4 in the presence of ghrelin significantly decreased triglyceride breakdown, indicate ghrelin dysregulates GLP-1 mediated functions. In rats, as expected, we observed increased serum non-esterified free fatty acids (NEFA) and increased hepatic triglycerides (TG) in ethanol-fed wild type rats while ethanol-fed KO rats showed similar serum NEFA levels and hepatic TG as controls. Intriguingly, serum NEFA levels were much lower in control-fed KO rats compared to their respective WT controls. In ethanol fed WT rats, we observed increased serum levels of GLP-1, and decreased insulin and adiponectin levels. Interestingly, ethanol-fed KO rats showed increased insulin sensitivity with moderate increase in insulin levels. Another intriguing observation was an increase in GLP-1 in the ethanol-treated wild type rats and normalization to control levels in KO-ethanol rats.

Conclusions These results indicate that increased GLP-1 levels seen after ethanol feeding is a compensatory increase due to impaired GLP-1 function (similar to insulin resistance-associated hyperinsulinemia). Thus, alcohol-induced increased ghrelin contributes to hepatic steatosis by modulating hormone mediated through gut-pancreas-adipose-liver axis.

A43 HARMFUL ALGAL BLOOM TOXIN MICROCYSTIN-LR EXACERBATES DEXTRAN SULFATE SODIUM INDUCED COLITIS IN A CD40 DEPENDENT MANNER

[1]Robin Su, [2]Apurva Lad, [3]Joshua D Breidenbach, [4]Emily Warner, [5]Casey Meyers, [4]Prabhatchandra Dube, [2]Fatimah K Khalaf, [4]Shungang Zhang, [2]Chrysan J Mohammed, [4]Andrew L Kleinhenz, [4]Thomas Blomquist, [4]Deepak Malhotra, [4]Steven T Haller, [6]David J Kennedy. *[1]The University of Toledo College of Medicine and Life Sciences, OH; [2]University of Toledo, Toledo, OH; [3]University of Toledo, Holland, OH; [4]The University of Toledo; [5]Wittenberg University*

10.1136/jim-2020-MW.88

Introduction/Background Harmful algal blooms (HABs) are on the rise globally and pose a serious health risk due to the

release of cyanotoxins. Microcystin-LR (MC-LR) is one of the most prevalent cyanotoxin released during HAB events and is a well-known hepatotoxin. The health effects of MC-LR in pre-existing disease states is not well characterized. We have previously shown that MC-LR has limited effects in the intestines of healthy mice, but has pronounced toxicity in the intestines of mice with dextran sulfate sodium (DSS)-induced colitis. In the setting of pre-existing colitis, MC-LR was observed to prolong body weight loss and detectable blood in the stool, worsen DSS-induced colonic shortening, increase DSS-induced colonic ulceration, and further exacerbate increases in DSS-induced inflammatory cytokines, such as TNF-α and IL-1β. In addition, we found that the TNF receptor superfamily member CD40 was significantly upregulated in colons of mice exposed to MC-LR with DSS-induced colitis.

Objective(s) We sought to test the hypothesis that MC-LR exacerbates DSS-induced colitis in a CD40 dependent manner.

Methods Wild type (WT) C57BL/6 and CD40 knockout (CD40KO) male mice on the C57BL/6 background were split into four exposure groups (n=6–10 per group): 1) control; 2) dextran sulfate sodium (DSS) only; 3) MC-LR only; and 4) DSS+MC-LR. Control mice were given regular drinking water for two weeks with sham oral gavage given daily during Week 2. DSS exposure alone mice were given 3% DSS drinking water during Week 1 and normal drinking water during Week 2, again with sham oral gavage given daily during Week 2. MC-LR exposure alone mice were given normal drinking water for 2 weeks with oral gavage of 1000ug/kg MC-LR daily during Week 2. DSS followed by MC-LR (DSS+MC-LR) exposure mice were given 3% DSS drinking water during Week 1 and normal drinking water during Week 2 with oral gavage of 1000ug/kg MC-LR daily during Week 2. Disease severity was determined based on the following parameters: body weight, stool grade, colon length, histological identification of colonic ulceration, and inflammatory marker regulation as assessed by qPCR.

Results MC-LR exposure alone had minimal overall effects in both WT and CD40KO mice. MC-LR exposure alone resulted in colonic shortening in both WT ($p<0.0001$) and CD40KO mice ($p<0.001$) compared to vehicle controls. In both WT and CD40KO mice, DSS exposure alone was observed to cause body weight loss, with full recovery in body weight following DSS removal during Week 2. Similarly, DSS exposure alone led to bloody stools in both WT and CD40KO mice, with full recovery following DSS removal during Week 2. In both WT and CD40KO mice, DSS exposure alone also led to colonic shortening ($p<0.0001$), colonic ulceration, and upregulation of TNF-α ($p<0.01$ in WT and $p<0.05$ in CD40KO) and IL-1β ($p<0.0001$ in WT and $p<0.01$ in CD40KO) compared to controls. DSS+MC-LR exposure led to prolonged decreases in body weight in both WT and CD40KO mice, however knocking out CD40 led to significantly less weight loss than in WT mice ($p<0.05$). While DSS+MC-LR exposure caused prolonged bloody stools without recovery following DSS removal in WT mice, knocking out CD40 led to full recovery of bloody stools following DSS removal. DSS+MC-LR exposure exacerbated DSS-induced colonic shortening, however, knocking out CD40 significantly attenuated the amount of colonic shortening ($p<0.0001$ vs WT). DSS+MC-LR exposure also led to the worsening of DSS-induced colonic ulceration, however, knocking out CD40, again, significantly decreased the amount of colonic ulceration ($p<0.001$ vs WT). DSS+MC-LR exposure also exacerbated DSS-induced inflammatory marker upregulation, however, knocking out CD40 significantly attenuated TNF-α expression ($p<0.0001$ vs WT).

Conclusions Our results suggest MC-LR exacerbates dextran sulfate sodium-induced colitis in a CD40 dependent manner.

Genetic and Molecular Medicine

B40 TRANSCRIPTOMIC ANALYSIS OF RESP18^{MUTANT} RAT KIDNEYS REVEALS UP-REGULATION OF RENIN-ANGIOTENSIN SYSTEM

Usman M Ashraf, Sivarajan Kumarasamy, Blair Mell. *University of Toledo College of Medicine and Life Sciences, Toledo, OH*

10.1136/jim-2020-MW.89

Introduction/Background The interplay between genetics and the environment play a vital role in the development and progression of hypertension and/or renal disease. Thus, identifying gene/genetic loci that contribute to hypertension and/or renal disease is fundamental in understanding these complex diseases. One such gene Regulated Endocrine Specific Protein 18 (RESP18), was found to have association with hypertension however the exact function of this gene is unknown. Previously, we have shown that a ZFN targeted disruption of Resp18 in Dahl SS rat genetic background (Resp18^{mutant}) aggravates salt-induced hypertension and renal injury on long term 2% high salt (HS) diet exposure.

Objective(s) The objective of the current study was aimed to investigate transcriptomic response in the Resp18^{mutant} rat kidneys on short term 2% HS diet treatment.

Methods We challenged the Resp18^{mutant} rats and SS rats with a short-term 1-week HS treatment, then measured blood pressure via radio telemetry. Glomerular filtration was measured via the transcutaneous clearance of fluorescein-isothiocyanate (FITC)-Sinistrin, and we conducted urine and serum analysis for creatinine and renin levels. To understand the transcriptomic response of the targeted disruption of Resp18, we performed RNA sequencing in both the Resp18^{mutant} and SS rat kidneys.

Results Using the RNA sequencing approach, we found that Resp18^{mutant} rats showed a differential expression of 25 genes, of which one was an upregulation of renin. Gene pathway enrichment analysis revealed alteration in the renin secretion pathway, and the renin-angiotensin system, along with other pathways such as FoxO signaling, p53 signaling pathway, and the endocrine and additional factor-regulated calcium reabsorbing pathway. In addition to RNA-seq, we also observed one week after the HS diet, the Resp18^{mutant} show, and an increase in systolic blood pressure. Resp18^{mutant} rats also exhibited a decrease in creatinine clearance and along with a reduction in Glomerular filtration rate (GFR). But more interestingly, we found that circulating renin levels were increased in the Resp18^{mutant} rats after one-week exposure to HS diet treatment.

Conclusions Therefore, these observations demonstrate that the targeted disruption of Resp18 result in an upregulation of renin-angiotensin system, an increased BP and a decreased kidney performance.

102 A POLYMORPHISM IN THE UGT1A9 GENE IS ASSOCIATED WITH NEUTROPENIA IN LUNG TRANSPLANT RECIPIENTS RECEIVING MYCOPHENOLIC ACID FOR IMMUNOSUPPRESSION

[1]Laneshia K Tague, [2]Derek Byers, [3]Ramsey Hachem, [2]Daniel Kreisel, [2]Andrew Gelman. [1]*Washington University in Saint Louis, Saint Louis, MO*; [2]*Washington University in Saint Louis*; [3]*Washing University in Saint Louis*

10.1136/jim-2020-MW.90

Introduction/Background Mycophenolic acid (MPA) is the most commonly used anti-proliferative agent post-lung transplantation. One of its major, therapy-limiting side effects is neutropenia, which occurs in up to a quarter of lung transplant recipients receiving MPA for immunosuppression. Neutropenia is a common reason for dose de-escalation or withdrawal of MPA, which have been shown to cause higher rates of allograft rejection. Previous work has uncovered several single nucleotide polymorphisms (SNPs) that regulate MPA metabolism, but the relationship between these SNPs and neutropenia in solid organs recipients receiving MPA remains unclear.

Objective(s) We aim to investigate the association between functional SNPs in key genes involved in mycophenolic acid metabolism and the subsequent development of neutropenia in lung transplant recipients receiving mycophenolic acid for immunosuppression.

Methods We conducted a single-center retrospective cohort study of adult lung transplant recipients from 2008 to 2013 receiving mycophenolic acid to evaluate genetic polymorphisms associated with neutropenia. Exclusion criteria included transplant before age 18, transplantation at another center, and patients undergoing re-transplantation. SNPs from the SLCO, UGT and ABBC2 families were chosen based on their previously reported effects on MPA metabolism. Our primary outcome was time to neutropenia, defined as an absolute neutrophil count less than 1500cells/mm3. Statistical analyses included student's t test and chi-square test for baseline demographic and clinical data. Time-to-event analyses were conducted utilizing Kaplan-Meier curves verified with the log rank test for equality of survivors and Cox Proportional Hazards regression modeling.

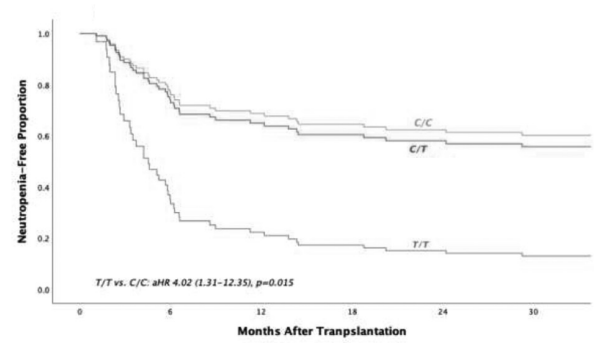

Abstract 102 Figure 1 Neutropenia-free survival by rs2741049 (UGT1A) genotype
Multivariable Cox Regression Modelling demonstrates that patients homozygous for the rs2741049 polymorphism remain with significantly poorer neutropenia-free survival when compared to patients with one or no copies of the polymorphism.

Results A total of 147 lung transplant recipients were included in the final analysis. 72 of the 147 (49%) patients experienced neutropenia after transplantation. Median time to neutropenia was 161 days (IQR 75–430). One SNP in the UGT1A9 gene, rs2741049, was found to be significantly associated with the time to development of neutropenia. This difference remained significant in Cox regression modelling with inclusion of age, sex and CMV mismatch status [table 1, figure 1, aHR 4.01 (1.31–12.35), p=0.015].

Conclusions A SNP in the UGT1A9 gene was significantly associated with the development of neutropenia in the post-lung transplant population receiving mycophenolic acid for immunosuppression. This is the first reported association between this SNP and neutropenia in a solid organ transplant population. Further investigation is warranted to validate this association and determine how to best utilize this finding to help predict the development of neutropenia and to help with medication management.

Abstract 102 Table 1 Multivariable cox regression modelling of neutropenia-free survival after lung transplantation

	aHR	95% CI	P VALUE
rs2741049 (reference C/C)			0.50
rs2741049 C/T	1.151	0.60 - 2.22	0.68
rs2741049 T/T	4.016	1.31 - 12.35	0.015
Recipient age at transplant (years)	1.001	0.98 - 1.02	0.89
Recipient Race (reference white vs. non-white)	1.648	0.53 - 5.09	0.39
CMV mismatch (reference: R-/D-)			0.11
CMV mismatch R-/D+	2.605	0.96 - 7.08	0.06
CMV mismatch R+/D-	0.889	0.20 - 3.93	0.88
CMV mismatch R+/D+	2.434	0.86 - 6.86	0.09
Recipient gender	0.772	0.41 - 1.46	0.42

A44 GLOBAL EPIGENETIC ALTERATIONS OF MESENCHYMAL STEM CELLS IN OBESITY: THE ROLE OF VITAMIN C REPROGRAMMING

[1]Mohsen Afarideh, [2]Roman Thaler, [2]Farzaneh Khani, [2]Hui Tang, [2]Kyra Jordan, [2]Sabena Conley, [2]Ishran M Saadiq, [2]Yasin Obeidat, [2]Aditya Pawar, [2]Alfonso Eirin, [2]Xiangyang Zhu, [2]Amir Lerman, [2]Andre JVan Wijnen, [2]Lilach O Lerman. *[1]Mayo Clinic, Rochester, MN; [2]Mayo Clinic*

10.1136/jim-2020-MW.91

Introduction/Background Obesity promotes dysfunction and impairs the reparative capacity of mesenchymal stem cells (MSCs), mirrored by alterations in their transcription, protein content and paracrine function. Whether these adverse effects are mediated by chromatin-modifying epigenetic changes remains unclear.

Objective(s) We tested the hypothesis that obesity imposes global DNA hydroxymethylation and histone tri-methylation alterations on swine abdominal tissue-derived obese compared to lean MSCs.

Methods Abdominal tissue-derived MSCs from female lean (n=7) and high-fat fed obese (n=7) domestic pigs were assessed using global epigenetic assays, before and after in-vitro co-incubation with the epigenetic modulator vitamin C (VIT-C) (50 μg/ml). Dot blotting was used to measure across the whole genome 5-hydroxyemthycytosine (5hmC) residues, and Western blotting to quantify in genomic histone 3 protein tri-methylated lysine 4 (H3K4me3), lysine 9 (H3K9me3) and lysine 27 (H3K27me3) residues. MSC migration and proliferation was studied in-vitro.

Results Obese MSCs displayed reduced global 5hmC and H3K4m3 levels, but comparable H3K9me3 and H3K27me3, compared to lean MSCs. Global 5hmC, H3K4me3, HK9me3 and H3K27me3 marks correlated with MSC migration and proliferation, as well as clinical and metabolic characteristics of obesity. Co-incubation of obese MSCs with VIT-C enhanced 5hmC marks, and reduced their global levels of H3K9me3 and H3K27me3.

Conclusions Obesity induces global genomic epigenetic alterations in MSCs, involving primarily genomic transcriptional repression, which are associated with MSC function and clinical features of obesity. Some of these alterations might be reversible using the epigenetic modulator VIT-C, suggesting epigenetic modifications as therapeutic targets in obesity.

Geriatrics

B41 ALGINATE OLIGOSACCHARIDE ALLEVIATES D-GALACTOSE-INDUCED H9C2 CARDIOMYOCYTES SENESCENCE VIA COUNTERACTING EFFECTS OF MICRORNA-34A ON MITOCHONDRIAL FUNCTION AND OXIDATIVE STRESS

[1]Wenjing Feng, [2]Shan Wang, [2]Meiping Feng, [2]Hui Pan, [3]Jia Liu, [4]Dongfeng Zhang, [2]Yongjun Mao. *[1]Department of Geriatrics, The Affiliated Hospital of Qingdao University; Department of Epidemiology and Health Statistics, Public Health College, Qingdao University, Qingdao; [2]Department of Geriatrics, The Affiliated Hospital of Qingdao University; [3]The Ohio State University College of Medicine; [4]Department of Epidemiology and Health Statistics, Public Health College, Qingdao University*

10.1136/jim-2020-MW.92

Introduction/Background Alginate oligosaccharide (AOS) has been shown to alleviate D-galactose-induced cardiac aging in mice by improving mitochondrial function and inhibiting oxidative stress in our previous study. Accumulating lines of evidence suggest that microRNA-34a (miR-34a) are associated with age-related diseases through regulating mitochondrial function and oxidative stress. However, it is unclear whether miR-34a is involved in AOS-mediated alleviation of D-galactose-induced cardiomyocytes senescence.

Objective(s) In this study we investigated the effects of miR-34a on AOS-mediated alleviation of H9c2 cardiomyocytes senescence induced by D-galactose.

Methods H9c2 cardiomyocytes were transfected with miR-34a mimic (50nM) or negative control RNA (50nM) using Lipofectamine RNAiMAX. Cell senescence was induced by D-galactose (200 mM) for 48h, senescent H9c2 cells were then treated with AOS (100 μg/mL) for 24h. After the above interventions, miR-34a expression was detected by qPCR. Senescence phenotype development was determined by senescence-associated β-galactosidase (SA-β-gal) staining. Protein expressions of p53, p21, p16, sirtuin 1 (SIRT1) and peroxisome proliferator-activated receptor gamma coactivator 1-alpha (PGC-1α) were analyzed by Western blot. Mitochondrial ultrastructure was analyzed by transmission electron microscopy. Mitochondrial membrane potential (MMP) and reactive oxygen species (ROS) were determined by and JC-1 and DHE staining, respectively. NADPH quantitation was examined by NADP+/NADPH Assay Kit.

Results In this study, we first found that D-galactose increased the expression of miR-34a, which was significantly downregulated by AOS. Meanwhile, AOS inhibited D-galactose-induced senescence phenotype development and the upregulation of senescence-related p53, p21 and p16 protein expression. The protective effects of AOS were suppressed by miR-34a mimic. We also found that AOS treatment increased the expression of SIRT1 and PGC-1α, and improved the mitochondrial ultrastructure and MMP, which were also abolished by miR-34a mimic. In addition, AOS significantly ameliorated D-galactose-induced ROS and NADPH production, and miR-34a mimic inhibited the anti-oxidative effect of AOS.

Conclusions Taken together, our results provide in vitro evidence that AOS alleviates D-galactose-induced H9c2 cardiomyocytes senescence through miR-34a-mediated regulation of mitochondrial function and oxidative stress.

105 IDENTIFICATION OF SUSPECTED DYSPHAGIA IN COMMUNITY-DWELLING OLDER ADULTS RECEIVING MEAL SUPPORT

[1]Nicole M Rogus-Pulia, [2]Atsuko Kurosu, [2]Fauzia Osman, [2]Rodolfo Pena-Chavez, [3]Allison Thompson, [4]Shannon Myers, [5]Pam VanKampen, [6]Sara Koenig, [2]Michelle Ciucci, [2]Jane Mahoney. *[1]University of Wisconsin-Madison, Middleton, WI; [2]University of Wisconsin-Madison; [3]Fresh Meals on Wheels Sheboygan County; [4]Wisconsin Institute for Healthy Aging; [5]Greater Wisconsin Agency on Aging Resources (GWAAR); [6]Wisconsin Department of Health Services, Bureau of Aging and Disability Resources, Office on Aging*

10.1136/jim-2020-MW.93

Introduction/Background Dysphagia, or swallowing dysfunction, is common in older adults. Early detection is essential to reduce dysphagia-related complications, such as malnutrition, dehydration, and aspiration pneumonia. However, dysphagia in community-dwelling older adults often remains untreated

until they are admitted to the hospital with or without dysphagia-related medical issues. Current estimates of the prevalence of dysphagia in community-dwelling older adults are highly variable with no current estimates for those receiving meal support. Additionally, it is unknown whether dysphagia is associated with other measures of physical function, such as ability to perform activities of daily living, or nutritional status in this population.

Objective(s) The purpose of this study was (1) to determine the prevalence of suspected dysphagia in a cohort of community-dwelling older adults receiving meal support and (2) to identify risk predictors associated with suspected dysphagia in this group.

Methods A cross-sectional study was conducted. Data were collected from 476 participants (78.5±11.1 years) across five participating 'Meals on Wheels' program sites. These data included demographic information (e.g., age, sex) as well as self-reported medical history (e.g., dysphagia diagnosis, pneumonia, hospitalization, dental status, difficulty chewing). A swallowing-related questionnaire (the 10-item Eating Assessment Tool (EAT-10)) was used to identify suspected dysphagia (score of 3 or higher). Nutrition risk and Activities of Daily Living (ADL) questionnaires were administered and total scores on each were calculated. Descriptive statistics as well as univariate and multivariate logistic regression analyses were conducted to examine associations among EAT-10 scores and these other risk predictors.

Results The prevalence of suspected dysphagia in community-dwelling older adults receiving meal support was 20.4%. The prevalence of self-reported dysphagia diagnosis was 9.4% with 84.8% of cases occurring in participants over 70 years old. Among the participants who had suspected dysphagia, 60% did not self-report a dysphagia diagnosis. Poor nutritional status (OR=2.5, p<0.001), difficulty chewing (OR=2.2, p=0.03), self-reported dysphagia diagnosis (OR=34.8, p<0.001) and prior hospitalization due to pneumonia (OR=1.88, p=0.04) were identified as risk predictors for suspected dysphagia.

Conclusions Approximately one in five community-dwelling older adults receiving meal support had suspected dysphagia identified by an EAT-10 score of 3 or higher. Suspected dysphagia was associated with greater nutrition risk, reduced chewing ability, a self-reported dysphagia diagnosis, and self-reported pneumonia history. Screening for dysphagia in the community-dwelling older adult population through administration of the EAT-10 may facilitate timely referral for swallowing evaluation and treatment, thus preventing negative health outcomes associated with dysphagia.

Hematology and Oncology

B43 PAPER BASED POINT-OF-CARE DEVICE FOR INTEGRATED ANEMIA DETECTION AND HEMOGLOBIN VARIANT IDENTIFICATION

[1]Ran An, [2]Yuncheng Man, [3]Jane A Little, [2]Umut A Gurkan. *[1]Case Western Reserve University, Cleveland, OH; [2]Case Western Reserve University, OH; [3]University of North Carolina, NC*

10.1136/jim-2020-MW.94

Introduction/Background Anemia affects over 2 billion people, which accounts for one-third of the world's population. Primary hemoglobinopathies, including Sickle Cell Disease (SCD) and Thalassemia are the 3rd prevalent causes of anemia. Anemia induced by SCD and Thalassemia may potentially induce severe and chronic diseases thus require consistent monitoring. The current gold standard for anemia testing and hemoglobin variant identification are complete blood count (CBC) using a hematology analyzer and High Performance Liquid Chromatography (HPLC). Both tests require state-of-the-art laboratory infrastructure and highly trained personnel. Such resources are typically scarce or non-existent in low- and middle-income countries, where both diseases are most prevalent. As a result, there is a critical need for portable POC tools that are highly accurate and have high throughput, to perform low cost integrated test for anemia and hemoglobin variant.

Objective(s) To develop and verify HemeChip+ platform based on the extensively tested previous version, HemeChip, as a point-of-care (POC) electrophoresis microchip, provides a solution for integrated anemia detection and hemoglobin variants identification within single test.

Methods HemeChip+ measures total hemoglobin level by comparing abundancy between total hemoglobin and a standard calibrator within the same test. 44 patient samples of were tested in this clinical study. Hemoglobin level measurement and hemoglobin variant quantification results were compared with clinical reference standards, with CBC and HPLC, respectively.

Results HemeChip+ hemoglobin levels demonstrated high accuracy within ±1.3 g/dL with a bias of -0.17 g/dL and mean error of 0.58 g/dL of CBC Hb levels in 44 subjects tested. The receiver operating characteristic analysis revealed that the test achieves a strong diagnostic performance with an area under the curve of 0.92. Hb levels and HemeChip + measured residual (r=-0.17) indicate that HemeChip+ performance remained consistent throughout the range of Hb levels tested. HemeChip+ demonstrated 100% sensitivity and specificity using Hb cutoff level of 13.0 g/dL for male subjects and 12.5 g/dL for female subjects to define anemia.

Conclusions HemeChip+ has demonstrated the feasibility of performing integrated anemia detection and hemoglobin variant identification. The area under ROC curve highlights the accuracy of HemeChip+ Hb measurement throughout the entire range of tested Hb levels.

B44 KP-17 INHIBITS METASTATIC ACTIVITY IN MULTIPLE CANCER CELLS

[1]AHMZ Ashraf, [2]Syeda H Afroze, [2]Ahmed F Pantho, [3]David C Zawieja, [4]Thomas J Kuehl, [5]Khanita Pudhom, [6]M Nasir Uddin. *[1]Baylor Scott and White Health, Temple, TX; [2]Orion Institute for Translational Medicine, Temple, TX; [3]Texas A&M University College of Medicine; [4]Orion Institute for Transnational Medicine, Emergent Biotechnologies; [5]Chulalongkorn University; [6]Texas A&M University College of Medicine, Orion Institute for Transnational Medicine, Emergent Biotechnologies*

10.1136/jim-2020-MW.95

Introduction/Background Ovarian cancer is the 6th leading cause of all related cancer deaths. Challenges in early diagnosis of this condition results in a survival rate of only five years for those diagnosed in advanced stages. Metastatic ovarian cancer can appear as a result of late diagnosis that tends to be aggressive and difficult to treat due to the

multiple karyotypes within ovarian cancer. In this research experiment, the ovarian cancer cell line, SK-OV-3, was used. The purpose of this study is to use a compound called KP-17 on SK-OV-3 cells in-vitro to determine how the proliferation, migration, and invasion of metastatic SK-OV-3 cells responds to the compound. KP-17 is derived from an endophytic fungus. Endophytic fungi are known to be potential sources for natural drug discovery and development. KP-17 is isolated from a genus of fungus known as Rhytidhysteron which is further isolated from the plant Azima sarmentosa, that is native to the mangrove area in Samutsakhon province in Thailand. KP-17 belongs to a rare family of fungal metabolites referred to as spirobisnaphthalenes. This compound contains a variety of distinctive structures which can initiate characteristic biochemical reactions that has the potential for anticancer activity.

Objective(s) The objective of this study is to elucidate the anti-cancer activity of the compound KP-17 on SK-OV-3 ovarian cancer cells by measuring the proliferation, migration, and invasion in a dose-dependent manner.

Methods *Cell culture.* Ovarian cancer cell line, SK-OV-3 (American Type Culture Collection), was grown in DMEM supplemented with 10% FBS. Cells were cultured at 37°C in a humidified atmosphere of 8.9% CO^2. *Migration and invasion assay.* Measurement of invasion activity was performed using an assay kit (CBA-100-C; Cell Biolabs). Confluent cultures of the SK-OV-3 ovarian cancer cells were removed using Accutase® (Sigma-Aldrich). Cell suspension containing 5.0×10^5cells/well in 0.5% FBS DMEM was prepared. Basal (DMSO) was the control and was added to the inside of each well. The KP-17 compound was added to each well in the 96-well plate at three different concentrations per 8 wells: 0.1 µl, 0.5 µl, and 1.0 µl. Cell migration and invasion were measured at 560 nm using a microplate reader. The cells were incubated with the KP-17 at 37°C with 8.9% CO_2 for 48 hours.

Proliferation assay. Measurement of proliferation activity was performed using XTT reagent. The DMEM-containing 10% FBS cultures were delivered in 96-well plates at 5.0×10^4 cells per well. Media containing XTT reagent was replaced after 48 hours of incubation with KP-17 compound. The plates were incubated in an atmosphere of 8.9% CO_2 at 37°C for 4 hours. The absorbance was measured at 490 nm by using a microplate reader.

Results KP-17 was effective in inhibiting proliferation, migration, and invasion in the SK-OV-3 ovarian cancer cell line. KP-17 exhibited the maximum anti-proliferative activity at concentrations of 0.5 µl and 1.0 µl.

Conclusions Our results determine the potent anticancer activity of KP-17 as the compound is seen to be able to affect the proliferation, migration, and invasion of SK-OV-3 cells. The next phase of this study is to understand the mechanism of action of this compound. This will be done by performing Western Blots to determine the up/down regulation of certain proteins that are involved in proliferation, migration, and invasion. In addition, an immunofluorescence assay using Annexin V stain will be performed to determine apoptotic signaling in the cancer cells. Afterwards, the anti-proliferative, invasive, and migratory efficacy of KP-17 and its toxicity will be tested on animal models. Our lab has previously studied the effects of different natural compounds on several ovarian cancer cell lines. Our past studies demonstrated the anti-cancer effects of a cardiotonic steroid, Cinobufotalin, and a phytochemical, 3,4',7-O-trimethylquercetin, on three different types of ovarian cancer cells. This study will greatly help to explore and discover another natural compound to be a `potential anti-cancer therapeutic agent for ovarian cancer.

B45 SICKLE RED BLOOD CELL ADHESION TO ICAM-1 IS BY FIBRINOGEN AND ASSOCIATES WITH A MORE SEVERE CLINICAL PHENOTYPE

[1]Erdem Kucukal, [2]Yuncheng Man, [3]Ran An, [4]Anton Ilich, [5]Erina Quinn, [6]Nigel S Key, [4]Jane A Little, [2]Umut A Gurkan. *[1]Case Western Reserve University, Cleveland Heights, OH; [2]Case Western Reserve University, OH; [3]Case Western Reserve University, Cleveland, OH; [4]University of North Carolina, NC; [5]Case Western Reserve University; [6]University of North Carolina*

10.1136/jim-2020-MW.96

Introduction/Background The clinical manifestations of sickle cell disease (SCD) are induced by enhanced cellular adhesion events in the microvasculature, leading to painful vaso-occlusive crises (VOC), and significant morbidity and early mortality in SCD. To date, a large group of endothelial- and sub-endothelial-associated molecules are recognized as mediators of sickle RBC adhesion to the vascular wall, including laminin, fibronectin, vascular cell adhesion molecule-1 (VCAM-1), and P-Selectin. However, there has been no systematic exploration of the adhesive interactions between sickle RBCs and intercellular adhesion molecule-1 (ICAM-1) despite the abundant expression of ICAM-1 on chronically activated and inflamed vasculature of SCD patients. Here, for the first time, we demonstrate that sickle RBCs adhere to ICAM-1 in a subject-specific manner, which is strongly modulated by fibrinogen. Additionally, above the physiologic shear rates, we show that a proportion of adherent RBCs roll on ICAM-1 in a shear-dependent fashion.

Objective(s) To characterize the unique adhesive interactions between sickle RBCs and immobilized ICAM-1 under physiologically relevant shear stress and to establish the mechanism (s) that promotes these interactions.

Methods Blood collection – De-identified non-SCD (HbAA) and SCD (HbSS and heterozygous/variant SCD) blood samples were collected in EDTA-containing vacutainers at University Hospitals Cleveland Medical Center (UHCMC) and CWRU (Cleveland, OH, Division of Hematology and Oncology), following informed consent, and according to Institutional Review Board approved protocol. A total number of 10 blood samples from 10 subjects without SCD (HbAA), 17 samples from 15 subjects with heterozygous SCD (HbS-variant), and 106 blood samples from 55 subjects with homozygous SCD (HbSS) were analyzed.

RBC adhesion experiments – 15 µl of whole blood samples were injected into ICAM-1 functionalized rectangular microfluidic channels (4 mm x 0.05 mm) under a physiologic shear stress of 1 dyne/cm^2. Next, the excess amount of blood was rinsed off using a buffer solution (1% BSA in PBS), and the adherent RBCs were imaged and quantified at 20X.

Inhibition experiments – For inhibition studies, either the whole blood samples were mixed with the specific antibody ($\alpha_4\beta_1$ or LFA-1) at 50 µg/mL for 1 hour at 37 °C, or the ICAM-1 functionalized microchannels were loaded with the specific agent (β_2, fibrinogen, or heparin) and incubated for 1 hours at 37°C.

Results Our results showed that HbSS RBCs had significantly greater adhesion to immobilized ICAM-1 than HbSC RBCs and HbAA RBCs (HbSS: mean adhesion± SD=1486 ±3312 per fov; HbSC: 54±59 per fov; HbAA: 3.5±1.4 per fov, $p<0.005$, Kruskal-Wallis with Dunn's multiple comparison – fov: field of view). We also observed a subject-specific and heterogeneous adhesion profile for HbSS RBCs, ranging between 6 and 19495 (per fov) for the entire study population. Notably, subjects with higher lactate dehydrogenase (LDH) levels and absolute reticulocyte counts (ARC) (n=21) had significantly higher RBC adhesion to ICAM-1 compared to those with lower LDH and ARC (n=55, 3159±4758 per fov vs 453±1159 per fov, $p=0.002$, Kruskal-Wallis with Dunn's multiple comparison). Low/high LDH and ARD levels were determined based on a k-means clustering analysis.

RBC adhesion to ICAM-1 also associated with subject HbF levels. We found that HbSS RBCs from subjects with higher HbF levels (n=18) had significantly lower adhesion to ICAM-1 compared to those with lower HbF levels (n=37, 283±455 per fov vs. 2127±3949 per fov, $p=0.007$, Mann-Whitney U-test). Moreover, 14 out of 37 subjects with lower HbF levels (<8.6%) had RBC adhesion that was higher than the mean adhesion level while this ratio was only 1 to 19 for HbF levels above 8.6%. The cut-off value of 8.6% was determined based on an earlier study, where it was associated with improved life expectancy.

We next performed adhesion inhibition experiments to determine possible mediators of HbSS RBC adhesion to immobilized ICAM-1. Inhibition of α4β1 integrin on the RBC membrane did not block the adhesion, indicating that the role of reticulocytes was likely limited. Then, we tested whether it would be mediated by β2 integrins that may exist on the red cell membrane, considering the role of β2-associated integrin in WBC-ICAM-1 interactions. However, neither the treatment of the blood samples with anti-LFA-1 nor pre-incubation of the ICAM-1 microchannels with recombinant human β2 protein exhibited any effect. Finally, RBC adhesion to ICAM-1 reduced by 45, 73, and 90% when the microchannels were pre-incubated with fibrinogen at concentrations: 5, 10, and 20 mg/mL respectively, indicating that RBC membrane bound fibrinogen could play a pivotal role in these adhesive interactions.

Interestingly, some of the adherent RBCs exhibited rolling behavior on ICAM-1, particularly at higher shear rates. The percentages of rolling RBCs to firmly attached RBCs were 43, 26, 14, 4, 0.4, and 0% at shear rates of 5000, 4000, 3000, 2000, 1000, and 500 s-1 respectively. Rolling velocities also depended on shear rate with a maximum of 8.4 μm/s at 5000 s-1 and minimum of 0 μm/s at 500 s-1. Based on these findings, we postulate that, under inflammatory conditions in which endothelial ICAM-1 levels are upregulated, HbSS RBCs roll in higher shear regions and firmly attach to the vasculature in post-capillary venules where shear rates are lower, thus contributing to increased resistance to blood flow and vaso-occlusion.

Conclusions The presented results point to a link between RBC adhesion to ICAM-1 and clinical phenotype for subjects with HBSS SCD. We further reveal the role of plasma fibrinogen in mediating HbSS RBC-ICAM-1 interactions and characterize the motion of adherent RBCs on ICAM-1, where they firmly adhered under low shear rates but roll with increasing velocities under high shear rates.

B48 INHIBITION OF CANCER BONE METASTASIS WITH A NOVEL BONE ANABOLIC AGENT

Teja Vallapuri, Colin Crean, John Chirgwin, Attaya Suvannasankha. *Indiana University School of Medicine*

10.1136/jim-2020-MW.97

Introduction/Background Cancer cells colonized to bone pathologically alter the bone niche to support the cancers' growth and survival. Multiple myeloma (MM) and metastatic solid tumors, particularly breast cancer (BC), activate osteoclasts and suppress osteoblasts leading to bone pain, fractures, cord compression, hypercalcemia, and an increased mortality risk. Current bone treatment strategies primarily target osteoclasts. Parathyroid related peptide (PTHrP), expressed by MM and breast cancer cells, activate osteoclast, facilitate tumor growth, and cancer cachexia. Clinical trials of PTHrP neutralizing antibody, however, showed limited tumor inhibition. BDDP is a novel PTH receptor-biased ligand, with both PTHrP inhibitory and bone anabolic effects. BDDP is currently under development for osteoporosis treatment.

Objective(s) We determined the effect of BDDP on tumor growth and bone homeostasis in myeloma and breast cancer bone metastasis models.

Methods In vitro effects of BDDP on bone genes and bone mineralization were tested in a co-culture assay of osteoblastic MC3T3-E1 cells ± human MM.1s cells. After 3 days in proliferative media, MC3T3-E1 were cultured ± human MM.1s cells in differentiation media. At Day 7, the expressions of genes with known roles in osteoblast differentiation were assayed by RT-PCR. At 25 days, nodular calcification was analyzed by Alizarin Red S staining and measured by colorimetric assay. In vivo effects of BDDP were evaluated in an intratibial transplant model. MDA-MB-231 BC cells expressing secreted luciferase were injected into the ipsilateral tibiae of Balb/$c^{nu/nu}$ mice. Mice were randomized to receive either BDDP (40 μg/kg/d) or vehicle via osmotic pump for 30 days. Following euthanasia, mice were subjected to Faxitron digital X-rays to detect osteolytic lesions and dual-energy x-ray absorptiometry (DEXA) scans to assess bone mineral content (BMC) and bone mineral density (BMD). Ipsilateral (tumor-injected) and contralateral (no tumor) tibiae were subjected to micro quantitative computed tomography (micro QCT) for 3D tibiae imaging and assessing tibiae trabecular changes.

Results MM.1s-treated MC3T3-E1 cells showed approximately a 5-fold reduction in osteoblast differentiation gene RUNX2 and a 3-fold reduction in BGLAP. This effect was attenuated by 100 nM BDDP by approximately 4-fold in both Runx2 and BGLAP. BDDP increased nodular calcification of MC3T3-E1. Nodular calcification was suppressed in MM.1s-treated MC3T3-E1 cells. This effect was reversed by BDDP. BDDP did not directly affect MM.1s and MDA-MB-231 growth in culture, measured by MTT assay, but showed dramatic tumor suppression in an MDA-MB-231 intratibial transplant model. Tumor burden assayed by serial serum luciferase assay showed control mice with detectable serum luciferase activity by 2 weeks after transplantation, while BDDP-treated mice had detectable signal by week 3. BDDP treated group had a 95% lower mean luciferase activity at 3 and 4-weeks post-transplant, compared to control group.

On Faxitron X-ray, tumor-injected tibiae had osteolytic lesions in all control mice, while there were no obvious lesions in BDDP-treated mice. Micro QCT of the tibiae showed small osteolytic lesions, below the detection of X-ray, were seen in BDDP treated mice, while gross destruction of bones was noted in control mice. Histology showed cortical breakage with extension of tumor into knee joint space in control mice, and lower tumor burden was noted in the intramedullary space. Osteoclast activity by TRAP staining was lower in BDDP treated mice. Bone mineral density (BMD) and bone mineral content (BMC) of the contralateral (non-tumor transplanted) tibiae did not differ between the two groups but BMD and BMC of the lumbar vertebrae were higher in the BDDP treated group, compared to control.

Conclusions BDDP reverses osteoblastic suppression by MM cells in vitro, as well as inhibiting tumor growth and attenuate tumor-induced osteolysis in the BC intratibial transplant model. Systemic bone anabolic effect of BDDPP was noted in the vertebrae of treated mice. Further testing of BDDP effect in prevention vs. treatment model and mechanistic studies in various bone cells and other cells within the bone microenvironment is ongoing. BDDP has a therapeutic value in the treatment of cancer bone metastasis.

B49 ABSTRACT WITHDRAWN

A45 RED BLOOD CELL ADHESION TO ERYTHROCYTE-DERIVED EXTRACELLULAR VESICLE-ACTIVATED MICROVASCULAR ENDOTHELIAL CELLS REFLECTS PATIENT-SPECIFIC CLINICAL PHENOTYPES IN SICKLE CELL DISEASE

[1]Ran An, [2]Yuncheng Man, [3]Jane A Little, [2]Umut A Gurkan. *[1]Case Western Reserve University, Cleveland, OH; [2]Case Western Reserve University, OH; [3]University of North Carolina, NC*

10.1136/jim-2020-MW.98

Introduction/Background Sickle cell disease (SCD) may lead to acute pain, chronic organ damage, hemolysis, vaso-occlusive crises, thrombosis and endothelial dysfunction. Red blood cells (RBCs) can spontaneously generate extracellular vesicles (EVs) which are known as vehicles for biomaterial exchange between cells. EVs may serve as surrogate biomarkers to represent the parent cells' activated states thus are of high clinical significance. EVs derived from RBCs have been associated with endothelial cell activation, hemolysis, oxygen saturation, pulmonary systolic pressure, as well as poor clinical outcome in SCD.

Objective(s) In this work, we performed in-vitro studies using a microfluidic model to assess human pulmonary microvascular endothelial cell (HPMEC) activation following exposure to EVs generated by RBCs from SCD patients. HPMEC activation was assessed using the direct biomarker of adhesion property of the RBCs from the same subject's blood sample.

Methods Blood samples were collected in anticoagulant EDTA tubes from 4 healthy subjects (homozygous HbAA), 10 SCD patients (homozygous HbSS), and 3 Hemoglobin SC Disease patients (heterozygous HbSC). RBCs from patient samples were used to generate EVs following published protocols. Derived EVs were incubated with HPMEC cells pre-cultured in microfluidic channels at 37°C for 2 hours. Remaining un-manipulated RBCs from the same blood sample were perfused through the microchannel at 1 dyne/cm^2 followed by a rinse step and quantification of adhered RBCs.

Results Samples from people with HbSS (N=10) were more adhesive to RBC derived MV-activated HPMECs than were samples from people with HbAA (N=4, p=0.006, Mann-Whitney). Notably, a heterogeneous EV-mediated RBC adhesion profile was seen among subjects with HbSS. No significant difference was observed between samples from people with HbSC (N=3) compared to HbSS and HbAA. To determine the impact of patient-specific clinical phenotypes on their adhesion profiles, we analyzed univariate models via the k-means clustering method and identified two subgroups with distinct sickle hemoglobin (HbS) levels. The number of adherent RBCs on EV-activated HPMECs was significantly lower in patients with recent transfusion (N=6) than patients without recent transfusion (N=4, p=0.043, Mann-Whitney), despite having a lower HbF level.

Conclusions We have shown that EVs derived from RBCs from SCD patients cause significant endothelial activation in vitro. Unlike other adhesion assays we have studied (e.g. LN), however, this pro-adhesive effect, studied under ambient conditions, is largely mitigated by transfusions. Our study suggests that SCD patients' circulating EVs are capable of causing endothelial dysfunction during a relatively short time course. Our results provide an in vitro approach to investigate the heterogeneous biological role that EVs may play in the vascular injuries of SCD patients.

A48 PREVALENCE AND SIGNIFICANCE OF SARCOPENIA AND OBESITY IN MULTIPLE MYELOMA PATIENTS UNDERGOING AUTOLOGOUS HEMATOPOIETIC CELL TRANSPLANTATION

[1]Alexis R Williams, [2]Dhiraj Baruah, [2]Aniko Szabo, [2]Jayshil J Patel, [2]Anita D'Souza. *[1]Medical College of Wisconsin, Milwaukee, WI; [2]Medical College of Wisconsin*

10.1136/jim-2020-MW.99

Introduction/Background Sarcopenia is the loss of muscle mass and when coupled with obesity, is termed sarcopenic obesity. Both are associated with adverse outcomes in solid cancers. The prevalence and outcomes related to reduced muscle mass are unknown in multiple myeloma (MM).

Objective(s) The primary objectives of this study were to determine the prevalence of sarcopenia and obesity in MM patients undergoing autoHCT, to determine any significant correlations between sarcopenia and baseline patient-, disease- and treatment-related characteristics, and to assess the impact of sarcopenia on early post-transplant course, progression-free and overall survivals.

Methods We identified 142 MM patients undergoing first autologous transplant at our center between 01/2013 and 12/2017 with a computerized tomography (CT) study within 6 months pre-transplant. We identified high-density muscle within the psoas at the L3 vertebral level using a

novel CT method. Patients were arbitrarily separated into two groups by percent high-density muscle using a >80% high-density cut-off to define healthy muscle and ≤80% high-density muscle as sarcopenia. We collected demographic, clinical, and outcomes variables including body mass index (BMI) at transplant. Complications including total days spent in hospital, ICU transfer, cardiovascular events (arrhythmia, heart failure), renal failure necessitating dialysis, respiratory failure necessitating intubation, and sepsis were assessed in the first 100 days after transplant. Cox proportional hazards model was fitted with% high-density muscle (≤80 versus >80) as the main effect for the primary endpoint, overall survival (OS).

Results The median age was 62.4 (range 38.2–78.7) years and 65% were males. Median BMI at transplant was 28.9 (range 17.8–46.1). A total of 72 (51%) patients had sarcopenia and 32 (23%) had sarcopenia and a BMI >30 kg/m^2. There were no significant differences between the sarcopenia group and the group without sarcopenia. One/more early complications were found in 22 (16%) patients. Cardiovascular events were the most common, accounting for 42% of all complications. Patients with sarcopenia had more cardiac complications (12.5%) than patients without (2.9%), p=0.03. Multivariate analysis showed no association of sarcopenia with OS but increasing BMI at transplant was associated with worse OS (hazard ratio: 1.10, 95% confidence interval: 1.01–1.20, p=0.03).

Conclusions We conclude that sarcopenia and obesity are prevalent in MM patients undergoing transplantation. While our study is limited by a small sample size, low incidence of post-transplant complications, and an arbitrary definition of sarcopenia, our preliminary analysis suggests an association of higher early post-transplant complications in those with sarcopenia and worse OS with obesity in MM.

Infectious Disease

B50 DEVELOPMENT AND VALIDATION OF A MACHINE LEARNING ALGORITHM TO PREDICT BACTEREMIA AND FUNGEMIA IN HOSPITALIZED PATIENTS

[1]Sivasubramanium Bhavani, [2]Zachary Lonjers, [3]Kyle Carey, [4]Majid Afshar, [4]Emily Gilbert, [2]Nirav Shah, [3]Elbert Huang, [5]Matthew Churpek. *[1]University of Chicago, Chicago, IL; [2]Northshore Hospital; [3]University of Chicago; [4]Loyola; [5]University of Wisconsin*

10.1136/jim-2020-MW.100

Introduction/Background Bacteremia and fungemia can cause life-threatening illness and carry mortality rates over 30%, with delays in antimicrobial therapy leading to further increases in risk of mortality. Blood cultures are the current gold standard to detect bacteremia and fungemia, but blood cultures have poor sensitivity and specificity and can often take more than 24 hours to result. This leads to unnecessary blood culture orders in low-risk patients and delayed or inadequate antimicrobial therapy in high-risk patients.

Objective(s) To predict the results of blood cultures using only routine data in the electronic health record (EHR) that is available prior to the blood culture order.

Methods The results of blood cultures over a ten-year period at two large tertiary medical centers were used to develop and validate logistic regression and gradient boosting machine (GBM) models to predict bacteremia and fungemia. All EHR data (e.g., vitals, labs, nursing assessments, processes of care) available before the blood culture order were included as predictors. The models were developed on the earliest 80% of admissions and validated on the most recent 20% to simulate prospective implementation. Model performance was evaluated using area under the receiver operator curve (AUC) values. Low and high-risk patients were identified using the lowest and highest decile of the machine learning model predicted risk, and the incidence of bacteremia, resistant organisms and mortality were compared between these risk categories.

Results There were 254,279 blood culture days – defined as 24-hour periods in which one or more blood cultures were ordered. In the validation cohort, there were 50,857 blood culture days, with 3,884 cases of bacteremia (7.6%) and 381 cases of fungemia (0.7%). The GBM model for bacteremia had significantly higher AUC (0.79 [95% CI 0.78–0.80]) than the logistic regression model (0.73 [95% CI 0.72–0.74]). The model identified a high-risk group with over 30 times the incidence of bacteremia as the low-risk group (30.2 vs 0.9%, p<0.001) and over 50 times the incidence of potentially resistant organisms (16.0 vs 0.3%, p<0.001). The majority of the most important variables in the GBM model were traditional vital signs such as temperature as well as interaction measures between vital signs, such as the product of respiratory and heart rates. The GBM model for fungemia had very high accuracy (AUC 0.87 [95% CI 0.85–0.89]). The high-risk fungemia group had 85 times the incidence of fungemia as the low-risk group (5.1% vs 0.06%, p<0.001).

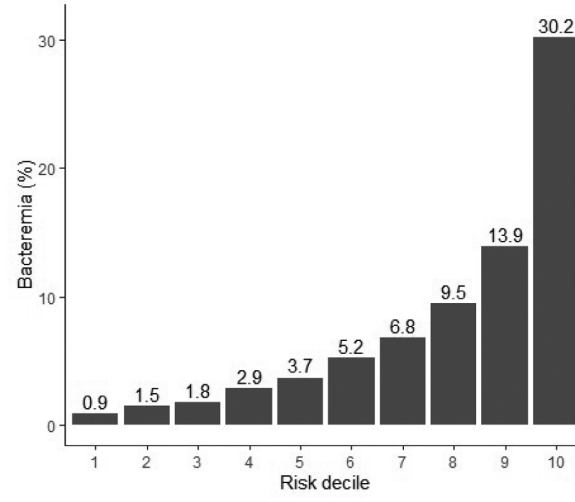

Abstract B50 Figure 1 Deciles of model predicted risk compared to the incidence of bacteremia
The gradient boosted machine (GBM) model predicted the risk of bacteremia using electronic health record (EHR) data available before the blood culture was ordered. The calibration of the model is shown here with deciles of predicted risk compared to the actual incidence of bacteremia in the validation cohort (n=50,857). Only 0.9% of patients in the lowest decile of predicted risk have bacteremia, while 30.2% of patients in the highest decile have bacteremia.

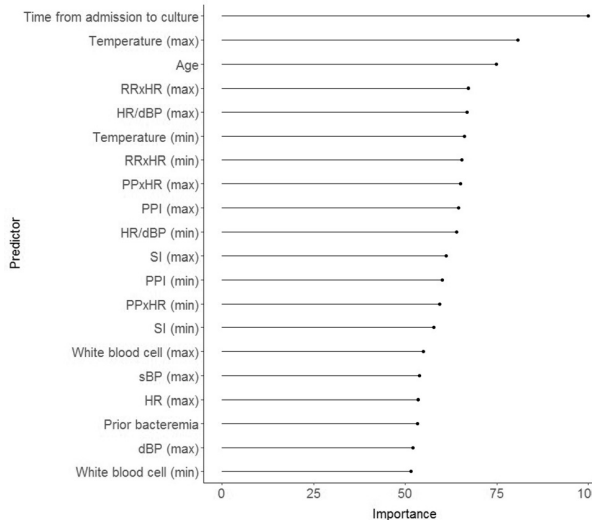

Abstract B50 Figure 2
Variable importance plot illustrating the most important predictors of bacteremia. Variable importance is measured by mean decrease in impurity adjusted to a scale of 0 to 100. In the gradient boosting machine (GBM) model, the length of time from admission to blood culture was the most important variable. The majority of the most important variables were traditional vital signs such as temperature as well as interaction measures between vital signs, such as the product of respiratory and heart rates. Age was also an important predictor, as was maximum and minimum white blood cell count. Definition of abbreviations: max – maximum; min – minimum; RR – respiratory rate; HR – heart rate; dBP – diastolic blood pressure; sBP – systolic blood pressure; PP – pulse pressure; PPI – pulse pressure index; SI – shock index.

Conclusions Our novel predictive model identified patients at low and high-risk for bacteremia and fungemia using only routine data in the EHR. Importantly, the model could decrease unnecessary blood cultures and increase timely antimicrobial coverage. Further research is needed to evaluate the cost-effectiveness and patient-oriented outcomes from model implementation in clinical practice.

B52 COST-EFFECTIVENESS ANALYSIS OF UV-C DISINFECTION TO PREVENT HOSPITAL-ONSET CLOSTRIDIOIDES DIFFICILE INFECTIONS IN ACUTE-CARE HOSPITALS

[1]Nathaniel Neptune, [2]Deverick Anderson. [1]*Duke University School of Medicine*; [2]*Duke University Medical Center*

10.1136/jim-2020-MW.101

Introduction/Background Clostridioides difficile infections (CDI) increase costs, length-of-stay, morbidity, and mortality for hospitalized patients. Patients admitted to high-risk rooms, defined as inpatient hospital rooms previously occupied by a patient with a CDI, are at an increased risk of acquiring hospital-onset C. difficile infections (HOCDI). High-risk rooms serve as a vector for CDIs because C. difficile spores often contaminate environmental surfaces after terminal room disinfection, the thorough disinfection hospitals perform to prepare a room for a new patient. Technologies such as automated ultraviolet (UV-C) light-emitting devices are designed to reduce environmental contamination and HOCDIs. However, UV-C devices introduce an additional cost for infection prevention. To date, a cost-effectiveness analysis of the use of a UV-C device during terminal room disinfection of high-risk rooms to prevent HOCDIs has not been completed.
Objective(s) The objective of this study was to determine the cost-effectiveness of using a UV-C device during terminal room disinfection of high-risk rooms to prevent HOCDIs.
Methods We evaluated the cost-effectiveness of adding a UV-C device to terminal disinfection compared to standard terminal disinfection without a UV-C device. The risks of HOCDI for both strategies were obtained from data collected during the Benefits of Enhanced Terminal Room (BETR) Disinfection study, a multicenter cluster-randomized crossover study. Other parameters were obtained from published literature or previous work. A Markov model was created, and decision analysis performed with TreeAge Pro 2019, R2 software to calculate projected costs and effectiveness for two disinfection strategies: 1) use of UV-C enhanced terminal room disinfection on no rooms and 2) use of UV-C enhanced terminal

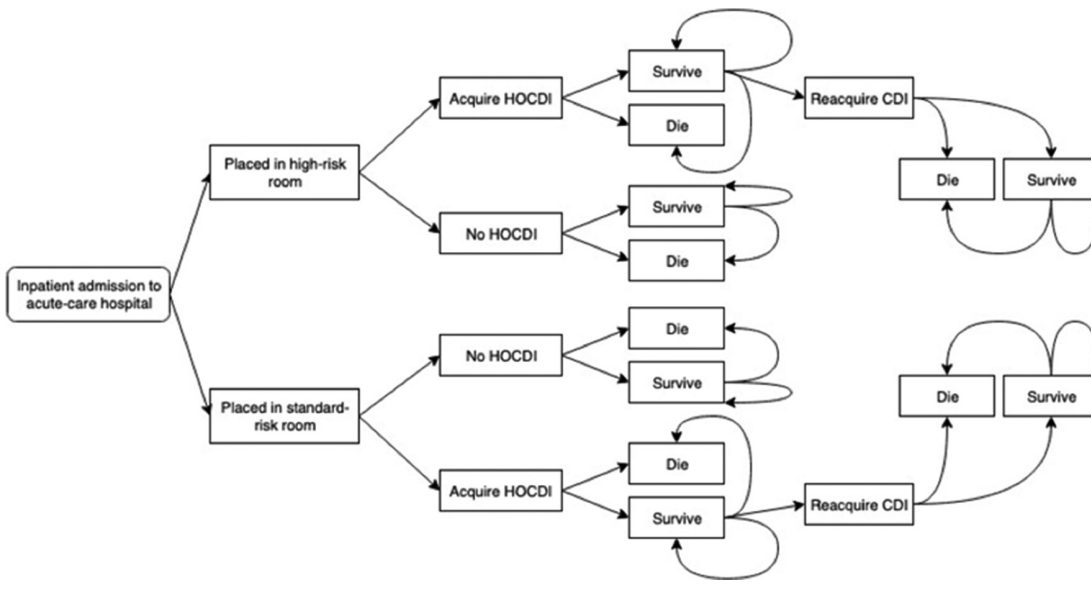

Abstract B52 Figure 1 Decision analysis pathway
Schematic of simplified diagram of the decision model. CDI, Clostridioides difficile infection; HOCDI, Hospital-onset Clostridioides difficile infection

room disinfection on high-risk rooms only. We defined effectiveness as the accrual of quality-adjusted life years (QALY). The incremental cost-effectiveness ratio (ICER) was calculated as the difference in the ratio of change in costs divided by the change in health effects for each cleaning strategy. The willingness-to-pay (WTP) threshold was set to $50,000 per QALY. The base case was a cohort of 20,000 annual patient admissions per UV-C device with a time horizon of 30-years. Hospital and outpatient costs and outcomes attributable to CDIs were projected for the entire time-horizon with a start age of 55 years. Simulated patients had varying rates of acquiring a HOCDI dependent upon the type of room they were admitted to and the disinfection strategy. In-hospital mortality varied based on the status of HOCDI acquisition.

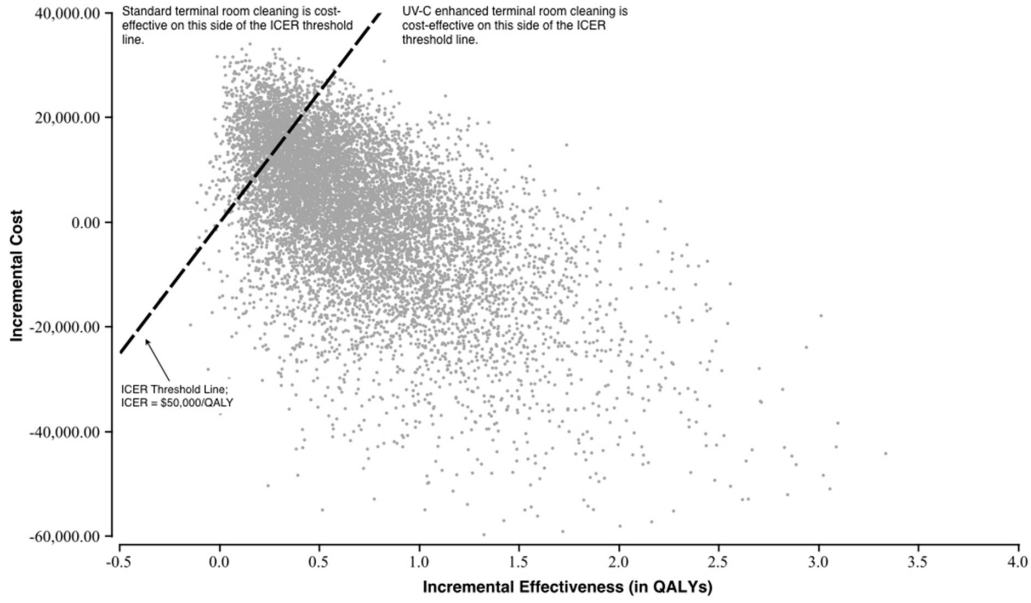

Abstract B52 Figure 2 Probabilistic analysis of UV-C enhanced terminal room cleaning versus standard cleaning
Incremental cost-effectiveness scatterplot of 10,000 Monte Carlo iterations. Each point represents the incremental cost-effectiveness ratio (ICER) of the UV-C enhanced cleaning strategy relative to the standard cleaning strategy. The UV-C enhanced cleaning strategy is cost-effective in 85.8% of iterations at willingness to pay threshold of $50,000/QALY. The UV-C enhanced cleaning strategy was dominant (less costly and more effective) in 36.6% of iterations.

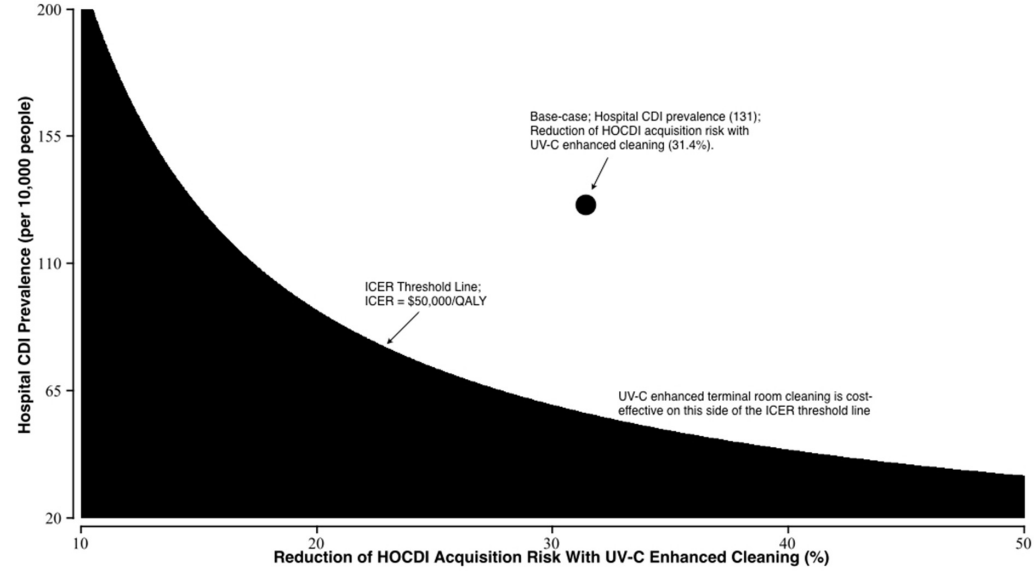

Abstract B52 Figure 3 Two-way sensitivity analysis of hospital CDI prevalence and reduction of HOCDI acquisition in high risk rooms cleaned with a UV-C device
Two-way sensitivity analysis evaluating the simultaneous effects of hospital CDI prevalence and the reduction of HOCDI acquisition risk with UV-C enhanced cleaning in high-risk rooms at a willingness to pay of $50,000/QALY. CDI, Clostridioides difficile infection; HOCDI, Hospital-onset Clostridioides difficile infection

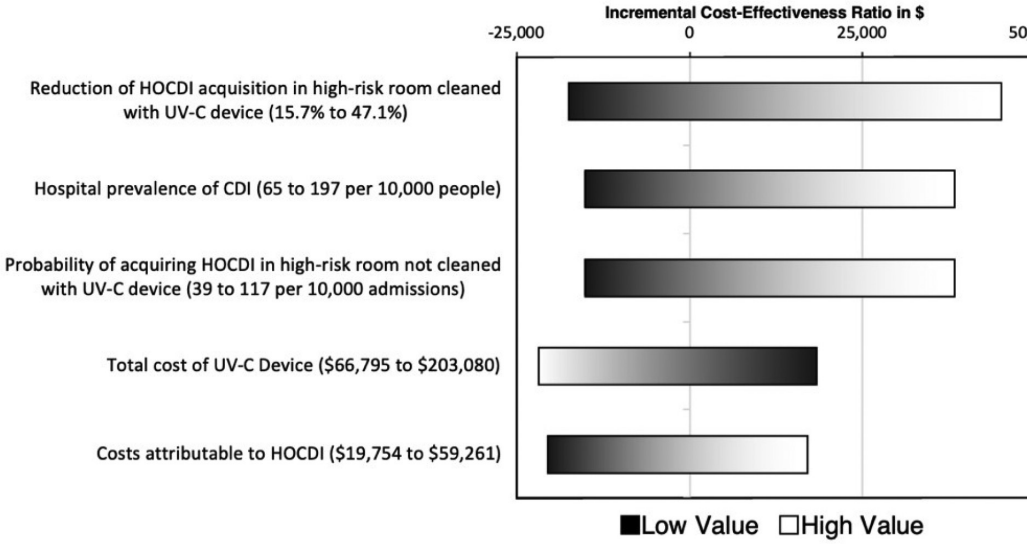

Abstract B52 Figure 4 One-way sensitivity analysis UV-C enhanced cleaning relative to standard cleaning
Tornado diagram displaying one-way sensitivity analysis of the 5 most influential parameters. No parameter has enough influence to increase the incremental cost-effectiveness ratio (ICER) above the $50,000/QALY threshold. CDI, Clostridioides difficile infection; HOCDI, Hospital-onset Clostridioides difficile infection

Patients who developed a HOCDI had a chance to develop a recurrent CDI, which resulted in additional costs; all CDIs resulted in a QALY decrement for the duration of the infection. For sensitivity analyses, parameters ranged from ±50% of the base-case values. We performed one-way sensitivity analyses of parameters and a probabilistic sensitivity analysis using 10,000 Monte Carlo simulations.

Results In the base case analysis, use of a UV-C device during terminal room cleaning in high-risk rooms adds an additional 0.68 QALYs and has an ICER of negative $1,761 per QALY gained relative to the strategy of no UV-C device use during terminal room cleaning. During sensitivity analysis, no single parameter had enough influence to increase the ICER above the WTP threshold. Three variables had the greatest impact on the ICER: 1) the effectiveness of a UV-C device preventing HOCDI in high-risk rooms, 2) hospital prevalence of CDIs, and 3) the risk of acquiring a HOCDI in a high-risk room cleaned without a UV-C device. In probabilistic sensitivity analysis, the UV-C enhanced cleaning strategy remained cost-effective in 85.8% of iterations.

Conclusions Adding the use of a UV-C device to terminal room cleaning is more effective and less costly than standard terminal room cleaning of high-risk inpatient rooms to prevent HOCDIs. This study adds to the body of evidence that use of a UV-C device during terminal room cleaning to prevent HO-CDIs is cost-effective and can result in a reduction of net costs. Further research is needed to confirm whether acute-care hospitals should be willing to pay to use a UV-C device during terminal room cleaning to prevent HO-CDIs or use alternate strategies.

A04 STREPTOCOCCUS PNEUMONIAE ACTIVATION OF NATURAL KILLER CELL IL-10 IN THE LUNG

Sarah E Clark. *University of Colorado Denver, Aurora, CO*

10.1136/jim-2020-MW.102

Introduction/Background The anti-inflammatory cytokine interleukin(IL)-10 is important for maintaining lung homeostasis. However, manipulation of IL-10 production prolongs infection for diverse microbial pathogens. Among these, Streptococcus pneumoniae is an opportunistic pathogen of the respiratory tract that activates the production of IL-10 during lung infection. S. pneumoniae both frequently colonizes the human nasopharynx and is a major cause of diseases including pneumonia, meningitis, otitis media and septicemia. Factors governing host susceptibility to S. pneumoniae disease remain unclear. This study addresses the cellular sources of IL-10 during S. pneumoniae infection and the impact of this response on protective immunity.

Objective(s) We investigated natural killer (NK) cells as a source of IL-10 production during S. pneumoniae infection. NK cells are innate lymphoid cells that produce immune regulatory cytokines including IFN-gamma and IL-10 during microbial infections. We examined the hypothesis that NK cell IL-10 production increases bacterial expansion in the lung, limiting host protection against infection.

Methods IL-10-GFP reporter mice were used to explore the potential for NK cell production of IL-10 in a pulmonary S. pneumoniae infection model. IL-10-deficient mice and NK cell-depleting antibodies were used to compare the effects of NK cells and IL-10 on bacterial burdens and recruitment of inflammatory myeloid cells to the lung. A co-culture system comprised of bone-marrow derived dendritic cells and purified lung NK cells was also used to determine the impact of exposure to a S. pneumoniae virulence protein on NK cell IL-10 production.

Results We find that NK cells are a major source of IL-10 in the lung during S. pneumoniae infection, and that the absence of either IL-10 or NK cells increases bacterial clearance, which correlates with reduced recruitment of inflammatory myeloid cells. We also identify a S. pneumoniae virulence protein that is sufficient to activate NK cell IL-10 production in a co-culture system in vitro.

Conclusions Collectively, these findings indicate that S. pneumoniae activates NK cell production of IL-10 in the lung. The consequences of NK cell IL-10 production during S. pneumoniae infection include reduced recruitment of inflammatory myeloid cells, which correlates with increased bacterial burdens in the lung. Overall, these data suggest that bacterial modulation of host IL-10 production reduces protection against a major respiratory tract bacterial pathogen.

A52 ATTRIBUTES OF NON-HIV U.S. MILITARY VETERANS IN CHICAGO, ILLINOIS WITH MYCOBACTERIUM AVIUM COMPLEX ISOLATED FROM THEIR LUNGS

[1]Christen Vagts, [2]Israel Rubinstein. *[1]University of Illinois at Chicago, Chicago, IL; [2]University of Illinois at Chicago*

10.1136/jim-2020-MW.103

Introduction/Background The presence of Mycobacterium avium complex (MAC) in the lung of non-HIV patients is increasingly recognized in Chicago, Illinois. Current ATS guidelines promulgate that diagnosis of MAC lung infection requires a constellation of bacteriological, clinical and imaging data. However, anti-infective therapy is not consistently administered to these patients.
Objective(s) The purpose of this study was to characterize clinical, imaging, and treatment attributes of non-HIV U.S. military veterans in Chicago, Illinois with MAC isolated from their lungs.
Methods Medical records of veterans followed at the Jesse Brown VA Medical Center (JBVAMC), Chicago, Illinois with a positive sputum or bronchoalveolar lavage fluid (BALF) for MAC between October 2008 and July 2019 were reviewed. Only veterans with at least 2 positive sputum cultures or one positive BALF culture for MAC were included. Demographics, co-morbidities, chest imaging, and anti-infective therapy were abstracted from each medical record. JBVAMC is a teaching affiliate of both the University of Illinois at Chicago (UIC) and Northwestern University (NU) and the corresponding pulmonary clinic was noted. Statistical analysis was performed using Mann-Whitney U test and Fisher's exact test as indicated. $P<0.05$ was considered statistically significant.
Results Nineteen patients with positive MAC cultures as outlined above were analyzed. Patients were predominantly males (90%), African-American (68%), and current or former smokers (84%). Median age at diagnosis was 74 years. Most had physician-diagnosed COPD (12/19; 63%) while 4 (21%) had other underlying lung disorders. Symptoms were reported by 10/19 (52%) patients. Lung imaging findings consisted of a combination of multiple nodules (n=14; 73%), bronchiectasis (n=9; 47%), tree-in-bud pattern (n=6; 31%) and cavities (n=4; 21%). Long-term, guideline-directed, triple anti-infective therapy was initiated in 52% of patients but only 50% of those patients were able to complete therapy. Seventeen patients (89%) were followed in pulmonary clinics, 9 by NU and 8 by UIC providers. Significantly more patients followed by UIC providers were started on treatment than those followed by NU providers ($p=0.015$). Symptoms and lung imaging findings at presentation were similar among treated and untreated groups. Six (32%) patients were deceased at the time of medical record review. Symptoms, lung imaging findings, and initiation of anti-infective therapy were similar among alive and deceased patients.
Conclusions Non-HIV U.S. military veterans in Chicago, Illinois with MAC isolated from their lungs present with distinct clinical, lung imaging and anti-infective therapy attributes. Initiation of anti-infective therapy at JBVAMC may be dependent, in part, on providers' proclivity.

Nephrology

B54 PERI-STENOTIC COLLATERAL CIRCULATION IN ATHEROSCLEROTIC RENOVASCULAR DISEASE: ASSOCIATION WITH KIDNEY FUNCTION AND RESPONSE TO TREATMENT

[1]Mohsen Afarideh, [2]Xin Zhang, [2]Christopher M Ferguson, [2]James F Glockner, [2]Amir Lerman, [2]Stephen C Textor, [2]Lilach O Lerman. *[1]Mayo Clinic, Rochester, MN; [2]Mayo Clinic*

10.1136/jim-2020-MW.104

Introduction/Background The significance of peri-stenotic collateral circulation (PCC) development around a stenotic renal artery is unknown.
Objective(s) We tested the hypothesis that PCC is linked to loss of kidney function and recovery potential in patients with atherosclerotic renovascular disease (ARVD).
Methods In a clinical setting, 34 patients with ARVD were prospectively assigned to medical therapy (MT) with or without revascularization based on clinical indications. The PCC was visualized using 3D multidetector computed tomography (MDCT), and defined relative to segmental arteries in essential hypertensive patients. PCC number before and 3-months after treatment was correlated with renal function, inflammation, and single-kidney volume, perfusion, and oxygenation estimated with MDCT and magnetic resonance imaging.
Results Thirty-four stenotic kidneys (STKs) from 30 patients were included in the analysis. PCC number correlated inversely with kidney volume. ARVD-STKs with baseline PCC (C-ARVD, n=13 patients) were associated with elevated 24-h urine protein and STK vein level of tumor necrosis factor-α, lower single-kidney volume and blood flow, and greater hypoxia than in patients with no PCC (NC-ARVD, n=17). Revascularization (but not MT alone) improved renal function and reduced STK vein inflammatory markers in both NC-ARVD and C-ARVD. In C-ARVD, revascularization also increased renal volume, blood flow, and oxygenation to levels comparable to NC-ARVD, and induced PCC regression. However, revascularization improved systolic blood pressure, plasma renin activity, and filtration fraction only in NC-ARVD.
Conclusions Patients with C-ARVD have greater kidney dysfunction, atrophy, hypoxia, and inflammation compared to NC-ARVD patients, suggesting that PCC does not effectively protect the STK in ARVD. Renal artery revascularization improved renal function in C-ARVD, but not hypertension or renin-angiotensin system activation. These observations may help direct management of patients with ARVD.

B55 PARAOXONASE 1 DELETION LEADS TO INCREASES IN THE PRO-INFLAMMATORY EICOSANOID 20-HETE AS WELL AS RENIN-ANGIOTENSIN SYSTEM ACTIVATION IN A DAHL SALT-SENSITIVE RAT MODEL OF CHRONIC KIDNEY DISEASE

[1]Fatimah K Khalaf, [1]Apurva Lad, [1]Chrysan J Mohammed, [2]Prabhatchandra Dube, [2]Jacob A Connolly, [2]Andrew L Kleinhenz, [2]Bella Z Khatib-Shahidi, [2]Noha Eid, [2]Deepak Malhotra, [2]Steven T Haller, [2]David J Kennedy. [1]*University of Toledo, Toledo, OH*; [2]*University of Toledo*

10.1136/jim-2020-MW.105

Introduction/Background Paraoxonase-1 (PON1) is a hydrolytic lactonase enzyme that synthesized in the liver and circulates attached to high density lipoproteins (HDL). Clinical studies have demonstrated an association between diminished PON-1 and progression of CKD however whether decreased PON-1 is mechanistically linked to renal injury is unknown.

Objective(s) We tested the hypothesis that lack of Pon-1 is mechanistically linked to progression of renal injury in CKD.

Methods Experiments were performed on control Dahl salt-sensitive rats (SS^{Mcwi}, hereafter designated SS rats) and Pon1 knock-out rats (designated SS-$Pon1^{em1Mcwi}$, hereafter designated SS-*Pon1* KO rats) generated by injecting a CRISPR targeting the sequence into SS^{Mcwi} rat embryos. The resulting mutation is a 7bp frameshift insertion in exon 4 of the Pon1 gene. First, in order to examine the renal protective role of PON-1 in vivo settings of CKD, ten-week-old, age-matched male rats were maintained on high salt diet (8% NaCl) for up to 5 weeks to initiate the salt-sensitive hypertensive renal disease characteristic of this model.

Results We have previously observed that SS-Pon1 KO demonstrated several hallmarks of increased renal injury noted by increased renal fibrosis, sclerosis and tubular injury compared to wild type SS rats. Upon examining the kidneys, SS-Pon1 KO demonstrate increased recruitment of CD68 positive immune cells in the renal interstitium, as well as increased expression of the key inflammatory genes (Timp-1, MCP-1, IL-6, COL1A1, and TGF-β) compared to the wild type SS rats (all $p<0.05$). SS-Pon1 KO rats also showed significant ($p<0.05$) decline in renal function along with increased renal oxidative stress compared to wild type SS rats despite no differences in blood pressure between the two groups as assessed both by tail cuff plethysmography as well as radiotelemetry. As PON-1 is known by to hydrolyze cytochrome p450 (cyt p450) pathway dependent arachidonic acid metabolites and as many of these metabolites have been known to mediate renal inflammation, we examined renal cortical levels in our model using LC-MS/MS. We noted that 20-HETE, a cyt p450 dependent arachidonic acid metabolite, was significantly ($p<0.05$) elevated in renal cortex from the SS-Pon1 KO compared to wild type SS rats. In addition to its effects on renal fibrosis and inflammation, 20-HETE is known to activate the renin-angiotensin system. Interestingly, we found that circulating levels of Angiotensin I (1–10), Angiotensin II (1–8), and Angiotensin (1–5), were significantly ($p<0.05$) higher in SS-Pon1 KO rats compared to wild type SS rats on high salt diet, while there was no difference in aldosterone.

Conclusions These findings suggest that disruption of PON-1 is accompanied by elevations in the pro-inflammatory eicosanoid 20-HETE in the renal cortex as well as renin-angiotensin system activation and leads to renal injury independent of blood pressure in a model of salt-sensitive hypertensive renal disease.

B04 KIDNEY FIBROSIS IS MITIGATED BY A DUAL ACTING FARNESOID X RECEPTOR AGONIST AND SOLUBLE EPOXIDE HYDROLASE INHIBITOR IN A MOUSE MODEL

[1]Abdul H Khan, [2]Anna Stavniichuk, [3]Daniel Merk, [2]John Imig. [1]*Department of Pharmacology and Toxicology, Medical College of Wisconsin, Milwaukee, WI, USA, Milwaukee, WI*; [2]*Department of Pharmacology and Toxicology, Medical College of Wisconsin, Milwaukee, WI, USA*; [3]*Institute of Pharmaceutical Chemistry, Goethe University Frankfurt, Germany*

10.1136/jim-2020-MW.106

Introduction/Background In Chronic kidney disease, renal fibrosis is a critical pathophysiological event and is the final common pathway in the progression of chronic kidney disease (CKD) to end-stage renal disease (ESRD). There has been little success in developing agents that can slow the progression of CKD to ESRD.

Objective(s) In the present study, we investigated the efficacy of an innovative dual-acting molecule, DM509, in mitigating renal fibrosis using the unilateral ureteral obstruction (UUO) renal fibrosis mouse model. DM509 acts concurrently as a farnesoid X receptor agonist and a soluble epoxide hydrolase inhibitor.

Methods C57BL/6J male mice went through either UUO or sham surgery (n=8/group). Mice were treated with either DM509 (10mg/kg/d) or vehicle in drinking water. Interventional DM509 treatment was started three days after UUO induction and continued for 7 days. Plasma and kidney tissue were collected at the end of the experimental protocol. Several biochemical, histopathological, immunohistopathological, and gene expression studies were carried out to determine the antifibrotic actions for DM509.

Results The UUO group exhibited elevated BUN compared to the sham group (77±10 vs. 44±15 mg/dL). DM509 treatment reduced BUN by 40%. UUO mice demonstrated marked renal fibrosis with higher kidney hydroxyproline content (267±46 vs. 53±14 μg/mg protein), collagen positive area (4.3±0.1% vs. 0.7±0.3%) compared to sham group. DM509 reduced hydroxyproline content by 41% and collagen positive area by 65%. Renal inflammation was evident in UUO mice with elevated kidney MCP-1, renal CD45 immune cell positive infiltration, and renal profibrotic gene expression (TNF-a, IL-6, IL-1b). Interventional DM509 treatment reduced renal inflammation in UUO mice. Renal fibrosis in UUO was associated with epithelial-to-mesenchymal transition (EMT) as UUO mice exhibited a 2 to 20-fold higher protein and gene expression of mesenchymal markers a-SMA, FSP-1, and FN, as well as a marked decrease in the epithelial marker, E-cadherin compared to sham group. UUO mice treated with DM509 had markedly reduced EMT. UUO mice also had tubular epithelial barrier injury with increased renal KIM-1, NGAL expression and lower claudin-1 and -5 expression compared to sham. DM509 treatment reduced tubular injury markers by 25–50% and maintained tubular epithelial integrity by restoring claudin expressions in UUO mice. Vascular inflammation was evident in UUO mice with 9 to 20-fold higher renal ICAM and VCAM gene expression

compared to sham that was reduced by 40–50% with DM509 treatment. Peritubular vascular density assessed by CD31 expression was reduced by 35% in UUO mice and DM509 mitigated vascular density loss.
Conclusions In conclusion, our data reveal that DM509 is a promising dual-acting antifibrotic agent that combats epithelial and vascular renal fibrotic pathological events.

B05 SIRTUIN-3 MEDIATES SEX DIFFERENCES IN ISCHEMIA-REPERFUSION AND AGING-RELATED KIDNEY INJURY

[1]Jenny S Pan, [2]Huiyun Shen, [3]David Sheikh-Hamad, [2]Qingtian Li. *[1]Baylor College of Medicine; MEDVAMC, Houston, TX; [2]Baylor College of Medicine; [3]Baylor College of Medicine; MEDVAMC*

10.1136/jim-2020-MW.107

Introduction/Background Acute kidney injury (AKI) is a common condition and is associated with increased morbidity, mortality, and the development/progression of chronic kidney disease. Kidney ischemia-reperfusion injury (IRI) is a common cause of AKI; but while the pathogenesis is better defined, the therapeutic options remain limited. There is accumulating evidence that biologic sex influences susceptibility to AKI, and sex hormones play a crucial role. We previously showed that a pathway from stanniocalcin-1 (STC1) mediated AMPK activation to induction of mitochondrial sirtuin-3 (mtSIRT3) suppresses ROS and confers resistance to kidney IRI. Our observations reveal increased baseline kidney expression of STC1, activated AMPK, and SIRT3 in female mice vs. males. Mitochondrial dysfunction and oxidative stress play key roles in the pathogenesis of ischemic AKI. We hypothesize that SIRT3, a major mitochondrial deacetylase, confers protection and mediates sex differences in response to kidney IRI.
Objective(s) Our study objectives are to: 1) examine in vivo whether transgenic overexpression of SIRT3 protects from kidney IRI; 2) examine whether sex differences in kidney mtSIRT3 expression mediate the observed sexual dimorphism in susceptibility to ischemic AKI; and 3) investigate the role of sex hormones in regulation of kidney mtSIRT3.
Methods We subjected wild-type (WT) or SIRT3 transgenic (Tg) male and female mice to bilateral kidney IRI (clamping of renal pedicles for 30 minutes with non-traumatic vascular clamps). We examined baseline kidney mtSIRT3 expression, and serum testosterone and estradiol (E2) levels in male and female WT mice at different ages: 1) 10 weeks (adolescent); 2) 3–6 months (mature adult); and 3) 18-months (old). Cultured 293T cells were treated with 17β-estradiol, testosterone or vehicle.
Results We observed higher kidney expression of mtSIRT3 and activity of AMPK in WT female mice compared with males. While there was age-dependent decline in kidney mtSIRT3 and AMPK activity, differential expression in males and females persisted. At age 6-months, SIRT3 Tg male mice displayed less tubular vacuolization, fibrosis and mitochondrial ROS vs. similarly aged WT male mice. Compared with WT male mice, SIRT3 Tg male mice demonstrated resistance to 30-minutes of kidney IRI characterized by: improved survival; preserved kidney function (creatinine clearance); decreased morphological damage and ROS production. SIRT3 Tg male mice tolerated IRI with survival and kidney function impairment similar to WT females. WT or SIRT3 Tg female mice display no measurable change in kidney function with 30-minutes of kidney IRI. In WT female mice, kidney mtSIRT3 expression correlates with both plasma E2 and testosterone levels; in WT male mice, kidney mtSIRT3 expression correlates with only plasma testosterone level. In cultured 293T cells, E2 treatment increased whole cell and mtSIRT3 protein expression, and SIRT3 mRNA in a dose-dependent manner. Testosterone treatment decreased mtSIRT3 protein expression in a dose-dependent manner, but had no effect on whole cell SIRT3 protein expression or SIRT3 mRNA. E2 treatment also increased estrogen receptor-β and estrogen related receptor-α mRNA expression.
Conclusions The data suggest that The data suggest that: 1) SIRT3 ameliorates kidney IRI and aging-related kidney injury; 2) decreased mtSIRT3 in males mediates the increased susceptibility to kidney injury; 3) sex steroids regulate mtSIRT3 expression; estrogen via transcriptional regulation and testosterone via inhibition of mitochondrial targeting. Our observations highlight the need for additional studies to better understand mechanisms underlying sex-specific differences in kidney disease and response to treatment.

A53 SYSTEMIC ENDOTHELIAL FUNCTION IS ASSOCIATED WITH RENAL DISEASE SEVERITY IN EARLY AUTOSOMAL DOMINANT POLYCYSTIC KIDNEY DISEASE (ADPKD)

[1]Walaa Elsekaily, [1]Kathleen Leistikow, [1]Fouad Chebib, [1]Peter Harris, [1]Lilach O Lerman, [1]Vicente Torres, [2]Maria V Irazabal. *[1]Mayo Clinic; [2]Mayo Clinic, Rochester, MN*

10.1136/jim-2020-MW.108

Introduction/Background In vitro studies have shown impaired endothelium-dependent relaxation of small resistance vessels in patients with ADPKD. Peripheral-arterial tonometry (PAT) provides, with high reproducibility and no operator dependency, non-invasive measures of nitric oxide-mediated endothelial response. However, no study has evaluated endothelial function by PAT in patients with ADPKD.
Objective(s) This pilot study tested the hypothesis that systemic endothelial dysfunction, as determined by PAT, would be detectable prior to development of hypertension and would correlate with renal disease severity determined by height adjusted total kidney volume (htTKV) in patients with ADPKD.
Methods Twelve young (18–40 years), early stage (eGFR >90 mL/min/1.73 m), normotensive (without blood pressure medication) patients with ADPKD and age/sex matched controls (2:1), underwent medical questionnaire, blood and urine collection, abdominal MRI for TKV and renal blood flow (RBF), and PAT for reactive hyperemia index (RHI, normal value ≥2) determination.
Results Main clinical and laboratory characteristics are shown in table 1. ADPKD patients presented with abnormal RHI levels, which correlated inversely with htTKV ($R=0.394$, $p=0.039$), and directly with RBF ($R=0.485$, $p=0.017$). There was no correlation between RHI, htTKV, or RBF and eGFR or other parameters listed in table.
Conclusions Systemic endothelial dysfunction as determined by PAT may be an early marker of vascular changes in patients with ADPKD, and is associated with renal disease severity. These observations may suggest systemic endothelial function as a diagnostic and therapeutic target in patients with ADPKD.

Abstract A53 Table 1 Clinical and laboratory characteristics of study participants

	ADPKD patients	Healthy volunteers	P-value
Gender (F/M)	11/1	5/1	N/A
Age (years)	28 ± 8	28 ± 6	0.759
BSA (m^2)	1.8 ± 0.2	1.8 ± 0.2	0.700
Smokers	None	None	N/A
GFR (ml/min/BSA)	107 ± 14	120 ± 4	0.081
SBP (24hrs) (mmHg)	117 ± 6	107 ± 6	0.155
DBP (24hrs) (mmHg)	79 ± 6	70 ± 7	0.131
HtTKV (ml/m)	319 (228-691)	175 ± 17	0.002
Class B (N)	6	---	
Class C (N)	6	---	
Class D (N)	0	---	
RBF (cc/min/BSA)	892 ± 134	941 ± 163	0.498
PAT index	1.88 ± 0.5	2.14 ± 0.6	0.548
Serum Creatinine (mg/dL)	0.9 ± 0.1	0.8 ± 0.1	0.680
Uric Acid (mg/dL)	4.4 ± 1.0	4.3 ± 1.1	0.929
Cholesterol Total (mg/dL)	169 ± 27	177 ± 13.5	0.457
HDL Cholesterol (mg/dL)	60 ± 9	69 ± 11	0.112
LDL (mg/dL)	94 ± 23	98 ± 13	0.662
Triglycerides (mg/dL)	77 ± 28	55 ± 24	0.180
hs-C-Reactive Protein (mg/L)	1.5 ± 0.5	0.6 ± 0.3	0.246
Lipoprotein, S (mg/dL)	7.7 ± 3.3	6.9 ± 3.6	0.847

A54 TRYPTOPHAN LEVELS PREDICT INCIDENT CARDIOVASCULAR DISEASE IN CHRONIC KIDNEY DISEASE

[1]Anna V Mathew, [2]Vetalise C Konje, [2]Sherwin Navaz, [2]Lixia Zeng, [2]Jaeman Byun, [2]TM Rajendiran, [2]Farsad Afshinnia. *[1]University of Michigan, Ann Arbor, MI; [2]University of Michigan*

10.1136/jim-2020-MW.109

Introduction/Background Non-traditional risk factors like inflammation and oxidative stress play an essential role in the increased cardiovascular disease (CVD) risk prevalent in chronic kidney disease (CKD). Tryptophan conversion to Kynurenine by indoleamine dioxygenase (IDO1) in the kynurenine pathway (KP) is linked to systemic inflammation and CVD in the general and dialysis population; However, the relationship of KP to incident CVD in the CKD population is unknown.

Objective(s) Our overall goal was to delineate the pathophysiological role of KP in incident CVD in CKD patients and mice models.

Methods We quantified IDO expression in aortic tissue and bone marrow cells by immunoblotting and immuno histiochemistry in CKD atherosclerosis mice models. IDO activity was measured by kynurenine to tryptophan ratio in aortic tissue and bone marrow cells in CKD atherosclerosis mouse model using targeted mass spectrometry. We also measured tryptophan metabolites using targeted mass spectrometry in 92 patients with a history of CVD (Old CVD); 46 patients with no history of CVD or new CVD during follow-up (No CVD); and 46 patients with no CVD history who developed CVD in the median follow-up period of 2 years (Incident CVD). The three groups are well-matched in age, gender, race, diabetes status, and CKD stage and only differed in total cholesterol and proteinuria.

Results IDO expression and activity were increased in atherosclerotic lesions and bone marrow derived tissue of CKD mice on high fat diet for 16 weeks compared to control mice with intact renal function. Tryptophan and kynurenine levels are significantly decreased in patients with 'Incident CVD' compared to the 'No CVD' or 'Old CVD' groups ($p=5.2E-7$; $p=0.003$ respectively). Kynurenic acid, 3-hydroxykynurenine, and kynurenine are all increased with worsening CKD stage ($p<0.05$). Increase in tryptophan levels at baseline was associated with 0.32 fold lower odds of 'Incident CVD' ($p=0.000014$) compared to the 'No CVD' group even after adjustment for classic CVD risk factors. Addition of tryptophan and kynurenine levels to receiver operating curve constructed from discriminant analysis predicting 'Incident CVD' using baseline clinical variables increased the area under the curve from 0.76 to 0.82 ($p=0.04$).

Conclusions In summary, KP is implicated in the early pathogenesis of new CVD in CKD both in in vivo animal models and clinical studies.

A55 TARGETED DISRUPTION OF PARAOXONASE 3 IN A DAHL SALT-SENSITIVE RAT MODEL OF CHRONIC KIDNEY DISEASE INCREASES RENAL CORTICAL PRO-INFLAMMATORY EICOSANOIDS

[1]Chrysan J Mohammed, [1]Fatimah K Khalaf, [2]Prabhatchandra Dube, [3]Tyler J Reid, [2]Jacob A Connolly, [2]Bella Z Khatib-Shahidi, [2]Andrew L Kleinhenz, [2]Steven T Haller, [2]David J Kennedy. *[1]University of Toledo, Toledo, OH; [2]University of Toledo; [3]University of Toledo College of Medicine and Life Sciences*

10.1136/jim-2020-MW.110

Introduction/Background Paraoxonase 3 (Pon3), is one of the three isoforms comprising the paraoxonase gene family. While

Pon1 and Pon2 are widely studied, there is a paucity of knowledge regarding Pon3. Pon3 is synthesized in the liver and can circulate bound to high-density lipoproteins, although there is significant expression in the kidney as well. Pon3 has the ability to metabolize eicosanoids, which can act as signaling molecules and have known roles in the pathophysiology of some renal diseases. Decreased Pon activity is associated with elevated levels of eicosanoid metabolites and adverse clinical outcomes. However, whether disruption of Pon3 is associated with changes in eicosanoids levels and renal damage is unknown.

Objective(s) We tested the hypothesis that targeted disruption of Pon3 results in elevated levels of pro-inflammatory eicosanoids and progression of renal injury.

Methods Ten week old, age-matched male control Dahl salt-sensitive (SS^{Mcwi}, hereafter called SS rats) and Pon3 mutant rats (designated SS-$Pon3^{em1Mcwi}$ hereafter called SS-*Pon3* KO rats) were maintained on low salt (0.3% NaCl) and high salt (8% NaCl) diets (Envigo, Teklad diets, Madison, WI) for eight weeks, to initiate salt-sensitive hypertensive renal disease characteristic of this model. SS-*Pon3* KO rats were created by injecting a CRISPR targeting the sequence into SS^{Mcwi} rat embryos, resulting in a 16bp frameshift deletion in exon 4 of the Pon3 gene.

Results We have previously observed that SS-Pon3 KO rats on eight weeks high salt diet demonstrated significantly increased renal injury characterized by increased fibrosis, hyaline cast formation, vascular hypertrophy and glomerular sclerosis, as well as significantly increased mortality. In the current study, we assessed blood pressure by radio telemetry and found that despite the noted phenotypic changes, there was no difference in blood pressure between SS-Pon3 KO and SS wild type. We then examined plasma levels of angiotensin and aldosterone via mass spectrometry and found that there were also no differences between the two groups. Furthermore, upon immunohistological analysis of the kidneys, we noted increased interstitial immune cell infiltration, including increased CD3 positive T cell recruitment in SS-Pon3 KO compared to SS wild type. Next, we used targeted lipidomic profiling with quantitative liquid chromatography–mass spectrometry to determine eicosanoid content in renal cortex from SS-Pon3 KO and SS wild type rats at the end of eight weeks of high salt diet. We found that hydroxyl fatty acids 5-HEPE and 5-HETE (5-lipoxygenase dependent arachidonic acid metabolites) were significantly ($p<0.05$) elevated in the renal cortex of SS-Pon3 KO compared to SS wild type rats. In addition to being mediators of inflammation, these metabolites are associated with renal cell injury and death. Furthermore, prostaglandin 6-keto-PGF1α, which has known links to renal inflammation, was significantly ($p<0.05$) increased in renal cortex of SS-Pon3 KO compared to SS wild type rats.

Conclusions These findings suggest that targeted deletion of Pon3 increases pro-inflammatory eicosanoids including hydroxy fatty acids (5-HETE and 5-HEPE) and prostaglandins (6-keto-$PGF_{1\alpha}$), as well as increases interstitial inflammation and renal damage independent of blood pressure.

A56 RENAL FIBROSIS CALCULATION: MAN AND MACHINE IS BETTER THAN MAN VS. MACHINE

[1]D Mohammed Saeed, [1]A Susma, [2]S Akkina, [1]A Karo, [1]S Sreedhar, [1]M Walsh, [1]S Setty.
[1]University of Illinois at Chicago, IL; [2]Loyola University Medical Center, Maywood, IL

10.1136/jim-2020-MW.111

Introduction/Background Interstitial fibrosis (IF) is an indicator of chronic renal damage in transplanted kidneys. It results from an accumulation of insults namely drug toxicity, infection and rejection. Manual scoring (MS) using Banff criteria is a very reproducible means of establishing the IF score of a renal transplant biopsy. But MS for smaller changes in IF is neither accurate nor reproducible. Thus the need for automation.

Objective(s) Since progressive renal fibrosis in transplanted kidney is not usually reflected in the serology. This study compares the automated method for early detection of fibrosis in kidney biopsies and compare it to serum creatinine and GFR at the time of the biopsy and in the previous three months. It also highlight the common problems associated with automated method.

Methods Paired kidney graft biopsies from 16 patients were obtained at an interval of 9±4 months. Serum creatinine and GFR at the time of biopsy and in the previous 3 months were compiled. Masson trichrome-stained whole slide images of the biopsies were scored using the Histolab program (Gothenburg, Sweden). Fibrosis scores were obtained of the renal

Abstract A56 Table 1 Summary of cases with serology and biopsy results

Patient number	Time interval between biopsies (months)	sCr* (mg/dl)	GFR* (ml/min)	Automated IF** (%)
1a	12	1.34	51	35
1b		1.38	42	6
2a	9	3.4	13	25
2b		1.04	64	9
3a	10	0.99	68	24
3b		1.4	55	9
4a	9	1.03	77	20
4b		1.10	71	25
5a	12	0.89	64	4
5b		0.95	64	23
6a	18	1.08	94	11
6b		1.41	75	18
7a	11	0.91	85	16
7b		0.91	84	73
8a	5	2.50	32	32
8b		2.40	34	19
9a	12	1.15	65	14
9b		1.02	75	3
10a	11	1.9	40	6
10b		1.7	46	13
11a	6	1.5	60	15
11b		1.5	53	7
12a	5	2	43	17
12b		1.8	49	2
13a	6	1.4	47	23
13b		1.45	47	27
14a	12	1.7	46	17
14b		1.8	41	7
15a	8	1.3	55	12
15b		1.16	67	12
16a	4	1.8	49	7
16b		1.3	64	35

* Average of values obtained at the time of biopsy and in the previous 3 months
** Interstitial fibrosis score

Abstract A56 Table 2 Tabulation of serum creatinine versus fibrosis in 16 patients

	No change in s creatinine	Increased s creatinine
No change in fibrosis	4	4
Increased fibrosis	6	2

cortex after excluding perivascular and periglomerular areas of fibrosis. Eyeball field-by-field scores, at 200x, were compiled. The automated method required the creation of a 'mask' for the area of fibrosis with adjustments to account for variability of staining i.e. differences in reagent lots, incubation times and tissue processing. Staining artifacts such as staining of tubular epithelial cytoplasm and tissue-edge artifacts are overcome by manual inspection.

Results The average fibrosis score obtained by the eyeball method was compared to the automated score. The results were considered discrepent if there was a difference in the trend i.e. increase instead of decrease or absence of change, the change between methods being ±20%. Only one pair of biopsies (6%) yielded discrepent results. Also, serum creatinine and GFR were compared to the automated fibrosis scores (table 1). In 6 pairs (37%), where both fibrosis and serology trended in the same direction. On the other hand, in 10 pairs of biopsies (62%), there was a mismatch between fibrosis and serology; in 6 pairs the fibrosis progressed whereas serology was within normal limits and in four pairs, the serology was abnormal without accompanying progression of fibrosis (table 2).

Conclusions Renal transplant subjects may have progressive renal fibrosis that is not reflected in the serology. Early detection with therapy modification could prolong the life of the graft. Finally, the automated method can be adjusted to detect areas of interest, highlighting the need for man and machine to work together to obtain a more accurate fibrosis score. Thus man and machine working in concert leads to higher performance and better patient care.

Neurology/Neurodegeneration

B56 ANALYSIS OF COGNITIVE IMPAIRMENT IN SOUTHWESTERN CLINICAL PARKINSON POPULATION AND RELATIONSHIP TO MOTOR SYMPTOM SEVERITY

[1]Emily Hoegh, [2]Matthew Chaung, [2]Scott Sherman. [1]*University of Arizona- College of Medicine Tucson, Tucson, AZ*; [2]*University of Arizona- College of Medicine Tucson*

10.1136/jim-2020-MW.112

Introduction/Background Although Parkinson Disease (PD) is primarily considered a movement disorder, cognitive decline is a major determinant of overall patient morbidity. The pathophysiology and treatment of motor and cognitive symptoms likely involves distinct brain regions and pathways. Novel therapies for cognitive symptoms are being developed, but first, we must understand the relationship between motor and cognitive status and the clinical picture of impairment across the many domains of cognitive to better develop targeted clinical trials.

Objective(s) We sought to determine the relationship between severity of PD manifestations utilizing standardized measures; the Unified Parkinson Disease Rating Scale (UDPRS) to assess motor symptoms and the Montreal Cognitive Assessment (MoCA) to assess cognitive impairment. We also sought to assess performance across cognition sub-domains as measured by the MoCA. We hypothesized that a positive correlation between the extent of motor and cognitive impairment exists in our local Southwestern PD population and that major cognitive deficits would be observed in delayed recall and visuospatial subdomains.

Methods Local clinical patients (n=16) in Tucson, Arizona with potential cognitive impairment were evaluated in the ON medication state utilizing the UPDRS Part III scale and MoCA as part of their routine care. We analyzed this data to determine the relationship of severity between motor and cognitive clinical presentations. Individual MoCA subdomain scores and total scores were standardized for comparison across subdomain.

Results It was found that most clinical cognition changes were due to impairment in visuospatial and delayed recall subdomains. The MoCA scores were as follows: Total 23/30 (±4.63), visuospatial 3.80/5 (±1.26), delayed recall 2.06/5 (±1.88). Analysis of motor impairment via UPDRS included only items tested across all subjects. The mean UPDRS score was 30.8/68 (±8.15). We carried out a correlation between the Total MoCA and UPDRS. The R^2 was 0.10 indicating no correlation between these measures. Additionally, no correlation was identified between UPDRS and impaired MoCA subdomains of delayed recall and visuospatial (R^2 was 0.008 and 0.07 respectively).

Conclusions We were surprised to find no significant correlation between motor and cognitive presentations in our population. This suggests that the pathophysiological processes underlying these two aspects of PD are different. Our future research will focus on the possibility that apolipoprotein E (APO-E) genotype and phenotype may correlate with cognitive impairment while leaving motor response to dopamine replacement therapy unaffected. APO-E is a known risk factor for the development of Alzheimer's Disease, but its role in PD dementia remains largely unknown. This determination is particularly important as treatments based on APO-E4 status (the neuro-steroid allopregnanolone, for example) are being developed at our institution and position for clinical trial.

107 UTILIZING IN VITRO MODELS OF INTRAVENTRICULAR HEMORRHAGE OF PREMATURITY TO SCREEN ANTI-INFLAMMATORY AND WHITE MATTER PROTECTIVE COMPOUNDS

[1]Brandon Miller, [2]Danielle Goulding, [2]Chirayukumar Pandya. [1]*Neurosurgery, Lexington, KY*; [2]*University of Kentucky, KY*

10.1136/jim-2020-MW.113

Introduction/Background Neonatal intraventricular hemorrhage (IVH) is a consequence of preterm birth. We have found that in vitro studies mimic certain aspects of our in vivo model of neonatal IVH including pro-inflammatory macrophage activation and white matter oxidative stress. We have used these in vitro models to test therapeutics that reduce macrophage activation and oxidative stress and our safe for use in humans.

Objective(s) To determine if hemoglobin induces similar features of inflammation and white matter injury in vivo and in

vitroTo determine if pharmacologic therapy can reduce inflammation and white matter injury in vitro.
Methods We utilized a rat model of neonatal intraventricular hemorrhage, stereotactically injecting 10µl or 15ul of 150 mg/ml hemoglobin into the lateral ventricle of post-natal day five Spague Dawley rat pups. A meso-scale detection ELISA was used to quantify inflammatory cytokines and Western blot was used to measure oxidative stress in the ipsilateral and contralateral hemisphere post injury. Immunohistochemistry was used to assess macrophage activation and oxidative stress. Morris water maze was used to test for behavioral deficits after injury. For in vitro experiments, mixed cortical cultures were obtained from post-natal day two rats and allowed to expand. Microglia and oligodendrocytes were isolated and exposed to different concentrations of hemoglobin. Outcomes after in vitro exposure to hemoglobin were assessed via meso-scale ELISA, immunohistochemistry, genetic analysis, and intracellular reactive oxygen species (ROS) levels using fluorescent dye DCF-DA.
Results Both in vivo and in vitro model systems demonstrated macrophage activation and oxidative stress in response to hemoglobin. The inflammatory profile in vitro mirrors the cytokine profile in vivo, both via gene expression analysis of monocyte chemoattractant protein-1, CCL2 (Chemokine C-C Motif Ligand 2) and inflammatory cytokine proteins. Immunohistochemistry shows that inflammation and oxidative stress are specifically elevated within white matter in vivo, peaking after the peak of macrophage activation. in vitro, hemoglobin directly elevates oxidative stress in oligodendrocyte progenitor cells. We tested the FDA-approved therapeutics azithromycin and phenelzine which showed the potential to reduce hemoglobin-induced inflammation and oxidative stress, respectively.
Conclusions In vitro models recapitulate many of in vivo features of neonatal IVH. This reductionistic strategy can be used to screen drugs that may have therapeutic efficacy for patients.

B06 GENETIC STRATEGIES TO TREAT VISION LOSS IN A MURINE MODEL OF USHER SYNDROME TYPE 1C

[1]Katelyn N Robillard, [2]Nicolas Bazan, [2]Jennifer Lentz. *[1]Louisiana State University Health Sciences Center – New Orleans, New Orleans, LA; [2]Louisiana State University Health Sciences Center – New Orleans*

10.1136/jim-2020-MW.114

Introduction/Background Usher syndrome Type 1C (USH1C) is an inherited form of deaf-blindness that affects Acadian populations in the United States and Canada. Specifically, the USH1C c.216G >A mutation encodes a truncated harmonin protein that disrupts photoreceptor and hair cell function. Antisense oligonucleotides targeting the 216A mutation transiently restore full-length harmonin, which correlates with short-term improvements in hearing, vestibular, and visual function in a mouse model of USH1C.
Objective(s) The goal of this study is to develop genetic strategies for long-term rescue of vision in a mouse model of USH1C. We hypothesize that AAV-mediated gene replacement and/or CRISPR gene-editing products will increase full-length wild type Ush1c expression and restore visual function to a mouse model of USH1C.
Methods An AAV vector that co-expresses Ush1c and GFP reporter was used to treat USH1C mice at different ages (P16, P21, P90). Analysis of transgene expression was performed using confocal scanning laser ophthalmoscopy (cSLO), immunohistochemistry (IHC), and polyacrylamide gel electrophoresis (PAGE). As an alternative approach, CRISPR base editor and nickase systems were designed to target the 216A mutation. Candidate reagents were screened by co-transfection of 293T cells with an USH1C minigene. Editing efficiency was determined by restriction fragment length polymorphism (RFLP) and chromatogram analyses.
Results cSLO detected AAV-mediated GFP localized to the treatment bleb in USH1C mice at 4-weeks posttreatment. IHC revealed that GFP localized to the outer nuclear layer (ONL) and photoreceptor inner/outer segments (IS/OS). Full-length Ush1c transcripts were also detected by PAGE analysis of retinal tissues harvested 4-weeks post-treatment in USH1C mice. For CRISPR-mediated gene editing, RFLP of the targeted region produced additional bands resulting from 216A >G editing. Sequence chromatograms also revealed a second G peak at the 216 location with up to 46% editing in sorted 293T cells.
Conclusions This study demonstrates successful AAV-mediated transgene expression in murine retina and successful CRISPR-mediated gene editing of the human USH1C c.216G >A mutation in cells. Future studies will determine long-term effects of these approaches on retinal structure, function, and visual perception using optical coherence tomography, electroretinography, and a visual cliff assay, respectively.

Other

B57 ABSTRACT WITHDRAWN

Pathophysiology

B20 NOT AS HARMLESS AS YOU THINK: MARIJUANA INDUCED CORONARY VASOSPASM

[1]Julien Feghaly, [2]Zachary Oman, [3]Abdul Rahman Al Hout, [2]Gretchen Grosch, [2]Debapria Das. *[1]St Louis University School of Medicine, St Louis, MO; [2]St Louis University School of Medicine; [3]St Elizabeth Hospital*

10.1136/jim-2020-MW.115

Introduction/Background Marijuana is the most common illicit drug used in the United States, particularly following legalization. Chronic use has been associated with vasospasms, angina, hypertension, arteritis and platelet aggregation. It has very rarely been associated with coronary vasospasm but is being more apparent as a cause of sudden cardiac death.
Case Presentation A 39-year-old female presented from home following an asystole cardiac arrest lasting 4 minutes; no shocks or medications given during resuscitation. She was an everyday tobacco and marijuana user, had no other cardiac risk factors, or personal or family history of cardiovascular disease. Electrocardiogram revealed ST-segment elevation in leads V2-V5 and depression in III and aVF. She was immediately taken for coronary angiography, which revealed normal coronary arteries. Troponin peaked at 0.130 ng/mL. Urine toxicology reported tetrahydrocannabinol (THC), along with

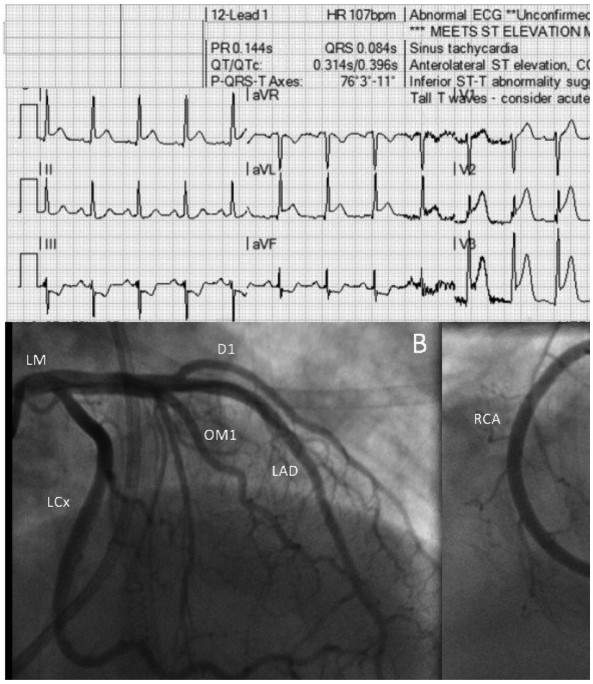

Abstract B20 Figure 1
A. ECG: reveling sinus tachycardia with ST-segment elevation in in leads V2-V5 and depression in III & aVF
B&C. Coronary angiography:
- Left main: Non-significant stenosis. It bifurcates into LAD and LCx.
- LAD: Non-significant stenosis. It is a moderate caliber vessel that gives rise to a large D1 and a small D2. LAD terminates by wrapping around the apex.
-LCx: No significant stenosis. It is moderate caliber vessel that gives to a large OM1 branch and then a small OM2 branch. It continues as a smaller vessel in the AV groove.
- RCA: No significant stenosis. It is a moderate caliber, dominant vessel that divides into RPDA and RPL branch.

hydrocodone which the patient took for pain and fentanyl given in the hospital. Following the cardiac arrest, she gradually recovered without cardiovascular support or medications.
Discussion In the absence of other etiologies or cocaine use, along with normal coronaries; we believe marijuana contributed to coronary vasospasm leading to cardiac arrest, initially appearing as ST-elevation myocardial infarction.

B23 OUT OF HOSPITAL CARDIAC ARREST SECONDARY TO SPONTANEOUS TENSION PNEUMOPERITONEUM

[1]Zarak Khan, [2]Randa T Alsayed, [2]Mohammad Alam, [2]Danekka Loganathan, [2]Narayana Gandham, [2]Narendra Khanchandani. *[1]St Mary Mercy Hospital, Livonia, MI, West Bloomfield, MI; [2]St Mary Mercy Hospital, Livonia*

10.1136/jim-2020-MW.116

Introduction/Background 'Pneumoperitoneum' is the accumulation of free gas in the peritoneal cavity. Common causes include ventilator-induced barotrauma, bowel perforation, endoscopic procedures and abdominal surgeries. Tension pneumoperitoneum is the excessive accumulation of free gas in the peritoneal cavity resulting in an acute rise in intra-abdominal pressure, causing hemodynamic instability. In rare cases it has led to cardiac arrest and we report one such case.

Case Presentation A 64-year-old man with history of hypertension and alcohol abuse was brought to emergency room with out of hospital cardiac arrest. He was found collapsed on the floor at home. His last known normal was 20 minutes prior to collapse. CPR was initiated by family and EMS was called. EMS noted empty beer cans at home near the patient. Patient was found to be in PEA arrest and resuscitated per ACLS protocol. ROSC was achieved at the scene and a King airway was placed to provide assisted ventilation. On arrival to ER patient's airway was changed to an endotracheal tube and resuscitation continued. Initial examination was remarkable for

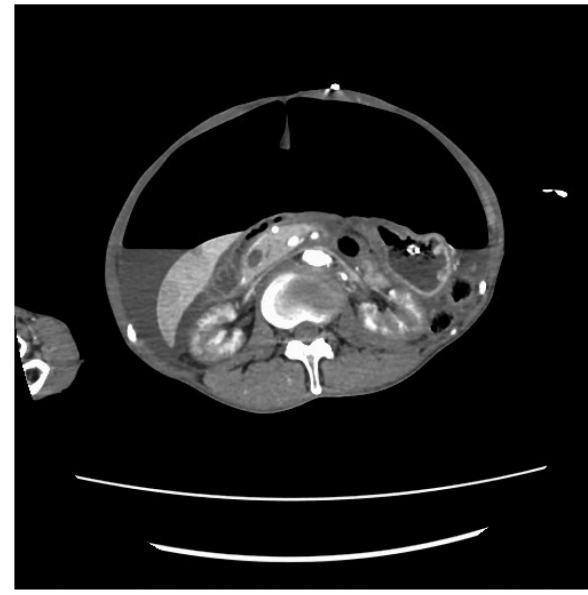

Abstract B23 Figure 1 Axial view of CT abdomen
CT Abdomen (Axial view) demonstrating pneumoperitoneum in the anterior abdomen

Abstract B23 Figure 2 Sagittal view of CT abdomen
CT Abdomen (Sagittal view) demonstrating pneumoperitoneum in the anterior abdomen

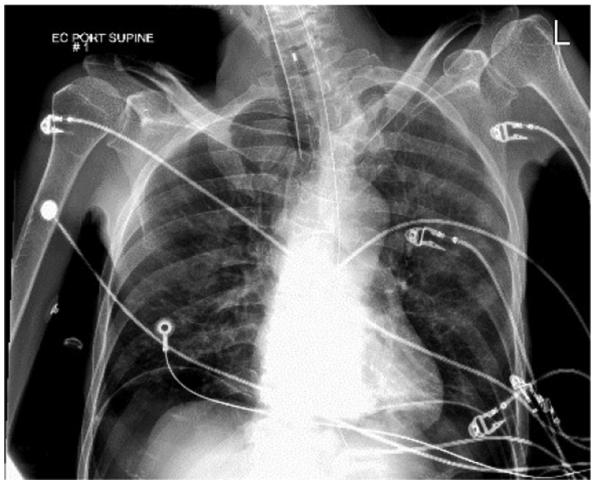

Abstract B23 Figure 3 X-ray chest
Chest x-ray demonstrating air under bilateral hemi-diaphragms concerning for pneumoperitoneum

Abstract B23 Figure 4 X-ray abdomen
Abdominal x-ray demonstrating Lucency involving the bilateral pericolic gutters concerning for pneumoperitoneum

an unresponsive gentleman in shock with a tensely distended and rigid abdomen. Patient had symptoms of abdominal pain for 2 days per family. Labs were significant for hemoglobin of 11.7 gm/dL, AST 435 units/L, ALT 236 units/L, lactic acid 13.4 mMol/L, alcohol level 19 mg/dL and ammonia 155 mcg/dL. CT scan of the abdomen showed large pneumoperitoneum, free fluid and compressed inferior vena cava. The patient was given broad-spectrum antibiotics and taken to the OR for emergency surgery. Intra-abdominal pressure was 28 mmHg in the OR using an indwelling foley catheter. Patient had a laparoscopy with initial release of accumulated gas. He was found to have a large 1.5 cm perforated gastric ulcer which was repaired laparoscopically. The patient was transferred to the ICU following the procedure. He had multiorgan dysfunction but stabilized with aggressive intensive care. However, he did not awaken and was declared brain dead 3 days after admission to hospital.

Discussion We believe our patient had tension pneumoperitoneum causing severe abdominal compartment syndrome leading to cardiovascular collapse and cardiac arrest. The rapid deterioration culminating in arrest suggests a mechanical component to the arrest rather than a pure hypovolemic and inflammatory state. The radiologic findings of a large pneumoperitoneum compressing the abdominal viscera into a central mass as well as compression of the inferior vena cava and medial displacement of the liver by air have previously been described with tension pneumoperitoneum. Smet *et al* described a case similar to ours of spontaneous tension pneumoperitoneum presenting with cardiac arrest. Emergency personnel should consider the possibility of tension pneumoperitoneum in patients with distended abdomen and preceding abdominal pain. Given the widespread availability of point of care ultrasound, rapid diagnosis of pneumoperitoneum can be made in the field or soon after arrival to ER. Emergent decompression with 16 G needle placed 2 cm below the umbilicus can be lifesaving.

Pediatrics

B16 PROSPECTIVE EFFECTS OF A GROUP-BASED MOTHER-DAUGHTER INTERVENTION FOR AFRICAN AMERICAN ADOLESCENT GIRLS ON MENTAL HEALTH SYMPTOMS AND SEXUALLY TRANSMITTED INFECTIONS

[1]Ashley Kendall, [2]Christina Young, [3]Bethany Bray, [3]Erin Emerson, [3]Sally Freels, [3]Geri Donenberg. [1]*University of Illinois at Chicago, Chicago, IL*; [2]*Stanford University*; [3]*University of Illinois at Chicago*

10.1136/jim-2020-MW.117

Introduction/Background There is a need for culturally tailored interventions that address the interrelated issues of mental health symptoms and HIV/sexually transmitted infection (STI) risk behaviors among African American adolescent girls. IMARA is a group-based mother-daughter intervention designed to address this gap. Our previous work showed that African American adolescent girls who received IMARA were 43% less likely than those from a mother-daughter health promotion control group to evidence a new STI 1 year later (relative risk = 0.57, 95% CI [0.36–0.89], p=0.01). The effects of IMARA on girls' mental health symptoms, and the possible role of mental health symptom improvement in the protective effect of IMARA against future STIs, remain unknown.

Objective(s) The primary aim of the present study was to test if (a) externalizing (e.g., aggression) and internalizing (e.g., anxiety, depression) symptoms improved more among girls who received IMARA than the health promotion control group over 6- and 12-month follow-up; and (b) symptom improvements were significantly stronger among girls who entered the study with high versus lower symptom levels, helping indicate to whom intervention resources should be

allocated. A secondary aim was to conduct exploratory analyses examining if mental health symptom improvements were partially associated with the protective effect of IMARA against new STIs by 1 year.
Methods African American girls 14–18 years old (N=199, mean age = 16.02 years) and their mothers were randomly assigned to IMARA or an equally intensive health promotion control group. Girls completed the Youth Self-Report of externalizing and internalizing symptoms at baseline, 6, and 12 months. They also provided urine samples that were screened via nucleic acid amplification testing for N. gonorrhoeae, C. trachomatis, and T. vaginalis at baseline and 12 months; positive cases were treated at each time point. Hierarchical linear modeling (HLM) analyzed the effects of IMARA on externalizing and internalizing symptom changes separately. Log binomial regression tested the effects of IMARA and mental health symptom change on STIs at 12 months. The University of Illinois at Chicago (UIC) IRB approved all procedures.
Results Among girls who entered the study with high, but not lower, externalizing symptoms (T-scores of greater than or equal to 60 and less than 60, respectively), those who received IMARA showed significantly greater reductions in externalizing symptoms than those from the control arm over 6- and 12-month follow-up, p=0.034. These improvements were associated with 12% of the protective effect of IMARA against new STIs at 1 year. Unexpectedly, IMARA did not appear to be associated with changes in internalizing symptoms, p>0.05.
Conclusions IMARA improved externalizing symptoms over a high-risk developmental period among African American girls with high, but now lower, baseline externalizing symptoms. These improvements may be linked with the protective effect of treatment against future STIs. The results underscore the importance of directing IMARA to the most symptomatic African American girls along the externalizing dimension. Future directions include examining the factors associated with the successful implementation of IMARA in real-world settings, moving the intervention from the present T3 phase into the T4 phase of the translational research continuum.

Pulmonary/Critical Care

B58 HUR PROMOTES MIRNA-MEDIATED UPREGULATION OF NFI-A PROTEIN EXPRESSION DURING MURINE SEPSIS

[1]Tuqa Alkhateeb, [2]Isatou Bah, [2]Ajinkya Kumbhare, [2]Dima Youssef, [3]Charles McCall, [2]Mohamed El Gazzar. *[1]East Tennessee State University College of Medicine, JOHNSON CITY, TN; [2]East Tennessee State University College of Medicine; [3]Wake Forest School of Medicine*

10.1136/jim-2020-MW.118

Introduction/Background Myeloid-derived suppressor cells (MDSCs) emerge when the acute sepsis stress response and emergency leukocytosis exhaust mature and functional innate immune phagocytes. Replacement of competent phagocytes with MDSCs during sepsis contributes to sustained life-threatening innate and adaptive immune failure, called 'immunoparalysis'. What controls sepsis induced MDSC development at the molecular level is unknown, and there are no molecular-based targeted treatments to reverse MDSCs. We previously reported that increases in microRNA (miR)-21 and miR-181b promote MDSCs in a sepsis mouse model by increasing expression of transcription factor NFI-A, but how NFI-A controls persistent MDSC expansion is unknown.
Objective(s) To determine how miR-21 and miR-181b control NFI-A expression to promote MDSC development during post-acute sepsis and identify a new druggable target.
Methods We generated Gr1+CD11b+ MDSCs for isolation by inducing polymicrobial sepsis in 8–10-week-old Balb/c mice with cecal ligation and puncture (CLP). Quantitative PCR assessed mRNA levels, and RNA immunoprecipitation defined interactions between NFI-A 3' untranslated region (3'UTR) and the RNA-binding proteins (RBPs) HuR, Ago1 and Ago2, and GU-rich element (GRE)-binding protein CUGBP1. A transfected luciferase reporter with miR-21 and miR-181b binding sites in the NFI-A 3'UTR and mutation of miRNA binding sites confirmed functional miRNA sites for mRNA stability.
Results We found that miR-21 and miR-181b limit NFI-A mRNA decay by recruiting the RNA-binding proteins HuR and Ago1 to the NFI-A mRNA 3'UTR. HuR interacted with Ago1 to form a complex that stabilized NFI-A mRNA and increased its protein level. In contrast, CUGBP1 counteracted HuR effect by degrading NFI-A mRNA. Transfecting MDSCs with luciferase reporter constructs containing an NFI-A 3'UTR fragment with miRNA binding site mutations confirmed our post-transcriptional mechanistic model of NFI-A upregulation in sepsis MDSCs.
Conclusions miR-21 and miR-181b post-transcriptionally control NFI-A expression by exchanging 3'UTR binding protein CUGBP1 with HuR. This axis potentially provides a new druggable target for reducing MDSCs and thus reversing chronic sepsis immunosuppression.

B59 CARMIL1 REGULATES PULMONARY ENDOTHELIAL BARRIER FUNCTION

[1]Patrick Belvitch, [2]Regaina Demeritte, [3]Joe Gn Garcia, [4]Steven Dudek. *[1]University of Illinois at Chicago, CHICAGO, IL; [2]University of Illinois at Chicago; [3]University of Arizona; [4]Division of Pulmonary, Critical Care, Sleep, and Allergy, University of Illinois at Chicago, States/Provinces*

10.1136/jim-2020-MW.119

Introduction/Background The acute respiratory distress syndrome (ARDS) results in loss of pulmonary endothelial barrier integrity resulting in alveolar flooding and impaired gas exchange. The pathologic mechanisms responsible for ARDS pathogenesis remain incompletely understood. Genetic variants in the gene encoding capping protein Arp2/3 complex myosin-I linker (CARMIL1) have been implicated in human ARDS outcomes through preservation of platelet count (Wei, *et al*. AJRCCM 2017). Based on the known cellular functions of CARMIL1 we hypothesized this protein may also contribute to endothelial barrier integrity.
Objective(s) To characterize the effects of altered CARMIL1 expression on endothelial barrier function.
Methods Human pulmonary artery endothelial cells (ECs) were treated with CARMIL1 siRNA (Santa Cruz) or scramble siRNA x 48 hrs followed by measurement of transendothelial electrical resistance (TER) by ECIS. The response to barrier enhancing sphingosine-1-phosphate (S1P 1 μM) or the S1P analogue tysiponate (Tys 1 μM) was determined. HPAEC membrane fractionations were obtained by

differential centrifugation. Protein expression level and phosphorylation status was measured by western blot. The ratio of phosphorylated myosin light chain (MLC)/total MLC was used as a surrogate for myosin light chain kinase (MLCK) activity.

Results Baseline TER was significantly reduced following treatment with siCARMIL1 compared to siControl (1042 ±20 Ohm vs 1238±28 Ohm; $p<0.01$). These changes in TER were correlated with a reduction in the p-MLC/total MLC ratio in siCARMIL1 cell lysate vs control (0.524 ±0.04 vs 0.866±0.06; $p<0.02$). Following treatment with S1P (1 μM), peak TER increased 25% over baseline in siControl cells but only increased 17% in siCARMIL1 cells. Additionally, TER elevations produced by S1P and Tys were not sustained following CARMIL1 knockdown as was observed in siControl treated cells. CARMIL1 membrane fraction protein levels increased 1.67-fold and 1.62-fold following S1P (1 μM) or Tys (1 μM) x 15 min compared to control conditions.

Conclusions CARMIL1 expression is required for baseline pulmonary endothelial barrier function and maximal response to barrier enhancing compounds. CARMIL1 is closely associated with the cell membrane under barrier enhancing conditions. Loss of CARMIL1 expression results in reduced MLCK activity. These results implicate CARMIL1 in endothelial functions critical to ARDS pathophysiology.

B60 LUNG ENDOTHELIAL CELL BARRIER DISRUPTION BY LPS IS ATTENUATED BY LITHIUM AND HALOPERIDOL

[1]Marco A Colamonici, [2]Yulia Epshtein, [3]Jeffrey R Jacobson. *[1]University of Illinois- Chicago; [2]UIC, Chicago, IL; [3]University of Illinois at Chicago*

10.1136/jim-2020-MW.120

Introduction/Background We have previously reported that claudin-5, a tight junctional protein, mediates lung vascular permeability in a murine acute lung injury (ALI) model induced by lipopolysaccharide (LPS). Recently, it has been shown that two antipsychotic medications, lithium and haloperidol, both dose-dependently increase expression of claudin-5 in vivo and in vitro, in brain endothelium. Notably, claudin-5 is highly expressed in both brain and lung tissues. However, the effects of these drugs on EC barrier function is unknown.

Objective(s) We hypothesized that lithium and haloperidol both upregulate lung EC claudin-5 and attenuate agonist-induced lung EC barrier disruption.

Methods Human pulmonary artery EC were pretreated with lithium or haloperidol at variable concentrations (0.1–10 mM) for 24 h. Cell lysates were subjected to Western blotting for claudin-5 and zona occludens-1 (ZO-1), another tight junctional protein. To assess effects on barrier function, EC were grown to confluence overlying gold-plated microelectrodes and were then pretreated for 24 h with lithium (0.1–10 mM), haloperidol (0.1–10 mM), or vehicle 24 prior to treatment with LPS (1 mg/ml). Measurements of transendothelial electrical resistance (TER) were recorded as a real-time assessment of barrier integrity.

Results Both lithium and haloperidol significantly upregulated claudin-5 and ZO-1 expression in a dose-dependent manner as assessed by Western blotting of cell lysates. Measurements of TER confirmed a significant attenuation of LPS-induced barrier disruption associated with treatment with either lithium or haloperidol.

Conclusions Our data confirm that both lithium and haloperidol upregulate the tight junctional proteins, claudin-5 and ZO-1 in lung EC. In addition, both drugs demonstrate vascular-protective effects. These findings suggest that lithium and haloperidol could represent novel therapies in the prevention and treatment of ALI and warrant further investigation in this context.

B61 TRPM2 AUGMENTS LUNG ENDOTHELIAL BARRIER FUNCTION AFTER RADIATION VIA SPHINGOLIPID SIGNALING

[1]Yulia Epshtein, [2]Weiguo Chen, [3]Huashan Wang, [4]Jeffrey R Jacobson. *[1]UIC, Chicago, IL; [2]University of Illinois at Chicago, Chicago, IL; [3]Univ of Illinois at Chicago; [4]University of Illinois at Chicago*

10.1136/jim-2020-MW.121

Introduction/Background We previously reported sphingolipid signaling is an important mediator of radiation-induced lung injury (RILI) although the mechanisms underlying these effects have not been fully defined. A potential molecule of interest in this regard in TRPM2 (transient receptor potential (melastatin) 2), an oxidant sensitive, non-selective cation channel expressed in the lung endothelium that is known to regulate endothelial cell (EC) permeability and cellular responses to radiation injury. Moreover, preliminary studies by our lab previously confirmed TRPM2-silenced EC demonstrated a significant attenuation of barrier enhancement induced by sphingosine 1-phosphate (S1P) as measured by transendothelial resistance (TER).

Objective(s) Thus, we hypothesized that TRPM2 is an important modulator of EC barrier responses to radiation via effects on sphingolipid signaling.

Methods Initially, to characterize the effects of radiation on lung EC TRPM2 expression we subjected cells to radiation (10 Gy) at various time points and performed Western blotting of lysates for TRPM2, as well as sphingosine kinase 1 (SphK1) and 2. To investigate the functional role of TRPM2 on EC barrier regulation, both after radiation and in response to S1P-mediated signaling, we measured TER in irradiated EC transfected with siTRPM2 and assessed effects on barrier enhancement by Tysiponate (Tys), an S1P analog. Next, irradiated EC were pretreated with an inhibitory peptide specific for TRPM2, synthesized by fusing a portion of the TRPM2 C-terminus with the tat-M2NX, and in separate experiments, we utilized 2'-deoxyadenosine 5'-diphosphoribose, a TRPM2 superagonist, to assess the effects on EC barrier responses both alone and in conjunction with Tys.

Results These experiments confirmed that EC TRPM2 and Sphk1/2 are upregulated after radiation. In addition, barrier enhancement of irradiated EC by Tys was significantly attenuated by the use of the TRPM2 inhibitory peptide. Moreover, the TRPM2 superagonist augmented EC barrier function by itself and had a synergistic effect on EC barrier enhancement by Tys.

Conclusions Our data confirm TRPM2 is an important mediator of EC barrier regulation by sphingolipids, both alone and in response to radiation. Further, we have identified a TRPM2 superagonist that now warrants further study as a

potential novel therapeutic molecule for patients either with or at risk for RILI or other inflammatory lung diseases.

B62 HEMIN INDUCED ENDOTHELIAL DYSFUNCTION CONTRIBUTES TO THE PATHOGENESIS OF PULMONARY HYPERTENSION DUE TO CHRONIC HEMOLYSIS

[1]Dustin R Fraidenburg, [2]Kelsey Holbert, [2]Janae Gonzales, [3]Kamryn Czysz. [1]*UIC, Chicago, IL*; [2]*University of Illinois at Chicago*; [3]*University of Denver*

10.1136/jim-2020-MW.122

Introduction/Background Pulmonary hypertension (PH) is a severe sequela of sickle cell disease (SCD) encountered in about 10% of patients and is an independent predictor of mortality. Hemolysis and nitric oxide scavenging are thought to play an important role in endothelial dysfunction and vascular remodeling leading to PH in SCD patients. Still, the precise pathogenesis leading to such a high burden of PH remains incompletely understood.
Objective(s) We hypothesize that products of intravascular hemolysis in patients with sickle cell disease lead to inflammation, increased endothelial proliferation, endothelial to mesenchymal transition (EndoMT), and ultimately contribute to the development and progression of PH in this cohort of patients.
Methods All experiments in the current study utilized commercially procured human pulmonary artery endothelial cells (HPAECs). Cell proliferation was determined by WST assay (Millipore) and PCNA expression. Migration was determined by wound assay and was done with electric cell-substrate impedance sensing (ECIS). Interleukin-6 (IL-6) and -8 (IL-8) secretion were evaluated by ELISA assay (BioLegend). Western blot analysis was used to determine protein expression of vimentin and alpha smooth muscle actin.
Results We identified increased proliferation by WST assay in HPAEC treated with 5 mM hemin compared to control ($p<0.001$). Similarly, PCNA expression was increased in hemin treated HPAEC. ECIS wound assay showed increased migration of HPAEC treated with hemin as compared to control. HPAEC treated with hemin also showed increased IL-6 ($p<0.001$) and IL-8 ($p<0.001$) secretion measured by ELISA. Increased protein expression of mesenchymal tissue markers, vimentin and alpha smooth muscle actin, were identified in HPAEC treated with hemin compared to control. Given the suggestion of increased EndoMT in HPAEC treated with hemin, we undertook experiments using an MLCK inhibitor, ML-7. Pretreatment with ML-7 almost fully prevented the increased proliferation seen in hemin treated HPAEC ($p<0.01$). Additionally, IL-6 and IL-8 secretion was blocked by pretreatment with ML-7, ($p<0.001$ for both).
Conclusions Low dose (5 mM) hemin exposure leads to dysfunction of HPAEC characterized by increased proliferation and migration as well as cytokine release. Hemin treatment seems to increase EndoMT as a potential mechanism for the development of PH in patients with chronic hemolysis. Targeting MLCK activity in HPAEC undergoing EndoMT may be a unique target in the early stages of PH development. Further work on these mechanisms will help to better understand the development and progression of PH in SCD while potentially unlocking unique therapeutic targets for this deadly complication.

B64 CIGARETTE SMOKE-INDUCED LUNG ENDOTHELIAL APOPTOSIS IS MODULATED BY CORTACTIN

[1]Mounica Bandela, [2]Eleftheria Letsiou, [3]Steven Dudek. [1]*Division of Pulmonary, Critical Care, Sleep, and Allergy, University of Illinois at Chicago, Chicago, IL*; [2]*Division of Pulmonary, Critical Care, Sleep, and Allergy, University of Illinois at Chicago, IL*; [3]*Division of Pulmonary, Critical Care, Sleep, and Allergy, University of Illinois at Chicago, States/Provinces*

10.1136/jim-2020-MW.123

Introduction/Background Cigarette smoke (CS) is the primary cause of Chronic Obstructive Pulmonary Disease (COPD) and induces apoptosis in lung endothelial cells (EC). We hypothesized a potential role for cortactin (CTTN) in CS-induced apoptosis in lung endothelial cells. CTTN is an actin-binding and barrier regulatory protein that is activated by Src-mediated tyrosine phosphorylation to promote actin rearrangement. We previously described a human genetic variant that alters CTTN phosphorylation at the functionally important Y486 site to affect lung endothelial actin dynamics.
Objective(s) The major goal of this study is to investigate the role of cortactin and its genetic variant during CS-induced lung EC apoptosis.
Methods CTTN protein levels in the lungs from CS-exposed mice (6 months) were analyzed using western blotting. CS-induced lung EC apoptosis was assessed by flow cytometry analysis (Annexin-V/7-AAD staining) and cleavage of caspase-3/PARP by western blot. The role of CTTN expression and function in this process was explored using cortactin siRNA, overexpression with Ds-Red-labeled wild type (WT) or genetic variant (SNP) CTTN, and SH3 domain peptide inhibitor.
Results CTTN protein expression was increased in lung tissues from CS-exposed mice. CS exposure increased CTTN tyrosine phosphorylation in cultured human lung EC within hours, with decreased phosphorylation of CTTN SNP compared to CTTN WT. Exposure of EC to CS for 24 hours enhanced cleavage of apoptotic markers caspase-3/PARP and significantly increased annexin (+) cell%. Reduction of cortactin expression by siRNA increased CS-induced apoptosis, while overexpressing DsRed WT CTTN (but not DsRed SNP CTTN) reduced apoptosis. Blocking the SH3 domain of CTTN with peptide inhibitor increased CS-induced apoptosis.
Conclusions Our study suggests that modulation of CTTN tyrosine phosphorylation during CS-induced lung EC apoptosis may have important functional effects during this key step in COPD pathogenesis.

B65 SMOOTH MUSCLE CELL SPECIFIC CAVEOLIN-1 DEFICIENCY ENHANCES THE PROGRESSION OFPULMONARY HYPERTENSION

[1]Haibin Li, [2]Ming Tang, [3]Suellen Oliveira, [4]Ayman Isbatan, [5]Zhenlong Chen, [5]Ying Jiang, [1]Maricela Castellon, [6]Dustin R Fraidenburg, [7]Wancai Yang, [1]Richard Mishall, [1]Jiwang Chen. [1]*Univesity of Illinois at Chicago*; [2]*Univesity of Illinois at Chicago, Chicago, IL*; [3]*Departments of Anesthesiology, UIC*; [4]*UNiversity of Illinois at Chiacago, Oak Lawn, IL*; [5]*UIC*; [6]*UIC, Chicago, IL*; [7]*Jining Medical University*

10.1136/jim-2020-MW.124

Introduction/Background Pulmonary hypertension (PH) is a chronic pulmonary vascular disease characterized by pulmonary arterial remodeling (PVR) and elevated pulmonary vascular resistance that eventually leads to right heart failure and

death. Caveolin 1 (Cav-1) has been reported to play a role in the development of PH.

Objective(s) The objective is to study the role of pulmonary artery smooth muscle cell (PASMC) specific Cav-1 in PAH.

Methods We generated smooth muscle cell specific Cav-1 deficient (Cav-1 $^{flox/flox}$ MHC Cre $^{+}$) mice. In three weeks after tamoxifen injections, the mice were exposed to normoxia or 10% FiO 2 for four weeks.Right ventricular systolic pressure (RVSP), right ventricle: left ventricle + septum (RV/LV+S) weight ratio and pulmonary artery remodeling via Aperio image software were measured. Pulmonary artery smooth muscle cells (PASMCs) isolated from Cav-1 $^{-/-}$ and WT siblings were used to study cell proliferation via BrdU assays. Strategies of silencing or overexpressing Cav-1 via adenovirus system were employed to examine their effect on hPASMC proliferation.

Results Under normoxic exposure, RVSP and RVH did not differ in Cav-1 $^{flox/flox}$ MHC Cre $^{+}$ mice between tamoxifen-induced and vehicle groups. After hypoxic exposure, the mice with tamoxifen induction developed significantly elevated RVSP, RVH and pulmonary vascular remodeling, compared to their vehicle group.The PASMCs isolated from Cav-1 $^{-/-}$ mice are more proliferative compared to wild type (WT) mice. In vitro silencing of Cav-1 in hPASMC promoted cell proliferation and overexpressing of Cav-1 inhibited cell proliferation.

Conclusions Using SMC specific Cav-1 knockout mice and isolated PASMCs, we demonstrate SMC Cav-1 expression plays an active role in regulating contractile protein expression and SMC proliferation.

B66 DEUBIQUITINASE USP13 PROMOTES FIBRONECTIN EXPRESSION BY STABILIZING SMAD4 IN LUNG FIBROBLAST CELLS

[1]Xinxin Liao, [2]Yanhui Li, [2]Jia Liu, [3]Daniel J Kass, [3]Mauricio Rojas, [2]Rama Mallapalli, [2]Jing Zhao, [2]Yutong Zhao. *[1]The Ohio State University College of Medicine, OH; [2]The Ohio State University College of Medicine; [3]The University of Pittsburgh*

10.1136/jim-2020-MW.125

Introduction/Background Fibronectin (FN) is a key component of the extracellular matrix and regulates cell adhesion, proliferation, migration and survival. TGF-β1 signaling plays a pivotal role in the expression of FN. The deubiquitinating enzymes participate in pathological mechanisms of human disorders by regulating proteins stability. In our previous study, the deubiquitinase USP13 has been shown to suppress lung inflammation. However, the role of USP13 in the expression of FN is unclear.

Objective(s) To investigate if deubiquitinase USP13 promotes fibronectin expression by stabilizing Smad4 in lung fibroblast cells.

Methods Human lung fibroblast cells (MRC5), lung fibroblast cells from idiopathic pulmonary fibrosis (IPF) patients, and primary lung fibroblast cells from USP13 deficient mice (USP13-KO) and C57BL/6 wild type (WT) were used for determining FN and Smad4 expression. C57BL/6 mice were challenged with intratracheal PBS or bleomycin (BLM) for 1–3 weeks. Smad4 half-life was examined by a cycloheximide (CHX) chase assay. Smad4 ubiquitination was measured by an in vivo ubiquitination assay.

Results USP13 protein levels were increased in both primary adult lung fibroblasts isolated from BLM (1 week)-challenged C57BL/6 mice and TGF-β1 (24 h)-treated primary mouse lung fibroblasts. USP13-KO mice showed reduced FN levels, compared with WT after BLM challenge for 3 weeks. The reduction in protein level and mRNA expression of FN were observed in the isolated lung fibroblasts from USP13-KO mice, compared with the cells from WT mice. Further, we examined the effect of USP13 on Smad4 expression and found that down-regulation of USP13 reduced Smad4 protein levels, without altering Smad4 mRNA expression. Overexpression of USP13 increased FN and Smad4 protein levels in MRC5 cells. Knockdown of USP13 decreased Smad4 half-life and promoted Smad4 ubiquitination.

Conclusions This is the first study to demonstrate that USP13 promotes FN expression by stabilizing Smad4 in lung fibroblast, indicating a role of USP13 in regulation of lung physiological function by maintenance of the extracellular matrix in lungs.

B67 IMMUNE CELL RECRUITMENT DURING INFLUENZA INFECTION IN MICE IS ALTERED BY CIGARETTE SMOKE EXPOSURE

[1]Wenxin Wu, [1]Lili Tian, [1]Wei Zhang, [2]J Leland Booth, [2]Vineet I Patel, [3]Erola Ainsua-Enrich, [3]Susan Kovats, [2]Jordan P Metcalf. *[1]University of Oklahoma Health Sciences Center; [2]University of Oklahoma Health Sciences Center, Oklahoma City, OK; [3]Oklahoma Medical Research Foundation*

10.1136/jim-2020-MW.126

Introduction/Background Influenza is a highly contagious, acute, febrile respiratory infection caused by a negative-sense, single-stranded RNA virus, which belongs in the Orthomyxoviridae family. Cigarette smoke (CS) exposure worsens influenza infection in terms of frequency and severity in both human and animal models.

Objective(s) We sought to determine the effect of CS exposure on immune cell recruitment to the lung during influenza infection in a mouse model.

Methods C57BL/6 mice with or without CS exposure for 6 weeks were inoculated intranasally with a single, non-lethal dose of the influenza A virus (IAV) A/Puerto Rico/8/1934 (PR8) strain. At 7 and 10 days after infection, lung and mediastinal lymph nodes (MLN) cells were collected to determine the numbers of dendritic cells (DC), neutrophils, total CD4+ and CD8+ T cells, and IAV-specific CD4+ and CD8+ T cells using flow cytometry.

Results CS exposure reduced numbers of CD103+ DCs in the lung and MLN of mice at day10, but not day7 post-infection. CS increased eosinophil number in mice with IAV infection at day10. CS exposure alone increased neutrophil numbers in mock-infected mice. IAV infection induced neutrophil in the lung, but CS exposure did not affect the number of neutrophil induced by IAV. Remarkably, CS increased total CD4+ and CD8+ T cell numbers in MLN in mice with IAV infection at day 7 and 10 compared to air-exposed mice. IAV-specific CD4+ and CD8+ T cells were increased by CS at day10. CS exposure also led to increased numbers of IAV-specific IFN-γ-bearing CD8+ T cells in the lung and MLN.

Conclusions Our results demonstrated that CS exposure alone induced neutrophil infiltration and inflammation in the lung. CS increased numbers of IAV antigen-specific CD4+ and CD8 + T cells, which produced more IFN-γ from day 7 after infection. CS-mediated induction of IFN-γ, CD4+ and CD8+

T cells may play a role in the increased mortality of the CS-exposed IAV-infected mice.

B68 NOVEL PHARMACOLOGICAL APPROACH FOR TREATMENT OF ACUTE RESPIRATORY DISTRESS SYNDROME

[1]Xinyan Qu, [2]Ben Hitchinson, [3]Avik Banerjee, [3]Shuangping Zhao, [3]Chongxu Zhang, [3]Vadim Gaponenko, [3]Yulia Komarova. [1]*university of illinois at chicago, chicago, IL*; [2]*University of Illinois at Chicago*; [3]*uic*

10.1136/jim-2020-MW.127

Introduction/Background Acute respiratory distress syndrome (ARDS) is a life-threatening condition associated with high mortality and long-term disability in survivors due to pulmonary insufficiency. It remains an area of unmet medical need, as the current management of ARDS patients is limited to supportive care. Here, we offer a novel pharmacological approach to treat ARDS by inhibiting microtubule accessory factor end binding protein 3 (EB3), which contributes to vascular leakage by amplifying pathological calcium signaling in endothelial cells.

Objective(s) The objective of this study is to develop and optimize novel drug-based compounds for future clinical studies, and investigate their therapeutic benefits in treating pulmonary edema, inflammation and mortality in pre-clinical models of ARDS.

Methods We have designed an EB3 allosteric inhibitor, UIC109, using Structure Activity Relationship (SAR) by NMR lead optimization studies. The dose-dependent effect of UIC109 on inhibition of calcium release from endoplasmic reticulum (ER) stores was determined using a robotically-integrated platform for high content screening. The Fluo-4 live-cell fluorescence imaging approach was utilized to monitor the changes in intracellular calcium concentration upon activation of calcium release from the ER in endothelial cells challenged with serine proteases α-thrombin. Furthermore, efficacy of UIC109 in treating vascular leakage, pulmonary edema, lung inflammation, and mortality was tested in mice challenged with endotoxin, underwent cecal ligation and puncture (CLP) surgery, or exposed to high volume mechanical ventilation.

Results UIC109 is a synthetic cyclic peptide of 902 Da with superior physicochemical characteristics and stability in human blood plasma and various storage conditions as compared to parent liner peptide and 60 other novel drug candidates tested in SAR studies. It demonstrates a *logP* of 0.74 and is cell permeable with $t_{1/2}$ uptake of 3.42±0.1 min by endothelial monolayers in vitro. UIC109 inhibits calcium release from ER stores at IC_{50} of 96.13±0.2 nM. Furthermore, UIC109 promptly restores lung tissue-fluid homeostasis and lung compliance at both early and late stages of lung injury induced by endotoxin, reduces inflammation of the lung, and markedly improves the survival of mice challenged with endotoxin or underwent CLP surgery. When administrated iv in mice at 20 h post-challenge with a lethal dose 90 of endotoxin (Lipopolysaccharides, LPS), it significantly improves survival rate from 10% to up to 75% with EC_{50} of 30 nM/kg bw. UIC109 also protects from vascular leakage and pulmonary edema in mice subjected to high volume mechanical.

Conclusions Based on the effects of UIC109 observed in mice, it is predicted to promptly restore respiratory function of injured lungs, increase the number of ventilator-free days, improve oxygenation of the lung and other organs, and decrease hospital mortality.

B69 PKG REGULATES PDE3A ACTIVATION THROUGH MODULATING ITS INTERACTION WITH HSP90

[1]Xiaomin Wu, [2]Haiyang Tang, [3]Evgeny Zemskov, [3]Xutong Sun, [3]Mannivannan Yegambaram, [4]Stephen M Black. [1]*The University of Arizona, Tucson, AZ*; [2]*The First Affiliated Hospital of Guangzhou Medical University, TUCSON, AZ*; [3]*University of Arizona*; [4]*The University of Arizona*

10.1136/jim-2020-MW.128

Introduction/Background Acute lung injury (ALI) secondary to sepsis is associated with significant morbidity and mortality. Patients with ALI exhibit disruption of the lung endothelial barrier that results in pulmonary edema and organ failure. There is no effective treatment for sepsis-induced ALI. Increasing our understanding the cellular and molecular mechanisms involved in pulmonary vascular endothelial barrier dysfunction may provide novel targets to develop new and effective therapies for ALI. Phosphodiesterases (PDEs) play a pivotal role in regulating cell signaling under both physiologic pathological circumstance through controlling cAMP and cGMP level. LPS (lipopolysaccharide), the major structural component of the Gram-negative bacterial outer membrane, is a major stimulus of ALI through disruption Endothelial Cells (ECs) barrier integrity. PDE3A specifically hydrolyze cAMP which protection EC barrier function, but the mechanism under PDE3A activation regulation is remain unknown.

Objective(s) In this study, we identified PDE3A features, one member of PDEs family, in LPS-induced Human Pulmonary Artery Endothelial Cells (HPAECs) barrier dysfunction.

Methods Protein expression levels were evaluated in cultured cells by western blotting, and band density quantified using Image-studio. PDE3A isoforms Open Reading Frame (ORF) were cloned from Human mRNA and fused with Flag-tag in pcDNA3 vector. Endotoxin-free plasmids were transient express in HEK293 cells using polyamine-mediated transfection. PDE3A phosphorylation at Ser654 antibody was custermerize generated at GenScript. Co-Immunoprecipitation (CoIP) was conducted to determine protein interaction. cAMP level were determined by using Cyclic AMP Assay Kit (Cell signaling, USA).

Results Three isoforms of PDE3A were identified (PDE3A1, PDE3A2 and PDE3A3) in human cells. Both of PDE3A2 and PDE3A3 express in HPAECs and were generated from one transcriptional mRNA with alternative translation start site. Transient co-expression with PKG plasmid in HEK293 cells, isoform 2 and 3 exhibited PKG-dependent phosphorylation at Ser654 site that has predictable role in regulation PDE3A activation. HPAECs barrier function dramatically break when exposure to LPS for 6 hrs, our data shown phosphorylation pS654 level were decreased by 19% with LPS-treatment (2 EU/ml) for 6 hrs (vs vehicle 6 hrs) in HPAECs, suggesting blocking phorsphory-PDE3A at S654 enhances it hydrolysis activity leads to decrease cAMP level, resulting in ECs barrier integrity disruption. Furthermore, we observed PDE3A directly interaction with Heat Shock Protein 90 (HSP90), HSP90 inhibition by 17-AAG (2 μM, 4 hrs) significantly reduces PDE3A binding affinity to 55% (vs vehicle), while cAMP level increased (~2 fold, vs vehicle), indicating

chaperon with HSP90 maintain PDE3A cAMP hydrolysis activation.

Conclusions Our results suggest PDE3A associates LPS-induced ECs barrier dysfunction through modulating PDE3A phosphorylation at Ser654 site. Regulation PDE3A phosphorylation may serve as a therapeutic strategy against ALI.

A05 ABO, A SMALL MOLECULE INHIBITOR OF INTEGRIN BETA4, ATTENUATES ACUTE LUNG INJURY IN MURINE MODELS

[1]Weiguo Chen, [2]Yulia Epshtein, [3]Jeffrey R Jacobson. *[1]University of Illinois at Chicago, Chicago, IL; [2]UIC, Chicago, IL; [3]University of Illinois at Chicago*

10.1136/jim-2020-MW.129

Introduction/Background We previously reported lung endothelial cell (EC) inflammation attenuated by simvastatin, an HMG CoA-reductase inhibitor, is mediated by decreased integrin β4 (ITGB4) phosphorylation. As statin drugs are recognized to have pleiotropic properties and to date have not proven to have significant clinical efficacy in lung vascular inflammatory syndromes including acute lung injury (ALI), strategies aimed precisely at inhibiting ITGB4 phosphorylation may prove to be more effective in this context. Preliminary data from our lab previously confirmed an attenuation of agonist-induced ITGB4 phosphorylation and EC cytokine expression after treatment with ABO (6-amino-2,3-dihydro-3-hydroxymethyl-1,4-benzoxazine), a small molecule inhibitor of ITGB4 phosphorylation (Y1494) via inhibition of annexin 7. Moreover, EC-specific ITGB4 knockout mice were found to have an attenuation of LPS-induced murine ALI.

Objective(s) We hypothesized that ABO represents a novel therapeutic molecule for ALI.

Methods To test our hypothesis, C57Bl/6 mice were pretreated with ABO (200 mg/kg, IP) or vehicle 1 h prior to LPS (1.25 mg/kg, IT). BAL was performed 24 h later and animals were sacrificed with lungs harvested for histologic evaluation. Measurements of BAL fluid protein, total cell counts, and cytokine levels were assessed. In addition, ITGB4 was immunoprecipitated (IP) from whole lung homogenates and subjected to Western blotting for p-Tyr. In separate experiments, ABO was administered to mice in a live MRSA ALI model followed by similar BAL fluid analyses.

Results These experiments confirmed a significant attenuation of LPS-induced lung injury associated with ABO treatment as measured by BAL fluid total protein, cell counts and cytokine levels (IL-6, TNFα, and IL-1β). Our results were further corroborated by changes evident on lung histology. Moreover, IP of ITGB4 from whole lung homogenates confirmed an attenuation of LPS-induced ITGB4 phosphorylation in animals treated with ABO. Additionally, ABO was also found to significantly attenuate MRSA-induced increases in BAL fluid protein levels, total cell counts, and cytokine levels.

Conclusions Our data suggest ABO may be highly effective in attenuating vascular inflammation via inhibition of ITGB4 phosphorylation and we have confirmed a protective effect of ABO administered in vivo in two distinct murine ALI models. These findings implicate ABO as a potentially novel and effective therapeutic molecule that warrants further investigation for the treatment of patients with or at risk for ALI.

A06 AUTOPHAGY REGULATES MUC5AC DEGRADATION DURING RESOLUTION OF MUCOUS CELL METAPLASIA IN AIRWAY DISEASE

[1]Kaitlin Hunt, [1]Katrina Kudrna, [2]Steven Brody, [3]John D Dickinson. *[1]University of Nebraska Medical Center; [2]Washington University School of Medicine; [3]University of Nebraska Medical Center, States/Provinces*

10.1136/jim-2020-MW.130

Introduction/Background Exacerbations of muco-obstructive airway diseases such as COPD and asthma are associated with epithelial changes and mucus plugging of airways. Mucous cell metaplasia (increased mucous cell number) and hyperplasia (increased size of mucous cells) are associated with a surge of MUC5AC production with cytoplasm packed with granules awaiting apical secretion. Molecular pathways leading to these alterations have been identified; however, the factors that regulate resolution are not understood. Following diminished immune response of Th2 inflammatory cytokines such as IL-13 and IL-33, the fate of the intracellular mucin granules of goblet cells is unknown. We considered that during resolution mucin granules may continue to be secreted or alternatively, degraded.

Objective(s) We previously demonstrated that a major protein degradation pathway, autophagy, is activated in airway epithelial cells in response to inflammatory Th2 cytokines causing mucous cell metaplasia. We hypothesized that the autophagosome-lysosome pathways are required for resolution of mucous cell metaplasia by degrading cytoplasmic MUC5AC.

Methods C57BL6/j mice globally deficient in autophagy regulatory protein, Atg16L1 hypomorph (HM) or wild type C57BL6/j (WT) were challenged with intra-nasal IL-33 over 5 days or saline. In a parallel experiment, mice were sensitized by intra-peritoneal injection (x3 over 5 days) and given nebulized challenge of OVA-albumen (x5 over 5 days). A subgroup of OVA challenged mice received neblized ATP (100 mM) for 30 minutes prior to euthanasia to assess for the response to a mucin secretory stimulant. Total lung mucin was assessed by immunoblotting for MUC5AC and MUC5B from mouse lung homogenates while intracellular mucin was assessed by immunostaining. Calu-3 airway epithelial cell line was utilized in vitro for ease of transfection and the capacity to produce distinct MUC5AC granules along the apical border while under air liquid interface (ALI) culture conditions.

Results In airway models of Th2 airway inflammation, the lysosomal markers, LAMP1 and LAMP2, were uniquely concentrated in the cytoplasm surrounding MUC5AC granules and not in ciliated cells, nor MUC5B positive cells from non-inflamed mice. Transmission electron microscopy revealed electron dense 0.5 micron granules consistent with lysosomes adjacent to mucin granules. Therefore, we assessed the effect of blocking the autophagy-lysosome degradation pathway. We found increased intracellular levels of MUC5AC, and to a lesser extent MUC5B by immunostaining and immunoblotting in Atg16L1^{HM} mice compared to WT after IL-33 or OVA challenge (**figure 1 A-E**). Upon airway nebulization of mucin secretory stimulant, ATP, however, we found, an equal decrease in intracellular mucin levels between the Atg16L1^{HM} and WT mice, indicating that the secretory function remains

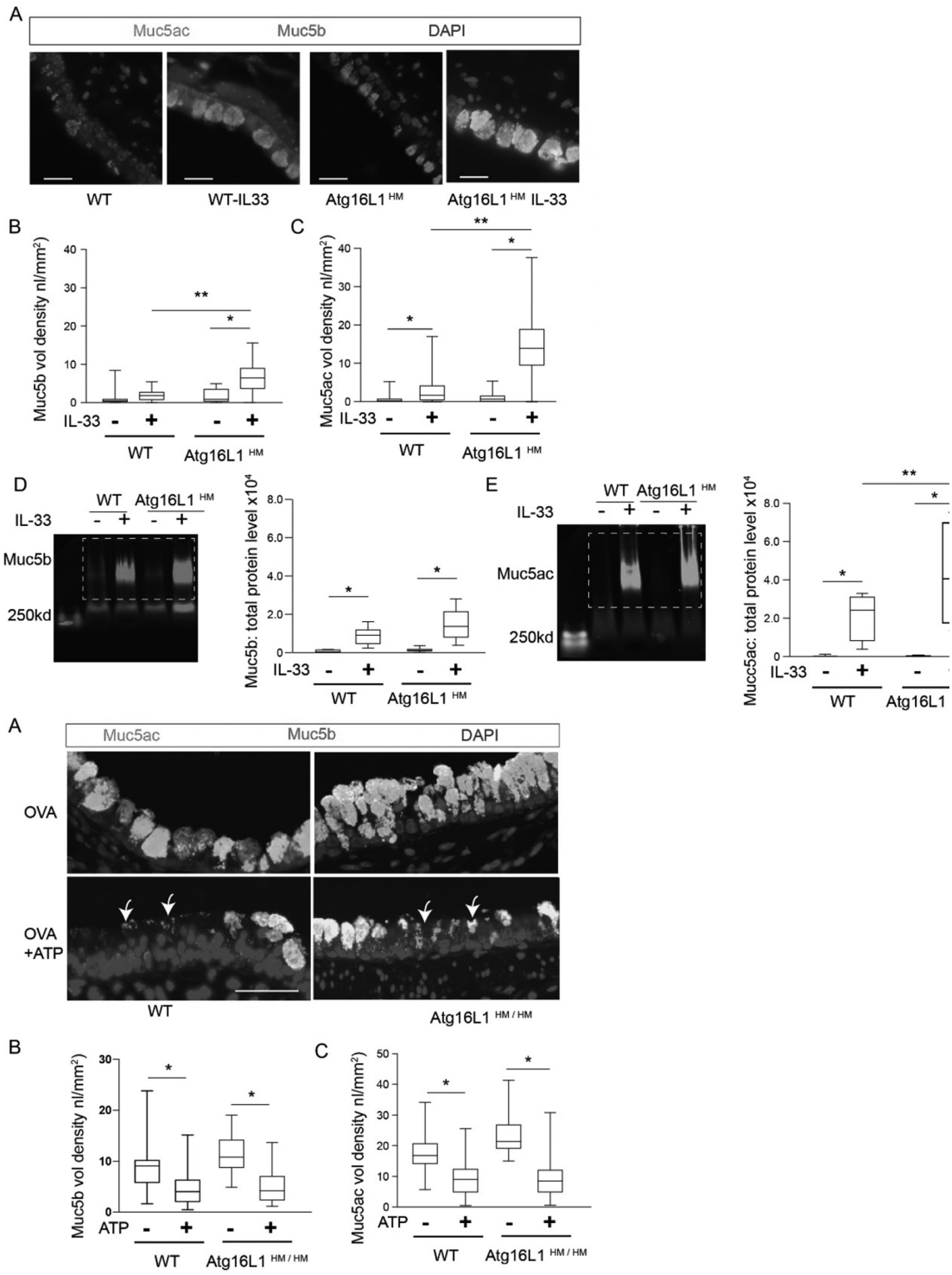

Abstract A06 Figure 1 **A)** Representative immunostaining images Muc5ac and Muc5b from WT and Atg16L1 ^{HM} mice ± IL-33. Scale bar is 20 microns. **B,C)** Quantication of staining area for Muc5ac and Muc5b. * denotes significant difference with IL-33, ** denotes significant difference with Atg16L1 vs WT. **D,E)** Representive immunoblotting with corresponding quantification with normalization to total protein for Muc5b and Muc5ac respectively. * denotes significant difference with IL-33, ** denotes significant difference with Atg16L1 ^{HM} vs WT. **F)** Representive images of Muc5AC and Muc5b immunostaining in OVA challenged WT and Atg16L1 ^{HM} mice ± nebulized ATP with corresponding quantnification of remaining intracellular mucin **(G, H)**. Scale bar is 50 microns. Arrows show mucous cells that have emptyed in response to ATP. * denotes significant difference in intracllular mucins between ATP and no ATP.

intact in autophagy-deficient mice (**figure 1F-H**). We then considered that the increased levels of mucins in the autophagy deficient mice were due to reduced mucin degradation. Mice that were challenged with airway IL-33 and allowed to recover for 10 days demonstrated persistent elevation of intracellular MUC5B and MUC5AC in Atg16L1^{HM} mice compared to WT mice. Indeed, the magnitude of the difference in mucin levels was greater relative to that measured during peak inflammation. Furthermore, lysosomal enrichment from whole lung homogenates showed persistent elevation of autophagy marker, LC3B II, during the resolution phase of mucous cell metaplasia. To determine if autophagy induction could drive intracellular mucins to a lysosomal degradation pathway, we treated Calu-3 cells with mTOR inhibitor, Torin1, and leupeptin to inhibit lysosomal enzyme activity. Torin1 treatment led to reduced cytoplasmic levels of MUC5AC with rescue when treated with leupeptin. In a parallel genetic approach, depletion of key autophagy protein, LC3B, led to a similar mitigation of torin1-induced MUC5AC degradation.

B07 ADMISSION NASAL EPITHELIAL GENE EXPRESSION PREDICTS DURATION OF ILLNESS IN CHILDREN WITH CRITICAL BRONCHIOLITIS

[1]Bria Coates, [2]Grant Hahn, [3]Sam Schmakel, [3]Kishore Anekalla, [3]Clarissa Koch, [3]Karen Ridge. *[1]Northwestern University, Chicago, IL; [2]Ann and Robert H. Lurie Children's Hospital of Chicago; [3]Northwestern University*

10.1136/jim-2020-MW.131

Introduction/Background Respiratory syncytial virus (RSV) is a ubiquitous single-stranded RNA virus that causes respiratory tract infections in both children and adults. The majority of RSV infections are mild, with symptoms confined to the upper respiratory tract. However, 2% of children infected with RSV prior to 1 year of age will require hospitalization. In a subset of hospitalized patients, RSV will cause severe, life-threatening lower respiratory tract disease. Despite the wide range in the clinical manifestations of RSV infection, the mechanisms associated with severe RSV lower respiratory infection (LRTI) are poorly understood.
Objective(s) To assess the feasibility of collecting nasal epithelial cells from children admitted to the Pediatric Intensive Care Unit with severe RSV LRTI and to use these cells to advance our understanding of the host response in critical bronchiolitis through evaluation of the nasal transcriptome.
Methods After obtaining informed consent, nasal scrapings from critically ill children less than 2 years of age with RSV LRTI were collected at Ann and Robert H. Lurie Children's Hospital of Chicago for gene expression analysis within 24 hours of admission. Negative controls were collected at well-child visits in a local outpatient clinic. Total RNA was isolated and following mRNA-enrichment, samples were sequenced using Illumina NextSeq 500.
Results High quality RNA could be extracted from nasal scrapings from children with severe RSV LRTI. Differential gene expression analysis and pairwise comparison between RSV-infected children and healthy controls revealed a significant number of differentially expressed genes that were enriched for pathways involved in inflammation and defense. Day of admission samples showed a unique inflammatory signature in subjects who would require greater than or equal to 5 days of supplemental oxygen compared to subjects who would require less than 5 days of supplemental oxygen. In addition, this early inflammatory signature was associated with intensive care unit and hospital length of stay.
Conclusions Collecting of nasal epithelial cells that yield high-quality RNA is safe and feasible in children with severe RSV LRTI. Early nasal epithelial gene expression predicts severity of illness and is associated with length of supplemental oxygen requirement, length of intensive care unit stay, and length of hospital stay. Further investigation may identify key differentially expressed genes that could serve as early biomarkers of severity of illness and subsequent intensive care unit needs in children with RSV LRTI.

B08 RECRUITMENT OF BONE MARROW DERIVED MONOCYTES INTO INFLAMED LUNGS IN HYPOXIC PULMONARY HYPERTENSION

[1]Rahul Kumar, [2]Claudia Mickael, [3]Biruk Kassa, [2]Linda Sanders, [2]Rubin Tuder, [4]Brian Graham. *[1]Zuckerberg San Francisco General Hospital, University of California San Francisco, USA, San Francisco, CA; [2]University of Colorado, Anschutz Medical Campus, USA; [3]Bachelor; [4]Zuckerberg San Francisco General Hospital, University of California San Francisco, USA*

10.1136/jim-2020-MW.132

Introduction/Background Hypoxia-induced pulmonary hypertension (PH) is a major cause of mortality and morbidity worldwide. TGF-β signaling is required for chronic hypoxic PH. Thrombospondin (TSP)-1 produced from bone marrow (BM) derived interstitial macrophages (IMs) activates TGF-β. However, the understanding the precursor of inflammatory IMs and mechanisms that drive these cells to egress from the BM compartment and be recruited into the lungs to cause hypoxic PH is largely unknown. Here, we hypothesized that under hypoxic conditions, the signals from lung-derived cytokines CCL2 and/or CCL7 causes Ly6chiCX3CR1low monocytes to be produced in the BM, leave the BM compartment, circulate and be recruited into the lungs, where they become pathologic TSP-1+ IMs.
Objective(s) 1: To determine that intravascular circulatory Ly6chiCX3CR1low monocytes are the precursors of TSP-1+ IMs in hypoxic PH. 2: To determine that lung-derived CCL2 cytokines signaling is required for the production and recruitment of TSP-1+IM precursor monocytes.
Methods Murine model of hypoxia-induced PH (10% F_iO_2 hypoxia exposure for 3 weeks) were used. Right heart catheterization and RV hypertrophy (Fulton Index) were measured to confirm PH phenotype. Flow cytometry (using single cell dispersion from whole lung) and qPCR was performed to quantify TSP-1$^+$IM precursors in the BM compartment. CCR2 ligands CCL2, CCL7 and CCL12 were quantified in the intravascular plasma and in whole lung lysates using ELISA. scRNAseq was performed on sorted IMs, using 500–1000 cells sequenced at 50k read pairs/cell (Illumina 10X Genomics Platform; analysis using Loupe Cell Browser v3.1.1). *CCR2*$^{-/-}$ BM cells were transplanted into lethally irradiated wildtype mice to determine the functional role of BM-derived Ly6c+ monocytes in hypoxic PH.
Results Flow cytometry and qPCR results showed higher expression of *Ccr2* in the BM compartment, while ELISA revealed higher levels of the CCR2 ligands, CCL2 and CCL7 in the intravascular compartment and in the lungs of the hypoxia-exposed wildtype mice. Flow cytometry revealed

higher expression of Ly6c in TSP-1^{+}IMs. scRNAseq further confirmed increased mRNA expression of *Ccr2*, *Ly6c* and *Thbs1* in IM subpopulations in hypoxia-exposed mice. Further, blocking the recruitment of Ly6c^{hi}CX$_3$CR1^{low} monocytes by transplanting *Ccr2*$^{-/-}$ BM cells into lethally irradiated wildtype mice attenuated hypoxic PH by lowering RVSP and Fulton Index.

Conclusions Bone marrow derived inflammatory Ly6c^{+} monocytes and their conversion to TSP-1^{+}interstitial macrophages may result into hypoxic PH.

B09 MRSA-INDUCED ENDOTHELIAL INJURY AND LUNG INJURY ARE REVERSED BY FTY720 S-PHOSPHONATE

[1]Lichun Wang, [2]Huashan Wang, [3]Steven Dudek. *[1]Univ of Illinois at Chicago, chicago, IL; [2]Univ of Illinois at Chicago; [3]Division of Pulmonary, Critical Care, Sleep, and Allergy, University of Illinois at Chicago, States/Provinces*

10.1136/jim-2020-MW.133

Introduction/Background Effective therapies are needed to preserve the lung vascular barrier that is disrupted during the Acute Respiratory Distress Syndrome (ARDS). Prior work has suggested that FTY720 S-phosphonate (Tys), an analog of the endogenous phospholipid sphingosine 1-phosphate (S1P) and the pharmaceutical compound FTY720, has potential to protect against endothelial barrier disruption in vitro and in vivo. An important mechanism by which Tys decreases permeability is by preserving expression of the barrier promoting S1P receptor 1 (S1PR1).

Objective(s) In this study we characterized the potential of Tys to protect against lung vascular injury induced by the ARDS stimulus methicillin-resistant Staph aureus bacteria (MRSA).

Methods Human pulmonary artery or microvascular endothelial cells (EC) were used for in vitro experiments. Immunoprecipitation, CHIP, ELISA, immunofluorescence microscopy and western blotting were performed per standard protocols. Heat-killed MRSA (HK-MRSA) was used in vitro, and intratracheal (IT) live MRSA was used in mice to induce lung injury in vivo.

Results HK-MRSA caused Rho activation, MLC phosphorylation, stress fiber formation, peripheral VE-cadherin loss, NF-κB phosphorylation, IL-6 and IL-8 release, and increased permeability in cultured human lung EC. All of these effects were inhibited by Tys (1 μM). HK-MRSA also induced epigenetic changes in lung EC, including methylation of histone H3 lysine 4. By chromatin immunoprecipitation (CHIP) analysis, HK-MRSA significantly enriched H3K9Ac in the NFAT binding region of the S1PR1 promoter. These epigenetic effects were inhibited by Tys treatment. In vivo, IT MRSA in mice causes a significant increase in BAL protein and total cell count levels compared to PBS (18 hours). Pretreatment or post-treatment with Tys significantly reduced BAL protein levels and BAL total cell count after MRSA compared to the vehicle control group. Compared to other potent S1PR1 agonists, RP001 or CYM5442, Tys exhibited prolonged barrier promotion in vitro and did not induce ubiquitination and degradation of S1PR1.

Conclusions Tys reverses many of the injurious effects of MRSA on lung EC in vitro and mice in vivo. These results suggest that S1PR1 agonists such as Tys may have potential utility in ARDS.

B10 UBIQUITIN E3 LIGASE NEDD4L SUPPRESSION PROMOTES LUNG FIBROBLAST DIFFERENTIATION AND EXTRACELLULAR MATRIX ACCUMULATION

[1]Qinmao Ye, [2]Shuang Li, [3]Yanhui Li, [4]Xinxin Liao, [5]Yingze Zhang, [2]Jiangning Tan, [6]Daniel J Kass, [3]Jing Zhao, [3]Yutong Zhao. *[1]Department of Physiology and Cell Biology, The Ohio State University College of Medicine; [2]Department of Medicine, The University of Pittsburgh; [3]The Ohio State University College of Medicine; [4]The Ohio State University College of Medicine, OH; [5]Department of Medicine and Human Genetics, The University of Pittsburgh; [6]The University of Pittsburgh*

10.1136/jim-2020-MW.134

Introduction/Background Background: Lung fibroblast differentiation and extracellular matrix (ECM) accumulation are hallmarks for Idiopathic Pulmonary Fibrosis (IPF). Ubiquitin E3 ligase Nedd4L negatively regulates TGF-β1 and LPA signaling by targeting TGF-β1 receptor I (TβRI), phospho-Smad2/3, and LPAR1 for ubiquitination and degradation, however, the role of Nedd4L in the pathogenesis of IPF has not been studied.

Objective(s) Objective: To investigate if Nedd4l expression decreases, lung fibroblast differentiation and extracellular matrix accumulation are promoted.

Methods Nedd4L mRNA and protein levels were analyzed by realtime PCR and immunoblotting in human primary lung fibroblasts from normal control and IPF patients, bleomycin-challenged lung tissues, and TGF-β1-treated human lung fibroblasts. Pulmonary fibrosis was induced by intratracheal injection of bleomycin.

Results By analysis of publically available microarray data, we found that Nedd4L mRNA levels were significantly lower in IPF cohorts, compared to normal healthy control subjects. Nedd4L protein levels in fibroblasts from IPF patients were decreased compared to normal control subjects. Reduction of Nedd4L levels directly correlates with FVC% predicated and DLCO% predicated. Nedd4L protein and mRNA expression were reduced in bleomycin (2 U/kg)-induced experimental pulmonary fibrosis. TGF-β1 treatment of HLF decreased Nedd4L protein and mRNA levels in a time-dependent manner, indicating that Nedd4L is reduced in fibrotic fibroblasts. Further, we investigated the role of Nedd4L in fibrotic responses. Overexpression of Nedd4L attenuated TGFβ-1-induced collagen I, FN, SMA levels. To elucidate the anti-fibrotic effect of Nedd4L in lung fibrosis, we delivered the Nedd4L-V5 gene to mouse lungs using an intratracheal (IT) lentiviral vector delivery system for 7 days prior to an intranasal bleomycin challenge. Lenti-Nedd4L-V5 attenuated bleomycin (2 U/kg, 3 wk)-increased FN, collagen levels, and lung fibrosis with extension into the adjacent alveolar parenchyma in mouse lungs.

Conclusions These data indicate that suppression of Nedd4L expression promoting TGF-β1 signaling and extracellular matrix accumulation. This study reveals that Nedd4L is a potential target for treating IPF.

A60 NON-MUSCLE MYOSIN LIGHT CHAIN KINASE ACTIVITY MEDIATES CELLULAR PROLIEFRATION AND MIGRATION IN BMPR2 DEFICIENT IN VIVO AND IN VITRO MODELS

[1]Mariam Anis, [2]Glen Marsboom, [2]Rachel Halstrom, [2]Noman Baig, [2]Jeffrey R Jacobson, [3]Dustin R Fraidenburg. *[1]University of Illinois at Chicago, Chicago, IL; [2]University of Illinois at Chicago; [3]UIC, Chicago, IL*

10.1136/jim-2020-MW.135

Introduction/Background Rationale: Pulmonary arterial hypertension (PAH) is characterized by a hyperproliferative and

apoptosis resistant phenotype in multiple vascular cell types. Non-muscle myosin light chain kinase (nmMLCK) is an essential component of the cellular cytoskeleton and we have previously reported that increased nmMLCK activity drives hyperproliferation, migration, and anti-apoptosis in human pulmonary artery endothelial cells (PAEC) induced by hypoxia and VEGF. Bone morphogenetic protein receptor II (BMPR2) plays an important role in the pathogenesis of PAH as the most common genetic mutation PAH. Our current study focuses on understanding nmMLCK activity in BMPR2 deficient PAEC and $BMPR2^{+/R899X}$ animal model.

Objective(s) We hypothesize that BMPR2 deficiency results in an increase in nmMLCK activity with downstream upregulation of ERK/MAPK pathways in both PAEC and the mouse model.

Methods PAEC were transfected with BMPR2 siRNA compared to scrambled siRNA using Lipofectamine (Thermo). Cell migration was assessed using both a scratch assay and electric cell-substrate impedance sensing (ECIS) wound healing assay. PAEC transfected with BMPR2 siRNA were also assessed for expression of proinflammatory cytokines including IL6 and IL8 using ELISA (Sigma Aldrich). Lung homogenates were utilized from mice bearing a heterozygous knock-in allele of a human BMPR2 mutation, R899X. Western blotting was used to determine protein quantification. Statistical analysis used t-test and ANOVA for comparisons between two groups and multiple groups, respectively.

Results PAEC transfected with BMPR2 siRNA showed increased proliferation both by WST assay and PCNA protein expression when compared to scrambled siRNA control ($p<0.05$). Increased migration was observed in BMPR2 silenced cells in both cell scratch ($p<0.05$) and ECIS wound healing assays ($p<0.001$). Treatment of BMPR2 silenced cells with the MLCK inhibitor, ML-7, resulted in decreased proliferation ($p<0.05$) and migration ($p<0.001$). BMPR2 transfected PAEC showed increased expression of IL-6 and IL-8 which was attenuated by ML-7 treatment ($p=0.034$). $BMPR2^{+/R899X}$ mice have higher right ventricular systolic pressures (RVSP) than controls and develop spontaneous pulmonary hypertension. Lung homogenates from $BMPR2^{+/R899X}$ mice demonstrate increased MLCK activity based on upregulation of myosin light chain phosphorylation as well as ERK phosphorylation compared to control.

Conclusions BMPR2 silenced PAEC are show increased proliferation and migration which is prevented by inhibition of MLCK. Similarly, BMPR2 transgenic mice which show decreased BMPR2 expression and develop spontaneous pulmonary hypertension have increased MLCK activity. These studies implicate nmMLCK as a novel potential contributor to the development and progression of PAH in both cellular and animal models.

A61 INHIBITION OF $GVPLA_2$ ATTENUATES MRSA-INDUCED INJURY OF LUNG ENDOTHELIUM

[1]Yu Maw Htwe, [2]Lucille Meliton, [3]Mounica Bandela, [4]Steven Dudek. *[1]Division of Pulmonary, Critical Care, Sleep, and Allergy, University of Illinois at Chicago, IL; [2]Division of Pulmonary, Critical Care, Sleep, and Allergy, University of Illinois at Chicago; [3]Division of Pulmonary, Critical Care, Sleep, and Allergy, University of Illinois at Chicago, Chicago, IL; [4]Division of Pulmonary, Critical Care, Sleep, and Allergy, University of Illinois at Chicago, States/Provinces*

10.1136/jim-2020-MW.136

Introduction/Background Methicillin-resistant Staph aureus (MRSA) is a common cause of the Acute Respiratory Distress Syndrome (ARDS). During ARDS, lung endothelial cell (EC) dysfunction and permeability increase, leading to life-threatening pulmonary edema. Prior work has suggested an important role for the enzyme group V phospholipase A_2 ($gVPLA_2$) in regulating EC permeability during inflammatory injury.

Objective(s) To advance our understanding of the role of $gVPLA_2$ during MRSA-induced injury to human lung EC.

Methods Human pulmonary artery EC (HPAEC) were used for these experiments. Permeability was assessed using the Electric Cell-substrate Impedance Sensing system (ECIS) to measure transendothelial resistance (TER). Heat-killed MRSA (HK-MRSA) was used to induce EC injury. Inhibition of $gVPLA_2$ was achieved with LY 311727 (global sPLA2 inhibitor) or MCL3G1 (monoclonal antibody directed against $gVPLA_2$). Immunofluorescence studies were performed to visualize stress fiber and gap formation. Supernatants from treated EC were collected and IL-8 levels determined by ELISA MAX Deluxe set (Biolegend, San Diego, CA). Gain of function experiments were performed using either transfection with the pCMV6-PLA2G5 expression plasmid (Origene), or by addition of recombinant human $gVPLA_2$ protein.

Results HK-MRSA causes a prolonged, statistically-significant, and dose-dependent increase in HPAEC permeability starting at 5–6 hours, which is attenuated in a dose dependent fashion by pretreatment with LY 311727 (50–100 μM) or MCL3G1 (25 μg/ml). Immunofluorescent studies demonstrate that HK-MRSA causes actin stress fiber and intercellular gap formation. Recombinant human $gVPLA_2$ protein enhanced HK-MRSA induced EC permeability. HK-MRSA increases IL-8 levels, which is enhanced by pCMV6-PLA2G5 transfection and decreased by LY 311727 and MCL3G1.

Conclusions HK-MRSA increases HPAEC permeability, IL-8 secretion, gap formation and stress fiber formation. These affects are attenuated by inhibition of $gVPLA_2$. Our findings suggest an important role for $gVPLA_2$ in mediating MRSA-induced endothelial injury and highlight it as a potential therapeutic target for ARDS.

A63 CATCHING NEUTROPHIL EXTRACELLULAR TRAPS (NETS) IN CF AIRWAYS

[1]Kristin M Hudock, [2]Margaret Collins, [2]Michelle Imbrogno, [3]Rory O'shaughnessy, [4]John Brewington. *[1]University of Cincinnati and Cincinnati Children's Hospital Medical Center, Cincinnati, OH; [2]University of Cincinnati; [3]CCHMC; [4]CCHMC and University of Cincinnati*

10.1136/jim-2020-MW.137

Introduction/Background This is a pivotal time in cystic fibrosis (CF), with the recent development of highly effective modulators to correct mutant CFTR function. Modulators do not control the excessive airway inflammation, that is driven by neutrophils, and leads to loss of lung function in CF. An immune component particularly relevant to CF is the generation of neutrophil extracellular traps (NETs) comprised of DNA, histones and immunomodulatory proteins, including myeloperoxidase (MPO), neutrophil elastase (NE) and IL-8. Individual components of NETs are increased in CF sputum and correlate with severity of CF lung disease, but the burden of NETs in CF airways remains unclear.

Objective(s) The objective of this study was to determine if NETs are present in significant quantities in CF and disease control lungs and if they correlate with lung function.
Methods NET complexes were measured in the supernatant of bronchoalveolar lavage (BAL) banked by the CCHMC Pulmonary Biorepository from nine children with CF and six disease controls (DCs) during clinical stability. DCs were race, gender and age-matched children with indwelling tracheostomies for upper airway disease. ELISAs were used to measure individual NET components: MPO, NE, IL-8 and citrullinated histones (CitH3) and sandwich ELISAs to quantify NET complexes: DNA-MPO, DNA-NE and DNA-IL-8. We utilized isolated NETs generated from three human subjects as positive controls.
Results CF children had significantly higher concentrations of free NE (0.78±0.25 vs 0.05±0.03ng/ml, p=0.044) and increased free MPO (2.84±0.37 vs 2.09±0.13ug/ml, p=0.06) protein than DCs in their BAL. Lower levels of NET-complexes DNA-MPO (1.10±0.32 vs 2.78±0.67AU, p=0.022), DNA-NE (0.47±0.09 vs 0.97±0.12AU, p=0.004) and DNA-IL-8 (0.26±0.06 vs 0.60±0.14 AU, p=0.035) were found in CF subjects compared to DCs. Higher protein concentrations of CitH3 were found in CF BAL compared to DC BAL (297.6±56.25 vs 97.2±32.94pg/ml, p=0.028). Elevated CitH3 concentrations tended to correlate (r=0.66, p=0.054) with higher percent forced expiratory volume in one second (FEV_1) in CF patients.
Conclusions NET complexes were observed in both pediatric CF and disease control lung lavage, with differences observed in free and NET-bound inflammatory mediators between the groups. Preliminary findings suggest elevated citrullinated histones correlate with better lung function, results which need to be confirmed in a larger group of CF patients. NETs may be a novel therapeutic target in CF that could be manipulated to control lung inflammation and prevent loss of lung function.

A64 BACTERIAL TOXINS STIMULATE LUNG EPITHELIAL CELLS TO RELEASE MITOCHONDRIA WITHIN EXTRACELLULAR VESICLES

[1]Eleftheria Letsiou, [2]Gustavo Teixeira Alves, [2]Martin Witzenrath, [3]Steven Dudek. *[1]Division of Pulmonary, Critical Care, Sleep, and Allergy, University of Illinois at Chicago, IL; [2]Division of Pulmonary Inflammation, Charité-Universitaetsmedizin Berlin, Germany; [3]Division of Pulmonary, Critical Care, Sleep, and Allergy, University of Illinois at Chicago, States/Provinces*

10.1136/jim-2020-MW.138

Introduction/Background Bacterial pneumonia is a major cause of acute lung injury. Lung epithelial cells are in the first line of defense against bacteria and their inflammatory products. Previous studies have demonstrated that pore-forming toxins (PFTs), such as the pneumococcal pneumolysin (PLY) and staphylococcal α-hemolysin (α-Toxin; α-T), cause mitochondrial dysfunction in the lung epithelium.
Objective(s) To explore the novel hypothesis that lung epithelial cells in response to PFTs release mitochondria within extracellular vesicles (EV).
Methods Experiments were performed in vitro using the lung epithelial cell lines A549 and MLE-12 (human and mouse alveolar epithelial type II cells, respectively) and Beas-2B (human bronchial epithelial cells). Cells were treated with PLY (100 ng/ml, 4 hours), α-T (0.5 μg/ml, 24 hours) or live streptococcus pneumoniae (S.pn.; MOI 50, 4 hours). Microvesicles (MVs), an EV subtype, were isolated from conditioned media through differential centrifugation. MVs were analyzed by nanoparticle tracking analysis (NTA), flow cytometry (FACS) after staining with annexin V (MV marker), and immunoblotting (IB). In separate experiments, cells were incubated with mitochondrial probes (MitoTracker DeepRed; MitoR), challenged with PLY, and the isolated MVs were analyzed by FACS.
Results In response to PFTs (PLY and α-T), A549, MLE-12, and Beas-2B release increased amounts of MVs (<1 μm in size) compared to untreated cells. IB analysis showed an increased expression of the mitochondrial protein, Tom20, in MV lysates derived from PFT-treated cells compared to controls. Stimulation of cells with live S.pn also results in significant production of MVs that express Tom20. To assess whether the MVs carry intact mitochondria, A549 were labeled with MitoTracker DeepRed, and then treated with PFTs. PFT-treated A549 release MVs that are double positive for annexin V and MitoR+.
Conclusions Our results demonstrate that bacterial pore-forming toxins stimulate the lung epithelium to release mitochondria embedded in microvesicles (mito-MVs). Future studies will elucidate the role of the mito-MVs in ALI.

A65 PROTEASOME INHIBITORS REDUCE C-MET IN NON-SMALL CELL LUNG CANCER CELLS

Yanhui Li, Su Dong, Arya Tamaskar, Heather Wang, Jing Zhao, Yutong Zhao. *The Ohio State University College Of Medicine*

10.1136/jim-2020-MW.139

Introduction/Background Non-small-cell lung cancer (NSCLC) is the most common type of lung cancer and accounts for 85% of all lung carcinomas. The hepatocyte growth factor receptor (c-Met) has been considered a potential therapeutic target for NSCLC. Proteasome inhibition induces cell apoptosis and has been used as a novel therapeutic approach for treating diseases including NSCLC; however, the effects of different proteasome inhibitors on NSCLC have not been fully investigated. The aim of this study is to determine a precise strategy for treating NSCLC by targeting c-Met using different proteasome inhibitors.
Objective(s) To investigate effects of proteasome inhibitors on non-small cell lung cancer cells.
Methods Three proteasome inhibitors, Bortezomib, MG132, and ONX 0914, were used in this study. We analyzed their effects on different NSCLC cell lines including A549, H441, H460, and H1299. c-Met protein and mRNA levels were analyzed by immunoblotting and Realtime PCR. Cell viability was examined to determine the effects of proteasome inhibitors on cell death.
Results Bortezomib (50 nM) significantly reduced c-Met levels and cell viability in A549, H1299, and H441 cells, while similar effects were observed in H460 cells when a higher concentration (~100 nM) was used. Bortezomib had no effect on c-Met gene expression in all four cell types. MG-132 at a low concentration (0.5 uM) diminished c-Met levels in H441 cells, while neither a low nor high concentration (~20 uM) altered c-Met levels in A549 and H460 cells. A higher concentration of MG-132 (5 uM) was required for decreasing c-Met levels

in H1299 cells. Furthermore, MG-132 induced cell death in all four cell types, while H441 cells were more susceptible to MG-132. MG-132 had no effects on c-Met mRNA levels. ONX 0914 reduced c-Met levels in H460, H1299, and H441 cells but not in A549 cells. H441 cells were more susceptible to ONX 0914. However, ONX 0914 did not alter cell viability in either H441 or A549 cells, while it induced cell death in H460 and H1299 cells.

Conclusions H1299 and H441 cells were susceptible to all three proteasome inhibitors, Bortezomib, MG132, and ONX 0914. H460 cells responded to all three inhibitors only at higher concentrations. A reduction in c-Met levels in A549 cells was only observed with Bortezomib. Not all the proteasome inhibitors reduced c-Met mRNA levels, which indicates that the reduction of c-Met is regulated by post-translational modifications and transcription, dependent on cell types. Most inhibitors mitigated cell viability in NSCLCs. This study reveals that different proteasome inhibitors produce varied inhibitory effects on NSCLS cell lines.

A66 ANTHRAX TOXINS INHIBIT HUMAN AIRWAY MACROPHAGE AND DENDRITIC CELL PHAGOCYTOSIS

Vineet I Patel, J Leland Booth, Jordan P Metcalf. *University of Oklahoma Health Sciences Center, Oklahoma City, OK*

10.1136/jim-2020-MW.140

Introduction/Background Bacillus anthracis is a worldwide concern as a Category A bioterrorism agent. B. anthracis spore exposure via the respiratory route causes inhalation anthrax; a disease with a high mortality rate. Once these spores germinate, they produce two toxins: lethal toxin (LT) and edema toxin (ET). LT is a combination of protective antigen (PA) and lethal factor (LF), and induces apoptosis of susceptible cell types. ET is a combination of PA and edema factor (EF), and functions as an adenylate cyclase. Both toxins are thought to impair immune cells during the course of anthrax pathogenesis, although their effects on lung immune cells remain unclear. We have previously described six subsets of airway and alveolar resident phagocytes (AARPs) found in the healthy human lung. We tested the susceptibility of AARPs to LT and ET, both in terms of induction of apoptosis, and inhibition of phagocytosis.

Objective(s) We tested the susceptibility of AARPs to LT and ET, both in terms of induction of apoptosis, and inhibition of phagocytosis.

Methods Human AARPs were tested for induction of apoptosis by Annexin V staining after incubation with LT and ET. Phagocytic inhibition was measured by preincubating AARPs with LT and ET, followed by their exposure to dye-labeled B. anthracis spores.

Results None of the AARP subsets were sensitive to LT-induced apoptosis at concentrations as high as 1000 ng/ml. Interestingly, apoptosis was induced to some degree in human B cells and T cells as a result of ET, rather than LT, exposure. After three hours of toxin preincubation, all six AARP subsets showed decreased spore phagocytosis by 30–50% after 30 minutes, but only with the combination of LT and ET. This effect was diminished by two hours of spore exposure. In contrast, blood immune cells showed inhibition of internalization after LT-preincubation alone, but only after two hours of spore exposure.

Conclusions Overall, our studies suggest that while human AARPs are resistant to anthrax toxin-induced apoptosis, their phagocytic abilities are transiently affected by them. The requirement for both LT and ET exposure for this effect to occur will require further investigation. This work implies that B. anthracis toxins may function together to impair AARP activity, and that inhibition of spore phagocytosis may be crucial for pathogen escape from the alveoli to cause systemic infection. Downregulation of phagocytosis by anthrax toxins may also cause impaired clearance of the pathogen if it also inhibits internalization of the vegetative form.

A67 THE DEUBIQUITINASE USP40 PROTECTS LUNG MICROVASCULAR CELLS FROM LPS-INDUCED INFLAMMATION AND BARRIER DYSFUNCTION

[1]Jiaxing Miao, [2]Jianxin Wei, [3]Rama Mallampalli, [3]Jing Zhao, [3]Yutong Zhao. *[1]The Ohio State University College of Medicine, OH; [2]The University of Pittsburgh; [3]The Ohio State University College of Medicine*

10.1136/jim-2020-MW.141

Introduction/Background Background: Lung microvascular inflammation and barrier disruption are the pathological hallmarks for acute lung injury. USP40, a newly recognized deubiquitinase, has been shown to regulate glomerular permeability in zebrafish. However, the role of USP40 in human vascular biology has not been reported.

Objective(s) Objective: To investigate if the deubiquitinase USP40 protects the lung microvascular endothelial cells from LPS-induced inflammation and barrier dysfunction.

Methods Human lung microvascular endothelial cells (HLMVECs) were used to investigate EC inflammation and barrier function. Transendothelial electrical resistance (TEER) was measured by an Electric Cell-substrate Impedance Sensing (ECIS) system to evaluate EC barrier function. ICAM1 expression were determined by immunoblotting. USP40 knockout (USP40 $^{-/-}$) mice were generated by the Crispr/Cas9 system.

Results Overexpression of USP40 attenuated LPS-induced NF-κB pathway by reducing phosphorylation of I-κB in HLMVECs. Further, we found that overexpression of USP40 significantly diminished LPS-induced ICAM1 expression, while knockdown of USP40 increased ICAM1 levels, suggesting that USP40 exhibits an anti-inflammatory property in ECs. To investigate the role of USP40 in EC barrier function, we examined the RhoA activation and MLC phosphorylation. Overexpression of USP40-V5 attenuated LPS-induced activation of RhoA and phosphorylation of MLC, as well as LPS-reduced TEER, while knockdown of USP40 by USP40 siRNA transfection increased LPS-induced EC permeability and gap formation in HLMVECs. USP40 deficient mice showed an increase in ICAM1 levels in lung tissues and BAL protein levels in intratracheal LPS (2 mg/kg, 24 h)-induced murine model of acute lung injury. LPS increased Evans blue leakage, BAL protein levels, and neutrophil influx, which were significantly decreased in lenti-USP40 delivered mice.

Conclusions Our observations are the first to reveal that USP40 reduces the severity of acute lung injury through diminishing the activation of NF-κB-mediated inflammation and RhoA-mediated EC permeability. This study provide a new target for treating acute lung injury.

A68 DEVELOPING TOOLS TO INCREASE PHYSICAL ACTIVITY AMONG MINORITY WOMEN WITH ASTHMA

[1]Caitlin Cooley, [1]Guilherme Balbim, [1]Lisa Sharp, [2]Sharmilee M Nyenhuis. [1]*University of Illinois at Chicago*; [2]*University of Illinois at Chicago, Chicago, IL*

10.1136/jim-2020-MW.142

Introduction/Background Physical inactivity among individuals with asthma is associated with poor asthma control and lung function, greater health care utilization, and poorer quality of life. A disproportionate number of African American women experience poor asthma control and asthma-related quality of life, greater healthcare utilization and high rates of physical inactivity. Given the connection between poor asthma outcomes and physical inactivity, using stakeholder input we have modified a physical activity (PA) intervention specifically for low-active African American women with asthma.

Objective(s) The objective of this current study is to further refine and assess the acceptability of modified video tools used in a PA intervention that addresses asthma-specific barriers to African American women with asthma.

Methods African American women with asthma were recruited from a minority-serving academic health system to participate in up to three qualitative focus group discussions (FGDs). Eligible women were: aged 18–70, had a physician-diagnosis of asthma and self-identified as African American. Two FGDs occurred prior to video tool modification. During FGD #1 and 2, the women were asked open ended questions about the existing video tools and how they should be modified for women with asthma. Both sessions were recorded, transcribed and coded by 2 independent coders. Emerging themes on how to modify the videos were created. Qualitative information from FGDs #1 and 2 were summarized and integrated into the video tools. After the new video tools were created, FGD #3 was conducted and a mixed methods approach was used to assess acceptability of the modified video tools. A 4-item summative evaluation was administered to assess satisfaction of the modified content, language and overall satisfaction of the new video tools. Qualitative data was also obtained from the women regarding overall satisfaction of the modified video tools through open-ended questions. This portion of FGD#3 was audiotaped, transcribed and coded by 2 independent coders for emerging themes of acceptability.

Results Nine women consented and invited to participate in the FGDs. Of the nine women, all attended the first FGD, six attended the second FGD and eight attended the third FGD. Themes from FGD #1 and 2 included: 1) modification of video structure (length, music, steps by step organization, topic layout and less distracting video environment) 2) modification of PA content to represent women of different ages and physical ability, female instructor leading stretches, proper footwear and attire for walking; 3) Addition of asthma content (talking with your doctor about asthma, asthma triggers, asthma medication use, managing asthma symptoms when walking). Based on the feedback, revisions to the video included: 1) shorter video length, less distracting environment and improved organization of topics with step order for information; 2) Revisions in the PA content included program safety (proper footwear and clothing attire, recommended medication procedure before PA and safe walking practice), female instructor leading stretching techniques and PA regimes to accommodate for age and physical ability; 3) Asthma content was revised to include communicating with your physician, asthma tips (avoidance of indoor and outdoor triggers, problem solving and breathing exercises) and benefits of PA for asthma. Overall, 100% of women found the revised video tools to be satisfied/very satisfied with the videos and had positive reactions to video structure (length, music, steps on how to increase PA) and the additional PA and asthma content.

Conclusions Stakeholder feedback in designing intervention tools leads to high participant acceptability. Additional studies that utilize these modified tools are needed to determine the efficacy of them tools to promote PA among African American women with asthma.

A69 SALUSIN-ß CONTRIBUTES TO THE DEVELOPMENT AND PROGRESSION OF PULMONARY HYPERTENSION

Haiyang Tang[1], Hui Wang[2], Xiaomin Wu[3], Stephen M Black[4], ying Han[5]. [1]*The First Affiliated Hospital of Guangzhou Medical University, TUCSON, AZ*; [2]*The University of Arizona, AZ*; [3]*The University of Arizona, Tucson, AZ*; [4]*The University of Arizona*; [5]*nanjing medical unversity, nanjing*

10.1136/jim-2020-MW.143

Introduction/Background Endothelial dysfunction is a hallmark feature and an important inducing factor of pulmonary arterial hypertension (PAH). We previous demonstrated the Salusin-β, an important vasoactive peptide, promotes vascular calcification via reactive oxygen species-mediated Klotho downregulation (Antioxid Redox Signal. 2019 Dec).

Objective(s) In this study, we investigate the roles of salusin-β, in endothelium-dependent vascular relaxation, and its signal pathways in the development and progression of pulmonary arterial hypertensive.

Methods Isometric tension experiment was performed to determine endothelium-dependent vascular relaxation by the degree of acetylcholine (ACh)-induced vascular relaxation. Isolated/perfused and ventilated lungs system was used to determine the hypoxic vasoconstriction. Animal models were used to determine the contribution of Salusin-β to chronic hypoxia-induced pulmonary hypertension.

Results Salusin-β level in plasma and its protein expressions of pulmonary artery (PA) in PAH rats was higher than that in control rats. Intravenous injection of salusin-β increased, while anti-salusin-β IgG decreased right ventricular systolic pressure (RVSP) of PAH rats. Salusin-β further deteriorated, while anti-salusin-β IgG improved, the decreased ACh-induced relaxation, endothelial nitric oxide synthase (eNOS) activity and nitric oxide (NO) level of PA in PAH rats. The NAD(P)H oxidase activity and reactive oxygen species (ROS) level of arteries of PAH rats were much higher than that of control rats, which was further increased by salusin-β, but decreased by anti-salusin-β IgG. ROS scavenger NAC or antioxidant apocynin significant inhibited, while SOD inhibitor DETC aggravated the effects of salusin-β, and eNOS inhibitor L-NAME inhibited the effects of anti-salusin-β IgG.

Conclusions Enhanced salusin-β activity is involved in attenuated endothelium-dependent vascular relaxation pathogenesis in PAH rats by stimulating NAD(P)H oxidase derived ROS generation and inhibiting eNOS activation and NO release. Scavenging salusin-β might improve endothelial function and prevent the development and progression of PAH.

A71 MOLECULAR REGULATION OF USP13 EXPRESSION IN MACROPHAGES IN RESPONSE TO LPS

[1]Fan Yu, [2]Lian Li, [3]Rama Mallampalli, [3]Jing Zhao, [3]Yutong Zhao. [1]*Department of Physiology and Cell Biology,The Ohio State University College of Medicine Columbus, Columbus, OH*; [2]*The Ohio State University College of Medicine Columbus*; [3]*The Ohio State University College of Medicine*

10.1136/jim-2020-MW.144

Introduction/Background Protein ubiquitination regulates protein degradation in the proteasome or lysosome systems, while the reaction can be reversed by deubiquitinases. Deubiquitinase USP13 has been reported to regulate the tumorigenesis by targeting PTEN and AKT/MAPK signaling. Our recent study showed that USP13 stabilizes an anti-inflammatory receptor, Sigirr. However, the molecular regulation of USP13 expression still remains poorly understood.

Objective(s) The objective of this study is to determine the molecular mechanism of USP13 in reducing bacterial acute infection-induced pro-inflammatory responses.

Methods In this study, the sepsis mice were induced by cecal ligation and puncture (CLP). Four or twenty-four hours after surgery, liver tissues from three groups (Sham, CLP 4h and CLP 24h) were collected for western blotting. Acute lung injury was induced by intratracheal (i.t) administration of lipopolysaccharide (LPS, 5 mg/kg), and intratracheal injection of PBS as control. Lung tissues were resected for western blotting after twenty-four hours. USP13 levels in LPS-stimulated Raw264.7 mouse macrophage and Kupffer cells were detected by real-time polymerase chain reaction (PCR) and western blotting.

Results We demonstrated that the protein levels of USP13 in CLP mouse livers and in i.t LPS mouse lungs were both significantly decreased compared to those in sham or control mice. The USP13 protein level and mRNA were also reduced in RAW264.7 macrophages and mouse Kupffer cells in response to LPS (100 ng/ml). Further, we found that LPS-reduced USP13 in Raw264.7 macrophages and mouse Kupffer cells were attenuated by pretreatment with JNK inhibitor II or C646 (CBP/p300 inhibitor).

Conclusions Our results indicate that USP13 protein levels are reduced in experimental acute inflammatory diseases and LPS-treated RAW264.7 macrophages and mouse Kupffer cells. JNK and CBP regulates USP13 expression in macrophages. This study will reveal a new anti-inflammatory pathway to reduce bacterial acute infection-induced pro-inflammatory responses.

Rheumatology/Immunology/Allergy

B73 ACUTE EXPOSURE TO AEROSOLIZED MICROCYSTIN-LR INDUCES ALLERGIC INFLAMMATORY GENE EXPRESSION IN HEALTHY HUMAN PRIMARY AIRWAY EPITHELIUM

[1]Joshua D Breidenbach, [2]Apurva Lad, [3]Robin Su, [4]James Willey, [4]Jeffrey Hammersley, [4]Thomas Blomquist, [4]Amira Gohara, [4]Mark Wooten, [4]Erin Crawford, [4]Nikolai Modyanov, [4]Deepak Malhotra, [4]Steven T Haller, [4]David J Kennedy. [1]*University of Toledo, Holland, OH*; [2]*University of Toledo, Toledo, OH*; [3]*The University of Toledo College of Medicine and Life Sciences, OH*; [4]*The University of Toledo*

10.1136/jim-2020-MW.145

Introduction/Background Harmful algal blooms (HABs) are on the rise globally and pose serious health concerns due to the release of cyanotoxins, which can be harmful to humans and the environment. Microcystin-LR (MC-LR) is one of the most prominently produced cyanotoxins and is a well-known hepatotoxin. We have recently shown that exposure to MC-LR exacerbates the development of pre-existing liver and inflammatory bowel disease. Exposure to MC-LR is typically investigated in the context of ingestion of contaminated water, however MC-LR has recently been detected in aerosols generated by bubble bursting, wave crashing, and recreational activities in the affected bodies of water. The human health effects of MC-LR aerosols on pulmonary function have not been extensively investigated and remain largely unknown.

Objective(s) The objective of this study was to determine the acute impact of algal toxin Microcystin-LR aerosol on human pulmonary epithelium.

Methods Airway epithelial cells were harvested and pooled from 14 healthy donors and used to reconstruct a ciliated, mucus-producing, airway epithelium in 3D air-liquid interface culture on transwell-plate inserts. These inserts were exposed to aerosolized solutions of 1 μM, 10 nM, and 100 pM MC-LR for 3 minutes a day for 3 days (9 minutes total over 3 days). RNA was isolated from well-plate inserts and cDNA was synthesized for RT-PCR measurements with a panel of genes chosen for assessment representing common pulmonary pathologies. Phenotypic characterization was also performed for tissue integrity, cell survival, mucociliary clearance, and cilia beating frequency.

Results A distinct shift in gene expression was detected by RT-PCR in MC-LR exposed airway epithelium. Several genes related to pulmonary allergic inflammatory response were significantly upregulated in MC-LR (1 μM) vs vehicle exposed cells [including TNF-alpha (8 fold increase), IL-6 (7 fold increase), CXCL8 (7 fold increase), CCL2 (4 fold increase), and CCL11 (3 fold increase), all $p<0.05$). These significant increases persisted even in the lowest dose MC-LR (100 pM) vs vehicle exposed cells (>2 fold increases in TNF-alpha, IL-6, and CXCL8; >1.5 fold increases in and CCL11, all $p<0.05$). Interestingly, no significant changes were noted in genetic markers associated with general pulmonary inflammation (NOS2, NOS3), fibrosis (CTGF, TGFB, EDN1), or carcinogenicity (CD36, XRCC1). Furthermore, no phenotypic alterations in tissue integrity, cell survival, mucociliary clearance, or cilia beating frequency were noted after the exposure protocol. The functional significance of the MC-LR induced inflammatory response toward immune cells is under active investigation.

Conclusions These results suggest the ability of MC-LR aerosol to drive exposed airway epithelium toward an allergic inflammatory response even in settings of acute, low dose exposure.

B74 THE BURDEN OF NEURO-PSYCHIATRIC SYMPTOMS IN A LARGE COHORT OF PATIENTS WITH NON-CLONAL MCAS

[1]Raied T Hufdhi, [2]Matthew Giannetti, [3]Matthew Hamilton, [2]Mariana Castells. [1]*University of Toledo, Sylvania, OH*; [2]*Harvard medical school/BWH, Boston, MA*; [3]*Harvard Medical School, Boston, MA*

10.1136/jim-2020-MW.146

Introduction/Background Non-clonal mast cell activation syndrome (MCAS) is defined by episodic and/or chronic

multisystem symptoms, response to medications and increased MC mediators. The burden of neuro-psychiatric symptoms in this population has not been characterized.

Objective(s) To assess the frequency and severity of neuro-psychiatric symptoms in patients with MCAS along with the impact on quality of life and productivity.

Methods We retrospectively reviewed the charts of 169 patients referred to the Brigham and Women`s Hospital Mastocytosis Center with mast cell activation symptoms and at least one elevated MC mediator.

Results All patients had MC-related symptoms, response to anti-MC medications, and at least one positive laboratory testing of MC mediator. Extensive testing was performed to exclude clonal MC disorders including KIT mutation in peripheral blood and, in some cases, bone marrow examination. 139 (82%) were females. Many patients had multiple system involvement. 130 (77%) with neuro-psychiatric symptoms. 145 (85%) had GI involvement, 148 (87%) cutaneous, 98 (58%) respiratory, 87 (51%) constitutional, and 92 (54%) skeletal, 67 (39%) had anaphylaxis and 58 (34%) required an ED visit. The neuro-psychiatric symptoms were prominent and were further analyzed. In this subset, the following were reported: headache 74 (43%), anxiety 61 (36%), depression 51 (30%), 50 (29%) poor concentration, and 47 (27%) memory loss. Interestingly, we found that 76 (23%) of the patients with MCAS were unable to work and more than half of these had applied for disability.

Conclusions Neuro-psychiatric symptoms are prevalent in patients with MCAS and likely have a significant impact on quality of life and productivity.

A73 ANTIOXIDANT THERAPY SIGNIFICANTLY ATTENUATES HEPATOTOXICITY FOLLOWING LOW DOSE EXPOSURE TO MICROCYSTIN-LR IN A MURINE MODEL OF DIET-INDUCED NON-ALCOHOLIC FATTY LIVER DISEASE

[1]Apurva Lad, [2]Andrew L Kleinhenz, [3]Joshua D Breidenbach, [1]Fatimah K Khalaf, [2]Prabhatchandra Dube, [2]Shungang Zhang, [4]Robin Su, [1]Jonathan Hunyadi, [1]Terry Hinds, [1]David D Baliu-Rodriguez, [1]Dragan D Isailovic, [2]Jacob A Connolly, [2]Bella Z Khatib-Shahidi, [2]Deepak Malhotra, [2]Steven T Haller, [2]David J Kennedy. *[1]University of Toledo, Toledo, OH; [2]The University of Toledo; [3]University of Toledo, Holland, OH; [4]The University of Toledo College of Medicine and Life Sciences, OH*

10.1136/jim-2020-MW.147

Introduction/Background Cyanobacterial blooms are an increasing problem worldwide. Microcystins are cyanotoxins produced as secondary metabolites by these cyanobacteria. Microcystin-LR (MC-LR) is one of the most abundant microcystin congeners and a known hepatotoxin. The current WHO guidelines for safe exposure to MC-LR have been extrapolated based on studies performed in healthy animal models. However, there is little data on the effects of these toxins in settings of common pre-existing liver diseases such as Non-alcoholic Fatty Liver Disease (NAFLD). Our previous studies demonstrated that chronic exposure to low doses of MC-LR (50 μg/kg and 100 μg/kg MC-LR, doses which do not induce hepatotoxicity in normal healthy mice) did induce hepatotoxicity marked with significant hepatic microvesicular lipid accumulation and oxidative stress in mice with NAFLD.

Objective(s) Based on these studies, we hypothesized that treatment with antioxidants could potentially act as a therapeutic in reducing the hepatotoxicity induced by low dose MC-LR exposure in NAFLD. In particular, we targeted two oxidative stress pathways that have been shown to be involved in NAFLD mediated oxidant stress [i.e. augmentation of the glutathione detoxification pathway with N-acetylcysteine and interruption of specific Src kinase-mediated oxidant signaling pathway with a novel peptide (pNaKtide)].

Methods Four groups of six-week old C57Bl/6J male mice (n=5–8 mice per group) were administered a choline-deficient 0.1% methionine containing high-fat diet (CDHFD) to induce NAFLD over a period of 6 weeks. During the 5th and 6th week, the mice continued to be fed on CDHFD and were gavaged with 15 total doses of vehicle (Control group, 300 μl of vehicle of water, n=5); 100 μg/kg of MC-LR every 24 hours (MC-LR only group, n=6), 100 μg/kg MC-LR and 25 mg/kg of the pNaKtide via intraperitoneal injection once a week at the end of week 5 and 6 (MC-LR+pNaKtide group, n=8); 100 μg/kg MC-LR and 40 mM N-acetylcysteine (NAC) administered in drinking water (MC-LR+NAC group, n=8). Weight and fat content (as assessed by nuclear magnetic resonance spectroscopy) were measured weekly. At the end of the study, 24-hour urine was collected for LC-MS/MS determination of MC-LR-Cysteine (MC-LR-Cys), an adduct formed during hepatic detoxification of MC-LR. Livers were assessed both histologically and by quantitative real-time PCR for hepatotoxicity.

Results After 4 weeks on CDHFD, all groups of mice showed significant increases in body weight and total fat content. Interestingly, while MC-LR exposure resulted in a significant increase in total fat content vs. vehicle during weeks 5 and 6, this was significantly attenuated in both the MC-LR+pNaKtide and MC-LR+NAC groups ($p<0.05$ for both). Liver weight was not significantly different between the 4 groups; however, histologic analysis revealed a significant increase in hepatic inflammation with MC-LR exposure which was attenuated in both the MC-LR+pNaKtide and MC-LR+NAC groups ($p<0.05$ vs MC-LR for both). Similarly, while quantitative real-time PCR from liver tissues revealed significant increases in markers of hepatotoxicity (OSMR, Serpine), inflammation (Fizz1, CD68, CD40, Itgam) and tissue remodeling (MMP2, MMP9, Col3a1) following exposure to MC-LR, these increases were significantly attenuated in the MC-LR+pNaKtide ($p<0.05$ vs MC-LR for OSMR, Serpine, Fizz1, CD68, CD40, Itgam, MMP2, MMP9, and Col3a1) and MC-LR +NAC mice ($p<0.05$ vs MC-LR for OSMR, Fizz1, CD40, MMP2, MMP9, and Col3a1). In preliminary results of a limited sample set (n=5/group) MC-LR+pNaKtide mice had a 100% increase in urinary excretion of the MC-LR-Cys metabolite ($p=0.09$ vs MC-LR) while MC-LR+NAC had a 126% increase in urinary excretion of the MC-LR-Cys metabolite ($p<0.05$ vs MC-LR).

Conclusions These results suggest that antioxidant therapy with NAC or pNaKtide may significantly attenuate hepatic injury following low dose exposure to MC-LR in a murine model of diet-induced NAFLD and that these effects may be due to increased MC-LR metabolism.